STATISTICAL THERMODYNAMICS OF FLUIDS
WITH ORIENTATION-DEPENDENT INTERACTIONS

APPLICATIONS TO WATER
IN HOMOGENEOUS AND HETEROGENEOUS SYSTEMS

N.A.M. BESSELING

STATISTICAL THERMODYNAMICS OF FLUIDS
WITH ORIENTATION-DEPENDENT INTERACTIONS

APPLICATIONS TO WATER
IN HOMOGENEOUS AND HETEROGENEOUS SYSTEMS

BIBLIOTHEEK
LANDBOUWUNIVERSITEIT
WAGENINGEN

STELLINGEN

I

Dat de 'gemiddeld-veld theorie' van Christenson e.a. repulsie voorspelt tussen twee oppervlakken in een medium van vloeibaar alkaan, wat in tegenspraak is met hun eigen metingen, is niet te wijten aan de gemiddeld-veld benadering maar aan de in hun berekening opgelegde uniforme dichtheid.

Christenson, H. K.; Gruen, D. W. R.; Horn, R. G.; Israelachvili, J. N.
J. Chem. Phys., 87, 1834-1841 (1987)

II

Er zijn veel verschillende 'gemiddeld-veld' benaderingen.

III

In de theorieën van Evers e.a. en van Böhmer en Evers voor de adsorptie van zwakke polyelectrolyten, zijn de entropie-bijdragen die samenhangen met de menging van de gedissocieerde en ongedissocieerde segmenten verwaarloosd.

Evers, O. A.; Fleer, G. J.; Scheutjens, J. M. H. M.; Lyklema, J.
J. Colloid Interface Sci., 111, 446-454 (1986)
Böhmer, M. R.; Evers, O. A.; Scheutjens, J. M. H. M. Macromolecules, 23, 2288 (1990)

IV

Rond apolaire (delen van) molekulen opgelost in water bestaat geen laag van watermolekulen die meer of sterkere onderlinge waterstofbruggen hebben.

Dit proefschrift, hoofdstuk IV.

V

De afleiding waarmee Leermakers en Scheutjens pretenderen aan te tonen dat in de membraan-vormings isotherm zoals door hen berekend, voor de thermodynamisch stabiele situatie moet gelden dat $\partial\left(A^{\sigma}/L\right)/\partial\theta_2^g < 0$, is niet juist.

Leermakers, F. A. M.; Scheutjens, J. M. H. M.
J. Chem. Phys., 89, 3264-3274 (1988) (vgl. 19 t/m 21).

VI

Voor de didactiek van de thermodynamica zou het beter zijn om de notatie van partiële afgeleiden meer in overeenstemming te brengen met de in andere vakgebieden gebruikelijke schrijfwijze, en in plaats van het aangeven van 'constant gehouden grootheden' door middel van subscribten, de argumenten van de te differentiëren functie weer te geven , b.v.

$$\frac{\partial G(n, p, T)}{\partial n} \quad \text{in plaats van} \quad \left(\frac{\partial G}{\partial n}\right)_{p,T}$$

VII

Het gescheiden etaleren van romans en romannetjes zoals in veel openbare bibliotheken gebeurt, werkt een eenzijdige ontwikkeling van het lezerspubliek in de hand.

VIII

Er is voor aankomende studenten een aantal goede redenen om exacte studies te mijden.

IX

De laatste twee letters in 'OIO' dienen slechts ter rechtvaardiging van een bezuiniging op salariskosten.

X

De economische waarde van een doctorsgraad is negatief.

XI

De tendens bij grote bedrijven om hun research meer 'business-gericht' te maken is enigszins onverenigbaar met het streven goede wetenschappers voor zich te laten werken.

XII

De weergave van de overeenkomsten en verschillen tussen de polyelectroliet-adsorptie-theorieën van Wiegel, Muthukumar en Böhmer door Van der Steeg e.a. is onjuist en derhalve hun verklaring voor de verschillen en overeenkomsten tussen de voorspellingen m.b.t. kritische desorptie eveneens.

Van der Steeg, H. G. M.; Cohen Stuart, M. A.; de Keizer, A.; Bijsterbosch, B. H.
Langmuir, 8, 2538-2546 (1992)

XIII

De auteursnamen bij een wetenschappelijke publicatie geven niet altijd juist weer wie aan het onderzoek hebben bijgedragen.

XIV

De vervanging van fosfaten in wasmiddelen is schadelijk voor het milieu.

XV

De BET-adsorptievergelijking is kwalitatief onjuist voor systemen waarbij het adsorbaat het adsorbens niet volledig bevochtigt.

XVI

Bij hun bespreking van de effecten van niet adsorberend polymeer op de stabiliteit van kolloïdale dispersies, gebruiken Fleer en Scheutjens op een verwarrende manier het begrip 'flocculation' waar zij het hebben over evenwichts-fasescheiding.

Fleer, G.J.; Scheutjens, J.M.H.M. in "Coagulation and Flocculation, Theory and Application",
B. Dobias, Ed., Surfactant Science Series Vol. 47, Marcel Dekker, New York (1993) 209-263.

Stellingen behorende bij het proefschrift *Statistical Thermodynamics of Fluids with Orientation-Dependent Interactions; Applications to Water in Homogeneous and Heterogeneous Systems.* N.A.M. Besseling, Wageningen 20 september 1993.

CONTENTS

CHAPTER I

GENERAL INTRODUCTION

1 WATER

On first sight, water seems to be rather uninteresting. It is a colourless, tasteless and odourless fluid. It cannot explode, it doesn't even burn. It is not at all rare and very cheap; we just bathe in it and drink it if nothing better is available. Every child knows what water is. Then, why should a generous OIO* salary be spent on research on water?

Upon second inspection water is extremely interesting. It is one of the most abundant compounds on earth and it is essential for the existence of life as we know it. It has various properties that makes it exceptional among low-molecular compounds and that are essential for its roles in biological and environmental systems. The heat capacity and heat of vaporisation are relatively high. This is important in stabilising the temperature of, for instance, individual humans as well as the global climate. At ambient pressure, water contracts upon melting and its isobaric density reaches a maximum at 4 $^{\circ}C$. This is of great ecological importance. Below the frozen surface of a lake, fish and other organisms can survive winter. Not only do many organisms live in water, all living beings consist for a large part of water. Water is the medium for all processes that constitute life. Some important phenomena in this respect are the formation of biological membranes and the conformation of proteins [1].

In the last two examples the so-called hydrophobic effect plays an important role. "Hydrophobic effect" is a somewhat vague term that is used in relation to the behaviour of water when it interacts with apolar molecules, fragments of molecules or with apolar surfaces. These are hydrophobic, which means that they tend to minimise their contacts with water. The solubility of apolar compounds in water is low and they tend to form a separate phase. Macromolecules such as proteins, tend to assume a conformation that minimises the contact between apolar parts and water. They usually have a globular conformation with the apolar parts enriching the inside. Association of lipids into

---

* OIO stands for 'Onderzoeker in Opleiding'.

biomembranes and of surfactants into micelles is driven by the hydrophobic nature of aliphatic chains of these molecules.

That the affinity between "like" molecules is larger than between unlike molecules is not at all restricted to apolar solutes in water. This is for instance reflected in Berthelot's principle [2], which states that the magnitude of the attraction between unlike molecules is the geometric mean of the values for the interactions between like molecules. What is special with apolar solutes in water, is the temperature dependence of the solubility; reflecting the roles of energetic and entropic contributions to the Gibbs energy of solvation. These point out that the origin of the low compatibility of water and apolar compounds is entropic, whereas the energetic effect is small and at low temperature even promotes compatibility.

It may be clear that an adequate understanding of water is essential for the understanding of numerous biological phenomena. Although much research, both experimental and theoretical, has been done on water, our understanding is still incomplete. In the present study aqueous systems will be investigated using a theory that accounts for local orientational correlations. Since this approach is quite versatile, the relations between the properties of individual water molecules and the behaviour of water at a large variety of circumstances can be clarified.

2 STATISTICAL THERMODYNAMICS

The aim of this branch of science, which is also known as *molecular thermodynamics, statistical mechanics* and *statistical physics*, is to infer macroscopic from microscopic properties. In the present study, the microscopic properties refer to molecules. Essentially, we consider the dependence of the interaction energy of the molecules upon relative positions, orientations and conformations. Macroscopic properties are properties that cannot be attributed to a single molecule or to a few ones, only to large collections of molecules. Examples are pressure, temperature, melting point, heat capacity. It is inappropriate to speak of the pressure of a methane molecule or of a melting water molecule. It is correct however, to speak of the melting of ice and the pressure of methane at some density and temperature.

Inferring the behaviour of a system consisting of a very large number of molecules from the properties of the individual molecules is not trivial. As the adjective *statistical* in the title of the present section suggests, probability plays a large role here (for a nice introduction to probability theory see ref. [3]). Gibbs has developed a general theoretical framework for the evaluation of macroscopic behaviour from molecular properties, the so called ensemble method. This is treated in numerous books on statistical thermodynamics, for instance refs. [4, 5]. In this method, the probability distribution of microscopic states is evaluated of systems for which macroscopic characteristics are given. This method will be used in the present study.

Another method that is often applied to the similar systems as will occur in this thesis is Molecular Dynamics Simulation. This is conceptually rather simple: Newton's laws of classical mechanics are applied to a box containing a finite number of molecules (typically a few tenths to a few hundreds). Realistic functions for the intermolecular interactions can be used. This method is rather (computer) time consuming. Only short intervals of real time can be simulated. Hence, one is not always certain that the equilibrium state of a system is reached. Especially the results for thermodynamic functions as entropy, chemical potentials etc. suffer from statistical uncertainties.

3 LATTICE MODELS FOR FLUID SYSTEMS

Often, molecules can be regarded as particles that satisfy the laws of classical mechanics. Accordingly, the Hamiltonian of a system, the energy as a function of phase-space coordinates, can be separated into a configurational-energy- and a kinetic-energy term. The configurational (is potential) energy of the system results from all interactions between the molecules and of the coupling with external fields, if present. This energy will generally depend on the configuration of the system, for instance on the distances between the molecules. Within the limits of classical mechanics, the configuration of a system and the velocity distribution of the molecules are independent. Partition functions can be written as products of a configuration- and a kinetic factor. The latter is fairly universal but the configurational properties are strongly system dependent. The great variety of macroscopic

phenomena is mainly due to these configurational properties. The present study concerns configurational properties and kinetic contributions are not considered.

Since often the systems we are interested in are very complicated on a molecular scale, we have to rely on models in which the most important properties of the molecules are captured as well as possible. The work described in this thesis is based on lattice models. In such models, molecules or molecular segments are confined to a regular lattice of sites. Consequently, the possible distances between molecules and angles that contacts between molecules make can vary only in a discrete way.

The title of the present section is somewhat paradoxical. It is well known that fluids have a disordered structure, unlike that of a regular lattice. One of the reasons why lattice models are applied to fluids is of a merely pragmatic nature; the configurational statistics are easier analysed on a discrete lattice than for a continuum. Confinement of the molecules to a lattice of sites will obviously reduce the configurational freedom and consequently the entropy. In many cases however, this shift of entropy per molecule will be more or less independent of temperature, composition etc.. Hence, within a lattice model *changes* of thermodynamic quantities upon changes of conditions will often be predicted rather well. As an a posteriori justification of this approach it might be added that in practice lattice models often work out surprisingly well.

For instance, Raoult's law, according to which the fugacity of one given component in a mixture is equal to its mole fraction, holds if the enthalpy does not change upon mixing and if the entropy of mixing n_1 molecules of species 1 and n_2 of species 2 equals

$$\Delta_{mix}S = k \ln \frac{(n_1 + n_2)!}{n_1! n_2!} \tag{1}$$

This expression can be derived from a model where the molecules are arranged on a lattice of $n_1 + n_2$ sites [4, 6]. The entropy of mixing in a fluid and on a lattice is similar.

In practice, eq. (1) holds if the molecular species do not differ too much in size and shape, and if interaction energies between molecules of species 1 (u_{11}), between molecules of species 2 (u_{22}), and between a

molecule of species 1 and one of species 2, (u_{12}) are similar, this means that $v_{12} = u_{12} - \frac{1}{2}(u_{11} + u_{22})$ has to be small. To approximate the mixing entropy by eq. (1) for cases where $v_{12} \neq 0$ is referred to as the Bragg-Williams- or random-mixing approximation. Establishing the origins and consequences of deviations of eq. (1) is one of the issues of the present study.

An important distinction between two groups of lattice models for fluid systems is that between models where sites are allowed to be vacant and models where all sites are occupied. Models of the first type are called lattice-gas-, lattice-fluid-, or hole models. In these models, density variations and pressure effects are accounted for. For the configurational statistics it is immaterial whether one deals with a lattice gas or with a model that does not contain vacancies. An n-component lattice gas is equivalent with a model without vacancies that contains $n + 1$ components. Only if one wants to infer thermodynamic quantities such as pressure, it is necessary to specify whether vacancies are present or if all sites are occupied by molecules.

In lattice models it is possible to accommodate molecules of various sizes. The size of a molecule is hence only discretely variable; a molecule occupies an integer number of sites. The entities occupying one site are called segments. The segments of a molecule can be of a different nature.

The discreteness inherent in lattice models implies that the "resolution" by which molecular details can be implemented and the results that are obtained, is restricted. For instance in a multilayer lattice model of a fluid adjoining a smooth surface, the oscillatory density profile cannot be dealt with if the size of the molecules equals that of the lattice sites (see however refs. [7, 8]).

It should be kept in mind that it is always somewhat arbitrary what to choose as a model for a certain molecule. In these choices one seeks a compromise the complexity of the model and the number of parameters, that is preferably small, and the accuracy of the results, which is preferably high.

4 NON-UNIFORM DISTRIBUTIONS, MEAN-FIELD APPROXIMATIONS AND SELF-CONSISTENT FIELDS

It is often convenient to formulate the expressions for the molecular distributions over locations orientations etc. in terms of self-consistent field equations. These express the density of molecules at a certain position, having a certain orientation etc. as a product of a normalisation factor and the weighting factor. The normalisation factor, usually the activity, is the same for all molecules of the same species. The weighting factor which accounts for interaction forces that a molecule in a certain position and orientation experiences will generally depend on position and orientation etc.. Such a mathematical formalism reflects that the molecules distribute themselves according to the forces they experience. This potential-energy field is always partly determined by these same molecules and hence related to the distribution of molecules over positions, orientations, conformations etc.. (see for instance [8-10])

The discussion of the following paragraphs reviews some aspects of what has been called the potential-distribution method. This has extensively discussed in the refs. [11-13]. I will here emphasise the relation with the self-consistent field formalism as, for instance, in the theory of Scheutjens and Fleer [9] and in the present study. As an example the density profile in one direction is examined. For this we can write rigorously

$$\rho(z) = \lambda \left\langle \exp - \frac{\Psi(\vec{r}, z)}{kT} \right\rangle \tag{2}$$

Here $\rho(z)$ is the number density in the plane z, $\lambda = \exp(\mu/kT)$ is the activity and $\Psi(\vec{r}, z)$ is the potential energy of a molecule at some position in the plane z. This energy is a function of the positions and orientations etc. of all molecules $\vec{r}$; $\langle \exp - \Psi(\vec{r}, z)/kT \rangle$ is the average of $\exp - \Psi(\vec{r}, z)/kT$ over all $\vec{r}$. If also an expression for $\langle \exp - \Psi(\vec{r}, z)/kT \rangle$ in terms of $\rho(z)$ were available, then we could in principle solve for the equilibrium distribution $\rho(z)$. Such a complete combination of expressions is referred to as "self-consistent field equations".

Equation (2) can be rewritten as

$$\mu = kT \ln \rho(z) - kT \ln\left\langle \exp{-\frac{\Psi(\vec{r}, z)}{kT}} \right\rangle = kT \ln \rho - kT \ln\left\langle \exp{-\frac{\Psi(\vec{r})}{kT}} \right\rangle \quad (3)$$

where $\mu = kT \ln \lambda$, ρ and $\langle \exp(-\Psi(\vec{r})/kT) \rangle$ are the averages over z of $\rho(z)$ and $\langle \exp(-\Psi(\vec{r}, z)/kT) \rangle$, respectively. Equation (3) is the statistical mechanical expression for the chemical potential. This expression is widely applied in the so-called "test-particle method" for the evaluation of the chemical potential from molecular simulations (i.e. molecular-dynamics, Monte Carlo). The quantity $-kT\ln\langle \exp{-} \Psi(\vec{r}, z)/kT \rangle$ is often referred to as "potential of the mean force" at z. The term $kT \ln \rho$ in eq. (3) is the ideal chemical potential, the next accounts for non ideality due to intermolecular interactions; $\langle \exp{-} \Psi(\vec{r})/kT \rangle^{-1}$ can be recognised as the activity coefficient.

The equations (2) and (3) are both completely general and exact within the framework of classical mechanics. They are derived from the classical configuration integral [11-13].

Although the meaning of $\langle \exp{-} \Psi(\vec{r}, z)/kT \rangle$ is quite clear, it is often extremely complicated to evaluate this quantity in terms of $\rho(z)$. Usually, it is necessary to make some assumption. Consider for instance the well-known lattice-gas model for isotropic molecules. In such a model the fraction of occupied sites in layer z is given by $\phi(z) = \rho(z)/v$, where v is the volume per lattice site and z indicates the lattice layer. To two or more molecules on the same site, an infinite energy is attributed and hence $\exp(-\Psi/kT)$ vanishes for such cases. This leads to a factor $1 - \phi(z)$ in the expression for $\langle \exp{-} \Psi(\vec{r}, z)/kT \rangle$. If there are no further interactions then this is the whole story and equation (2) can be rewritten rigorously as $\rho(z) = \lambda(1 - \phi(z))$. However, in the case that molecules on nearest-neighbour sites have an interaction energy u, the potential energy of a molecule with n nearest-neighbours equals nu. A factor $\langle \exp(-nu/kT) \rangle$, the average over all configurations of $\exp(-nu/kT)$, should be added. For $\langle \exp(-nu/kT) \rangle$ no exact expression is available.

In the so-called the Bragg-Williams approximation (also called zeroth-order- or random-mixing approximation) the molecules on each layer are assumed to be distributed at random. Hence, the number of nearest-neighbours of a molecule in layer z, is given by $q\langle \phi(z) \rangle = q_{\pm}\phi(z-1) + q_0\phi(z) + q_{\pm}\phi(z+1)$, where q_0 and $q_{\pm}$ are the number of

nearest-neighbour sites in the same layer and in an adjoining layer, respectively. Each site has $q = q_0 + 2q_{\pm}$ nearest neighbours. Accordingly, the potential energy of a molecule at some site (that is not occupied by another molecule) in layer z is $q\langle\phi(z)\rangle u$ and equation (2) is approximated by [12, 13]

$$\rho(z) = \lambda(1 - \phi(z))\exp{-\frac{q\langle\phi(z)\rangle u}{kT}} \tag{4}$$

This expression is equivalent with the self-consistent field theory of Scheutjens and Fleer [9] applied to molecules that occupy one site at a time (the present parameter is related to the Flory-Huggins parameter for the interaction between a molecule and vacancy as $\chi = -\frac{1}{2}qu$).

For non-zero nearest-neighbour interactions it is inconsistent to assume that the molecules are distributed randomly within the layers and that the environment of each site and its occupation are stochastically independent. In fact, all molecules find / create themselves a "potential-energy dip". The lowering of the potential energy due to this ordering is partly compensated by a lowering of entropy. That is why the inaccuracies in the Bragg-Williams values for the energy and entropy are always much larger than for the Helmholtz energy. Often this last quantity are predicted rather well. As we will see in the following chapters this is not the case for compounds with strongly orientation-dependent intermolecular interactions such as water. That is the reason we use the more accurate quasi-chemical approximation in the present study.

A quantity like $q\langle\phi(z)\rangle u$ is sometimes called a "mean potential". In mean field approximations, the "potential of the mean force" is approximated by the "mean potential". Mathematically, in calculating the mean potential, the sequence of taking the average and the exponential of the potential energy is inverted. It is important to note the effect upon calculated temperature dependencies: the mean potential $q\langle\phi(z)\rangle u$ is independent of temperature whereas the corresponding potential of mean force varies with temperature. This is obviously directly related to the defects of the Bragg-Williams approximation in determining the values of energy and entropy. Sometimes the discrepancies due to the approximations are

compensated by making some ad hoc assumption about some temperature dependence for u.

In the present study we will not use the Bragg-Williams approximation but the quasi-chemical approximation (also called Bethe-Guggenheim approximation or first-order approximation) [4, 6]. This accounts for correlations in the occupations of neighbouring sites. It is assumed that the occurrence of a contact does not depend on other contacts. This is not exact for lattices with closed rings of sites. It is interesting to note that the Bragg-Williams approximation can be obtained from the quasi-chemical one as the limiting result for an infinitely large lattice coordination number [6].

Apart from disregarding short-range ordering, the occurrence of all long-range ordering within the layers is also precluded in the equation (4) and in its first-order alternative. Only inhomogeneity in the z direction, which allows for the existence of a density gradient normal to a macroscopic interface, is accounted for. It is a general feature of mean field approaches that one has to specify the possibilities for long-range ordering (symmetry breaking). Examples of forms of long-range order are: density heterogeneity in some direction, as discussed here (or in two directions as in ref. [10]), nematic ordering in systems with a homogeneous density and the formation of super-lattice structures [6]. Usually, the smaller the symmetry one assumes for a system, the more complicated the evaluation.

5 ORIENTATION-DEPENDENT INTERMOLECULAR INTERACTIONS

The differences between the results from the zeroth- and first-order approximation for isotropic molecules are only quantitative and usually not very large [6]. Especially if intermolecular interactions depend on the relative orientations of molecules, it is of great importance to account for correlations. Not only does each molecule influence the local composition in its neighbourhood. It also influences the orientations of the neighbouring molecules. The possibilities for the molecules to find and create "potential-energy dips" are larger in the case of orientation-dependent intermolecular interactions. This has important consequences for the macroscopic properties of such compounds.

The temperature dependence of the thermodynamic properties of systems containing molecules with orientation-dependent interactions is often very different from that of simple isotropic molecules. As has been suggested long ago by Hirschfelder et al., the occurrence of closed-loop coexistence curves can be explained by orientation-dependent intermolecular interactions [14]. As will be demonstrated in a number of chapters of the present thesis, the well know anomalous properties of water can also be explained by the strongly orientation-dependent interactions (i.e. hydrogen bonds) between water molecules.

Of all compounds that possess orientation-dependent intermolecular interactions, water is undoubtedly the most interesting. It exhibits many anomalous properties that are due to these interactions. There are still many open questions as to the relations between the macroscopic behaviour of water and the properties of the individual molecules.

Applying the zeroth-order approximation (Bragg-Williams / random-mixing), the effects of orientation-dependence of intermolecular interactions cannot be reproduced. Within that approach, molecules with orientation-dependent interactions show the same behaviour as isotropic ones. This fault is due to unweighted averaging over relative orientations, which is implicit in the zeroth-order approximation. Consequently, in calculating the properties of homogeneous systems in zeroth-order approximation, the orientation-dependent interaction energy between anisotropic monomers can just as well be replaced by an effective isotropic interaction energy. This effective interaction energy is calculated by averaging the intermolecular interactions over all orientations of the two molecules: $\sum_{o,p} u_{AB}^{op} / \sum_{o,p} 1$ where o and p are orientations of monomers A and B respectively. Hence, the results of the zeroth-order approximation are often qualitatively wrong if applied to molecules with orientational interactions.

In the present study, the first-order approximation, which does account for correlation effects, is generalised so that compounds like water can be modelled.

6 OUTLINE OF THIS THESIS

The present study deals with the development of a lattice theory that is applicable to systems containing molecules with orientation-dependent interactions. In the following chapter this theory is introduced in a rather general fashion. That chapter mainly consists of a derivation of the self-consistent field equations and of the expressions for thermodynamic quantities for an arbitrary combination of monomeric species. Further, some illustrations of the capabilities of the method are given.

In chapter III, a lattice-fluid model for water is introduced and analysed according to the theory introduced in chapter II. Results on the properties of water, its structure, equation of state and liquid-vapour equilibrium and of the liquid-vapour interface are presented and discussed.

In chapter IV, the same model for water is applied to the molecular interpretation of the hydrophobic effect.

Chapter V deals with the structure of water near inert interfaces and with the hydration forces between interfaces ensuing from overlap of solvation layers. This chapter is again based on the model for water that was introduced in III.

In Chapter VI, some other aspects of the behaviour of water near interfaces is investigated: vapour adsorption and wetting phenomena.

In the chapters II to VI, a molecule occupies only one lattice site. In chapter VII this restriction is relaxed. The theory of chapter II is generalised to account for chain molecules that occupy a number of connected sites. A propagator formalism is derived that allows for an efficient evaluation of the distribution of chain conformations.

REFERENCES

1   Israelachvili, J. *Intermolecular & Surface Forces*; Academic Press: London, 1992.
2   Lyklema, J. *Fundamentals of Interface and Colloid Science*; Academic Press: London, 1991.
3   Feller, W. *An Introduction to Probability Theory and its Applications*; Wiley: New York, 1970.
4   Hill, T. L. *Introduction to Statistical Thermodynamics*; Addison-Wesley: 1962.
5   McQuarrie, D. A. *Statistical Mechanics*; Harper and Row: 1976.
6   Guggenheim, E. A. *Mixtures*; Fowler, R. H., et al.; Clarendon: Oxford, 1952.

7   Israëls, R.; Meijer, L. A. (1992). Personal communication: The Scheutjens Fleer theory applied to small branched molecules at a smoothe surface reproduces an oscilatory density profile.

8   Björling, M. in *Polymers at Interfaces*, edited by (Thesis, University of Lund, Sweden, Lund, 1992) pp. V:2-V:32. "Self consistent field theory for hard sphere chains close to hard walls".

9   Scheutjens, J. M. H. M.; Fleer, G. J. *J. Phys. Chem.*, *83*, 1619-1635 (1979) "Statistical theory of the adsorption of interacting chain molecules. 1. Partition function, segment density distribution, and adsorption isotherms".

10   Leermakers, F. A. M.; Scheutjens, J. M. H. M. *Biochim. Biophys. Acta, 1024*, 139-151 (1990) "Statistical thermodynamics of association colloids. IV. Inhomogeneous membrane systems".

11   Jackson, J. L.; Klein, L. S. *Phys. Fluids, 7*, 228-231 (1963) "Potential distribution method in equilibrium statistical mechanics".

12   Widom, B. *J. Chem. Phys.*, *39*, 2808-2812 (1963) "Some topics in the theory of fluids".

13   Widom, B. *J. Stat. Phys., 19*, 563-574 (1978) "Structure of interfaces from uniformity of the chemical potential".

14   Hirschfelder, J.; Stevenson, D.; Eyring, H. *J. Chem. Phys., 5*, 896-912 (1937) "A theory of liquid structure".

CHAPTER II

STATISTICAL THERMODYNAMICS OF MOLECULES WITH ORIENTATION-DEPENDENT INTERACTIONS IN HOMOGENEOUS AND HETEROGENEOUS SYSTEMS

A lattice theory is presented for homogeneous and heterogeneous systems containing molecules with orientation-dependent interactions. Correlations due to interactions are accounted for in first-order (quasichemical) approximation by allowing variations of the distribution of intermolecular contacts. To model heterogeneous systems, parallel lattice layers are allowed to be differently occupied. A partition function, written as a sum over distributions of molecules over orientations and locations and of intermolecular contacts, is derived for any collection of monomeric species. Using a maximum-term argument, self-consistent field equations are derived for the equilibrium distributions. These equations are solved numerically. Allowing lattice sites to be vacant, free-volume effects can be accounted for. Expressions are obtained for energy, entropy, chemical potentials, pressure and surface tension. The capabilities of the method are illustrated by applying it to a number of specific systems, one of which exhibiting a closed-loop coexistence curve. Properties are investigated of coexisting phases and of the interface between them.

1 INTRODUCTION

In lattice models for fluids, molecules are confined to a regular array of sites in which distances and angles are discrete. Such coarse-grained models are often useful in relating thermodynamic behaviour to molecular properties and obtaining semi-quantitative expressions for thermodynamic functions of complicated systems. The using of lattice models for fluids is justified by the consideration that the reduction of the molecular entropy, due to the confinement of the molecules to lattice sites, is more or less independent of temperature and composition. So this simplification does not greatly affect changes in the thermodynamic quantities, although it does alter the standard state.

Well-known examples of successful applications of lattice models are mixtures of small molecules [1, 2] and of mixtures containing polymers [1-3]. Effects of free-volume changes in pure fluids and fluid mixtures have been investigated by including vacant sites in the model. Such models are referred to as lattice-gas, lattice-fluid, or hole models [1, 4-8].

Various approximate methods to derive thermodynamic properties of lattice models for interacting molecules have been developed [1, 2]. The most simple is the *Bragg-Williams* or *random-mixing* approximation. Guggenheim refers to it as the *zeroth-order* approximation. This approximation assumes the occupation of the sites to be stochastically independent although non-zero interaction energies are allowed for. The more accurate *Bethe-* and *quasi-chemical* approximations, that Guggenheim demonstrated to be equivalent, are usually referred to as the *first-order* approximation [2]. This accounts for correlations between nearest neighbours, but assumes pairs of sites to be independently occupied. The existence of closed rings of sites is disregarded. Hence this approximation is sometimes referred to as the *dendritic* approximation. It is known to give exact results for one-dimensional systems [1]. More generally, it is exact for *Cayley-tree lattices* or *Bethe lattices* (lattices that contain no closed rings of sites) [9]. Higher approximations have been developed in which the interdependence within larger clusters of sites is

accounted for [2, 10, 11]. These are more difficult to apply to complex situations and using larger basic clusters does not generally guarantee more exact results.

Especially for systems containing molecules with orientation-dependent interactions, where the intermolecular interaction depends on the relative orientations of the molecules, it is important to account for correlations. It can easily be shown that, according to the zeroth-order approximation, which neglects all correlations, homogeneous isotropic systems containing molecules with orientation-dependent interactions show the same behaviour as systems that contain only isotropic molecules. Such a treatment fails in reproducing the more complicated temperature dependence of thermodynamic quantities of compounds with orientation-dependent interactions. For instance, the miscibility in a binary system can be increasing with decreasing temperature, and even a closed-loop coexistence curve with a lower critical solution temperature that is smaller than the upper critical solution temperature can occur.

A simple way to formulate a lattice theory that reproduces such a phase diagram is to treat the parameter that accounts for the intermolecular interactions as a function of temperature. Then, it has the character of a free energy instead of an energy. However, such a treatment does not give any clue for a molecular explanation of the temperature dependence.

The first quantitative statistical-thermodynamic treatments based on a physical model of binary mixtures of molecules with orientation-dependent interactions are due to Barker and co-workers [12-15] and to Tompa [16]. They used the above-mentioned first-order approximation. It was demonstrated by Barker and Fock that orientation-dependent interactions can lead to closed-loop coexistence curves with both upper- and lower critical solution temperatures [14]. This occurs with mixtures in which there is a net attraction between unlike molecules in some relative orientations, whereas in most relative orientations there is a net repulsion between unlike molecules. The coexistence curves obtained by Barker and Fock are somewhat 'narrow shaped'; the difference between the compositions of coexisting phases seems to be too small. Bodegom and Meijer [17] have argued that this is partly due to imperfections of the first-order approximation. By using larger

basic clusters of sites, they obtained larger differences between the compositions of coexisting phases. On the other hand, it has been shown that a change of the physical model itself, increasing the ratio between the numbers of repulsive and attractive relative orientations of unlike molecules, also leads to larger differences between the compositions of coexisting phases [17, 18]. In the original Barker-Fock model, the mixture is symmetrical with respect to exchanging the components. As a consequence, thermodynamic functions and coexistence curves are also symmetric in this respect. The Barker-Fock approach has been generalised and applied to liquid-vapour phase diagrams of models for alkanes, alcohols [19, 20], to a model for aqueous polymer solutions [21], and to mixtures adjoining inert surfaces [22].

Various other models, that are easier to evaluate than the Barker-Fock model, have been introduced to incorporate orientation-dependent interactions including so-called *decorated-lattice* and *double-lattice* models where different types of lattice-sites are defined [18, 23-26], and models where 'internal' states are attributed to the molecules or their segments [8, 27-36]. Some of these models apply to mixtures containing molecules of different sizes, polymers included [26, 31-33, 35, 36]. In these models, one large molecule occupies a number of connected lattice sites. Some of these models are isomorphic with the spin-$\frac{1}{2}$ Ising model. So, some exact results can be obtained [24, 25, 34].

The application of lattice models is not restricted to homogeneous systems. Allowing parallel lattice layers to be differently occupied, interfaces can be investigated [22, 37-40]. Fluid interfaces [37, 38, 40-42] as well as the behaviour of fluids adjoining inert flat surfaces [22] have been modelled in this way. Adsorption of low- [1] and high- [43-45] molecular weight compounds at solid surfaces is an important phenomenon to which lattice models are successfully applied. In some of this work on interfacial systems, the first-order approximation was applied [22, 41, 42]. Kurata [41] and Parlange [42] dealt with a fluid interface of isotropic monomers. Smirnova investigated mixtures adjoining an inert boundary which was taken to be a model for fluid interfaces [22].

In the present paper we present a generalisation of the first-order quasi-chemical treatment for both homogeneous and heterogeneous systems, the latter including fluid interfaces and fluids adjoining inert surfaces. These systems may contain any combination of monomer types, with or without orientation-dependent interactions. The generalisation towards chain molecules will be presented in a subsequent chapter. In sections 2 and 3, the model is described in general terms and most symbols by which the state of the system is described are introduced. The combinatory analysis of the configurations of the system is presented in section 4. This forms the basis of the partition functions that are formulated in section 5. In that same section the self-consistent field equations for the equilibrium configuration are derived from the partition function. In section 7, expressions for thermodynamic quantities are given. In the sections 8, 9 and 10 it is explained how the equations can be applied to various situations. Finally, to illustrate the capabilities of the present theory, in section 11 numerical results for a number of specific model systems are presented and discussed. Extensive results on a lattice-gas model for water are presented in a subsequent chapter.

2 GENERAL DESCRIPTION OF THE MODELS

To be able to count the configurational micro states of the fluid, the volume V that contains the fluid is divided into a regular lattice of N identical sites. The volume of a site is denoted by v, so $V = Nv$. This lattice does not change with temperature or composition. The lattice serves as a system of coordinates, on which distances and angles are discrete rather than continuous. Each lattice site is surrounded by a fixed number, the lattice coordination number q, of nearest-neighbour sites.

For the moment we will restrict the treatment to molecules occupying one lattice site. Such model molecules are called monomers. The surface of a monomer consists of q faces that are confined to be directed towards nearest neighbour lattice sites. Hence, to a monomer of type A, a discrete number ω_A, of distinguishable orientations can be assigned. This number is

determined by the arrangement of different faces on the monomer surface. For example, an isotropic monomer, which has only one type of face, does not have distinguishable orientations (hence, $\omega_A = 1$). A monomer with one labelled face has q distinguishable orientations because the labelled face can have q directions. Faces are characterised by their mutual interactions, as will be discussed in detail in the next section. In the present chapter, the term *direction* will be restricted to a face, *orientation* to a monomer and *configuration* to a complete system.

In order to deal with systems that are spatially inhomogeneous in one direction, the lattice is divided into M parallel layers, each denoted by a ranking number z, which runs from 1 until M. Each layer can be filled differently. So inhomogeneities in the direction normal to the layers are possible. The number of sites in each layer is denoted by L. The number L is proportional to the surface area of the system $A = La$ where a is the cross-sectional surface area of one lattice site. The surface area will be taken to be infinite so that edge effects can be ignored and the system can be considered as macroscopic. By choosing appropriate boundary conditions for the outer layers, a virtually infinite fluid, or a fluid adjoining a solid surface can be modelled.

Allowing lattice sites to be vacant, *free-volume* effects, volume changes associated with changes of temperature, composition and pressure, can be accounted for. Empty lattice sites are referred to as *vacancies*. In the literature, the terms *holes* and *voids* are also used. In the statistical analysis, vacancies can be treated as just another type of monomer. In the subsequent sections the term *monomer* will be used accordingly for vacancies as well as for molecules. The choice whether one of the monomers is interpreted as vacancy can be postponed until the calculation of macroscopic thermodynamic properties such as pressure and chemical potentials. This will be discussed in section 7.

The number of monomers of type A having orientation o that are located in layer z is denoted by $n_A^o(z)$. The complete set of values of $n_A^o(z)$, for all A, o and z, is denoted by $\left\{ n_A^o(z) \right\}$. The number of monomers of type A at layer z is given by $n_A(z) = \sum_o n_A^o(z)$, and the total number of monomers of type A by $n_A = \sum_z n_A(z)$. The number of

faces of type α at layer z, pointing in direction d, is $n_\alpha^d(z)$. These numbers are directly related to the distribution of monomers over layers and orientations:

$$\sum_{A,o} n_A^o(z) q_{A\alpha}^{od} = n_\alpha^d(z) \tag{1}$$

for each α, z and d. The factor $q_{A\alpha}^{od}$ denotes the number of faces of type α with direction d, belonging to a monomer of type A with orientation o, it can have values 0 or 1.

The number of contacts between faces of type α with direction d at sites of layer z, and faces of type β, is denoted by $n_\alpha^d(z)_\beta$. If the layer z, and direction d, of a face α, are specified, then the layer and direction of the face that makes contact with α are fixed. It has the opposite of d, denoted as $-d$. It is located at layer z', by which we denote the layer at which d is directed from a site at layer z. So $n_\alpha^d(z)_\beta = n_\beta^{-d}(z')_\alpha$. The complete distribution of contacts is denoted as $\left\{ n_\alpha^d(z)_\beta \right\}$.

For the distribution of contacts and faces the relation

$$\sum_\beta n_\alpha^d(z)_\beta = n_\alpha^d(z) \tag{2}$$

should hold for each α, z and d.

According to this condition in combination with eq. (1), all layers contain the same number of monomers. If one additional independent constraint is satisfied, which equates the total number of monomers and the total number of sites,

$$\sum_A n_A = ML \tag{3}$$

where sum extends over all monomer types (vacancy included), then it follows that $\sum_A n_A(z) = L$ for all z and $\sum_{\alpha,\beta} n_\alpha^d(z)_\beta = \sum_\alpha n_\alpha^d(z) = L$ for all d and z.

Site fractions for monomers, faces and contacts are defined as $\phi_A^o(z) \equiv n_A^o(z)/L$, $\phi_A(z) \equiv n_A(z)/L$, $\phi_\alpha^d(z) \equiv n_\alpha^d(z)/L$ and $\phi_\alpha^d(z)_\beta \equiv n_\alpha^d(z)_\beta/L$, respectively. In addition, we introduce $\theta_A \equiv n_A/L$, the amount of component A expressed in equivalent lattice layers. Obviously, θ_A equals $\sum_z \phi_A(z)$.

The quantities $\phi_A^o(z)$, $\phi_A(z)$, $\phi_\alpha^d(z)$ can be considered as probability distributions for sites at layer z to be occupied in a certain way. The joint probability distribution for the occupation of pairs of nearest-neighbour sites, $\phi_\alpha^d(z)_\beta$, is related to the nearest-neighbour distribution function:

$$\psi_\alpha^d(z)_\beta \equiv \frac{\phi_\alpha^d(z)_\beta}{\phi_\beta^{-d}(z')} \tag{4}$$

which is the conditional probability of α, provided that it is located at layer z, has direction d and makes contact with a face of type β.

Moreover, the nearest-neighbour correlation function can be defined as

$$g_\alpha^d(z)_\beta \equiv \frac{\psi_\alpha^d(z)_\beta}{\phi_\alpha^d(z)} = \frac{\phi_\alpha^d(z)_\beta}{\phi_\alpha^d(z)\phi_\beta^{-d}(z')} \tag{5}$$

Note that $\phi_\alpha^d(z)_\beta = \phi_\beta^{-d}(z')_\alpha$ and $g_\alpha^d(z)_\beta = g_\beta^{-d}(z')_\alpha$ but $\psi_\alpha^d(z)_\beta \neq \psi_\beta^{-d}(z')_\alpha$. In case the occupation of nearest-neighbour sites is stochastically independent, the joint probability for the occupation of these sites (such that a certain type of contact occurs) is simply given as a product of the probabilities for the occupation of each of the sites:

$$\phi_\alpha^{*d}(z)_\beta = \phi_\alpha^d(z)\phi_\beta^{-d}(z') \tag{6}$$

This will be referred to as the random distribution of contacts. In this case, for each α, the nearest-neighbour distribution, given by $\psi_\alpha^{*d}(z)_\beta = \phi_\alpha^d(z)$, is independent of β, and the nearest-neighbour correlation function, $g_\alpha^{*d}(z)_\beta$, equals 1 for each α, β, d and z.

3 INTERACTION ENERGIES

To account for the hard core repulsion between molecules, not more than one monomer is allowed on a single lattice site. Monomers on nearest-neighbour sites have an interaction energy that might depend on their relative orientation. Dependence of the interaction energy on rotation around the connection line between monomers is not accounted for; the interactions between monomers

only depends on the faces that are in contact. It is further assumed that pair-interaction energies are additive and that only nearest-neighbour interactions contribute.

For x different faces there are $(x^2 - x)/2$ independent interaction parameters. (The matrix of energies for $\alpha\beta$ contacts is symmetrical with respect to exchange of α and β; for each type of face a potential-energy reference state has to be chosen). *Exchange energies* are defined such that these vanish for contacts between faces of the same type; *Contact energies* vanish for contacts with a vacancy. Contact energies are denoted by $u_{\alpha\beta}$, exchange energies by $v_{\alpha\beta}$. These two types of parameters are related as

$$v_{\alpha\beta} = u_{\alpha\beta} - \tfrac{1}{2}\left(u_{\alpha\alpha} + u_{\beta\beta}\right) \tag{7}$$

Consequently, $u_{\alpha\beta} = v_{\alpha\beta} - v_{\alpha0} - v_{\beta0}$, where the subscript 0 stands for vacancy.

We will use exchange energies throughout the present chapter. In this way, all types of monomers as well as the vacancies, are treated in the same way. Expressions for various quantities in terms of interaction energies are given in APPENDIX III.

The configurational part of the internal energy of a system is given in terms of exchange energies as

$$U\left(\left\{n_\alpha^d(z)_\beta\right\}\right) = \tfrac{1}{2} \sum_{\alpha,\beta,d,z} n_\alpha^d(z)_\beta v_{\alpha\beta} \tag{8}$$

where the sum extends over all contacts; the factor $\tfrac{1}{2}$ corrects for duplicate occurrence of each contact in the sum.

4 COMBINATORY FORMULA

We will derive an approximate formula for $\Omega\left(\left\{n_A^o(z)\right\},\left\{n_\alpha^d(z)_\beta\right\}\right)$, the number of configurations in which specified distributions of monomers, $\left\{n_A^o(z)\right\}$, and contacts, $\left\{n_\alpha^d(z)_\beta\right\}$ are simultaneously realised.

Generally, the distribution of contacts differs from the random distribution, $\left\{n_\alpha^{*d}(z)_\beta\right\}$; low energy contacts are preferred and the occupations of neighbouring sites are correlated, both with respect to the types of monomers involved, as well as to their orientations.

This is ignored in the zeroth-order (Bragg-Williams, random-mixing) approximation where the distribution of contacts is presumed to be random as given by eq. (6). The first-order (quasi-chemical) approximation that will be applied here is more accurate though not exact. The interdependence of all contacts on a lattice is solely accounted for by the over-all constraints (1), (2) and (3). In an exact treatment, eqs. (1) and (2) should hold not only for the system as a whole, but also locally, for each cluster of sites. Whereas the zeroth-order approximation assumes the occupation of sites to be stochastically independent, the present first-order treatment assumes pairs of sites to be independent. It is presumed that all faces of the same type at the same layer and direction have the same probability distribution of contacts, given by the nearest-neighbour distribution function. This distribution is irrespective of the type of monomer to which a face belongs, nor of other contacts in which that monomer is involved. Accordingly, the present treatment is equivalent to a first-order Markov approximation for the occupation of chains of sites. The nearest-neighbour distribution function, $\psi_\alpha^d(z)_\beta$ as defined by eq. (4), represents the transition probability for the occupation of subsequent sites. Within this approximation, the expression for the degeneracy of a system with given $\left\{n_A^o(z)\right\}$ and $\left\{n_\alpha^d(z)_\beta\right\}$ is of the form

$$\Omega\left(\left\{n_A^o(z)\right\}, \left\{n_\alpha^d(z)_\beta\right\}\right) = \frac{f\left(\left\{n_A^o(z)\right\}\right)}{\left(\displaystyle\prod_{\alpha,\beta,d,z} n_\alpha^d(z)_\beta!\right)^{1/2}} \qquad (9)$$

Here factorials $n_\alpha^d(z)_\beta!$ account for indistinguishability of contacts between identical faces. The numerator $f\left(\left\{n_A^o(z)\right\}\right)$ is some function of the distribution of monomers over layers and orientations for which an expression has to be found. Since $\Omega\left(\left\{n_A^o(z)\right\}, \left\{n_\alpha^d(z)_\beta\right\}\right)$ is a continuous function of the distribution of contacts, the following condition must be satisfied:

$$\Omega\left(\left\{n_A^o(z)\right\}, \left\{n_\alpha^{*d}(z)_\beta\right\}\right) = \Omega\left(\left\{n_A^o(z)\right\}\right) = \frac{L!^M}{\displaystyle\prod_{A,o,z} n_A^o(z)!} \qquad (10)$$

where $\Omega\!\left(\left\{n_A^o(z)\right\}\right)$ indicates the number of ways to arrange a collection of monomers with distribution $\left\{n_A^o(z)\right\}$ on the lattice. The right-hand side of eq. (10) can be recognised as a product of M multinomial coefficients, one for each layer. The factorial $L!$ equals the number of ways to arrange L distinguishable monomers on a layer of L sites. Factorials $n_A^o(z)!$ account for indistinguishability of monomers of the same type and orientation. The second equality of eq. (10) is exact. The random distribution of contacts, $\left\{n_\alpha^{*d}(z)_\beta\right\}$ maximises $\Omega\!\left(\left\{n_A^o(z)\right\},\left\{n_\alpha^d(z)_\beta\right\}\right)$ with respect to variations of $\left\{n_\alpha^d(z)_\beta\right\}$ under condition (2). It will be proven in section 5 that this is consistent with expression (6) but for the moment we will proceed without bothering about an expression for the $n_\alpha^{*d}(z)_\beta$'s. In eq. (10) we have simply substituted the maximum term $\Omega\!\left(\left\{n_A^o(z)\right\},\left\{n_\alpha^{*d}(z)_\beta\right\}\right)$ for the full sum $\sum_{\left\{n_\alpha^d(z)_\beta\right\}}\Omega\!\left(\left\{n_A^o(z)\right\},\left\{n_\alpha^d(z)_\beta\right\}\right)$. By doing so, a proportionality constant between these two quantities is disregarded. This is justified because it has no consequences for thermodynamic and configurational results.

From eqs. (9) and (10) it follows that

$$\Omega\!\left(\left\{n_A^o(z)\right\},\left\{n_\alpha^d(z)_\beta\right\}\right) = \frac{L!^M}{\prod_{A,o,z} n_A^o(z)!}\left(\prod_{\alpha,\beta,d,z}\frac{n_\alpha^{*d}(z)_\beta!}{n_\alpha^d(z)_\beta!}\right)^{1/2} \tag{11}$$

The second factor on the right-hand side accounts for correlations between the occupation of neighbouring sites. The exponent $\frac{1}{2}$ is needed since in the product over α, β, d and z, each type of contact is counted twice. With Sterling's theorem for large n: $\ln n! = n \ln n - n$, with $\frac{1}{2}\sum_{\alpha,\beta,d,z} n_\alpha^{*d}(z)_\beta \ln \phi_\alpha^{*d}(z)_\beta = \sum_{\alpha,d,z} n_\alpha^d(z)\ln\phi_\alpha^d(z)$, which follows from eq. (6), and with $\frac{1}{2}\sum_{\alpha,\beta,d,z} n_\alpha^d(z)_\beta \ln\phi_\alpha^d(z)_\beta - \sum_{\alpha,d,z} n_\alpha^d(z)\ln\phi_\alpha^d(z) = \frac{1}{2}\sum_{\alpha,\beta,d,z} n_\alpha^d(z)_\beta \ln g_\alpha^d(z)_\beta$. which follows from eq. (4), eq. (11) can be rewritten as

$$\ln\Omega\!\left(\left\{n_A^o(z)\right\},\left\{n_\alpha^d(z)_\beta\right\}\right) = -\sum_{A,o,z} n_A^o(z)\ln\phi_A^o(z) - \frac{1}{2}\sum_{\alpha,\beta,d,z} n_\alpha^d(z)_\beta \ln g_\alpha^d(z)_\beta \tag{12}$$

Here the last term accounts for correlations between the occupations of neighbouring sites. In case of random formation of contacts, it vanishes, otherwise it is negative.

5 PARTITION FUNCTIONS AND THE SELF-CONSISTENT FIELD

The configurational canonical partition function, $Q(\{n_A\}, L, T)$, can be written in terms of the degeneracy, $\Omega(\{n_A^o(z)\}, \{n_\alpha^d(z)_\beta\})$, and the potential energy $U(\{n_\alpha^d(z)_\beta\})$:

$$Q(\{n_A\}, L, T) = \sum_{\{n_A^o(z)\}, \{n_\alpha^d(z)_\beta\}} \Omega(\{n_A^o(z)\}, \{n_\alpha^d(z)_\beta\}) \exp - \frac{U(\{n_\alpha^d(z)_\beta\})}{kT}$$

$$(13)$$

where the sum extends over all distributions $\{n_A^o(z)\}$ that satisfy condition (3) and over all $\{n_\alpha^d(z)_\beta\}$ such that the saturation constraints (2) are satisfied (with the numbers of faces related to the numbers of monomers by eq. (1)); the symbol k represents Boltzmann's constant.

The characteristic thermodynamic function for the independent variables $\{n_A\}$, L and T is the Helmholtz energy: $F = -kT \ln Q(\{n_A\}, L, T)$. We define the partial Helmholtz energy of component A as

$$f_A \equiv \left(\frac{\partial F}{\partial n_A}\right)_{A, T, \{n_{B \neq A}\}} \tag{14}$$

In section (7), it will be shown how these partials are related to chemical potentials and pressure.

The partition function for an ensemble of systems where for each system $\{f_A\}$ and M are fixed instead of $\{n_A\}$ is obtained as a Laplace transform of $Q(\{n_A\}, L, T)$:

$$\Xi(\{f_A\}, M, L, T) = \sum_{\{n_A\}} Q(\{n_A\}, L, T) \exp \sum_A \frac{n_A f_A}{kT} \tag{15}$$

where the sum extends over all distributions $\{n_A\}$ that satisfy condition (3). The characteristic function for the variables $\{f_A\}$, M, L and T is given by $F - \sum_A n_A f_A = \gamma A = -kT \ln \Xi(\{f_A\}, M, L, T)$ where γ is the interfacial tension.

In the thermodynamic limit, in the present case for large L, the most probable distributions of contacts and of monomers dominate the equilibrium properties. At these distributions the summands of

the right-hand sides of eqs. (15) and (13), are maximal under the constraints (2) and (3). It is convenient to locate this maximum by means of the multiplier method of Lagrange. Hence, an unconstrained function, $\mathcal{L}\big(\{n_A^o(z)\},\{n_\alpha^d(z)_\beta\}\big)$, is formulated by adding to the constrained function for each constraint an undetermined multiplier times a term which vanishes if the constraint is satisfied:

$$\mathcal{L}\big(\{n_A^o(z)\},\{n_\alpha^d(z)_\beta\}\big) = \ln\Omega\big(\{n_A^o(z)\},\{n_\alpha^d(z)_\beta\}\big) - \frac{U\big(\{n_\alpha^d(z)_\beta\}\big)}{kT} + \sum_A \frac{n_A f_A}{kT}$$

$$+ \sum_{\alpha,d,z} \lambda_\alpha^d(z)\left(\sum_\beta n_{\alpha\beta}^d(z) - n_\alpha^d(z)\right) + \lambda\left(\sum_A n_A - LM\right) \qquad (16)$$

where $\ln\Omega\big(\{n_A^o(z)\},\{n_\alpha^d(z)_\beta\}\big)$ is given by eq. (12) (where it is convenient to write $\frac{1}{2}\sum_{\alpha,\beta,d,z} n_\alpha^d(z)_\beta \ln\phi_\alpha^d(z)_\beta - \sum_{\alpha,d,z} n_\alpha^d(z)\ln\phi_\alpha^d(z)$ for $\frac{1}{2}\sum_{\alpha,\beta,d,z} n_\alpha^d(z)_\beta \ln g_\alpha^d(z)_\beta$.), $U\big(\{n_\alpha^d(z)_\beta\}\big)$ is given by eq. (8).

The most probable distributions $\{n_A^o(z)\}$, $\{n_\alpha^d(z)_\beta\}$, as well as the Lagrangian multipliers λ and all $\lambda_\alpha^d(z)$'s are obtained from the set of equations

$$\frac{\partial\mathcal{L}}{\partial n_\alpha^d(z)_\beta} = -\ln\phi_\alpha^d(z)_\beta - 1 + \lambda_\alpha^d(z) + \lambda_\beta^{-d}(z') - \frac{v_{\alpha\beta}}{kT} = 0 \qquad (17)$$

for each α, β, d and z,

$$\frac{\partial\mathcal{L}}{\partial n_A^o(z)} = -\ln\phi_A^o(z) - 1 + q + \sum_{\alpha,d} q_{A\alpha}^{od}\big(\ln\phi_\alpha^d(z) - \lambda_\alpha^d(z)\big) + \lambda + \frac{f_A}{kT} = 0 \quad (18)$$

for each A, o and z, simultaneously with the eqs. (2) and (3). To arrive at eq. (18), we have made use of $\partial n_\alpha^d(z)/\partial n_A^o(z) = q_{A\alpha}^{od}$ which follows from eq. (1).

As can be shown easily, equation (17) is consistent with a mass-action law for contacts: $\phi_\alpha^d(z)_\beta\phi_\beta^d(z)_\alpha\big/\big(\phi_\alpha^d(z)_\alpha\phi_\beta^d(z)_\beta\big) = \exp\big(-2v_{\alpha\beta}/kT\big)$, resembling the condition for chemical equilibrium. This is why the present approximation is called *quasi-chemical.*

We will not proceed from the mass-action relations as such but introduce a factor $G_\alpha^d(z) \equiv \phi_\alpha^d(z)\exp\big(\frac{1}{2} - \lambda_\alpha^d(z)\big)$ for each α, d and z. Hence, eq. (17) can be rewritten as

$$\phi_\alpha^d(z)_\beta = \frac{\phi_\alpha^d(z)\phi_\beta^{-d}(z')}{G_\alpha^d(z)G_\beta^{-d}(z')}\exp-\frac{\upsilon_{\alpha\beta}}{kT} \tag{19}$$

The factor $G_\alpha^d(z)$ accounts for saturation of faces of type a at layer z having direction d: the constraints (2) should be satisfied. By summation over all β, in eq. (19), and combining with eq. (2) we obtain equation

$$\frac{1}{G_\alpha^d(z)}\sum_\beta\left(\frac{\phi_\beta^{-d}(z')}{G_\beta^{-d}(z')}\exp-\frac{\upsilon_{\alpha\beta}}{kT}\right) = 1 \tag{20}$$

for each α, d and z.

If all exchange energies vanish as compared to kT then eqs. (19) with (20) lead to $\phi_\alpha^d(z)_\beta = \phi_\alpha^d(z)\phi_\beta^{-d}(z')$. Hence, at the random distribution of contacts as given by eq. (6), $\Omega\!\left(\left\{n_A^o(z)\right\},\left\{n_\alpha^d(z)_\beta\right\}\right)$ is at its maximum with respect to variations of $\left\{n_\alpha^d(z)_\beta\right\}$.

By rearranging eq. (18), we will formulate a more convenient expression for the distribution of monomers: $G_A^o(z)$ is defined so that

$$\phi_A^o(z) = \Lambda_A G_A^o(z) \tag{21}$$

where $\Lambda_A = \exp(f_A/kT)$. As the factor $G_A^o(z)$ measures the probability to find a monomer of type A, having orientation o, in layer z, it is referred to as *monomer weighting factor*. The quantity $-kT\ln G_A^o(z)$ is the non-ideal part of the partial Helmholtz energy of a monomer of type A having orientation o, located at layer z. Such a quantity is often referred to as *potential of mean force*. The monomer weighting factor can be factorised as

$$G_A^o(z) = C\prod_{\alpha,d} G_\alpha^d(z)^{q_{A\alpha}^{od}} = C\prod_d G_A^{od}(z) \tag{22}$$

where we have introduced a factor $C \equiv \exp\!\left(\lambda-1+\frac{1}{2}q\right)$. As they represent the contribution of a face to the monomer weighting factor, the $G_\alpha^d(z)$ are referred to as *face weighting factors*. In the last expression of eq. (22), the factors $G_A^{od}(z)$ are face weighting factors that are labelled by the monomer type and orientation they belong to. It will be shown that $C = 1$ in homogeneous systems. The quantity

$-kT \ln C$ accounts for the excess work of creating space for a monomer in the inhomogeneous system as compared to a homogeneous bulk phase with which the inhomogeneous system is at equilibrium; $-(kT/v)\ln C$ can be interpreted as an excess tangential pressure, averaged over all layers. Mathematically, this contribution is a consequence of condition (3). If for each component A, Λ_A is known, then C is obtained from eq. (3).

The density distribution of component A is normalised by the factor Λ_A. Summation over all orientations o and layers z, of the left- and right-hand side of eq. (21) leads to an expression for Λ_A:

$$\Lambda_A = \frac{\theta_A}{\sum_{o,z} G_A^o(z)} \tag{23}$$

Although the eqs. (15) to (22) where derived for systems with fixed $\{f_A\}$ (or, equivalently, $\{\Lambda_A\}$), eq. (23) makes it possible to normalise any component A by fixing either Λ_A or θ_A. Hence the system is open or closed, respectively for that component.

If $\{\theta_A\}$ is specified, then in eq. (21) for the distribution of monomers, the factor C in each monomer weighting factor is cancelled by a factor $1/C$ in the normalisation factor as calculated by eq. (23). So, the value of C is irrelevant for the configuration of the system and hence for the configurational entropy and energy. However, the value of C has to be known to calculate partial contributions to the free energy such as the f_A's. It will be shown in section (7) that for any system C can be obtained from the condition that for homogeneous systems $C = 1$.

Until now we kept the treatment general by discriminating between all lattice directions. By imposing or assuming a higher symmetry for a system, a reduction of the number variables can be achieved. This will be considered further in APPENDIX I.

Relations like (21) and (23) resemble expressions occurring in the *potential-distribution-* or *test-particle* formulation of the statistical theory of fluids [5, 38, 39, 46]. In contrast with Widom's treatment of the lattice gas of isotropic molecules and its liquid-vapour interface, in the present approach, vacancies are handled as species. The weighting factor for a monomer located at layer z, $\left\langle \exp(-\Psi/kT) \right\rangle_z$ in

the notation of Widom [38], is in our notation given by $\Lambda_0 G_A(z) = \phi_0(z) G_A(z)/G_0(z)$, where subscript A indicates the molecules and 0 vacancies. The normalisation factor in Widom's formulation is the activity $\exp(\mu_A/kT)$, where μ_A is the chemical potential. The relation between f_A as defined by eq. (14) and μ_A is discussed in section (7). (Apart from this difference, Widom used the zeroth- instead of the first-order approximation, as we do at present, and he did not account for orientation effects.)

6 BOUNDARY CONDITIONS

Numerical calculations are necessarily restricted to a system consisting of a finite number of layers. It is necessary to specify the contents of the layers adjacent to such a system.

If the model fluid continues beyond boundary layer z'' (1 or M), a reflecting boundary can be placed in the middle of that layer: $G_\alpha^{-d}(z''-z) = G_\alpha^{d}(z''+z)$. Alternatively, letting $G_\alpha^{-d}(z'' \pm 1 - z) = G_\alpha^{d}(z''+z)$ implies placement of a reflecting boundary between layer z'' and $z'' \pm 1$. If reflecting boundaries are half or one lattice layer apart, the system is necessarily homogeneous.

It is also possible to model a fluid adjoining an inert solid surface by using the appropriate boundary condition. A solid surface can be modelled as a layer with fixed composition in the sense that there is a fixed distribution of faces exposed to the outer layer of the fluid. Components of the fluid cannot enter the solid: inside the solid their weighting factors are zero. Only the preferential adsorption energies, the differences between the values of $v_{\alpha\beta}$ (where β refers to faces of the solid surface), influence the configuration. Within a lattice model, the surface tension of an inert surface adjoined by a fluid consisting of one type of isotropic monomers has no entropic contributions and is simply given by $\gamma a = \sum_{d,\beta} \phi_\beta^{d}(s.s.) v_{\alpha\beta}$, where $\phi_\beta^{d}(s.s.)$ denotes the fraction of faces belonging the solid surface with direction d, that are of type β, and α is the face type belonging to the monomeric component. Often, we are not interested in the absolute values of the surface tension and will make an arbitrary choice for a reference level. For instance the $v_{0\beta}$'s, where the subscript 0 indicates vacancy and β the face(s) of the surface, can be chosen to be zero. This

implies that the surface in vacuum is the reference state for the surface tension of the inert surface. Such a choice is immaterial for all other properties of the system.

By way of illustration, for a mixture of isotropic components 1 and 0, the Henry coefficient of adsorption of component 1 at a surface with only faces of type 2, is given by $K_1^{ads} = \lim_{\phi_1(\infty) \to 0} \phi_1(1)/\phi_1(\infty) = \exp\left((v_{02} - v_{12})/kT\right)$. Here $v_{12} - v_{02}$ is the preferential adsorption energy of component 1 with respect to component 0. If the mixture is athermal the adsorption isotherm is given by $\phi_1(1)/\phi_0(1) = K_1^{ads} \phi_1(\infty)/\phi_0(\infty)$. This can be identified as Langmuir's adsorption equation. It is obtained as a limiting result of the present treatment. This shows that a range of actual interfacial phenomena can be retrieved.

7 THERMODYNAMIC FUNCTIONS

The statistical analysis presented above applies both to lattice-gas models, containing vacancies, and to models where no vacancies are present. The intensive quantity f_A is defined in such a way (see eq. (14)), that it applies to vacancy as well as to molecular species. The fundamental thermodynamic equation for the independent variables T, A and $\{n_A\}$ is given by:

$$dF = -SdT + \gamma dA + \sum_A f_A dn_A \tag{24}$$

By integration, the characteristic thermodynamic function (thermodynamic potential) for these variables, the Helmholtz energy, is obtained:

$$F = \gamma A + \sum_A f_A n_A \tag{25}$$

The partial f_A of each molecular component A can be related to the chemical potential but it is not identical to it because in the list of variables that are kept constant upon partial differentiation (eq. (14)), the number of vacancies is included. In accordance with conventions the chemical potential is defined as

$$\mu_A \equiv \left(\frac{\partial G}{\partial n_A}\right)_{p,A,T,\{n_{B \neq A,0}\}} = \left(\frac{\partial F}{\partial n_A}\right)_{V,A,T,\{n_{B \neq A,0}\}} = f_A + pv \qquad (26)$$

where G is the Gibbs energy. The condition of constant V is equivalent with constant N; similarly the condition that A is constant is equivalent with constant L. According to the second equality, μ_A is the change of the Helmholtz energy due to the exchange of a vacancy by a molecule.

If no vacancies are accounted for in a specific model, this implies that the partial molecular volumes are constant: $(\partial V/\partial n_A)_{p,T,\{n_{B \neq A}\}} = v$. In a lattice gas, as in reality, the partial molecular volume, $(\partial V/\partial n_A)_{p,T,\{n_{B \neq A,0}\}}$, of each molecular component A is not constant since $(\partial n_0/\partial n_A)_{p,T,\{n_{B \neq A,0}\}}$, the amount of vacancy that comes with a monomer of type A varies. In this case, the pressure is related to f_0 where the subscript 0 indicates vacancy:

$$p \equiv -\left(\frac{\partial F}{\partial V}\right)_{A,T,\{n_{A \neq 0}\}} = -\frac{1}{v}\left(\frac{\partial F}{\partial n_0}\right)_{A,T,\{n_{A \neq 0}\}} = -\frac{f_0}{v} \qquad (27)$$

The fluid can be regarded as a mixture of vacancies and molecular components, the pressure as the osmotic pressure difference between the fluid and vacuum. From the relations between the f_A's and the chemical potentials and the pressure, and from the conditions $V = v\sum_A n_A$ and $dV = v\sum_A dn_A$, it follows that in the equations (24) and (25) $\sum_A f_A dn_A$ and $\sum_A f_A n_A$ can be replaced by $-pdV + \sum_{A \neq 0} \mu_A dn_A$ and $\sum_A f_A n_A$ by $-pV + \sum_{A \neq 0} \mu_A n_A$, respectively. Hence, it is reaffirmed that the present relations (24) and (25) are consistent with the familiar expressions for the Helmholz energy.

The configurational energy of a system in equilibrium is obtained by substituting the most probable distribution of contacts, as given by eq. (19), into eq. (8). The configurational entropy can be obtained using Boltzmann's law $S = k \ln \Omega\left(\left\{n_A^0(z)\right\}, \left\{n_\alpha^d(z)_\beta\right\}\right)$. In the combinatory formula the most probable distributions $\left\{n_A^0(z)\right\}$, as given by eq. (21) with (22), and $\left\{n_\alpha^d(z)_\beta\right\}$, as given by (19), should be substituted. This leads to

$$\frac{S}{Lk} = -\sum_A \frac{\theta_A f_A}{kT} - M \ln C + \frac{U}{kT} \qquad (28)$$

Consequently, the Helmholtz energy, $F = U - TS$, can be expressed as

$$\frac{F}{LkT} = \sum_A \frac{\theta_A f_A}{kT} + M \ln C \qquad (29)$$

The interfacial tension is given by $\gamma A = F - \sum_A n_A f_A$. Accordingly, we obtain

$$\frac{\gamma a}{kT} = M \ln C \qquad (30)$$

This expression for the interfacial tension reconfirms the remarks made in section 5 on the interpretation of the quantity C as it appeared in eq. (22).

In relation to this, it can be noted that the expression for the Lagrangian function $\mathcal{L}\left(\left\{n_A^o(z)\right\}, \left\{n_{ab}^d(z)\right\}\right)$ as given by eq. (16) is not unique. The constraints can be used to eliminate variables or to add terms. For instance, a term of the form $g(n(z), z) = \sum_z f(n(z), z)(n(z) - L)$, where $n(z) = \sum_{A,o} n_A^o(z)$, could be added, such that for each A and o, and z, $\partial g / \partial n_A^o(z) = g'(z)$ is finite. Since $n(z) - L$ vanishes for each z if the constraints (2) and (3) are satisfied, such alteration of the Lagrangian is immaterial for the calculated distributions and thermodynamic quantities. However, the set of simultaneous equations that define C and the $G_\alpha^d(z)$'s and, hence, the resulting values for these quantities are altered. Instead of a single factor C in eq. (22), the product $C \exp g'(z)$ appears. Consequently, to the right-hand side of eqs. (28), (29) and (30), a term $\sum_z g'(z)$ is added. The functional dependence of $f(n(z), z)$ on the distribution of monomers is immaterial for the calculated configurations and thermodynamic quantities. The present formulation was chosen for its relative simplicity. The arbitrariness in the choice of $f(n(z), z)$ is the counterpart of the fact that there is no unique way to define microscopic pressure tensor and hence the profile of the tangential pressure (see for instance [39]). A measurable property as the interfacial tension, which can be calculated from the integral of the tangential-pressure profile, is invariant with respect to the chosen profile [39].

8 HOMOGENEOUS SYSTEMS

For homogeneous systems the parameter z can be omitted. Since there is no interfacial tension it follows from eq. (30) that $C = 1$. Equation (20) has to be satisfied for each type of face and each direction. These simultaneous equation can be solved quite easily by a Newton iteration. According to the Phase Rule and the condition $\sum_A \phi_A = 1$, the variables T, $\{f_A\}$ and $\{\phi_A\}$ are not all independent. The site fraction of one of the components is fixed by that of all others. If there are x components (vacancy included), then out of all ϕ_A's but one, all f_A's and T, x variables can be fixed. The others follow. The distribution of monomeric orientations and of contacts can be calculated from the equations (19) and (21).

9 COEXISTING PHASES

The appropriate conditions for a number of homogeneous phases 1, 2, . . . to coexist are that the temperature is the same in each phase and that for each component A

$$f_A^{\,1} = f_A^{\,2} \dots \quad \text{or} \quad \Lambda_A^{\,1} = \Lambda_A^{\,2} \dots \tag{31}$$

This is equivalent to the condition that the temperature, the chemical potential of each molecular component as well as the pressure are the same in each phase. The Λ_A's are given by eq. (23). For a given temperature eq. (31) and for each separate phase, eq. (20) has to be satisfied for each α and d. In APPENDIX II, a numerical method for this problem is discussed in detail.

10 HETEROGENEOUS SYSTEMS

In the present model, a heterogeneous system consists of M plan-parallel layers. The contents of each layer may be different.

At a fixed temperature, for all components (vacancy included) but one, a normalisation condition must be specified: either the total amount per cross-sectional lattice site surface area θ_A is fixed if the system is closed with respect to component A or, if the system is open with respect to this component, Λ_A may be fixed. Alternatively, the volume fraction in a homogeneous bulk system that is in

equilibrium with the heterogeneous system can be fixed. For each component A, Λ_A has the same value for different systems that are at equilibrium.

As stated before, for homogeneous systems C should equal 1. The value of C for an inhomogeneous system that is at equilibrium with a homogeneous system can be inferred since for each component A, the value of Λ_A is identical for systems that are at equilibrium. A homogeneous bulk system serves as a reference for the values of C for any inhomogeneous system with which it is at equilibrium.

If the heterogeneous system contains a fluid interface, then the two coexisting homogeneous phases can be found. Generally, if in one of these homogeneous phases C is set 1, in the other it will often have some value unequal to 1, if it is presumed that in each phase the value for Λ_A is equal for each component A. Equivalently, if it is presumed that in each of the two bulk phases $C = 1$, the values for Λ_A are often not equal in each phase. This apparently anomalous phenomenon is related to layering transitions, first-order phase transitions that occur upon gradually shifting the profile with respect to the lattice layers by varying the over-all composition of the inhomogeneous system. The composition of the bulk phases and values of partial free energies vary periodically. The periodicity corresponds to a shift of the profile of precisely one lattice layer. This phenomenon has also been called 'lattice artefact' [47]. Unambiguous results for fluid interfaces are obtained by determining the overall composition of the inhomogeneous layered system for which there the C values of the two homogeneous systems equal 1. Then these will be proper coexisting phases.

For each system, all face weighting factors $G_\alpha^d(z)$ and volume fractions $\phi_A^0(z)$ are determined completely by equations (20), (21) and condition (3). These equations describe the self-consistent molecular field (in terms of face weighting factors) and a distribution of monomers over orientations and positions plus a distribution of contacts.

Details on the numerical methods are given in APPENDIX II.

Table 1

exchange energies

v	1'	1"	2'	2"
1'	0	0	v	$-0.333v$
1"	0	0	$-0.333v$	$-0.333v$
2'	v	$-0.333v$	0	0
2"	$-0.333v$	$-0.333v$	0	0

11 APPLICATION TO SPECIFIC SYSTEMS

In this section the capabilities of the present theory will be illustrated. To that end, we shall compare the properties of three model systems, called A, B and C. Further elaborations, especially to a lattice-gas model for water will be worked out in a subsequent chapter [48].

As mentioned in section 1, Barker and Fock [14] studied the phase behaviour of a binary mixture. Each monomer has one 'special' face that deviates from its other faces. In our nomenclature, these monomers have q orientations since the 'special' face of a monomer can have q directions. The two monomer types will be denoted as 1 and 2, the 'special' faces of these monomers as 1" and 2" respectively, the other faces as 1' and 2'. This is illustrated for a two-dimensional case in fig. 1. The 'special' face has a strong affinity for all faces of monomers of the other type. If unlike monomers make contact without the involvement of a special face the exchange energy is positive. This energy will be denoted as v. All interactions in the model of this section are quantified in terms of v in table 1. We refer to this model as A.

In the second system, B, monomer 2 has the same properties as in model A but the other monomer is isotropic, all its faces are identical. The interactions are the same as in A, apart from the fact that the 'special' faces 1" are not present. Column and row 1" can be disregarded in table 1. Obviously this model is not symmetric with respect to exchange of component 1 and 2.

Table 2

contact energies

u	1'	2'	2"
1'	0	0	0
2'	0	$0.6667v$	$-0.6667v$
2"	0	$-0.6667v$	$-2v$

To accentuate the effects of the orientation-dependence of the interactions, results for a binary mixture of isotropic monomers (model C) are also shown. In this case only the 1'-2' interactions are relevant. For this case, an analytical expression has been derived in first-order approximation for the upper critical solution temperature [1, 2].

$$\frac{v}{kT} = \ln\frac{q}{q-2} \qquad (32)$$

Of these models, A and C are symmetric with respect to exchange of the monomer types. B and C can be interpreted as lattice gases by considering component 1 as vacancies. For lattice-gas models, it is probably more according to intuition to quantify the interactions in terms of contact energies instead of exchange energies (see eq. (7) and APPENDIX III). These values, corresponding to these of table 1 are given in table 2.
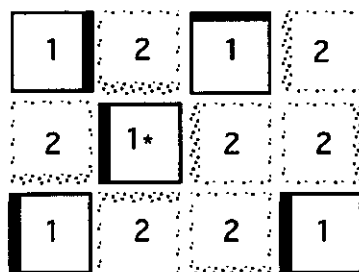

Figure 1.   *Two dimensional illustration of model A. The 'special' faces are indicated by bold lines. In this cut-out of the lattice, a monomer of type 1 (indicated with a *) is solubilised by three monomers of type 2 that are oriented with their 'special' face towards it.*
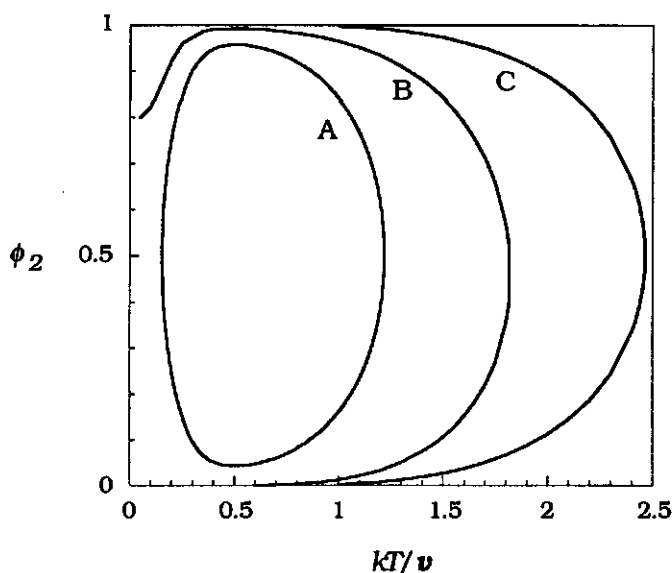
Figure 2. *Phase diagrams of model A, B and C.*

In the calculations a simple cubic lattice will be used; $q = 6$; the number of nearest neighbours is 4 within the same layer and 1 in each adjacent layer.

Model A has a closed-loop coexistence curve with an upper critical solution temperature (UCST) and also a lower critical solution temperature (LCST) as has been shown before by Barker and Fock. The temperature scale of Barker and Fock seems to be wrong; their UCST is even higher than given by eq. (32), which applies to systems where the orientation-dependent attraction between unlike monomers is absent.

Upon lowering the temperature towards the LCST, the concentration of component 1 in the phase that is rich in 2 as well as the concentration of component 2 in the phase that is rich in 1 increases until the two components become completely miscible at the LCST. Below a certain temperature, the molecules of one type are, upon decreasing temperature, increasingly able to solubilise those of the other type. At low temperatures, monomers of type 1 get predominantly coordinated by 2"-faces of monomers of type 2. In the same way, monomers of type 2 get predominantly coordinated by 1"-
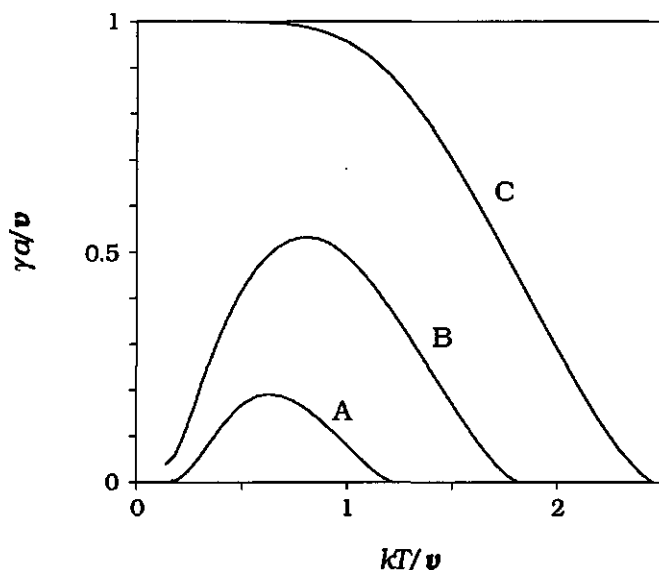
Figure 3. *Interfacial tension between the coexisting phases as a function of temperature for the models* A, B *and* C.

faces. This explains the increasing mutual solubility at decreasing temperatures.

In model B, the concentration of component 2 in the coexisting phase that is rich in 1 is higher than in A. This concentration increases with temperature over the whole temperature range. The monomers of type 1 are not able to solubilise those of type 2. Hence this system does not have a LCST. The concentration of component 1 in the phase that is rich in 2 does show an increase upon decreasing temperature due to solubilisation of monomers 1 by 2.

System B can be interpreted as a lattice gas, by identifying component 1 as vacancy. Then the phase with a high density ϕ_2 can be identified as the liquid and the coexisting phase with a low density as the vapour. The density of the coexisting liquid has a maximum as a function of temperature. Experimentally, such behaviour is observed with water. Extensive results on a more accurate model for water will be presented in the following chapter [48].
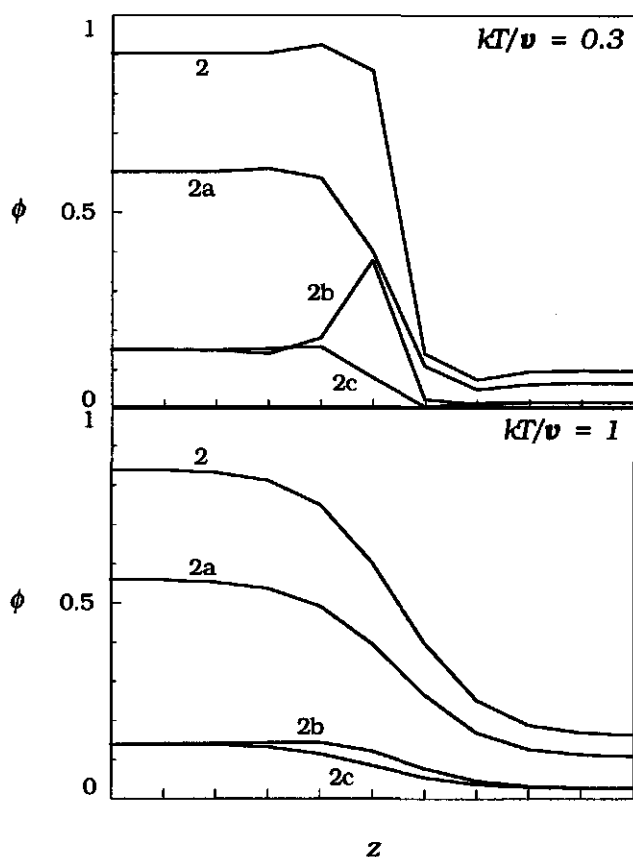
Figure 4. *Density profiles of the interfacial region for model A at two temperatures. The profiles of the various orientations of 2 are indicated by 2a (the four orientations with face 2" directed laterally), 2b (orientation with 2" pointing towards the phase rich in 1, at the right) and 2c (orientation with 2" pointing towards the phase rich in 2, at the left). To be sure that boundary effects are absent, the calculation were made for much larger numbers of layers than are shown in the plot. Calculated points are connected by straight lines.*

The interfacial tension between the coexisting phases of the three model fluids are plotted in fig. 3 for the complete temperature range. For model A, the interfacial tension vanishes both at the LCST and at the UCST, as expected. Starting from the LCST, the interfacial tension increases with temperature, until it reaches a maximum. In this temperature range the interfacial entropy, $s^s \equiv (\partial S/\partial A)_{T,V,n} =$

$-(\partial\gamma/\partial T)_{A,V,n}$ is negative; this indicates that the interface is more ordered than the bulk of the coexisting fluids. With model B such interfacial ordering also occurs. For model C, at 0 K, a phase where $\phi_1 = 1$ and $\phi_2 = 0$ coexists with a phase where $\phi_1 = 0$ and $\phi_2 = 1$. The interface between these phases is perfectly sharp and the interfacial entropy vanishes as well as the entropy in the bulk of the coexisting fluids. At this point, the interfacial tension is purely energetic and is given by $\gamma a = v$. Upon increasing temperature, the interfacial tension decreases until it vanishes at the UCST.

For model A, the density profiles in the interfacial region of component 2 and the contributions of its various orientations are plotted in fig. 4 for two temperatures. The density profile of component 1 is neither plotted nor discussed separately since this is an exact mirror image of that of component 2.

In the bulk phases, each of the 6 orientations contributes equally to the density of a component. However, in the interfacial region, this is not the case. Curve 2a gives the contribution of the four orientations for which the deviating face, 2", is directed laterally. In the interfacial region, orientation 2b has a higher density than in the bulk. With this orientation, face 2" is directed towards the phase that is rich in monomers of type 1. As expected, this ordering in the interfacial region is more pronounced at low temperatures. At the layers in the negative z-direction, adjacent to the layer where 2b has a maximum, 2c has a maximum. Adjacent to this layer, 2a has a maximum and 2b a minimum. The various densities exhibit oscillations with an amplitude that decays with increasing distance from the interface.
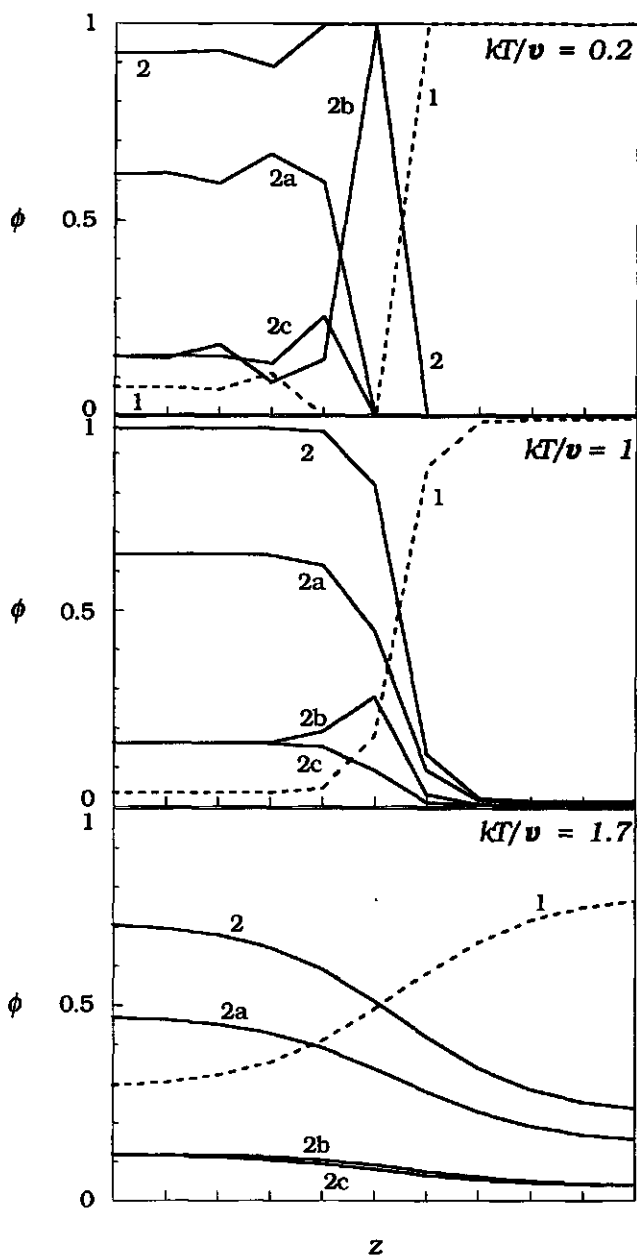
Figure 5. *Density profiles of the interfacial region for model* B *at three temperatures. Components 1 and 2. are indicated as well as the profiles of the various orientations: 2a (four orientations with face 2" directed laterally), 2b (orientation with 2" pointing to the right) and 2c (orientation with 2" pointing to the left).*
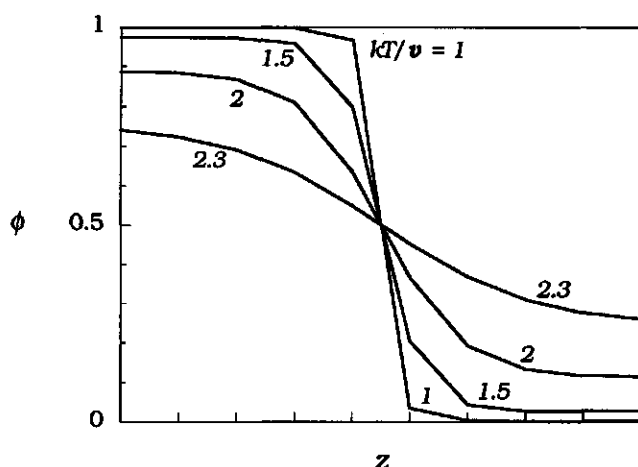
Figure 6.   *Density profiles of component 2 for model C at different temperatures. Values of kT/v are indicated along the curves*

At intermediate temperatures, the profile of component 2 in model B is similar to that in model A (see fig. 5). However, that of component 1 is very different. Since these are isotropic monomers, they cannot have any orientational ordering. Hence, he interface is strongly asymmetric. At low temperatures, where in model A the components become miscible again, the interface of model B gets stratified (see fig. 5, the plot for $kT/v = 0.2$). Then the concentration of 1 and of 2a have a series of maxima on the 2-side of the interface. These layers are adjoined by layers where ϕ_{2b} and ϕ_{2c} have maxima at the lower-, and upper- z-direction respectively. This layered structure allows optimal solubilisation of monomers 1 by 2.

The oscillations occurring in the density profiles of models A and B are of a somewhat different nature than the density oscillations that are known to occur with spherical molecules near a flat surface. In the latter case, the oscillations are due to the repulsive short range interactions between the molecules and the surface and between the molecules themselves. These oscillations have a periodicity of about the molecular diameter. The oscillations in the present model are related to the orientation-dependent attractive interactions between the monomers of different species. Monomers of one species tend to

be coordinated by monomers of the other species. Such associates
have a diameter of 3 lattice layers and hence the oscillations have
such a periodicity.

To make a comparison, also some density profiles for model C are
shown, in fig. 6. Here the composition varies monotonously between
the two coexisting phases. The density profile of component 1 is the
mirror image of that of 2.

12 CONCLUDING REMARKS

In this chapter we have derived a theory for molecules with
orientation-dependent interactions. By accounting for local
correlations due to the intermolecular interactions, the temperature
dependence of the behaviour of such systems is reproduced. By
accounting for spatial variations of the density, interfacial systems
can be handled.

The capabilities of the method where illustrated by some specific
systems. In one of these, the orientation-dependent intermolecular
interactions lead to a closed loop coexistence curve. A different
mechanism that gives rise to lower critical solution points can be
modelled as well: including a third component (for instance
vacancies), that has a different affinity for each of the two original
components might induce an additional lower critical solution
temperature and high temperature phase separation [6, 9]. This
phenomenon is very important in polymer solutions at high
temperatures (see for instance refs. [31, 33, 49, 50]). This can be
combined with the orientation effects as in model A or B of the
previous section. In this way the complete phase behaviour and its
relation to molecular parameters of various binary mixtures could be
reproduced at least semiquantitatively. Moreover, the properties of
the interfaces between the coexisting phases can be examined.

One of the most interesting compounds in which orientation-
dependent interactions are important is water. In the next chapter
we will apply the formalism of the present chapter to a lattice-gas
model for water. In this way it appears possible to reproduce various
anomalous properties of water both for homogeneous- and for
interfacial aqueous systems.

The treatment is formulated in a general way in the present chapter such that it applies to any combination of monomers. Often it is important to account for different sizes of molecules and for aspects of the molecular structure such as branching. Hence in a future chapter the formalism will be generalised further in order to account for chain molecules that occupy a number of connected lattice sites.

APPENDIX I *REDUCTION OF THE NUMBER OF VARIABLES*

In the previous sections it was assumed that densities have a gradient in one direction only (the z-direction, normal to the layers). The distributions of faces and contacts over the directions of the lattice were allowed to vary. If a higher symmetry is imposed on the system by letting the distributions be uniform within subsets of directions, the number of variables can be reduced considerably. For instance, directions that have the same angle with respect to the z-axis can be taken together in a subset. Let us denote such a subset by D. Then $G_\alpha^d(z) = G_\alpha^D(z)$ for every $d \in D$. Weighting factors for different monomeric orientations are equal if the faces have directions that belong to the same D. Such orientations are said to belong to the same subset of orientations, O. We define $G_A^O(z) \equiv \sum_{o \in O} G_A^o(z)$, where all terms of the sum are equal. Then formula (22) can be rewritten as

$$G_A^O(z) = \omega_A^O C \prod_{\alpha, D} G_\alpha^D(z)^{q_{A\alpha}^{OD}} \tag{I.1}$$

where ω_A^O is the number of orientations belonging to the set O. In eq. (I.1), $q_{A\alpha}^{OD} = \sum_{d \in D} q_{A\alpha}^{od}$ is the number of faces of type α in a direction belonging to D of a monomer of type A in an orientation belonging to the set O. Note that $\phi_\alpha^d(z) = n_\alpha^d(z)/L$ equals $\phi_\alpha^D(z) = n_\alpha^D(z)/q^D L$ for every $d \in D$.

Volume fractions of monomers are given by

$$\phi_A^O(z) = \Lambda_A G_A^O(z). \tag{I.2}$$

The original equations (21) and (22) can be considered as special cases of eqs. (I.1) and (I.2).

For homogeneous systems the parameter z can be omitted. When in addition the system is isotropic, we do not have to distinguish different subsets of directions and the superscripts D and O can be also omitted. If such a homogeneous, isotropic system is athermal (all $v_{\alpha\beta}$ equal 0) then each G_A^o equals 1. Consequently, $G_A = \sum_o G_A^o = \omega_A$, each ϕ_A^o equals Λ_A, and $\phi_A = \sum_o \phi_A^o$ equals $\omega_A \Lambda_A$. If the system consists of monomers of type A only; $\phi_A = 1$, then Λ_A equals $1/\omega_A$.

APPENDIX II *NUMERICAL METHODS*

In the previous sections it has been shown that distributions of contacts and monomers are determined by the face weighting factors $G_\alpha^d(z)$, and vice versa. The set of equations can be solved using a modified Newton iteration method such as implemented in the FORTRAN program by Powell [51] or the more powerful SIMULA program by Scheutjens [52]. We define a number of variables x_i, from which all properties of the system can be derived, and need an equal number of equations $f_i(\{x_i\}) = 0$, that are equivalent to eqs. (20) to (21). Obviously, various sets of variables and equations can be defined that are equivalent to the self-consistent field equations. In order to obtain converging iterations, the functions f_i should be formulated such that they are as linear as possible. Moreover, the Jacobian matrix of partial derivatives, $\partial f_i/\partial x_j$, should be as symmetric as possible, the largest values should be concentrated around its main diagonal and the sensitivity to each parameter should be equal (all $\partial f_i/\partial x_j$ should be about the same if $|i - j|$ is the same).

In the subsequent sections the following averages will be used:

$$\overline{x_\alpha}^\alpha = \frac{\sum_\alpha x^\alpha}{\sum_\alpha 1} \qquad \overline{x^d}^d = \frac{\sum_d x^d}{q} = \frac{\sum_D q^D x^D}{q} \qquad \overline{x(z)}^z = \frac{\sum_z x(z)}{M}$$

In the average over all face types, the face types of a solid surface are not included.

Scheme I, general method.

The variables are defined as:

$$x_\alpha^D(z) \equiv \ln G_\alpha^D(z) - \overline{\ln G_\alpha^D(z)}^\alpha + \overline{\ln G_\alpha^D(z)}^{\alpha,d} + \frac{\ln C}{q} \qquad (\text{II}.1)$$

These variables may be interpreted as the logarithms of alternatively defined face weighting factors. From this expression follows that

$$\overline{x_\alpha^D(z)}^\alpha = \overline{x_\alpha^D(z)}^{\alpha,d} = \overline{\ln G_\alpha^D(z)}^{\alpha,d} + \frac{\ln C}{q} \qquad (\text{II}.2)$$

and

$$x_\alpha'^D(z) \equiv x_\alpha^D(z) - \overline{x_\alpha^D(z)}^\alpha = \ln G_\alpha^D(z) - \overline{\ln G_\alpha^D(z)}^\alpha \qquad (\text{II}.3)$$

According to eq. (I.1) it is possible to compute the monomeric weighting factors from the variables:

$$G_A^O(z) = \omega_A^O \exp \sum_{\alpha,D} q_{A\alpha}^{OD} x_\alpha^D(z) \qquad (\text{II}.4)$$

Applying eqs. (II.4) and (I.2) all $\phi_A^O(z)$ can be computed if the normalisation conditions for the components are specified. A component A can be normalised by giving Λ_A. Using eq. (23) it can also be computed from a given total amount in equivalent lattice layers, θ_A in one of the systems that are in equilibrium. Since eq. (1) can be rewritten as $\sum_{A,O} \phi_A^O(z) q_{A\alpha}^{OD}/q^D = \phi_\alpha^D(z)$ also all $\phi_\alpha^D(z)$ can be calculated.

Appropriate functions are

$$f_\alpha^D(z) \equiv 1 - \frac{1}{\displaystyle\sum_{A,O} \phi_A^O(z)} + \overline{x_\alpha^D(z)}^\alpha - \overline{x_\alpha^D(z)}^{\alpha,d} - g_\alpha^D(z) + \tfrac{1}{2}\left(\overline{g_\alpha^D(z)}^\alpha + \overline{g_\alpha^{-D}(z')}^\alpha \right)$$

$$(\text{II}.5)$$

where

$$g_\alpha^D(z) \equiv -x_\alpha'^D(z) + \ln \sum_\beta \frac{\phi_\beta^{-D}(z')}{\exp\left(x_\beta'^{-D}(z') + \dfrac{v_{\alpha\beta}}{kT} \right)} \qquad (\text{II}.6)$$

If the self-consistent field equations (20) and (21) with (22) are satisfied, all $f_\alpha^D(z)$ vanish: It is obvious that the first two terms of eq. (II.5) have to cancel. The second two terms cancel according to eq.

(II.2). According to eqs. (20) and (II.3) $g_\alpha^D(z)$ equals $\overline{\ln G_\alpha^D(z)}^\alpha + \overline{\ln G_\alpha^{-D}(z')}^\alpha$, for each α, D and z, and hence cancels the last term.

Taking the average over all layers of the left and right hand side of eq. (II.2) and substituting $\overline{\frac{1}{2} g_\alpha^D(z)}^{\alpha,d,z}$ for $\overline{\ln G_\alpha^D(z)}^{\alpha,d,z}$ an expression for C can be obtained:

$$\ln C = \overline{x_\alpha^D(z)}^{\alpha,d,z} - \frac{1}{2}\overline{g_\alpha^D(z)}^{\alpha,d,z} \qquad (II.7)$$

The distribution of contacts can be obtained using eq. (19) with

$$G_\alpha^D(z)G_\alpha^{-D}(z') = \exp\left(x_\alpha'^D(z) + x_\alpha'^{-D}(z') + \overline{g_\alpha^D(z)}^\alpha \right) \qquad (II.8)$$

If there is an inert surface adjacent to the fluid, additional variables have to be introduced. The distribution of faces belonging to an inert surface is fixed. For these faces we define the variables:

$$x_\alpha^D(z) \equiv \ln G_\alpha^D(z) \qquad (II.9)$$

and functions:

$$f_\alpha^D(z) \equiv -g_\alpha^D(z) + \frac{1}{2}\left(\overline{g_\alpha^D(z)}^\alpha + \overline{g_\alpha^{-D}(z')}^\alpha \right) \qquad (II.10)$$

In eqs. (II.9) and (II.10) the subscript α refers to faces belonging to the solid surface, $g_\alpha^D(z)$ is still given by eq. (II.6).

The interfacial tension can be calculated from the variables according to

$$\frac{\gamma a}{kT} = \sum_{z,d,\alpha} \phi_\alpha^d(z)x_\alpha^d(z) - \frac{1}{2}\sum_{z,d,\alpha,\beta} \phi_{\alpha\beta}^d(z)\left(x_\alpha'^d(z) + x_\beta'^d(z) + \overline{g_\alpha^d(z)}^\alpha \right)$$

$$(II.11)$$

Usually, calculations are made on two systems that are in equilibrium, an inhomogeneous interfacial system and the corresponding homogeneous bulk system. The latter is adequately represented by half a layer between reflecting boundaries.

According to the Phase Rule and the condition $\sum_A \phi_A = 1$, normalisation conditions for components are not all independent. As

a consequence, using this iteration scheme for a system consisting of more than one layer, the equations (II.5) are not independent if all components are normalised by fixing θ_A. Therefore, of one component the site fraction in the bulk $\phi_B(\infty)$ is computed as $1 - \sum_{A \neq B} \phi_A(\infty)$. If, for all components but one, bulk concentrations or Λ_A are given, all unknown Λ_A can be computed first by a separate iteration for the bulk. However, if for one or more components θ_A in the multilayer system is given, then the bulk iteration has to be carried out each time the functions (II.5) are to be computed during the iteration for the multilayer system. Since this is rather time consuming, we often apply Scheme II.

Scheme II, System with fixed overall composition.

If for one of a set of systems (usually an interfacial- and a bulk system) that are at equilibrium with each other the overall composition is fixed, then it is a good strategy to compute the internal equilibrium of that system first, using the following iteration method. Each component is normalised by a given amount, θ_A. In order to avoid the functions to be dependent, they have to be supplemented by an additional term (the right hand side of eq. (II.7)). This implies that $\ln C$ will be iterated to zero for this system. Using scheme *I*, the resulting values of Λ_A can be used for normalisation in a computation for any system that is at equilibrium with the first system.

One of the systems has to be homogeneous in order to have a reference level for C. A homogeneous system is adequately represented by half a lattice layer between reflecting boundaries. From the condition that C equals 1 or homogeneous systems, a factor is obtained by which for each of the systems that are at equilibrium the values of C, and hence all $G_A^O(z)$'s, Λ_A's etc. can be renormalised afterwards.

Scheme III, coexisting homogeneous phases.

To compute the properties of two coexisting homogeneous phases the following method can be used:

The iterated variables, x_i, are related to face weighting factors as:

$$x_\alpha^D(p) \equiv \ln G_\alpha^D(p) - \overline{\ln G_\alpha^D(p) - \ln\left(\frac{m}{1-m}\right)}^{\alpha,D,p} \tag{II.12}$$

where p denotes the phase and m is the fraction of the total volume that is occupied by phase 1. According to (II.12), m can be computed from the variables: $\sum_{\alpha,D,p} x_\alpha^D(p) = \ln(m/(1-m))$. Let

$$G_\alpha'^D(p) = \exp\left(x_\alpha^D(p) - \overline{x_\alpha^D(p)}^{\alpha,D,p}\right) = aG_\alpha^D(p) \tag{II.13}$$

The volume fractions in each phase are computed using:

$$\phi_A^O(p) = \Lambda_A' G_A'^O(p) \tag{II.14}$$

with

$$G_A'^O = \omega_A^O \prod_{\alpha,D} G_\alpha'^D(p)^{q_{A\alpha}^{OD}} = a^q G_A^O \tag{II.15}$$

and $\Lambda_A' = \Lambda_A/a^q$ is the same for each phase and can be obtained from:

$$\Lambda_A' = \frac{m\phi_A(1) + (1-m)\phi_A(2)}{mG_A'(1) + (1-m)G_A'(2)} \tag{II.16}$$

The average composition of the two phases has to be given and it has to be within the miscibility gap in order to obtain separation into coexisting phases. Optimum performance of the iteration is obtained when the resulting m has a value close to $\frac{1}{2}$.

Appropriate functions are

$$f_\alpha^D(p) \equiv 1 - \frac{1}{\sum\limits_{A,O} \phi_A^O(p)} + g_\alpha^D(p) - \overline{g_\alpha^D(p)}^{\alpha,D,p} \tag{II.17}$$

where

$$g_\alpha^D(p) = \ln G_\alpha'^D(p) - \ln \sum_\beta \frac{\phi_\beta^{-D}(p)}{\exp\left(\ln G_\beta'^{-D}(p) + \dfrac{v_{\alpha\beta}}{kT}\right)} \tag{II.18}$$

The equations $f_i = 0$ are solved for the variables, x_i. Then the equations (20) and (31) are satisfied. The first two terms on the

right-hand side of eq. (II.17) cancel because the sum of all volume fractions is equal to 1. The third term equals $2\ln a$ for each α, D and p, hence it cancels the fourth term. The value for a can be used to obtain $G_\alpha^D(p)$ from $G_\alpha'^D(p)$, $G_A^O(p)$ from $G_A'^O(p)$ and Λ_A from Λ_A'.

APPENDIX III   *FROM EXCHANGE- TO INTERACTION ENERGIES*

So far, exchange energies, $v_{\alpha\beta}$, have been used for quantifying interactions. In this way, all faces are handled in the same way, those of vacancies included. Some results might be more intuitive when expressed in terms of interaction energies, $u_{\alpha\beta}$. These are defined such that all values for 'contacts with vacancies' are zero. Results consistent with this choice of the potential-energy reference can be obtained by making the following substitutions: replace

$$v_{\alpha\beta} \qquad \text{by} \qquad u_{\alpha\beta} = v_{\alpha\beta} - v_{\alpha 0} - v_{\beta 0} \quad \text{(See eq. (7))}$$

Consequently, replace

$$U\left(\left\{n_\alpha^d(z)_\beta\right\}\right) \qquad \text{by} \qquad \tfrac{1}{2}\sum_{\alpha,\beta,d,z} n_\alpha^d(z)_\beta u_{\alpha\beta} =$$

$$U\left(\left\{n_\alpha^d(z)_\beta\right\}\right) - \tfrac{1}{2}\sum_{\alpha,\beta,d,z} n_\alpha^d(z)_\beta \left(v_{\alpha 0} + v_{\beta 0}\right)$$

Moreover, replace

$$G_\alpha^d(z) \qquad \text{by} \qquad G_\alpha^d(z)\exp\left(v_{\alpha 0}/kT\right)$$

These satisfy eq. (20) if there the $v_{\alpha\beta}$'s are replaced by $u_{\alpha\beta}$'s. The distribution of contacts can be calculated by replacing the $v_{\alpha\beta}$'s by $u_{\alpha\beta}$ in eq. (19)). Obviously, the values of monomer weighting factors also change. Consequently, replace

$$f_A \qquad \text{by} \qquad f_A - \sum_\alpha q_{A\alpha} v_{\alpha 0}$$

The pressure p is invariant with respect to these substitutions, as should be.

APPENDIX IV   *SYMBOLS*

subscripts:

     A, B monomer types, all upper case roman subscripts refer to monomer types. 0 refers to vacancies.

     α, β face types. All lower case Greek subscripts refer to face types. A, 0 refers to the face of vacancies.

superscripts

     o monomer orientation.

O   set of monomer orientations.

d   direction (of a face or contact).

D   set of directions.

If in an equation the parameters d, $-d$, z and z' appear they are related as follows: $-d$ indicates the opposite of direction d; z indicates the layer from which the face with direction d originates, z' the layer at which it is pointing.

In the following list, each parameter o or d can be replaced by O or D.

A surface area

a $= A/L$, cross-sectional surface-area per lattice site

C normalisation constant for the whole system

f_A partial Helmholtz energy of component A, defined in eq. (14)

F Helmholtz energy

$g_{\alpha\beta}^d(z)$ $= \phi_{\alpha\beta}^d(z)/\phi_\alpha^d(z)\phi_\beta^{-d}(z')$, nearest-neighbour correlation function, see eq. (5)

G Gibbs energy

$G_A^o(z)$ weighting factor for a monomer of type A, in orientation o and layer z, introduced in eq. (21)

$G_\alpha^d(z)$ face weighting factor of a face of type α, with direction d, located in layer z, introduced in eq. (19)

k Boltzmann's constant

L number of lattice sites in a layer

$\mathcal{L}$ Lagrange function, given by eq. (16)

M number of layers

N number of lattice sites in a system

n_A total number of monomers of type A in a system

$n_A^o(z)$ number of monomers of type A, with orientation o in layer z

$n_\alpha^d(z)$ number of faces of type α, with direction d, in layer z

$n_{\alpha\beta}^d(z)$ number of contacts between faces of type α, having direction d, in layer z and faces of type β. An asterisk indicates the random value

p pressure

$Q(\{n_A\}, L, T)$ canonical partition function, given by eq. (13)

q	coordination number of the lattice, identical to the number of nearest neighbours of each site
q^D	number of directions belonging to set D
$q_{A\alpha}^{od}$	number of faces of type α, with direction d, on a monomer of type A, having orientation o (possible values are 0 and 1)
$q_{A\alpha}^{OD}$	number of faces of type α, with direction belonging to subset D, on a monomer of type A, having an orientation belonging to O (possible values: 0, 1, . . q^D)
S	entropy
T	absolute temperature
U	potential energy, see eq. (8)
$u_{\alpha\beta}$	interaction energy for an $\alpha\beta$-contact
V	volume of the system
v	$= V/N$ volume of one lattice site
$v_{\alpha\beta}$	exchange energy for an $\alpha\beta$-contact
z	layer number
γ	surface tension
θ_A	$= n_A/L$
Λ_A	$= \exp(f_A/kT)$
$\lambda_\alpha^d(z), \lambda$	undetermined multipliers associated with constraints (2) and (3) respectively
μ_A	chemical potential, see eq. (26)
$\Xi(\{f_a\}, M, L, T)$	partition function for an ensemble of systems with fixed $\{f_a\}$, M, L, and T, given by eq. (15)
$\phi_A^o(z)$	$= n_A^o(z)/L$, site fraction in layer z of monomers of type A, in orientation o
$\phi_\alpha^d(z)$	$= n_\alpha^d(z)/L$, fraction of faces in layer z, with direction d, that are of type α
$\phi_{\alpha\beta}^d(z)$	$= n_{\alpha\beta}^d(z)/L$, fraction of faces in layer z, with direction d, that are of type α and make contact with a face of type β
$\psi_{\alpha\beta}^d(z)$	$= \phi_{\alpha\beta}^d(z)/\phi_\beta^{-d}(z')$, nearest-neighbour distribution function: conditional probability of α at direction d of a site of layer z, that makes contact with a face of type β. see eq. (4)
Ω	combinatory factor

ω_A number of orientations of a monomer of type A

ω_A^O number of orientations of a monomer of type A, belonging to the subset of orientations O

REFERENCES

1   Hill, T. L. *Introduction to Statistical Thermodynamics*; Addison-Wesley: 1962.

2   Guggenheim, E. A. *Mixtures*; Fowler, R. H., et al.; Clarendon: Oxford, 1952.

3   Flory, P. J. *Principles of Polymer Chemistry*; Cornell: Ithaca/London, 1971.

4   Lee, T. D.; Yang, C. N. *Phys. Rev.*, *87*, 410-419 (1952) "Statistical theory of equations of state and phase transitions. II. Lattice gas and Ising model".

5   Widom, B. *J. Chem. Phys.*, *39*, 2808-2812 (1963) "Some topics in the theory of fluids".

6   Trappeniers, N. J.; Schouten, J. A.; Ten Seldam, C. A. *Chem. Phys. Lett*, *5*, 541-545 (1970) "Gas-gas equilibrium and the two-component lattice-gas model.".

7   Kleintjens, L. A.; Koningsveld, R. *Sep. Sci. Techn.*, *17*, 215-233 (1982) "Mean field lattice-gas discription of the system of CO_2 and H_2O".

8   Walker, J. S.; Goldstein, R. E. *Phys. Lett.*, *112A*, 53-56 (1985) "Interaction-driven asymetric coexistence curves and the singular diameter".

9   Wheeler, J. C.; Widom, B. *J. Chem. Phys.*, *52*, 5334-5343 (1970) "Phase equilibrium and critical behaviour in a two-component Bethe-lattice gas or a three-component Bethe-lattice solution".

10   Kikuchi, R. *Phys. Rev.*, *81*, 988-1003 (1951) "A theory of cooperative phenomena".

11   Hijmans, J.; De Boer, J. *Physica*, *21*, 471-516 (1955) "An approximation method for order-disorder problems".

12   Barker, J. A. *J. Chem. Phys.*, *20*, 1526-1533 (1952) "Cooperative orientation effects in solutions".

13   Barker, J. A. *J. Chem. Phys.*, *21*, 1391-1394 (1953) "Cooperative orientation in solutions. The accuracy of the quasi-chemical approximation".

14   Barker, J. A.; Fock, W. *Disc. Faraday Soc.*, *15*, 188-195 (1953) "Theory of upper and lower critical solution temperatures".

15   Barker, J. A.; Smith, F. *J. Chem. Phys.*, *22*, 375-380 (1954) "Statistical thermodynamics of associated solutions".

16   Tompa, H. *J. Chem. Phys.*, *21*, 250-258 (1953) "Quasi-chemical treatment of mixtures of orientated molecules".

17   Bodegom, E.; Meijer, P. H. E. *J. Chem. Phys.*, *80*, 1617-1624 (1983) "Coexistence and spinodal curves in directionally bonded liquids using the four-cluster approximation".

18   Andersen, G. R.; Wheeler, J. C. *J. Chem. Phys.*, *69*, 2083-2088 (1978) "Directionallity dependence of lattice models for solutions with closed loop coexistence curves".

19   Smirnova, A. N. *Pure & Appl. Chem.*, *61*, 1115-1122 (1989) "New versions of quasichemical models for fluids with orientation effects".

20   Smirnova, N. A.; Victorov, A. I. *Fluid Phase Equilibria, 34*, 235-264 (1987) "Thermodynamic properties of pure fluids and solutions from the hole group-contribution model".

21   Prange, M. M.; Hooper, H. H.; Prausnitz, J. M. *AIChE Journal, 35*, 803-813 (1989) "Thermodynamics of aqueous systems containing hydrophilic polymers or gels".

22   Smirnova, N. A. *Fluid Phase Equilibria, 2*, 1-25 (1978) "Lattice model for the surface region of solutions consisting of different-sized molecules with orientation effects".

23   Mulholland, G. W.; Rehr, J. J. *J. Chem. Phys., 60*, 1297-1306 (1973) "Coexistence curve properties of Mermin's decorated lattice gas".

24   Wheeler, J. C. *J. Chem. Phys., 62*, 433-439 (1974) ""Exactly soluble" two-component lattice solution with upper and lower critical solution temperatures".

25   Andersen, G. R.; Wheeler, J. C. *J. Chem. Phys., 69*, 3403-3413 (1978) "Theory of lower critical solution points in aqueous mixtures".

26   Hu, Y.; Lambert, S. M.; Soane, D. S.; Prausnitz, J. M. *Macromolecules, 24*, 4356-4363 (1991) "Double-lattice model for binary polymer solutions".

27   Walker, J. S.; Vause, C. A. *Phys. Lett, 79A*, 421-424 (1980) "Theory of closed-loop phase diagrams in binary fluid mixtures".

28   Vause, C. A.; Walker, J. S. *Phys. Lett., 90A*, 419-424 (1982) "Effects of orientational degrees of freedom in closed-loop solubility phase diagrams".

29   Walker, J. S.; Vause, C. A. *J. Chem. Phys., 79*, 2660-2676 (1983) "Lattice theory of binary fluid mixtures: Phase diagrams with upper and lower critical solution points from a renormalization-group calculation".

30   Goldstein, R. E.; Walker, J. S. *J. Chem. Phys., 78*, 1492-1512 (1982) "Theory of multiple phase separations in binary mixtures: Phase diagrams, thermodynamic properties, and comparisons with experiments".

31   Ten Brinke, G.; Karasz, F. E. *Macromolecules, 17*, 815-820 (1983) "Lower critical solution temperatures behaviour in polymer blends: Compressibility and directional-specific interactions".

32   Goldstein, R. E. *J. Chem. Phys., 80*, 5340-5341 (1984) "On the theory of lower critical solution points in hydrogen-bonded mixtures".

33   Sanchez, I. C.; Balazs, A. C. *Macromolecules, 22*, 2325-2331 (1989) "Generalization of the lattice-fluid model for specific interactions".

34   Huckaby, D. A.; Bellemans, A. *J. Chem. Phys., 81*, 3691-3693 (1984) "An exactly solvable two-component solution having a "closed-loop" phase diagram".

35   Karlström, G. *J. Phys. Chem., 89*, 4962-4964 (1984) "A new model for upper and lower critical solution temperatures in poly(ethylene oxide) solutions".

36   Sjöberg, Å.; Karlström, G. *Macromolecules, 22*, 1325-1330 (1988) "Temperature dependence of the phase equilibria for the system poly(ethylene glycol)/dextran/water. A theoretical and experimental study".

37   Ono, S.; Kondo, S. in *Encyclopedia of Physics*, edited by Flügge, S. (Springer, Berlin, 1960) pp. 134-280. "Molecular theory of surface tension in liquids".

38   Widom, B. *J. Stat. Phys., 19*, 563-574 (1978) "Structure of interfaces from uniformity of the chemical potential".

39 Rowlinson, J. S.; Widom, B. *Molecular Theory of Capillarity*; Baldwin, J. E., et al.; Clarendon: Oxford, 1982.

40 Roe, R. J. *J. Chem. Phys.*, *62*, 490-499 (1975) "Theory of the interface between polymers or polymer solutions.I. Two component system".

41 Kurata, M. *Busseiron Kenkyu*, *39*, 77-86 (1951) "Bethe approximation for surface layers". In Japanese.

42 Parlange, J. Y. *J. Chem. Phys.*, *48*, 169-173 (1967) "Phase transition and surface tension in the quasichemical approximation".

43 Scheutjens, J. M. H. M.; Fleer, G. J. *J. Phys. Chem.*, *83*, 1619-1635 (1979) "Statistical theory of the adsorption of interacting chain molecules. 1. Partition function, segment density distribution, and adsorption isotherms".

44 Scheutjens, J. M. H. M.; Fleer, G. J. (1980) "Statistical theory of the adsorption of interacting chain molecules. 2. Train, loop, and tail size distribution".

45 Evers, O. A.; Scheutjens, J. M. H. M.; Fleer, G. J. *Macromolecules*, *23*, 5221-5233 (1990) "Statistical thermodynamics of block copolymer adsorption. 1. Formulation of the model and results for the adsorbed layer structure".

46 Jackson, J. L.; Klein, L. S. *Phys. Fluids*, *7*, 228-231 (1963) "Potential distribution method in equilibrium statistical mechanics".

47 Barneveld, P. A.; Scheutjens, J. M. H.; Lyklema, J. *Langmuir*, *8*, 3122-3130 (1992) "Bending moduli and spontaneous curvature. 1. Bilayers and monolayers of pure and mixed nonionic surfactants".

48 Besseling, N. A. M. "Statistical thermodynamics of water I:". to be published.

49 Patterson, D. *Macromolecules*, *2*, 672-677 (1969) "Free volume and polymer solubility. A Qualitative View".

50 Koningsveld, R.; Kleintjens, L. A. *Croat. Chem. Acta*, *60*, 53-89 (1987) "Polymers and thermodynamics".

51 Powell, M. J. D. in *Numerical methods for nonlinear algebraic equations*, edited by Rabinowitz, P. (Gordon and Breach, London, 1970) pp. 115-161. "A fortran subroutine for solving systems of nonlinear algebraic equations".

52 Scheutjens, J. M. H. M. "Newton.sim". A Simula class for unconstrained optimization.

CHAPTER III

EQUILIBRIUM PROPERTIES OF WATER
AND ITS LIQUID-VAPOUR INTERFACE

A previously formulated self-consistent field lattice theory for molecules with orientation-dependent interactions is applied to a lattice-gas model for water. The theory is a generalisation of the quasi-chemical treatment and hence accounts for local correlations. The calculated equation of state and liquid-vapour phase diagram agree at least qualitatively with the experimental behaviour of water. The well-known anomalous behaviour of water as reflected in the maximum of the isobaric density is reproduced by the theory. Within this model it is possible to analyse the relation between this behaviour and the hydrogen-bonded structure of water. Interfacial properties of water are also investigated. Although the calculated interfacial tension is lower than is experimentally found, the trends are reproduced. The theoretical liquid-vapour interfacial tension shows a minimum in its temperature coefficient, as is found experimentally. At intermediate temperatures, the calculated interfacial thickness and the density decay length is an order of magnitude larger than for simple molecules, and has a minimum as a function of temperature.

1 INTRODUCTION

In the preceding chapter [1] we introduced a self-consistent field lattice theory for homogeneous as well as heterogeneous systems that may contain molecules with orientation-dependent interactions. The theory is based on the *first-order quasi-chemical* approximation for lattice models of systems with interacting molecules [2, 3]. We will refer to this theory as first-order self-consistent field (FOSCF) theory. The first-order approximation accounts for local correlations, which are particularly important in fluids containing molecules with orientation-dependent interactions, especially for the temperature dependence of their thermodynamic properties. If molecules have orientation-dependent interactions then their orientations will be correlated.

Of compounds that possess orientation-dependent intermolecular interactions, water is an interesting example, both from a scientific and from a practical point of view. As is well known, water has a rather exceptional behaviour. Liquid water has an open structure and its density shows a maximum with isobaric variation of temperature. The isothermal compressibility has a minimum with varying temperature. At about atmospheric pressures, ice contracts upon melting into liquid water. Water has a large heat capacity and a high melting and boiling point as compared to other compounds of similar molecular mass. The surface tension, γ, of water is relatively high, and $-d\gamma/dT$, which equals the surface entropy, passes through a maximum with varying temperature [4-6]. whereas for simple compounds, such as argon, both γ and $-d\gamma/dT$ are monotonously decreasing functions [6].

The most intriguing properties of water, especially to biologists and biochemists, are referred to by the term *hydrophobic effect*. This notion is used in relation to the interaction between water and apolar solutes and apolar macroscopic surfaces. Especially the interpretation of the temperature dependence of this hydrophobicity or, equivalently, of the role of entropy and energy has been a problem. Some phenomena where the hydrophobic effect plays a role

are: micellisation of amphipolar molecules, formation of biological membranes [7] and folding of proteins [8-10].

Macroscopic solid surfaces also influence the structure of adjacent fluid water. This is relevant for adsorption and wetting phenomena at such surfaces, and for the solvent-structure-originated contribution to the interaction between surfaces, the so-called hydration forces [11-13].

It is clear that the roles of repulsive and attractive intermolecular forces in water is quite different from simple fluids consisting of more or less isotropic molecules. It is well known, that the structure of simple fluids is mainly determined by short-range repulsive intermolecular forces. The cohesive energy is mainly due to the attractive Van der Waals interactions. The structure of water is to a large extent determined by the attractive directional forces, usually denoted as hydrogen bonds. These give rise to a locally anisotropic structure.

Many attempts to formulate a molecular explanation for the above-mentioned macroscopic properties of water started from assumptions about the microscopic structure of liquid water. In one model, water was pictured as a mixture of finite clusters of various sizes that are continuously breaking down and rebuilding. Frank and Wen introduced the term *flickering clusters* for this [14]. A quantitative statistical theory based on this physical picture which has drawn a lot of attention was developed by Némethy and Scheraga [15].

According to an alternative view, first put forward by Bernal and Fowler [16], liquid water is regarded as a macroscopic hydrogen-bonded network. Similarly as with the cluster model, in this network the hydrogen bonds are reshuffling all the time. It can be imagined that a (not too large) apolar molecule can be accommodated in this network without reducing the number of hydrogen bonds between water molecules. This reduces the entropy, but does not cost much energy [17]. Various theories starting from the network view of water have been presented [18-20].

The above mentioned theories all start from some assumption about the microscopic structure of water. It is not easy to judge whether or not such a view is correct. Often, the same experimental

observations can be explained from contradicting models. Hence, methods of a more ab-initio nature are needed.

Computer simulations (molecular dynamics, Monte Carlo) start from a model for the intermolecular interactions and do not need any further assumptions on the structure of the liquid. Since application of these methods to water have become possible some twenty years ago [21, 22] they have been of great help to the study of water. This applies to homogeneous fluid water [20-29], as well as to aqueous interfacial systems [30-35]. Simulations are restricted to rather small systems and short intervals of real time (often too short to reach thermodynamic equilibrium). Often the results suffer from large statistical uncertainties.

Water has also be studied by extending the methods used for simple fluids. These involve integral equations [36-38] or cluster expansions for the pair correlation function [39, 40]. In principle, one only needs to specify the intermolecular interactions and need not make further assumptions on the microscopic structure of the fluid. However, this approach meets with mathematical difficulties if the interactions are complicated and strongly orientation-dependent, as with water. It is inevitable to introduce further approximations and even then it remains difficult to obtain detailed numerical results on thermodynamic properties. At the moment, extension of these methods towards heterogeneous aqueous systems seems to be far out of reach.

Yang at al. have developed a density-functional theory for the aqueous liquid-vapour interface [41, 42]. As these authors indicate themselves, for homogenous fluid water this theory leads to a simple 'Van der Waals' expression for the Helmholtz energy. This is due to certain mean-field averaging of the anisotropic correlations. Hence their theory is not able to reproduce the anomalous behaviour of homogeneous liquid water and it is not surprising that the agreement between theoretical and experimental interfacial properties such as the surface tension is poor.

Lattice-gas theories can be considered as coarse-grained alternatives to the continuum theories of classical fluids. Since the present chapter is on a lattice-gas theory, some previous applications to aqueous systems will be reviewed in some detail. In lattice models,

distances and angles vary discretely rather than continuously. Density variations are accounted for by allowing lattice sites to be vacant. In lattice gases, the intermolecular interactions are similar to those in continuum models; the intermolecular repulsion at short separation is accounted for by excluding multiple occupancy of the lattice sites. The interaction energy of the molecules located on neighbouring sites can have some finite value. Lattice-gas models have been rather successfully applied to aqueous systems [43-53]. Bell [43] used the body-centred cubic lattice (see fig. 1), as we do. In his model, the intermolecular interactions are quantified by three parameters, one for the hydrogen bond, one for the interaction between molecules on nearest neighbour sites that are not hydrogen bonded, and one that quantifies an energy penalty against close packing. In Bell's model, this energy penalty is implemented in a rather unrealistic way: if to a triad of sites consisting of two next-nearest neighbours and their common nearest neighbour (for instance sites A, B and C in fig. 1) are completely occupied by water molecules, an additional positive energy is assigned. In the present chapter it will be shown that it is unnecessary to introduce an energy-penalty in such an artificial way. Bell evaluated his model using the quasi-chemical approximation for clusters of four sites. An improved statistical analysis of Bell's model based on the cluster-variation method has been presented by Meijer and co-workers [51-53]. These theories were all restricted to homogeneous systems.

So far, for water no theory exists that can be applied to systems as complicated and diverse as mixtures with apolar or amphiphilic components, and fluid-fluid and fluid-solid interfaces. As a consequence, the understanding of aqueous behaviour is still incomplete. The relations between the various idiosyncrasies of water are hence not yet completely understood.

In the present chapter a lattice-gas theory is introduced that can be applied homogeneous and to interfacial aqueous systems. In the model for water the dependence of the intermolecular interactions upon the orientations of the molecules is accounted for (section 2). In section 3 the relevant details of the first-order self-consistent field (FOSCF) theory are briefly reviewed [1]. For reasons of comparison, in section 4 results on a fluid consisting of radially

symmetrical molecules are presented. In the last two sections, the behaviour of water according to the present theory is presented and discussed. Section 5 is devoted to the properties of the homogeneous fluid. Section 6 deals with the properties of the interface between the coexisting liquid and vapour.

In subsequent chapters, the present theory will be applied to find a molecular interpretation of the "hydrophobic effect" [54]. Moreover, the behaviour of water at solid surfaces will be studied, including phenomena as "hydration forces" between planar surfaces [55], vapour adsorption and wetting phenomena [56].

2 A LATTICE MODEL FOR WATER

As in a previous paper [1], the volume V that contains the fluid is divided into a regular lattice of N identical sites. The volume of one site, V/N, will be denoted by v. The lattice does not change with temperature or composition. It serves as a system of coordinates on which distances and angles are discrete. To model water the body-centred cubic (bcc) lattice is a good choice because it has tetrahedral angles. The bcc lattice has a coordination number of eight: each lattice site is surrounded by eight nearest neighbours. In two ways, the bcc lattice can be subdivided into two tetrahedral (diamond) sublattices, each with a coordination number of four. Hence, the bcc lattice can be occupied in such a way that locally the monomers are ordered tetrahedrally while this does not imply the existence of long range tetrahedral ordering.

In the present chapter sites can either be vacant or occupied by water molecules. Empty lattice sites are referred to as *vacancies.*

To model heterogeneous systems, the lattice is divided into M parallel layers of L sites in such a way that each site has four nearest neighbours within the same layer and two in each of the two adjacent layers. The total surface area is denoted by A and the cross-sectional area per site is given by $a = A/L$. Each layer is denoted by a ranking number z, which runs from 1 until M. Each layer can be filled differently. We will be dealing with systems with an infinitely large surface area and hence an infinitely large L. Calculations are restricted to a finite number of layers. Hence, boundary conditions
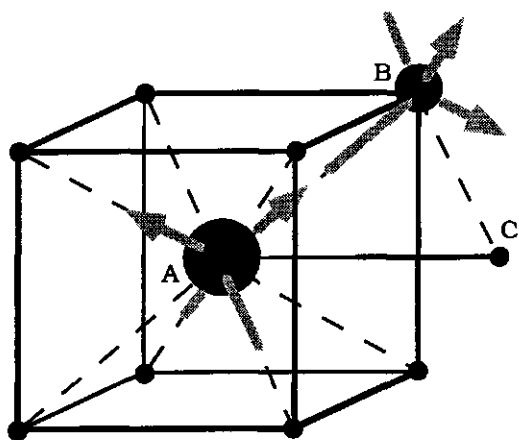
Figure 1. *Ten sites of the body-centred cubic lattice. Around site A its eight nearest neighbours and a next-nearest neighbour C. Sites A and its nearest neighbour B are occupied by water molecules. Arrows indicate proton donors, headless sticks indicate proton acceptors (lone pairs of electrons). The two molecules make contact through a hydrogen bond.*

defining the situation beyond the first and the last layer have to be specified. To model systems where the fluid is imagined to continue beyond these boundary layers, reflecting boundaries can be placed in the middle of, or adjacent to a boundary layer. Adjacent solid surfaces can be modelled by specifying a surface with fixed properties. Systems with solid surfaces will be elaborated in a subsequent chapter.

For a quantitative comparison of experimental results with those from the lattice model, the dimensions of the lattice site have to be specified. An estimate is obtained from the density of natural ice (ice Ih at 273.16 K; 916.8 kg/m^3) assuming this density to correspond to that of a half-filled bcc lattice ($\phi_w = \frac{1}{2}$). In this way a value of 1.632 10^{-29} m^3 is obtained for the lattice site volume v. This corresponds to 2.767 10^{-10} (m) for the distance between the centres of nearest neighbours, of 7.221 10^{-20} m^2 for the cross-section per lattice site, and of 2.260 10^{-10} m for the spacing between the lattice layers. The distance between the centres of the lattice sites is consistent with the value of 2.77 10^{-10} m for the O-O distance in ice at 0 ^{0}C as measured by X-ray diffraction [57].

The water molecule is modelled as a monomer. Of its eight faces, two represent the protons. These will be referred to as *proton-donor faces* or *D*. Two other faces represent the *lone electron pairs*, called *proton-acceptor faces* and are indicated by *A*. These four·faces have a tetrahedral geometry. The four remaining *indifferent* faces, indicated by *I*, also have a tetrahedral geometry. In the present model, the faces are confined to be directed towards nearest-neighbour sites. Consequently, in this model the water molecule has 12 distinguishable orientations. A contact between a proton-donor face and a proton-acceptor face will be considered as a hydrogen bond. Only in 18 out of the total of 144 distinguishable configurations of two neighbouring water molecules a hydrogen bond is formed between them. The way water molecules are accommodated in a bcc lattice is illustrated by fig. 1. A survey of the different types of contact between water molecules can be found in table I. In this table, 'degeneracy' means the number of ways to realise a certain type of contact if two neighbouring lattice sites are occupied by water molecules; these degeneracies sum up to 144.

From the number of different faces that are present in the model for pure water, there are in principle six independent interaction parameters for intermolecular contacts [1]. To keep the number of parameters low and considering that mainly the difference between the hydrogen bond and other modes of intermolecular interaction is responsible for the anomalous properties of water, the same value for the interaction energy was assigned to all types of contact between water molecules, except for the hydrogen bond. These two interaction energies will be denoted by u_{Hb} and u_{nHb} for the hydrogen bond and for other contacts between neighbouring water molecules respectively. It should be noted that in this way the proton-donor and proton-acceptor faces are modelled as being identical, except for the fact that they are complementary with respect to formation of hydrogen bonds. To keep the number of adjustable parameters low, u_{Hb} and u_{nHb} are assumed to be independent of temperature, density, density gradients etc.

The values for the interaction energies were obtained by fitting the experimental pressure and liquid density at coexistence with vapour at 273.16 (K). This temperature was chosen since the size of

Table I

contacts between water molecules

contact type	degeneracy	u/k K
D-A	18	$u_{Hb}/k = -2414.23$
D-D	9	$u_{nHb}/k = 210.2$
A-A	9	$u_{nHb}/k = 210.2$
D-I	36	$u_{nHb}/k = 210.2$
A-I	36	$u_{nHb}/k = 210.2$
I-I	36	$u_{nHb}/k = 210.2$

the lattice site was obtained from the density of ice at this temperature. The values for u_{Hb} and u_{nHb} are included in table I. In obtaining these values, the pressure was most sensitive to the hydrogen-bond strength u_{Hb} whereas the liquid density was most sensitive to u_{nHb}. The existence of a repulsive intermolecular interaction at distances of the order of the hydrogen-bond length for non-hydrogen-bonding orientations is often neglected in discussions on water. That it exists is not unexpected if one inspects models for the electrical charge distribution in the water molecule. This repulsion is responsible for the open structure of water and ice at not too high pressure. Our value, for the hydrogen-bond energy is quite reasonable; it corresponds to −20.0733 kJ/mol of hydrogen-bonds. This is close to the experimental value. From experiments on dimer formation in vapour at 373 K, a value of −22.8 ± 2.9 kJ/mol is obtained for the electronic interaction energy [58]. The corresponding value if changes due to loss of translational and rotational kinetic energy and gain of vibrational energy upon dimer formation are accounted for, is −18.1 ± 1.3 kJ/mol (see also table 2-2 of ref. [59]).

Using temperature-independent values for the interaction parameters and for the lattice dimensions, changes of the intermolecular vibrations with varying temperature are disregarded. Moreover, it is assumed that all entropy changes due to formation of contacts are accounted for in the configurational counting.

In the present chapter the interactions are quantified by 'interaction energies', $u_{\alpha\beta}$. These are defined such that all $u_{\alpha 0}$

vanish. In a previous chapter [1] differently defined parameters were used. Those where referred to as 'exchange energies', $v_{\alpha\beta}$, and defined such that they vanishes for contacts between identical faces. This difference implies different reference states for the potential energy of the faces, the weighting factors and most thermodynamic quantities

Since the occupation of the lattice layers is allowed to be different, density gradients normal to layers can exist in the present model. Instead of, or in addition to this, another kind of symmetry breaking can occur: two intertwining tetrahedral sublattices can become differently occupied. This can be regarded as crystallisation e.g., formation of ice. Two distinct crystalline states can form in this model, an 'open' and a 'close-packed' structure. In the open form, one tetrahedral sublattice is (mainly) occupied by water molecules that are (nearly) all connected by hydrogen-bonds. The other sublattice is (mainly) empty. This can be identified as "ice Ic" which is found experimentally as a metastable state which resembles "ice Ih", the natural form of ice at atmospheric pressure [57].

Pauling has obtained an approximate value of $k\ln\frac{3}{2}$ per molecule for the residual entropy of perfect four-coordinated ice [60]. It has been shown that the approximations in Pauling's calculation are equivalent to the first-order quasi-chemical approximation [61]. In the present chapter, we apply this approximation to the model described above, which is more elaborate than that of Pauling. It can be shown that Pauling's value is the low-temperature limit of the present theory (APPENDIX I).

In the close-packed crystalline state that can exist in the present model, the two intertwined tetrahedral lattices are both occupied and the water molecules are hydrogen-bonded to molecules on the same sublattice. This structure has a density of about twice that of the tetrahedral open form. It can be identified as "ice VII" which exits at high pressure [57].

3 FIRST-ORDER SELF-CONSISTENT FIELD THEORY

In a previous chapter we derived a general first-order self-consistent field theory for models like the one described above [1].

This theory is based on the first-order approximation, also called quasi-chemical approximation: correlations within each pair of nearest neighbour sites is accounted for but the occurrence of closed rings of sites is disregarded. At given normalisation conditions, the distribution of monomers over orientations and layers can be related to a molecular field. This field is quantified by *face weighting factors*. These can be expressed in terms of the monomeric distribution. The configuration for which the molecular field and the monomeric distribution are self consistent is identified as the equilibrium state of the system.

In the previous section, the model for the water molecule was introduced. It will be indicated as species 1. In the following statistical analysis, vacancies will be treated as just another isotropic monomer type. It will be indicated as species 0. For each distinguishable orientation of each component we can write

$$\phi_A^o(z) = \Lambda_A G_A^o(z) \tag{1}$$

where $\phi_A^o(z)$ is the fraction of sites in layer z, occupied by monomers of type A in orientation o. Here A can stand for a vacancy or for a water molecule. By division of the site fractions by the lattice-site volume, number densities are obtained. As $G_A^o(z)$ measures the probability to find such a monomer in layer z, it is referred to as a *monomer weighting factor*. The quantity $-kT \ln G_A^o(z)$ is a *potential of mean force* for a monomer of type A with orientation o at layer z. It contains the energies of the contacts of the monomer with surrounding monomers and the entropy of the ensuing local order. This ordering is related to the non-randomness of the distribution of contacts.

The normalisation factor Λ_A is uniform for all locations and orientations of monomer type A. It has been shown that $\Lambda_A = \exp(f_A/kT)$ where $f_A \equiv (\partial F/\partial n_A)_{A,T,\{n_{B \neq A}\}}$ and F is the Helmholtz energy [1]. Summation over orientations o and layers z, of the left and right hand side of eq. (1) leads to

$$\Lambda_A = \frac{\phi_A}{G_A} \tag{2}$$

where $\phi_A = \sum_{o,z} \phi_A^o(z)/M$ is the fraction of sites occupied by component A, averaged over all layers; similarly, $G_A = \sum_{o,z} G_A^o(z)/M$. By fixing for a component either Λ_A or ϕ_A we are dealing with a system that is open or closed for that component respectively.

The f_A's can be related to the pressure and the chemical potentials. The pressure of a lattice gas can be related to f_0 where the subscript 0 indicates vacancies.

$$p \equiv -\left(\frac{\partial F}{\partial V}\right)_{A,T,\{n_{A\neq0}\}} = -\frac{1}{v}\left(\frac{\partial F}{\partial n_0}\right)_{A,T,\{n_{A\neq0}\}} = -\frac{f_0}{v} \qquad (3)$$

For the chemical potential of component A we can write

$$\mu_A \equiv \left(\frac{\partial G}{\partial n_A}\right)_{p,A,T,\{n_{B\neq A,0}\}} \equiv \left(\frac{\partial F}{\partial n_A}\right)_{V,A,T,\{n_{B\neq A,0}\}} = f_A - f_0 = kT\ln\frac{\phi_A}{G_A\Lambda_0} \qquad (4)$$

Here $-kT\ln(G_A\Lambda_0)$ can be identified as the Gibbs energy of solvation of molecule A by its environment. This quantity differs from $-kT\ln G_A$, by the term $-kT\ln\Lambda_0 = pv$ (see eq. (3)). This last term equals the work of creating space for the monomer.

Within the quasi-chemical approximation, the monomer weighting factor can be expressed as [1]

$$G_A^o(z) = C\prod_{\alpha,d} G_\alpha^d(z)^{q_{A\alpha}^{od}} = C\prod_d G_A^{od}(z) \qquad (5)$$

As they represent the contribution of a face to the monomer weighting factor, the $G_\alpha^d(z)$ are referred to as *face weighting factors*. A face type can be identified by the monomer type and orientation to which it belongs; $G_A^{od}(z)$ is the weighting factor of the face with direction d of a monomer of type A, with orientation o, that is located in layer z. The normalisation factor C equals 1 for homogeneous systems. The interfacial tension can simply be written as [1]

$$\frac{\gamma a}{kT} = M\ln C \qquad (7)$$

Equation (1) gives the density distribution for all monomeric orientations. Moreover, information on intermolecular correlations is obtained in terms of the distribution of contacts. The site fraction of contacts, $\phi_\alpha^d(z)_\beta = n_\alpha^d(z)_\beta/L$, is given by [1]

$$\phi_\alpha^d(z)_\beta = \frac{\phi_\alpha^d(z)\phi_\beta^{-d}(z')}{G_\alpha^d(z)G_\beta^{-d}(z')}\exp{-\frac{u_{\alpha\beta}}{kT}} \tag{8}$$

The site fractions of faces $\phi_\alpha^d(z) = n_\alpha^d(z)/L$ are directly obtained from the distribution of monomers: $n_\alpha^d(z) = \sum_{A,o} n_A^o(z)q_{A\alpha}^{od}$. Here $q_{A\alpha}^{od}$ quantifies the way faces are arranged on the surface of a monomer of type A. It equals 1 if the face at direction d of a monomer of type A having orientation o, is of type α, otherwise it equals 0. For the present choice for the reference level of the molecular potential energy of intermolecular interactions, as implied by the use of interaction parameters $u_{\alpha\beta}$, all $G_\alpha^d(z)$'s equal 1 at infinitely low density. The appearance of the face weighting factors in the expressions for the monomer distribution (eqs. (1) and (5)) as well as in the expressions for the distribution of contacts, manifests the relation between these features.

If the occupation of neighbouring sites would be uncorrelated, the distribution of contacts would be given by

$$\phi_\alpha^{*d}(z)_\beta = \phi_\alpha^d(z)\phi_\beta^{-d}(z') \tag{9}$$

To obtain the distribution of contacts according to the quasi-chemical approximation (see eq. (8)), $\phi_\alpha^{*d}(z)_\beta$ has to be multiplied by the Boltzmann factor of the contact energy. Moreover, the saturation constraints $\sum_\beta \phi_\alpha^d(z)_\beta = \phi_\alpha^d(z)$ have to be satisfied. This is accounted for by the factors $G_\alpha^d(z)$. If the normalisation conditions for the components of the system are specified, these constraints, together with eq. (8) and eq. (1) with (5) and (6) constitute a complete set of self-consistent field equations. These can be solved numerically by the methods described in reference [1].

It is convenient to define the nearest-neighbour distribution function as the probability of an α-face, provided that it has direction d, that it is located at layer z and that it makes contact with a face of type b . It is given by the expression

$$\psi_\alpha^d(z)_\beta \equiv \frac{\phi_\alpha^d(z)_\beta}{\phi_\beta^{-d}(z')} \qquad (10)$$

If the contacts are formed randomly $\psi_\alpha^d(z)_\beta$ equals $\phi_\alpha^d(z)$ for each β. As a special this we define the hydrogen-bonding ratio for proton-donor faces as $\psi_A^d(z)_D$, similarly for acceptors we have $\psi_D^d(z)_A$. Here A and D stand for proton-donor and acceptor faces, respectively. For homogeneous isotropic systems the indices d and z can be omitted and $\psi_{AD} = \psi_{DA} = \alpha$. This quantity is plotted in fig. 7 as a function of T and ϕ.

The total configurational energy of a system can be written in terms of numbers of contacts and interaction-energy parameters as

$$U = \tfrac{1}{2} \sum_{\alpha,\beta,d,z} n_\alpha^d(z)_\beta u_{\alpha\beta} \qquad (11)$$

The configurational entropy is given by

$$\frac{S}{k} = - \sum_{A,o,z} n_A^o(z) \ln \phi_A^o(z) - \tfrac{1}{2} \sum_{\alpha,\beta,d,z} n_\alpha^d(z)_\beta \ln \frac{\psi_\alpha^d(z)_\beta}{\phi_\alpha^d(z)} \qquad (12)$$

The first term on the right-hand side can be recognised as the ideal entropy of mixing the monomers, that have a certain distribution over orientations and layers. The other term accounts for the entropy lowering due to local ordering. In the case of random mixing, as would occur if all contacts had the same energy (if $u_{\alpha\beta} - \tfrac{1}{2}\left(u_{\alpha\alpha} + u_{\beta\beta}\right)$ would vanish for each $\alpha\beta$), the ordering contribution to the entropy vanishes.

In eqs. (11) and (12) the equilibrium distribution of monomers and of contacts, given by eqs. (1) and (8), should be substituted. Both the energy and the entropy of the system are related to the distribution of contacts, that is to the correlations of the positions and orientations of the molecules.

In the same way as the occupation of the lattice layers is handled, the occupation of intertwining sublattices can be treated and the formation of crystalline structures can be handled. In all equations of the present section, the parameter z can be supplemented or replaced by a parameter indicating sublattices. As yet we will not try

to perform calculations on these order-disorder transitions. In the present chapter the intertwining sublattices are not allowed to be differently occupied. Hence the formation of ice-like states will not be considered.

4 THE BEHAVIOUR OF ISOTROPICAL MONOMERS

To emphasise the effects of the orientation-dependent nature of the intermolecular interactions in water, we will first review some properties of a lattice model for isotropic monomers. In this section, the same bcc lattice will be utilised as with the model for water. This model will be evaluated within the same first-order approximation as the model for water. There is only one independent interaction-energy u.

From the interaction energies occurring in the model for water, we could calculate an "unweighted average over relative orientations" for the interaction energy between water molecules $u^{av} = \frac{1}{8}u_{Hb} + \frac{7}{8}u_{nHb} = -471.4k$. In this way orientational correlations are ignored. The differences between the results in present section and in the following two sections are due to these orientational correlations.

Since the model is symmetrical with respect to exchanging the molecules and the vacancies, the coexistence curve is symmetrical around $\phi_1 = \phi_0 = \frac{1}{2}$. The critical density is given by $\phi_1 = \phi_0 = \frac{1}{2}$. The critical conditions for this model within first-order approximation are given by some simple explicit expressions [2, 3]. The critical temperature is given by $u/kT = -2\ln(q/(q-2))$. So, for the bcc lattice, for which the lattice coordination number $q = 8$, the critical temperature is $T^* = -1.7380 u/k$. Below this temperature two phases with different densities, liquid and vapour, can coexist. The critical pressure is given by $p^* v/kT^* = 0.15902$ or $p^* = -0.27638 u/v$, where v is the volume of a lattice site. The phase diagram of this model is plotted in fig. 2.

Substitution of the above-mentioned "orientation-averaged" value of the water-water interaction energy leads to a critical temperature 819.3 K. The Bragg-Williams expression for the critical temperature, in which all correlations are ignored, is $qu/kT = -4$ [2, 3]
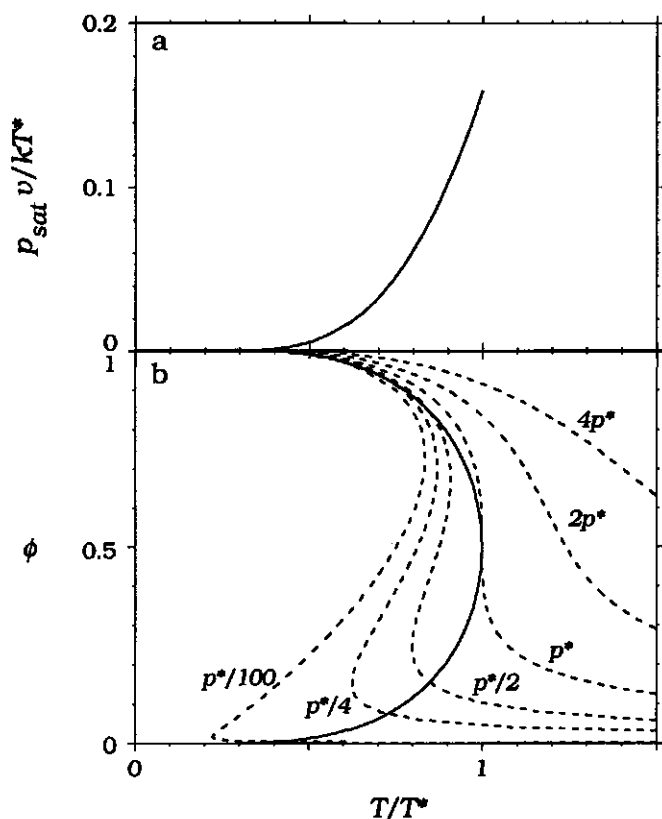
Figure 2. *Phase diagram of the system with isotropic monomers on a bcc lattice. Saturation pressure as a function of temperature (a) and coexistence curve (b). In addition to the binodal, in the ϕ-T diagram, also isobaric densities at various pressures are plotted (dashed curves). The values of the pressure are plotted along with the curves, p^* indicates the critical pressure, T^* the critical temperature.*

which corresponds to a temperature 942.8 K if for u the orientation-averaged water-water interaction is substituted. In the next section, where the orientational correlations are accounted for, a much lower value is obtained. This illustrates that mean-field averaging always leads to an underestimation of the stability with respect to phase separation.

The molecular entropy, energy and enthalpy are calculated as

$$s = S/n = S/\phi N, \quad u = U/\phi N \quad \text{and} \quad h = (U + pV)/n \quad = \quad (U/N - f_0)/\phi$$
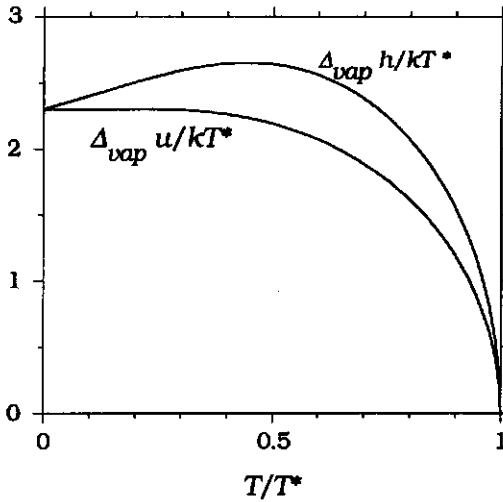
Figure 3. *Molecular energy and enthalpy of vaporisation of isotropic monomers as a function of temperature. Note that $T\Delta_{vap}s$ equals $\Delta_{vap}h$.*

respectively. Here we have omitted the subscript, and have written just n and ϕ for the number and site fraction of molecules. The molecular entropy, energy and enthalpy of vaporisation are calculated as $\Delta_{vap}s = s^{vap} - s^{liq}$, $\Delta_{vap}u = u^{vap} - u^{liq}$ and $\Delta_{vap}h = h^{vap} - h^{liq}$, respectively. These quantities are plotted in fig. 3. At 0 (K), $\Delta_{vap}h = \Delta_{vap}u = \frac{1}{2}qu$ so $\Delta_{vap}h/kT^* = \Delta_{vap}u/kT^* = 2.3014$.

Upon increasing temperature, $\Delta_{vap}u$ decreases until it vanishes at the critical temperature. The difference between the enthalpy and the energy of vaporisation is the work of expansion upon vaporisation. This work vanishes at 0 K since the saturation pressure vanishes there. At the critical temperature it vanishes as well since the density of liquid and vapour become equal there. Obviously $\Delta_{vap}h/T$ equals $\Delta_{vap}s$ and $\Delta_{vap}g = g^{vap} - g^{liq} = \mu^{vap} - \mu^{liq} = 0$. For a one component system (contains one type of molecules and vacancies) $g = G/n$ equals μ as defined by eq. (4).
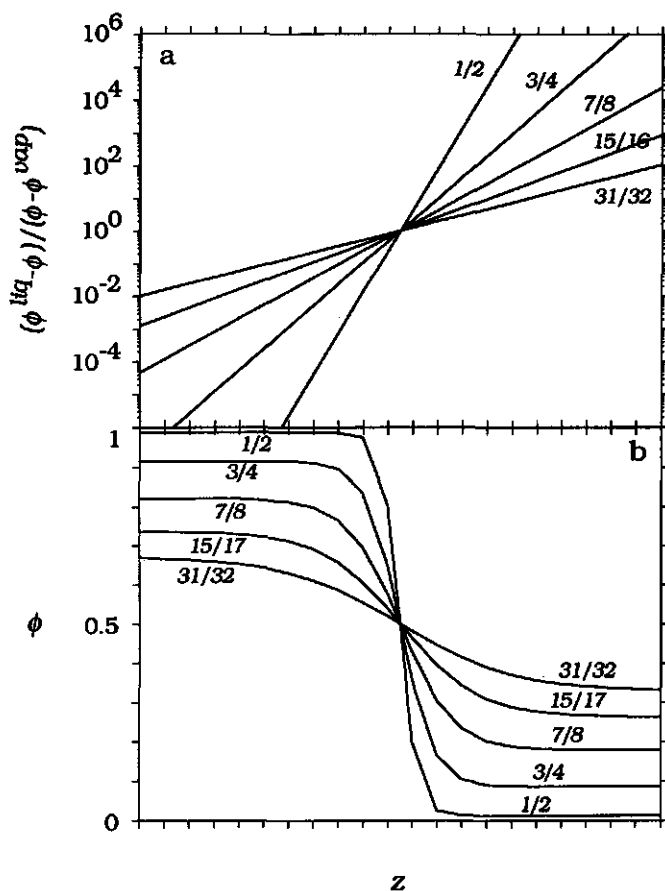
Figure 4. a. *Profiles of the interfacial region at various temperatures. Values of T/T^* are indicated.* b. *Logarithmic plots of $\left(\phi^{liq} - \phi\right)\big/\left(\phi - \phi^{vap}\right)$ at the same temperatures. Values of the density decay length, ξ, equal 0.3461 lattice layers at $T = \frac{1}{2}T^*$, 0.6638 at $T = \frac{3}{4}T^*$, 1.051 at $T = \frac{7}{8}T^*$, 1.566 at $T = \frac{15}{16}T^*$ and 2.269 at $T = \frac{31}{32}T^*$. The ticks on the z-axis indicate the centres of the lattice layers on which the centres of the monomers are located. To guide the eye calculated values are connected by straight lines. To avoid boundary effects, the calculations were performed on a much larger number of layers than is shown in the plots.*

In addition to these properties of the homogeneous fluid and its liquid-vapour equilibrium, we are also interested in the structure and thermodynamics of the liquid-vapour interface. As expected, the
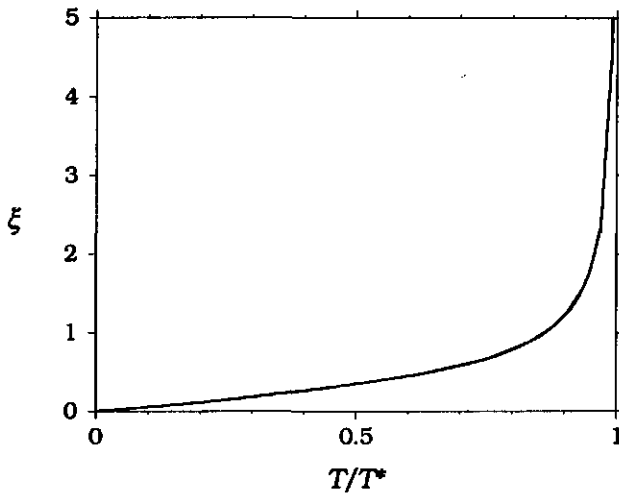
Figure 5. *Density-decay length at the liquid-vapour interface as a function of temperature. ξ is given as a number of lattice layers.*

profile is symmetric with respect to exchanging molecules and vacancies. For not too low temperatures, a plot of $\ln\left(\left(\phi^{liq}-\phi\right)/\left(\phi-\phi^{vap}\right)\right)$ versus z, is linear (see fig. 4). Hence, the density profile satisfies an equation of the form $\phi(z) = \frac{1}{2}\left(1-\phi^{liq}+\phi^{vap}\right)\tanh(z/2\xi)$ where ξ is the density decay length; for isotropic monomers the present treatment leads to a similar density profile as the mesoscopic Van der Waals theory of the liquid interface [6, 62, 63]. At lower temperature, the profile does not satisfy the tanh dependence anymore. In the region where the density is close to its bulk value, the exponential decay towards bulk density, $\phi(z)-\phi^{bulk} \sim \exp(-z/\xi)$, persists at low temperatures.

The density-decay length, ξ, vanishes at absolute zero and increases with increasing temperature. At the critical temperature it diverges. In fig. 5, ξ is plotted from the absolute zero to the critical temperature. Close to the critical point ξ satisfies a power law: $\xi \sim \left(T-T^*\right)^{-\nu}$ where the critical exponent ν equals $\frac{1}{2}$, as is expected for any mean-field type treatment [6]. Also for other critical exponents, the classical mean-field values are found.
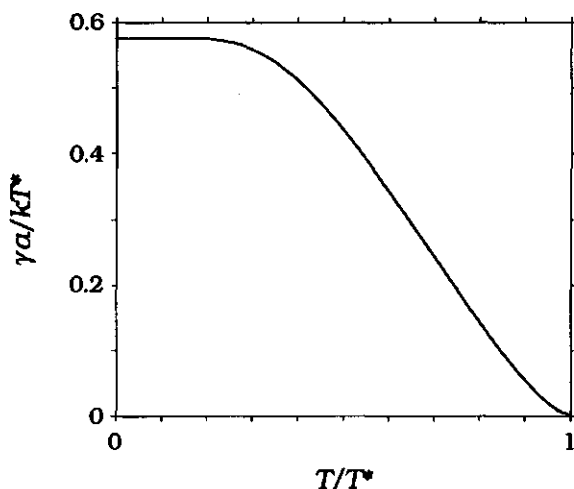
Figure 6. *Interfacial tension of the liquid-vapour interface of isotropic monomers as a function of temperature.*

The liquid-vapour interfacial tension is plotted in fig. 6. At $T = 0$ K, the densities of the coexisting phases are given by $\phi = 1$ and $\phi = 0$, and the interface is perfectly sharp. The interfacial tension at this point is given by $\gamma a = -\frac{1}{2} q^1 w$ where q^1 is the number of contacts of a lattice site with sites of one of the adjacent layers. In the present model q^1 has a value of 2. Hence, $\gamma a / kT^* = 0.57537$ at 0 K. From this value it decreases until the critical temperature is reached, where it vanishes. At 0 K, the interfacial entropy, $s^s = (\partial S / \partial A)_{T,V,n} = -d\gamma/dT$ vanishes (since γ is the interfacial tension of coexisting phases there are no variables but T, we can hence write a total- instead of a partial differential quotient). The interfacial entropy increases upon increasing temperature until it reaches a maximum. At this point, the interfacial tension as a function of temperature has an inflection. Upon further increase of temperature s^s decreases until it vanishes at the critical temperature. It has been suggested that the occurrence of an inflection in the interfacial tension as a function of temperature is typical for water and that it is "a pale reflection of the more marked anomalies in density, compressibility, etc.". [6]. The calculations on the present model with isotropic monomers, that does not have these anomalies, indicate that it is a more general

effect. The experimental observation of this behaviour might be prevented by crystallisation; the triple point might be located at a higher temperature than the temperature where the inflection in the fluid-interfacial tension would occur.

5 HOMOGENEOUS FLUID WATER

To develop some insight into the idiosyncrasies of water, we will now examine some aspects of the structure of homogeneous liquid water that are obtained in the present theory. Due to the orientation-dependent interactions between water molecules, the properties are not symmetric with respect to exchange of molecules and vacancies as in the model of the previous section. An important characteristic of the structure of fluid water is the ratio of the average number of hydrogen-bonds per water molecule, and the maximum of this number, which equals 2. We refer to this quantity as the 'hydrogen-bonding ratio'. In section 3 we introduced the symbol α for this quantity.

For the present lattice model, the low density limit of α is given ·exactly as well as within the first-order approximation of the present theory by

$$\lim_{\phi \to 0}\left(\frac{\alpha}{\phi}\right) = \frac{1}{4}\exp-\frac{u_{Hb}}{kT} \tag{15}$$

The factor $\frac{1}{4}$ is needed because only two out of eight faces of a neighbouring water molecule are able to form a hydrogen-bond with some selected proton donor or acceptor. Equivalently, only three out of twelve orientations of the neighbouring water molecule are suited.

The random mixing value for the hydrogen-bonding ratio, α, is $\frac{1}{4}\phi$ at each temperature which is the limiting value at high temperature. The interactions between water molecules lead to a pronounced non-randomness i.e. to much local order. From fig. 7, showing α over the whole density range and over a large range of temperatures, we see that α is much larger than the random-mixing value.
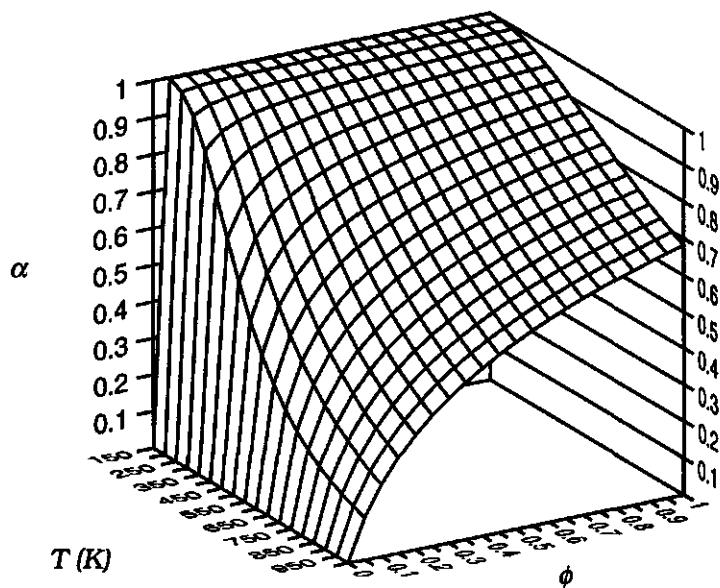
Figure 7. *Hydrogen-bonding ratio, α as a function of temperature and density. Calculated points are connected by straight lines.*

According to the classical theory of gelation and cluster formation [64, 65] (for a review on gelation, see ref. [66]), various characteristics of the hydrogen-bonded structure can be calculated from the value of α. It is inherent to the present first-order approximation as well as to the classical theory of gelation and cluster formation that the (hydrogen) bonds are distributed randomly. By this, it is not meant that the hydrogen-bonding ratio has its random-mixing value, but that each proton-acceptor and donor has an equal probability to be involved in a hydrogen bond, irrespective of other contacts of the molecule to which it belongs. Within this approximation, the fraction of water molecules occupied in b hydrogen bonds is given by the binomial distribution [19, 25] and equals $\binom{4}{b}\alpha^b(1-\alpha)^{4-b}$ where the binomial coefficient $\binom{4}{b}$ = $4!/(b!(4-b)!)$. Consequently, the concentration of non-hydrogen-bonded water molecules is very small over a very large range of temperatures and densities. Simple expressions for various other structural properties of water that can be calculated from α are given in [25].

According to classical gelation theory, the critical value for α, above which a macroscopic network exists, is given by $\alpha^* = 1/(f-1)$,
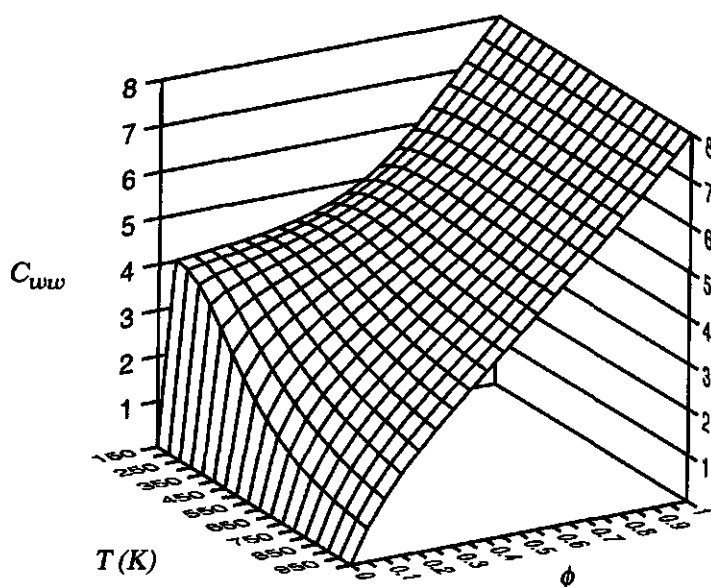
Figure 8. *Coordination number of the water molecules as a function of temperature and density. Calculated points are connected by straight lines.*

where f is the functionality of a monomer. In the present model, for the formation of hydrogen-bonds between water molecules a value of four should be used for f. The hydrogen-bonding ratio, plotted in fig. 7, and the curve at which $\alpha = \frac{1}{3}$, as plotted in fig. 12, indicate that over a large range of temperatures and densities water should be regarded as a macroscopic percolating hydrogen-bonded network and not as a collection of finite clusters. This is consistent with various molecular-dynamics simulations [20, 25-28]. It is interesting to note that the liquid-vapour critical point is located within the network regime.

Various theories for water have been developed from the assumption that water has a gel-like structure [18, 19, 67, 68]. These theories use the hydrogen-bonding ratio as an input parameter. The present theory is of a more ab-initio character since the hydrogen-bonding ratio and various other properties are calculated from a model for the molecules and the intermolecular interactions. The present theory also has a larger range of applicability since it also

accounts for situations where the hydrogen-bonding ratio is as low as it is in the vapour phase.

It should be noted that we do not say anything about kinetic properties; the statement that water has a network structure does not preclude that the lifetime of the hydrogen-bonds might be very short.

In fig. 8, the coordination number of the water molecules is shown for the same circumstances as in fig. 7. Within the present model this quantity ranges from 0 to 8, the coordination number of the lattice.

For the low-density limit of the average coordination number, we can write a simple closed formula:

$$\lim_{\phi \to 0} \left(\frac{C_{ww}}{\phi} \right) = \frac{1}{\omega} \sum_{\alpha} q_{\alpha} \sum_{o} \exp \frac{-u_{\alpha}^o}{kT} = \frac{1}{q} \sum_{\alpha} q_{\alpha} \sum_{\beta} q_{\beta} \exp \frac{-u_{\alpha\beta}}{kT} \qquad (16)$$

Here $\omega = 12$ is the number of possible orientations of the water molecule in the present model. The sum over α extends over all face types of the water molecule and q_{α} is the number of faces of type α that a water molecule has. The sum over o extends over all orientations and u_{α}^o is the energy of a contact between a face of type α (of a water molecule) and a neighbouring water molecule with relative orientation o.

The random-mixing value for the coordination number is 8ϕ for each temperature. According to the present theory, this limiting result is attained at high temperature. With decreasing temperature, the influence of the orientation-dependent interactions is becoming increasingly important. At low densities and temperatures there is a strong deviation from the random-mixing value.

At not too high temperatures, the hydrogen bonds are responsible for the increase of the coordination number towards a value of about four for densities lower than $\phi = \frac{1}{2}$. Then, the four indifferent faces of the water molecule are mostly coordinated by vacancies. The coordination number for liquid water at ambient conditions (ϕ slightly larger than $\frac{1}{2}$ (see fig. 12), $T \approx 300$ (K)) is approximately 4.5. This is consistent with X-ray measurements [69].
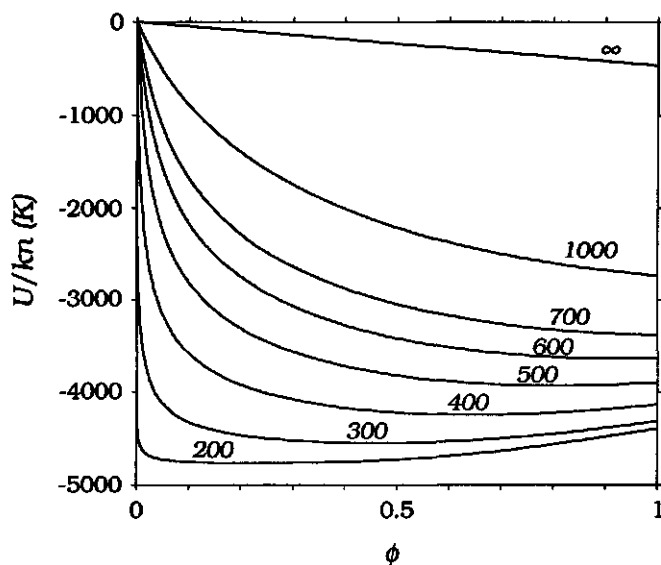
Figure 9. *Mean molecular cohesive energy (U/kn given in K) as a function of density at various temperatures. Temperatures are indicated along the curves. At infinite temperature, random-mixing occurs.*

The tetrahedral coordination of water molecules does not imply that fluid water has a long-range tetrahedral structure. In our calculations the tetrahedral sublattices of the bcc lattice are equally occupied. This precludes the formation of long-range tetrahedral ordering.

It is remarkable that at constant density, the coordination number as a function of temperature has a maximum. This is due to the increasing effectiveness of the repulsive interactions upon decrease of the temperature. The temperature of this maximum increases with increasing densities. Both the hydrogen-bonding ratio and the coordination number as a function of temperature show an inflection.

The cohesive energy per molecule can be calculated from the distribution of contacts and the interaction energies of table I (eq. (11)). In case of random mixing, the average number of intermolecular contacts would be 8ϕ per molecule. Of these contacts, 1 out of 8 would then be a hydrogen bond. Consequently, the mean

molecular cohesive energy would decrease linearly with density: $U/kn = (u_{Hb} + 7u_{nHb})\frac{1}{2}\phi/k = -471.4\phi$ K. This occurs only at infinite temperature.

According to the present theory, the mean molecular cohesive-energy is concave as a function of density at finite temperatures. This is shown in fig. 9. Upon increase of the density from $\phi = 0$, the molecular energy first decreases steeply due to hydrogen-bond formation. Especially if the temperature is not too high, the increase of the number of hydrogen bonds per molecule levels off at intermediate density. Upon further increase of the density, mainly the number of repulsive contacts increases and hence the molecular energy. Such an increase of the molecular energy upon density is quite uncommon among simple fluids. This anomaly of water will be shown to be closely related to the so-called hydrophobic effect.

According to eq. (12), the entropy of the fluid can be related to the distribution of contacts. The contribution to the entropy density due to the non-randomness of the distribution of contacts is given by; $S^{exc}/kN = -\frac{1}{2}\sum_{\alpha,\beta,d} \phi_{\alpha\beta}^d \ln(\phi_{\alpha\beta}^d/\phi_{\alpha\beta}^{*d})$. The coordinate z can be omitted now since we are considering homogeneous systems. Obviously this contribution vanishes for a completely vacant system ($\phi = 0$). At low temperatures this ordering contribution is important.

The liquid-vapour phase equilibrium is be related to the non-linearity of the Helmholtz energy as a function of composition. Coexisting phases can be identified as phases with different compositions for which the Helmholtz energy, $F(\phi)$, has a common tangent, such that the Helmholtz energy is higher than this tangent for intermediate compositions (fig. 10). Equivalently, the compositions of the coexisting phases satisfy the set of equations

and
$$p^{liq} = p^{vap}$$
$$\mu^{liq} = \mu^{vap} \tag{13}$$

or, again equivalently

$$f_0^{liq} = f_0^{vap}$$
$$f_1^{liq} = f_1^{vap} \tag{14}$$
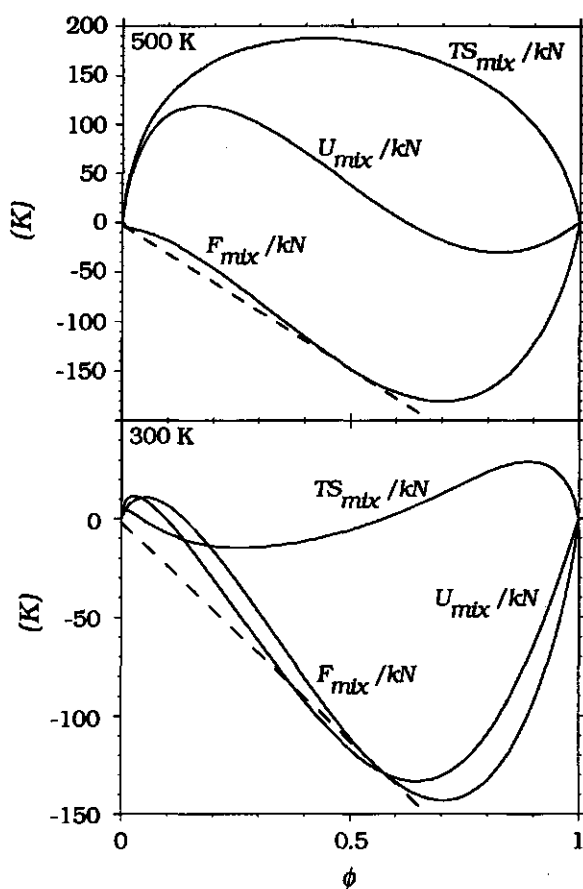
Figure 10. *Helmholtz energy of mixing water molecules and vacancies and its energetic and entropic contributions as a function of density at two temperatures. The dashed line is the double tangent of the Helmholtz energy of mixing; it meets the curve F_{mix}/kN at coexisting compositions.*

where the subscripts 1 and 0 indicate water and vacancies respectively.

We will use 'mixing terminology' for the liquid-vapour equilibrium since liquid-vapour equilibrium of a pure fluid is very similar to the phase equilibrium in a binary mixture. This holds especially for lattice models, where vacancies can be handled as just another type of monomer.

The Helmholtz energy of mixing, $F_{mix}(\phi)$, is obtained by subtracting from the total Helmholtz energy, $F(\phi)$, the terms $\phi F(1) - (1-\phi)F(0)$ that are linear in density. Hence, $F_{mix}(\phi)$ vanishes for the pure systems $\phi = 0$ and $\phi = 1$. The same applies to its energetic and entropic contributions. Obviously, $S(0)$ vanishes. By virtue of the present choice of the reference state for the potential energy of the faces also $U(0)$ and hence $F(0)$ vanish. Positive contributions to F_{mix} promote phase separation. Negative contributions promote mixing. The Helmholtz energy of mixing, $F_{mix}(\phi)$, can be subdivided into an entropic contribution, $-TS_{mix}(\phi)$, and an energetic one $U_{mix}(\phi)$.

The entropy of mixing, $S_{mix}(\phi)$ contains an ideal contribution due to random mixing, which is always positive and promotes mixing. From the first term on the right-hand side of eq. (12) it follows that $S_{mix}^{id.}(\phi)/N = -k(\phi \ln \phi + (1-\phi)\ln(1-\phi))$ for a 'binary' (containing molecules and vacancies) isotropic system. In addition to this, there is a contribution due to ordering $S_{mix}^{exc}(\phi)/N$. Within the present theory, this contribution can be derived from the second term on the right-hand side of eq. (12). As can be seen in fig. 10, at lower temperature this contribution can be so large that the mixing entropy can become negative.

Usually, if no strong directional interactions play a role, the mixing energy, $U_{mix}(\phi)$, is positive and promotes phase separation. For water this is different. Especially at lower temperatures $U_{mix}(\phi)$ is negative at higher densities (see fig. 10). This extends the regime of liquid density that is stable with respect to phase separation (compare figs. 2.b and 12) and explains why liquid water at ambient conditions has an open structure.

As can be seen in fig. 11 and 12, some characteristic features of the equation of state and the liquid-vapour phase behaviour of water are reproduced at least semiquantitatively by the theory.

For the present model for water, values of $p_{sat}v/kT^{*}$ are lower than for a system of isotropic monomers at the same values of T/T^{*}, and the agreement with the experimental behaviour of water is much better (compare figs. 11.a and 2). The theory even underestimates somewhat the experimental values.

In contrast to the zeroth-order (random-mixing, Bragg-Williams) treatment of systems containing two types of monomers and to the
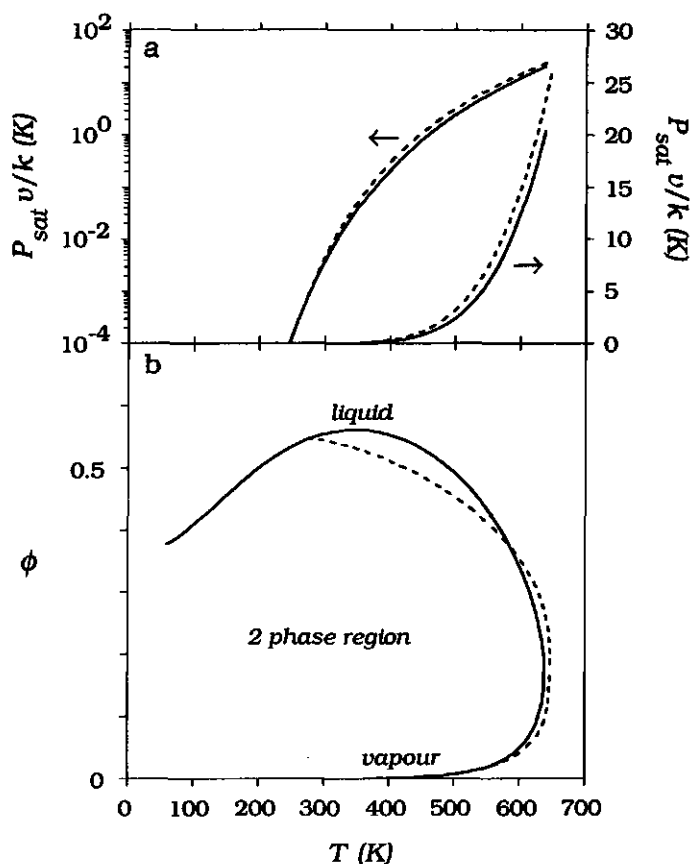
Figure 11. *Liquid-vapour phase diagram of water. a: saturated vapour pressure, b: binodal. Drawn curves (————) are theoretical; dashed curves (------) are from experimental results.*

first-order (quasi-chemical) treatment of isotropic monomers of the previous section, the binodal curve for the present model for water is asymmetric with respect to exchange of the monomer types (water molecules and vacancies). The density of the liquid coexisting with vapour and the isobaric density at various pressures have a maximum as a function of temperature. According to our calculations, the temperature of maximum isobaric density decreases with increasing pressure (see fig. 12). This is also found experimentally [70]. The theoretical maximum is more pronounced and occurs at a higher temperature than is found experimentally.
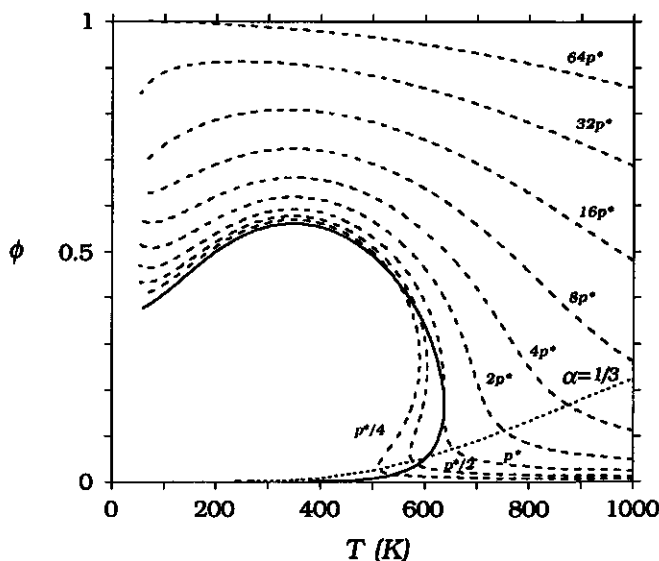
Figure 12. *Theoretical isobaric densities at various pressures* (------, p^* *is the critical pressure*). *The liquid-vapour coexistence curve* (———) *encloses the two-phase region where the isobars show a Van der Waals loop. The dotted curve* (·······) *applies for* $\alpha = \frac{1}{3}$. *At larger densities,* $\alpha > \frac{1}{3}$ *and hence the hydrogen-bonds form a macroscopic network according to the classical gelation criterion.*

At the theoretical critical point, $T^* = 639.0$ K, $\phi^* = 0.16539$ and $p^*v/k = 20.595$ K. In the plot of the experimental coexistence curve in fig. 11, the density maximum can hardly be seen. For obvious reasons, the experimental curve does not extend below 0 °C.

The difference between the theoretical and experimental density maximum might be explained by the fact that we only accounted for density variations due to changes of the average site occupation. We did not account for any increase of the average hydrogen-bond length. Assuming that this contribution to the thermal expansion of liquid water can be approximated by extrapolation from the thermal expansion of ice, the anomalous density increase with temperature would extend up to about 50-60 °C [17]

In calculating the theoretical curve, crystallisation was not allowed; tetrahedral sublattices were not allowed to be differently

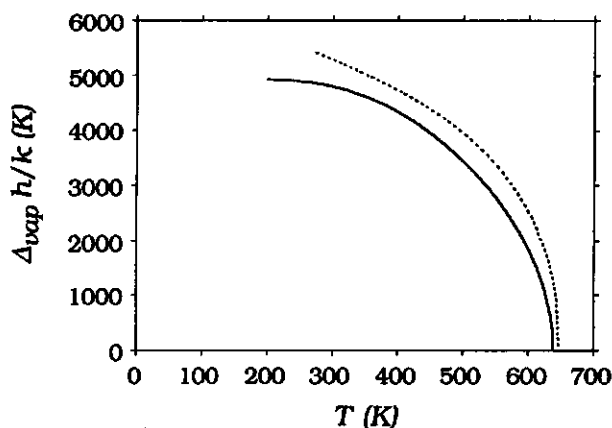Figure 13. *Molecular enthalpy of vaporisation of water ($\Delta_{vap} h/T$ equals molecular entropy of vaporisation $\Delta_{vap}s$). Experimental result ($\cdots\cdots$), theoretical result (———).*

occupied. So, for the low temperature regime we are dealing with a supercooled fluid. The experimental isobaric density of liquid water shows a pronounced decrease on supercooling. At about 228 K it seems to have the same density as ice Ih [70]. Theoretically, at 200.6 K the density of the coexisting liquid is $\phi = \frac{1}{2}$.

The calculated values for the molecular heat of vaporisation are over the whole temperature range somewhat lower than the experimental ones. The value of $\Delta_{vap}h/kT^*$ calculated for the present model is far higher than that for isotropic monomers on the same lattice at the same values of T/T^* (compare figs. 13 and 3). This is another manifestation of the high energy density of liquid water due to the hydrogen bonds. Although quantitative agreement with experiment is not perfect, the present model for water is an important improvement as compared to the model with isotropic monomers, also with respect to the heat of vaporisation.

According to simple thermodynamic reasoning, the anomalous density increase with increasing temperature is related to an anomalous increase of entropy with increasing density:

$$\left(\frac{\partial V}{\partial T}\right)_{p,n_1} = -\left(\frac{\partial S}{\partial p}\right)_{T,n_1} = -\left(\frac{\partial S}{\partial V}\right)_{T,n_1}\left(\frac{\partial V}{\partial p}\right)_{T,n_1}$$

where the first equality derives from $dG = -SdT + Vdp + \mu_1 dn_1$. In a thermodynamically stable system, $(\partial V/\partial p)_{T,n}$ is negative. Hence, $(\partial V/\partial T)_{p,n}$ and $(\partial S/\partial V)_{T,n}$ have the same sign. Usually they are positive; the entropy of a fluid usually increases upon increasing volume and the density decreases with increasing temperature. With water at low temperatures this is different.

In the present model, expansion corresponds to addition of vacancies: $(\partial S/\partial V)_{T,n_1} = s_0/v$ where $s_0 = (\partial S/\partial n_0)_{T,n_1}$. From $dF = -SdT + f_0 dn_0 + f_1 dn_1$, the Maxwell relation $s_0 = -(\partial f_0/\partial T)_{n_0,n_1}$ is derived. The partial entropy of a vacancy, s_0 can be divided into an *ideal* and a *non-ideal* contribution. The ideal contribution, which accounts for the increase of the translational freedom of the molecules due to an increasing volume, is equal to s_0 of an athermal lattice gas. By differentiation of the first term of the right-hand side of eq. (12) we obtain $-k \ln \phi_0$ for this ideal term (we are considering homogeneous systems now, so the coordinate z can be omitted). Obviously, this equals the ideal term of $-f_0/T$ (see eq. (2)). The term, $-k \ln \phi_0$, is always positive, and the non-ideal term must be smaller than $k \ln \phi_0$ in order to render $(\partial S/\partial V)_{T,n}$ and $(\partial V/\partial T)_{p,n}$ negative. The non-ideal contribution to the partial entropy is a result of ordering. In the present theory, it is directly related to the distribution of contacts (see eq. (12)). For water, such ordering is more important than for most other liquids where $(\partial V/\partial T)_{p,n}$ and $(\partial S/\partial V)_{T,n}$ are positive for all temperatures. This is due to the strong directional interactions of the water molecules. Upon expansion of liquid water the number of hydrogen bonds decreases only slightly. In the expanded fluid the number of ways to realise those hydrogen bonds is reduced hence the molecules loose orientational freedom.

A similar entropy lowering upon expansion as found with cold water, is also observed with polymer networks for which the entropy is lowered upon uptake of solvent at constant temperature. With swelling of a polymer network the chains of the network are stretched and can assume fewer conformations and the segments of the chains loose orientational and translational freedom. As already

stated, the structure of water can be pictured as a macroscopic, hydrogen-bonded network. The similarity between liquid water at low temperatures and polymer networks does not only apply to its structure, but also holds for some thermodynamic properties.

6 THE LIQUID-VAPOUR INTERFACE OF WATER

In the previous sections we discussed the properties of homogeneous water including the liquid-vapour phase equilibrium. Now we will examine the interfacial region between liquid and vapour where the density decreases from liquid to vapour. This density profile can be characterised by two distinct decay lengths. The decay of the density towards the liquid is much slower. For instance, at 295 K ξ^{vap} = 0.2156 layers = 0.04872 nm and ξ^{liq} = 2.803 lattice layers = 0.6334 nm. This liquid decay length for water exceeds that of isotropical monomers at similar reduced temperatures by a factor of about ten.

Recall that for isotropic monomers the profile of the liquid vapour interface is symmetrical with respect to exchange of holes and molecules (see fig. 4). For that system, the density decay lengths on the liquid and vapour sides of the interface are the same, and similar to the vapour decay length of water at the same reduced temperature. In fig. 16 the decay lengths are plotted for the complete temperature range.

A measure of the interfacial thickness that is often given as the result of neutron reflection [71] and X-ray reflection experiments [72] is the standard deviation of the normalised derivative of the density profile, usually denoted by the symbol σ. In a lattice model this can be calculated as $\sigma^2 = \sum_z z^2 \left(\phi^{vap} - \phi^{liq}\right) \Delta\phi(z) - \left(\sum_z z\left(\phi^{vap} - \phi^{liq}\right)\Delta\phi(z)\right)^2$ where $\Delta\phi(z) = \phi\left(z + \frac{1}{2}\right) - \phi\left(z - \frac{1}{2}\right)$. We obtain σ = 2.822 lattice layers for the profile of fig. 14 at 295 K. In fig. 16 the calculated σ is plotted for the whole relevant temperature range.

It should be noted that in our calculation capillary waves are disregarded. This may lead to an underestimation of the interfacial thickness, and to an overestimation of the interfacial tension [73].
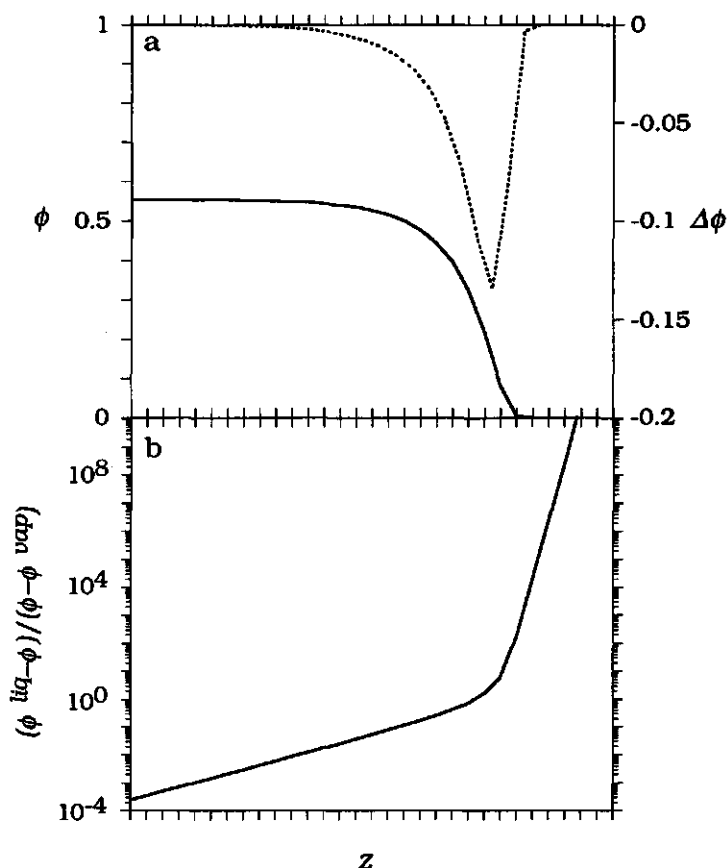
Figure 14. a: *Density profile of the liquid vapour interface at 295 K. To guide the eye, calculated points are connected by the drawn curve* ——— *. The dotted curve* ------- *connects the points $\Delta\phi(z) = \phi\left(z+\frac{1}{2}\right) - \phi\left(z-\frac{1}{2}\right)$ (only defined at such z that $z\pm\frac{1}{2}$ is an integer).* b: *Plot of $\ln\left(\left(\phi^{liq} - \phi\right)\big/\left(\phi - \phi^{vap}\right)\right)$, where ϕ^{liq} and ϕ^{vap} are the density of the liquid and the vapour, respectively. Ticks on the z-axis indicate centres of lattice layers.*

Usually, the thickness of a fluid interface and the density decay length increase with temperature until the critical temperature, at which they diverge, such as shown in fig. 5. However, according to our calculations this is not the case for the water, for which the interfacial thickness has a minimum at about 450 K. The increasing

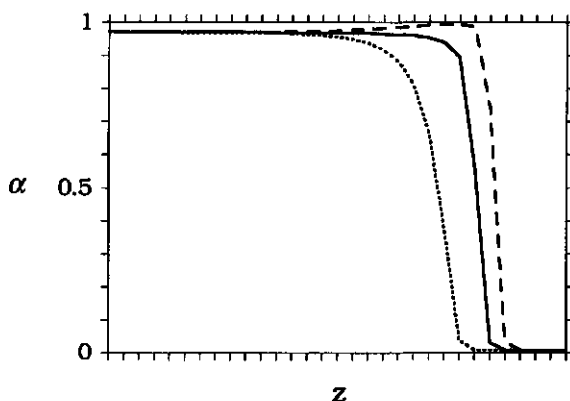Figure 15. *Hydrogen-bonding ratio of H-donor and acceptor faces in the interfacial region at 295 K. With the present set of parameters, the hydrogen-bonding ratio of donor and acceptor faces are equal. Dashed – – –, solid —— and dotted ······ curves are for donors and acceptors that are directed towards the liquid (negative z-direction), laterally, and towards the vapour (positive z-direction), respectively.*

thickness upon decreasing temperature is mainly due to the behaviour at the liquid side of the interfacial region (see fig. 14). The density decay length of the liquid also has a minimum which is found at a somewhat higher temperature. This behaviour is obviously due to the associated, hydrogen-bonded structure of water which is promoted upon lowering the temperature. In liquid water, the free-energy cost associated with a gradient of the density (as for instance reflected in the coefficient of the "squared-gradient term" of the Van der Waals- / Cahn-Hilliard theory [6, 62, 63]) is higher than in simple fluids. This is due to the reduced possibilities for hydrogen-bonding of proton donors and acceptors directed towards a region of lower density (see fig. 15). To our best knowledge, such behaviour of the interfacial thickness and the density-decay length of liquid water has not been predicted so far. It still awaits experimental confirmation.

Our set of interaction parameters is such that the proton donors and acceptors are similar, apart from being complementary in forming hydrogen-bonds. For this reason, the orientational distribution of the water molecules is the same in the interfacial
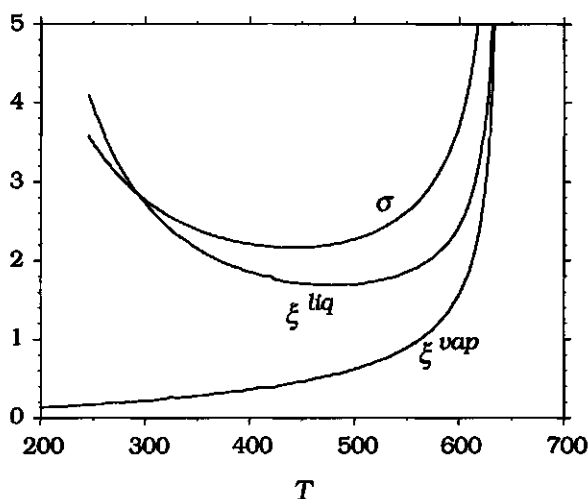
Figure 16. *Interfacial thickness σ, Density decay length of the liquid,* ϕ^{liq}, *and of the vapour* ϕ^{vap}, *given in lattice layers, the layer spacing is* 2.260 Å.

region as in the two homogeneous bulk phases; all orientations are equally probable.

An important structural feature that emerges from the present evaluation is related to correlations in the interfacial region. These are highly anisotropic. At not too high temperatures, the hydrogen-bonding ratio is high at liquid density whereas at vapour density it is low (see fig. 7). Hence, in the interfacial region the hydrogen-bonding ratio, α, decreases going from liquid to vapour. This decrease is steeper than the decrease of density. In the interfacial region, the hydrogen-bond ratios of the proton donors and acceptors strongly depends on their directions. Donors and acceptors directed towards the vapour 'see' a relatively low density and as a consequence their hydrogen-bonding ratio is relatively low. This is plotted in fig. 15 for the same interfacial region as pictured in fig. 14.

Experimentally, the liquid-vapour interfacial tension of water as a function of temperature is convex at lower temperatures and has an inflection at about 250 °C [4]. So, the interfacial entropy as a function of temperature, $s^s = (\partial S/\partial A)_{T,V,n_w} = -d\gamma/dT$, has a maximum there. Below this temperature the interfacial entropy of the aqueous liquid-
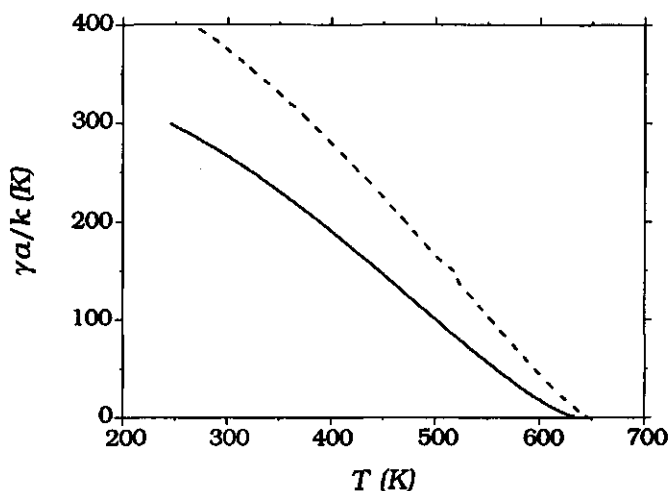
Figure 17. *The interfacial tension of the aqueous liquid-vapour interface, experimental [4] (· · · · · ·) and theoretical result (——).*

vapour interface increases with temperature. It has been suggested that this inflection of the interfacial tension is related to the well-known anomalies of homogeneous water [6]. However, in section 4 we have shown that a lattice gas of isotropic monomers, that does not have any of the anomalous properties that are so typical for water, also shows such an inflection. This indicates that the inflection of the liquid-vapour interfacial tension is at least not exclusively due to the orientation-dependent nature of the intermolecular interactions.

The values of $\gamma a / k T^*$ for the water model are fairly similar to those for isotropic monomers at the same values of T/T^*. Over the whole temperature range, the theoretical interfacial tension is lower than the experimental value. This discrepancy seems to be more serious than for various properties of homogeneous systems. This might be due to the fact that neglect of the long-range character of the dispersion forces is of more consequence in the surface as it is for bulk phases. The values for the two interaction parameters were determined by a fit of liquid-vapour phase-coexistence at 273.16 K. These same values are used throughout all other calculations including those of the liquid-vapour interface.

Even so, the liquid-vapour interfacial tension as calculated here, is much closer to the experiment than the result from the density-

functional theory by Yang at al.. [41, 42]. In our opinion, this is due to the more accurate way in which we have accounted for the anisotropic correlations in homogeneous as well as in heterogeneous water.

8 CONCLUDING REMARKS

The present lattice theory for water in which orientation-dependent intermolecular interactions and the ensuing local correlations are accounted for, is capable of reproducing semiquantitatively various properties of water. The origins of the differences between the anomalous behaviour of water and the behaviour of isotropic molecules is clarified.

It is straightforward to apply the present method to a large range of circumstances, including water at solid surfaces, in slits between such surfaces and aqueous solutions. This will be elaborated in coming chapters.

APPENDIX I *THE RESIDUAL ENTROPY OF PERFECT ICE*

For homogeneous systems where K sublattices of J sites each, are allowed to be differently occupied, the combinatory formula that is the basis of the present first-order treatment (eq. (11) of ref. [1]) can be rewritten as

$$\Omega\left(\left\{n_A^o(s)\right\},\left\{n_{\alpha\beta}^d(s)\right\}\right) = \frac{J!^K}{\displaystyle\prod_{s,A,o} n_A^o(s)!} \prod_{s,d,\alpha,\beta}\left(\frac{n_{\alpha\beta}^{*d}(s)!}{n_{\alpha\beta}^d(s)!}\right)^{\frac{1}{2}}$$

$$= \frac{J^{JK}}{\displaystyle\prod_{s,A,o} n_A^o(s)^{n_A^o(s)}} \prod_{w,d,\alpha,\beta}\left(\frac{n_{\alpha\beta}^{*d}(s)^{n_{\alpha\beta}^{*d}(s)}}{n_{\alpha\beta}^d(s)^{n_{\alpha\beta}^d(s)}}\right)^{\frac{1}{2}} \qquad (I.1)$$

Here s indicates the separate sublattices. We have made use of Sterling's theorem for large n: $n! = (n/e)^n$. The configurational entropy is given by Boltzmann's equation: $S = k \ln \Omega$.

The bcc lattice can be subdivided into two intertwining tetrahedral sublattices ($K = 2$). In low pressure ice close to 0 K all water molecules are found on one tetrahedral sublattice, that we will indicate by $w = 1$. The other tetrahedral sublattice, that we will indicate by $w = 2$, is completely vacant. So the number of water molecules, n_1, and vacancies, n_0, are given by $n_1 = n_0 = J = \frac{1}{2}N$ (N being the total number of sites of the system). There are four directions to go from a site to a site belonging to the same sublattice and also four directions to go to sites of the other sublattice. Each water molecule is tetrahedrally coordinated by four other water molecules that are hydrogen-bonded to the central molecule. Each water molecule is also tetrahedrally coordinated by four vacancies that are located on the other sublattice ($w = 2$). Each vacancy is tetrahedrally coordinated by four vacancies and by four water molecules that are located on sublattice 1. Only with six of the twelve possible orientations of the water molecule the proton donors and acceptors are directed towards sites of the same sublattice. These six orientations are equally probable, so each occurs at a frequency of $\frac{1}{6}J$. The J vacancies, for which no orientations can be distinguished, are all located on sublattice 2. Substitution into the first factor of eq. (I.1) results in 6^J. This would be the number of configurations of the J water molecules of which the proton donors and acceptors are directed towards other water molecules.

For perfect ice, this number is reduced by the condition all hydrogen bonds should be intact: $n_{AD}^d(1) = n_{DA}^d(1) = \frac{1}{2}J$ and $n_{DD}^d(1) = n_{AA}^d(1) = 0$ for each d. For the distribution of molecules over orientations given before, the numbers of contacts between molecules on sublattice 1, if formed at random, are given by: $n_{AD}^{*d}(1) = n_{DA}^{*d}(1) = n_{DD}^{*d}(1) = n_{AA}^{*d}(J) = \frac{1}{4}J$ for each direction d. For contacts between sites of different sublattices: $n_{10}^{*d}(1) = n_{01}^{*d}(2) = n_{10}^d(1) = n_{01}^d(2) = J$ for each d. Contacts between sites of sublattice 2 can only be between vacancies, so $n_{00}^{*d}(2) = n_{00}^d(2) = J$ for each d. Substituting these values into the second factor on the right-hand side of eq. (I.1) a value of $\left(\frac{1}{4}\right)^J$ is obtained. Hence we obtain $\left(\frac{3}{2}\right)^J$ for the number of configurations of J water molecules of ice.

This equals Pauling's result [60, 61] and hence it is demonstrated that our model and the first-order statistical treatment that we apply

is consistent with Pauling's result for the residual entropy of ice and that Pauling's result follows from the present theory as a limiting case for low temperature.

REFERENCES

1   Besseling, N. A. M. "Statistical thermodynamics of molecules with orientation-dependent interactions in homogeneous and heterogeneous systems". Chapter II, Ibid.
2   Guggenheim, E. A. *Mixtures*; Fowler, R. H., et al.; Clarendon: Oxford, 1952.
3   Hill, T. L. *Introduction to Statistical Thermodynamics*; Addison-Wesley: 1962.
4   Volyak, L. D. *Dokl. Akad. Nauk. SSSR*, *74*, 307-310 (1950) "Surface tension of water as a function of temperature".
5   Grigull, U.; Bach, J. *Brennst.-Wärme-Kraft*, *18*, 73-75 (1966) "Die Oberflächenspannung und verwandte Zustandsgrößen des Wassers".
6   Rowlinson, J. S.; Widom, B. *Molecular Theory of Capilarity*; Baldwin, J. E., et al.; Clarendon: Oxford, 1982.
7   Evans, D. F.; Ninham, B. W. *J. Phys. Chem.*, *90*, 226-234 (1986) "Molecular forces in the self-organization of amphiphiles".
8   Privalov, P. L.; Gill, S. J. *Pure & Appl. Chem.*, *61*, 1097-1104 (1989) "The hydrophobic effect: a reappraisal".
9   Privalov, P. L.; Gill, S. J. *Adv. Protein Chem.*, *39*, 191-234 (1988) "Stability of protein structure and hydrophobic interaction".
10   Creighton, T. E. *Proteins: Structures and Molecular Properties*; Freeman: New York, 1983.
11   Pashley, R. M.; Israelachvili, J. N. *J. Colloid Interface Sci.*, *97*, 446-455 (1984) "DLVO and Hydration Forces between Mica Surfaces in Mg2+, Ca2+, Sr2+ and Ba2+ Chloride Solutions".
12   Claeson, P. M. *Progr. Colloid & Polymer Sci*, *74*, 48-54 (1987) "Experimental Evidence for Repulsive and Atractive Forces not accounted for by conventional DLVO theory".
13   Rand, R. P.; Parsegian, V. A. *Biochim. Biophys. Acta*, *778*, 224-228 (1989) "Hydration forces between phospholipid bilayers".
14   Frank, H. S.; Wen, W. Y. *Discuss. Faraday Soc.*, *24*, 133 (1957) "Structural aspects of ion-solvent interaction in aqueous solutions: a suggested picture of water structure".
15   Némethy, G.; Scheraga, H. A. *J. Chem. Phys.*, *36*, 3382-3400 (1962) "Structure of water and hydrophobic bonding in proteins. I. A model for the thermodynamic properties of liquid water".
16   Bernal, J. D.; Fowler, R. H. *J. Chem. Phys.*, *1*, 515-548 (1933) "A theory of water and ionic solution, with particular reference to hydrogen and hydroxyl ions".
17   Gibbs, J. H. *Ann. New York Acad. Sci.*, *303*, 10-19 (1977) "On the Nature of Liquid Water".
18   Gibbs, J. H.; Cohen, C.; Fleming III, P. D.; Porosoff, H. *J. Sol. Chem.*, *2*, 277-299 (1973) "Toward a model for liquid water".

19   Stanley, H. E. *J. Phys. A: Math. Gen*, *12*, 329-337 (1979) "A polychromatic correlated-site percolation problem with possible relevance to the unusual behaviour of supercooled H2O and D2O".

20   Stanley, H. E.; Blumberg, R. L.; Geiger, A. *Phys. Rev. B*, *28*, 1626-1629 (1983) "Gelation models of hydrogen bond networks in liquid water".

21   Rahman, A.; Stillinger, F. H. *J. Chem. Phys.*, *55*, 3336-3359 (1971) "Molecular Dynamics study of liquid water".

22   Stillinger, F. H.; Rahman, A. *J. Chem. Phys.*, *57*, (1972) "Molecular study of temperature effects on water structure and kinetics".

23   Postma, J. P. M.; Berendsen, J. C.; Haak, J. R. *Faraday Symp. Chem. Soc.*, *17*, (1982) "Thermodynamics of cavity formation in water".

24   Postma, J. P. M. *MD of H2O. A Molecular Dynamics Study of Water*; Thesis Groningen State University: 1985.

25   Blumberg, R. L.; Stanley, H. E. *J. Chem. Phys.*, *80*, 5230-5241 (1984) "Connectivity of hydrogen bonds in liquid water".

26   Bagchi, B.; Gibbs, J. H. *Chem. Phys. Lett.*, *94*, 253-258 (1983) "Agreement between the gelation and molecular dynamics models of the hydrogen-bond network in water".

27   Geiger, A.; Stillinger, F. H.; Rahman, A. *J. Chem. Phys.*, *70*, 4185-4193 (1978) "Aspects of the percolation process for hydrogen-bond networks in water".

28   Geiger, A.; Stanley, H. E. *Phys. Rev. Lett.*, *49*, 1895-1898 (1982) "Tests of universality of percolation exponents for a three-dimensional continuum system of interacting waterlike particles".

29   Poole, P. H.; Sciortino, F.; Essmann, U.; Stanley, H. E. *Nature*, *360*, 324-328 (1992) "Phase behaviour of metastable water".

30   Matsumoto, M.; Kataoka, Y. *J. Chem. Phys.*, *88*, 3233-3245 (1988) "Study on liquid-vapour interface of water. I. Simulational results of thermodynamic properties and orientational structure".

31   Wilson, M. A. *J. Chem. Phys.*, *88*, 3281-3285 (1988) "Surface potential of the water liquid-vapor interface".

32   Wilson, M. A.; Pohorille, A.; Pratt, L. R. *J. Phys. Chem.*, *91*, 4873-4881 (1987) "Molecular Dynamics of the water liquid-vapor interface".

33   Townsend, R. M.; Rice, S. A. *J. Chem. Phys.*, *94*, 2207-2218 (1991) "Molecular dynamics studies of the liquid-vapor interface of water".

34   Berkowitz, M. L.; Raghavan, K. *Langmuir*, *7*, 1042-1044 (1991) "Computer Simulation of a Water/Membrane Interface".

35   Delville, A. *Langmuir*, *8*, 1796-1805 (1992) "Structure of liquids at a solid interface: An application to the swelling of clay by water".

36   Pratt, L. R.; Chandler, D. *J. Chem. Phys.*, *67*, 3683-3704 (1977) "Theory of the hydrophobic effect".

37   Pettitt, B. M.; Rossky, P. J. *J. Chem. Phys.*, *77*, 1451-1457 (1982) "Integral equation predictions of liquid state structure for waterlike intermolecular potentials".

38   Ichiye, T.; Chandler, D. *J. Phys. Chem.*, *92*, 5257-5261 (1988) "Hypernetted chain closure reference interaction site method theory of structure and thermodynamics for alkanes in water".

39 Dahl, L. W.; Andersen, H. C. *J. Chem. Phys.*, *78*, 1962-1979 (1982) "Cluster expansions for hydrogen-bonded fluids. III. Water".

40 Dahl, L. W.; Andersen, H. C. *J. Chem. Phys.*, *78*, 1980-1993 (1983) "A theory of the anomalous thermodynamic properties of liquid water".

41 Yang, B.; Sullivan, D. E.; Tjipto-Margo, B.; Gray, C. G. *Mol. Phys.*, *76*, 709-735 (1992) "Density-functional theory of water liquid-vapour interface".

42 Yang, B.; Sullivan, D. E.; Tjipto-Margo, B.; Gray, C. G. *J. Phys.: Condens. Matter*, *3*, 109-125 (1991) "Molecular orientational structure of the water liquid/vapour interface".

43 Bell, G. M. *J. Phys. C: Solid State Phys.*, *5*, 889-905 (1972) "Statistical mechanics of water: lattice model with directed bonding".

44 Fleming III, P. D.; Gibbs, J. H. *J. Stat. Phys.*, *10*, 157-173 (1973) "An adaptation of the lattice gas to the water problem".

45 Flemming III, P. D.; Gibbs, J. H. *J. Stat. Phys.*, *10*, 351 378 (1973) "An adaptation of the lattice gas to the water problem. II. Second-order approximation".

46 Herrick, D. R.; Stillinger, F. H. *J. Chem. Phys.*, *65*, 1345-1356 (1976) "Quantizatation for lattice-gas models of water".

47 Bell, G. M.; Salt, D. W. *J. Chem. Soc. Faraday Trans. II*, *72*, 76-86 (1976) "Three-dimensional lattice model for the water/ice system".

48 Lavis, D. A.; Christou, N. I. *J. Phys. A: Math. Gen.*, *10*, 2153-2169 (1977) "The dielectric constant of a bonded lattice model for water".

49 Wilson, G. L.; Bell, G. M. *J. Chem. Soc. Faraday Trans. II*, *74*, 1702-1722 (1978) "Lattice model for aqueous solutions of non-electrolytes".

50 Heilmann, O. J.; Huckaby, D. A. *J. Stat. Phys.*, *20*, 371-383 (1979) "Phase transitions in lattice gas models for water".

51 Meijer, P. H. E.; Kikuchi, R. *Physica*, *109A*, 365-381 (1981) "Phase diagram of water based on a lattice model".

52 Meijer, P. H. E.; Kikuchi, R.; Van Royen, E. *Physica*, *115A*, 124-142 (1982) "Extended lattice model of water: two-sublattice, two-orientation model".

53 Van Royen, E.; Meijer, P. H. E. *Physica*, *127A*, 87-112 (1984) "Dependence of the phase diagram on the coupling parameters in water-lattice models".

54 Besseling, N. A. M. "On the molecular interpretation of the hydrophobic effect". Chapter IV, Ibid.

55 Besseling, N. A. M. "Hydration Forces between Planar Surfaces". Chapter V, Ibid.

56 Besseling, N. A. M. "Water-Vapour Adsorption, Wetting, Capillary Condensation in Slits.". Chapter VI, Ibid.

57 Franks, F. in *Water. A Comprehensive Treatise 1*, edited by Franks, F. (Plenum, New York-London, 1972) pp. 115-149. "The properties of ice".

58 Curtis, L. A.; Frurip, D. J.; Blander, M. *J. Chem. Phys.*, *71*, 2703-2711 (1979) "Studies of molecular association in H2O and D2O vapors by measurement of thermal conductivity".

59 Joesten, M. D.; Schaad, L. J. *Hydrogen Bonding*; Marcel Dekker: New York, 1974.

60 Pauling, L. *J. Am. Chem. Soc.*, *57*, 2680-2685 (1935) "The Structure and Entropy of Ice and Other Crystals with Some Randomness of Atomic Arrangement".

61 Hollins, G. T. *Proc. Phys. Soc.*, *84*, 1001-1016 (1964) "Configurational statistics and the Dielectric Constant of Ice".

62 Rowlinson, J. S.; Van der Waals, J. D. *J. Stat. Phys.*, *20*, 197-244 (1979) "Translation of J. D. van der Waals' "The thermodynamic theory of capillarity under the hypothesis of a continuous variation of density"". This translation by Rowlinson is probably the best accessible version of Van der Waals' paper. It contains references to the original versions.

63 Cahn, J. W.; Hilliard, J. E. *J. Chem. Phys.*, *28*, 258-267 (1958) "Free Energy of a Nonuniform System. I. Interfacial Free Energy".

64 Flory, P. J. *Priciples of Polymer Chemistry*; 1953.

65 Stockmayer, W. H. *J. Chem. Phys.*, *11*, 45-55 (1943) "Theory of Molecular Size Distribution and Gel Formation in Branched-Chain Polymers".

66 Stauffer, D.; Coniglio, A.; Adam, M. *Adv. Polym. Sci.*, *44*, 103-158 (1982) "Gelation and Critical Phenomena".

67 Cohen, C.; Gibbs, J. H.; Fleming III, P. D. *J. Chem. Phys.*, *59*, 5511-5516 (1973) "Condensation and gelation: Clarification of Stockmayer's analogy".

68 Stanley, H. E.; Teixeira, J. *J. Chem. Phys.*, *73*, 3404-3422 (1980) "Interpretation of the unusual behaviour of H_2O and D_2O at low temperatures: Tests of a percolation model".

69 Narten, A. H.; Danford, M. D.; Levy, H. A. *Discuss. Faraday Soc.*, *43*, 97-107 (1967) "X-ray diffraction study of liquid water in the temperature range 4-200 °C".

70 Angell, C. A. in *Water: A Comprehensive Treatise*, edited by Franks, F. (Plenum, New York, 1982) pp. "Supercooled water".

71 Penfold, J.; Thomas, R. K. *J. Phys.: Condens. Matter*, *2*, 1369-1412 (1989) "The Application of the Specular Reflection of Neutrons to the Study of Interfaces".

72 Braslau, A.; Pershan, P. S.; Swislow, G.; Ocko, B. M.; Als-Nielsen, J. *Phys. Rev. A*, *38*, 2457-2470 (1988) "Capillary waves on the Surface of Simple Liquids Measured by X-ray Reflectivity".

73 Kayser, R. F. *Phys. Rev. A*, *33*, 1948-1956 (1986) "Effect of Capillary Waves on Surface Tension".

CHAPTER IV

ON THE MOLECULAR INTERPRETATION
OF THE HYDROPHOBIC EFFECT

The temperature dependence of the solubility of apolar compounds in water is examined. We indicate that the hydrophobic effect and the anomalous variation of the isobaric density of water with varying temperature have the same molecular basis. By means of a previously introduced lattice-gas based on a first-order (quasi-chemical) approximation, these macroscopic phenomena are related to the orientation-dependent intermolecular interactions of water. In this approach, it is not necessary to make assumptions on the occurrence of "iceberg"-like structures around apolar solutes. The model, not only involves the strong directional attraction, known as the hydrogen bond. Repulsive interactions that operate at the same intermolecular separation as the hydrogen bond, but at different relative orientations also appear to be important. The negative solvation entropy of apolar molecules is related to changes of the local ordering of the water molecules similar to those occurring upon expansion of pure water. The negative solvation enthalpy of small apolar molecules is due to reduction of the number of repulsive non-hydrogen bonding interactions between neighbouring water molecules. Calculations on an extended flat hydrophobic surface indicate that the anomalous aspects of the solvation thermodynamics do not occur with bulky apolar particles.

1 INTRODUCTION

Various macroscopic properties of water are still not understood very well from a molecular point of view. The well-known maximum of the isobaric density as a function of temperature is one of them. Another example is the behaviour of water as a solvent for apolar molecules which has been a subject of scientific debate for more than sixty years now. The solubility of apolar compounds in water has a minimum with varying temperature, indicating that the role of entropy and enthalpy are unusual as compared to other solutions. At ambient conditions, i.e. at moderate temperature and pressure, the low solubility appears to be due to a strongly negative entropy of solvation, whereas the solvation enthalpy is small and up to about room temperature even negative. For this anomalous behaviour of water as the solvent for apolar molecules, often the term *hydrophobic effect* is used. This phenomenon has drawn much attention over the past decades, especially since it is of major importance, not only for the behaviour of simple aqueous solutions, but also for the conformation of proteins and for the formation of micelles and biological membranes [1-5].

It has been understood for a long time that hydrogen bonds, strongly attractive directional interactions, play an important role in water. For instance, the open, approximately four-coordinated structure of ice and liquid water at ambient conditions has been explained from the tendency of water molecules to form four hydrogen bonds with other water molecules in tetrahedral geometry. In our opinion however, this explanation is not complete. If each water molecule is surrounded by eight others, it is also possible for each water molecule to be involved in four hydrogen bonds. Actually such a situation is known to occur at very high pressure, for instance in *ice VII*, that consists of two intertwined tetrahedral structures, such that each molecule has eight neighbours to four of which it is hydrogen bonded. The four-coordinated open tetrahedral form *ice Ic* and the rather similar commonly occurring form *ice Ih* exist at low pressures [6]. That close packing does not occur at low pressures must be due to repulsive forces between non-hydrogen bonded water

molecules that are at a separations of comparable magnitude as the length of the hydrogen bond.

Considering the distribution of electrical charge over the water molecule (for instance as in ref. [4]), it is not unexpected that the interaction between two water molecules that have the proper separation, but not the relative orientation required to form a hydrogen bond is, on the average, repulsive.

In our opinion, it is the balance between orientation-dependent attractive and repulsive interactions that leads to the open, approximately four-coordinated structure of water at ambient conditions, to the anomalous temperature dependencies of the isobaric density and of the solubility of apolar molecules (as well as to other properties that will not be discussed here).

2 STATISTICAL THERMODYNAMICS OF SOLVATION

Generally, the configurational chemical potential of a compound a can be expressed in statistical mechanical terms as

$$\mu_a = kT \ln \rho_a - kT \ln \left\langle \exp\left(-\frac{\Psi_a}{kT}\right)\right\rangle \tag{1}$$

The potential energy of an a-molecule due to interactions with all other molecules, Ψ_a, is a function of the positions and orientations of all molecules. The weighting factor $\langle \exp(-\Psi_a/kT)\rangle$ is the canonical average of $\exp(-\Psi_a/kT)$ [7-10]. The quantity $-kT \ln\langle \exp(-\Psi_a/kT)\rangle$ is often referred to as the "potential of the mean force".

As was mentioned in the introduction, the solubility of apolar compounds is low. This implies that the Gibbs energy of solution, the change of Gibbs energy upon transfer of an apolar molecule from a fixed position in an apolar medium to a fixed position in water $\Delta_{tr}(a \rightarrow w)g$, is high. This quantity is related to the solubility in water, and to the potentials of the mean force in either medium as [11]

$$\Delta_s g = -kT \ln \frac{\rho_a{}^w}{\rho_a{}^a} = -kT \ln \frac{\langle \exp(-\Psi_a/kT)\rangle^w}{\langle \exp(-\Psi_a/kT)\rangle^a} \tag{2}$$

where we have, as we will do hereafter, used the shorthand notation $\Delta_s g$ for $\Delta_{tr}(a \to w)g$; $\rho_a{}^w$ and $\rho_a{}^a$ are concentrations (number densities) of the apolar compound a in water and in an apolar phase a, respectively.

What has caused much puzzlement among scientists for about 60 years, was the finding that for many non-polar solutes the solubility in water has a minimum at about room temperature. The precise value of the temperature of minimum solubility is somewhat different for each apolar compound. The Gibbs-Helmholtz relation

$$\Delta_s h = -T^2\left(\frac{\partial(\Delta_s g/T)}{\partial T}\right)_p \tag{3}$$

implies that the solvation enthalpy changes sign, from negative to positive, at the temperature of minimum solubility. Consequently, in combination with the relation

$$\Delta_s g = \Delta_s h - T\Delta_s s \tag{4}$$

it is inferred that the high positive value of $\Delta_s g$ is at ambient conditions due to a strongly negative entropy of dissolution. The trends of the temperature dependencies of $\Delta_s g$ and its enthalpic and entropic contributions are as shown in fig. 3.

This behaviour is quite unusual as compared to non-aqueous solutions. Usually, $\Delta_s h$ is positive. This is in accordance with the common wisdom that the attractive interaction between like molecules is stronger than between unlike molecules [4, 12]. This is for instance reflected in Berthelot's principle ("geometric-mean rule") [12, 13].

The current explanation of the anomalous phenomena, invokes the formation of a highly structured shell of water molecules, a so-called 'iceberg', around apolar (parts of) molecules [4, 14-16]. Hence, the negative entropy of solution. The exothermic solution enthalpy is often explained by an increase of the number of hydrogen bonds upon addition of an apolar molecule [4, 15] or by assuming that hydrogen bonds in the 'solvation shell' are stronger than in bulk water [17]. Especially these explanations of the enthalpy effect appeared to us as unsatisfactory.

Rather recently, attention has been drawn to the occurrence of a maximum of $\Delta_s g$ at elevated temperature [18], indicating that there the solvation entropy, for which we can write $\Delta_s s = -(\partial \Delta_s g / \partial T)_p$, changes sign from positive to negative (see also fig. 3). Some authors state that at this temperature hydrophobic hydration disappears [16, 18]. Obviously, that is merely a linguistic statement, an attempt to redefine the term "hydrophobic". It does not bring us closer to a physical explanation of the phenomena.

It is our goal to interpret the macroscopic findings in terms of a molecular picture. To that end, we present an analysis, based on a detailed statistical-thermodynamic treatment of fluids with orientation-dependent interactions [19, 20].

3 A LATTICE THEORY FOR WATER

The model presented here is the same as that of ref. [20]. There, the properties of water, its liquid-vapour phase-equilibrium and the liquid-vapour interface are examined.

To facilitate the configurational analysis, the molecules are confined to a body-centred cubic lattice of N sites. This lattice possesses tetrahedral angles. Each site is surrounded by eight nearest neighbours. A site can be vacant or occupied by a water molecule or a small apolar molecule. Vacant lattice sites are indicated by subscript v, water molecules by w and apolar molecules by a. A value for the volume per lattice site, denoted as v, is determined by equating the density of ice with that of a half-filled bcc lattice. In this way $v = 1.632 \ 10^{-29} \ \text{m}^3$ is obtained. It will be convenient to express the density of a certain component A in terms of the fraction of sites occupied by A: $\phi_A = n_A / N = v \rho_A$, $\rho_A = n_A / V$ is the number density.

To account for the anisotropy of water molecules, we distinguish different faces. Two of these stand for protons; two others for lone pairs of electrons. These four faces are arranged tetrahedrally on the surface of the molecule. The remaining four faces are called 'indifferent'. Not only are the molecules confined to lattice sites, also their faces are confined to be directed towards nearest-neighbour sites. So, in the present model a water molecule has 12 orientations.
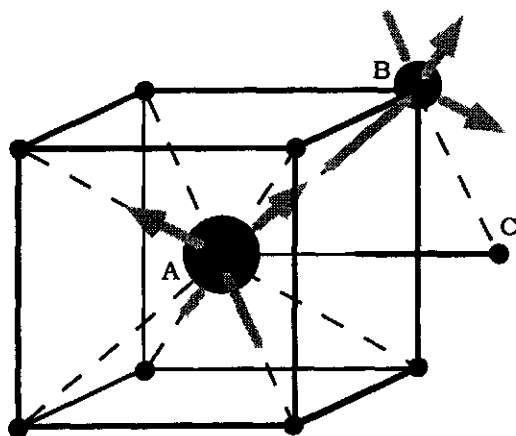
Figure 1. *Ten sites in a bcc lattice. Site A is surrounded by its eight*
nearest neighbours. One of the next-nearest neighbours is indicated (C).
Two water molecules are indicated by solid balls bearing arrows and
sticks, indicating respectively the protons and the lone pairs of
electrons. The molecules, interact through a hydrogen bond.

A contact between a proton and a 'lone pair' is identified as a
hydrogen bond. If two nearest-neighbour sites are occupied by water
molecules, only in 18 out of the 144 viable configurations of this pair
a hydrogen bond exists. To such a contact, an energy of u_{Hb} is
attributed. To all non-hydrogen bonding contacts between water
molecules, an energy $u_{\neq Hb}$ is assigned.

One way to determine these parameters is by fitting the density
and pressure of the liquid at coexistence with vapour, at 0 °C, In this
way values $u_{Hb} = -20.1$ kJ/mol and $u_{\neq Hb} = 1.75$ kJ/mol are obtained
[20]. These values are used throughout all calculations of the present
chapter. Our value of the hydrogen bond energy is close to the
experimental value [21]. It should be noted that the non-hydrogen
bonded contacts are repulsive.

The cohesive energy of the system can be calculated from the
distribution of contacts:

$$U = \sum_{\alpha \leq \beta} n_{\alpha\beta} u_{\alpha\beta} = n_{Hb} u_{Hb} + n_{\neq Hb} u_{\neq Hb} \qquad (5)$$

where $u_{\alpha\beta}$ and $n_{\alpha\beta}$ are the energy and the number of $\alpha\beta$-contacts, respectively. The last expression applies to the present model for water; n_{Hb} and n_{*Hb} are the numbers of hydrogen bonds and non-hydrogen bonded contacts between water molecules.

To derive the thermodynamic properties for this model, we have generalised the first-order quasi-chemical approximation [22, 23] for systems containing molecules with orientation-dependent interactions [19, 20]. A general derivation of the theory is presented elsewhere [19]. In the present section we will review some aspects that are most relevant for the present purpose. Most important is the fact that the occupancies of neighbouring sites are correlated; the contacts are not formed randomly. According to the quasi-chemical approximation, this can be described by mass-action laws for contacts. Generally,

$$\frac{\left(\frac{1}{2}n_{\alpha\beta}\right)^2}{n_{\alpha\alpha}n_{\beta\beta}} = \exp\left(\frac{u_{\alpha\alpha} + u_{\beta\beta} - 2u_{\alpha\beta}}{kT}\right) \tag{6}$$

where the subscripts α and β can indicate any of the face types that are present: 'proton', 'lone pair', 'indifferent', 'vacancy' and 'apolar'.

At infinite temperature, contacts are formed at random. Then the number of water-water contacts is $4n_w\phi_w$. Of these contacts, 1 out of 8 is a hydrogen bond. The random numbers of contacts between water molecules and vacancies and between two vacancies are $8n_w\phi_v$ $= 8n_v\phi_w$ and $4n_v\phi_v$, respectively.

At finite temperatures, contacts are not formed at random. Low-energy contacts are preferred. This gives rise to a certain local ordering and to a negative entropy contribution. It can be shown [19, 20] that in first-order quasi-chemical approximation the entropy reduction S^{exc} due to correlations is given by

$$S = S^{id} + S^{exc} \tag{7.a}$$

with

$$S^{id} = -k\sum_A n_A \ln\frac{n_A}{N\omega_A} \tag{7.b}$$

and

$$S^{exc} = -k \sum_{\alpha \le \beta} n_{\alpha\beta} \ln \frac{n_{\alpha\beta}}{n_{\alpha\beta}^\infty} \tag{7.c}$$

Here S^{id} is the entropy of mixing randomly the molecules and vacancies; ω_A is the number of orientations of a monomer of type A. If the contact were formed at random, i.e. if all contacts would have the same energy, then the ratio $n_{\alpha\beta}/n_{\alpha\beta}^\infty$ would be equal to unity for each type of contact and the excess entropy would vanish.

Equation (7) is in line with (6). Equation (6) can by derived by minimising the configurational Helmholtz energy $F = U - TS$, where the energy is given by eq. (5) and the entropy by (7), with respect to the distribution of contacts. By the same token, substituting the expression for the distribution of contacts (6) into eq. (5) for the energy, and integrating $U = \left(\partial(F/T)/\partial(1/T) \right)_{n_w, n_v, \dots}$ from $1/T = 0$ to $1/T$, an expression for the Helmholtz energy is obtained and hence expression (7) for the entropy.

Since it applies to molecular components as well as to vacancies, the partial quantity defined as

$$f_A \equiv \left(\frac{\partial F}{\partial n_A} \right)_{T, \{n_{B \ne A}\}} \tag{8}$$

is very convenient in evaluating lattice models. For f_A the expression

$$f_A = kT \ln \frac{\phi_A}{G_A} \tag{9}$$

can be written. This equation defines G_A which can be interpreted as a weighting factor for species A. It can be written as a product of an orientational degeneracy factor ω_A and of face weighting factors:

$$G_A = \omega_A \prod_\alpha G_\alpha^{q_{A\alpha}} \tag{10}$$

where $q_{A\alpha}$ is the number of α-faces belonging to a molecule of type A (or to a vacancy). The G_α's are given by the implicit equations

$$G_\alpha = \sum_\beta \frac{\phi_\beta}{G_\beta} \exp-\frac{u_{\alpha\beta}}{kT} \qquad (11)$$

Since the interaction energies $u_{\alpha\beta}$ are defined in such a way that they vanish for "contacts with vacuum", all G_α equal unity for very low density.

The f_A's can be related to the pressure and the chemical potentials. The pressure of a lattice gas can be related to f_v where the subscript v indicates vacancies.

$$p \equiv -\left(\frac{\partial F}{\partial V}\right)_{T,\{n_{A\neq v}\}} = -\frac{1}{v}\left(\frac{\partial F}{\partial n_v}\right)_{T,\{n_{A\neq v}\}} = -\frac{f_v}{v} \qquad (12)$$

For the chemical potential of molecular components we can write

$$\mu_A \equiv \left(\frac{\partial G}{\partial n_A}\right)_{p,T,\{n_{B\neq A,v}\}} \equiv \left(\frac{\partial F}{\partial n_A}\right)_{V,T,\{n_{B\neq A,v}\}} = f_A - f_v \qquad (13)$$

Comparing equations (1), (9) and (13) reveals that, according to the present theory:

$$\left\langle \exp-\frac{\Psi_A}{kT}\right\rangle = \frac{G_A \Lambda_v}{v} = \frac{\phi_v G_A}{v G_v} \qquad (14)$$

where $\Lambda_v = \exp(f_v/kT)$.

The Gibbs energy change of transfer of an apolar molecule a from phase a to w can be expressed in terms of the weighting factors of eqs. (9) and (10):

$$\Delta_s g = kT \ln\frac{G_a(a)}{G_a(w)} \qquad (15)$$

4 ISOBARIC DENSITY OF PURE WATER

The isobaric densities and liquid-vapour coexistence curve, calculated from this model are shown in fig. 2. These results resemble at least qualitatively the experimental findings. The anomalous maximum isobaric density is reproduced. This supports the view that the essential physics is captured in the present model.
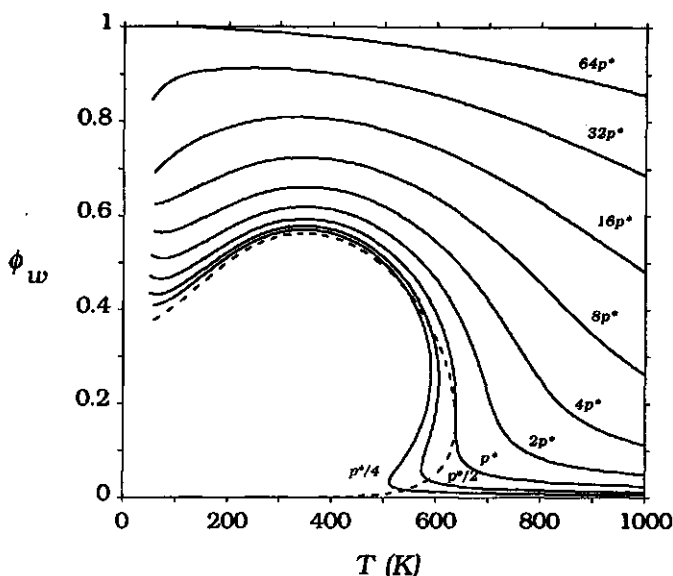
Figure 2. *Theoretical isobaric density at various pressures* ———, *p^* is the theoretical critical pressure, 1.7423 10^7 Pa). The liquid-vapour coexistence curve ------ encloses the two-phase region where the isobars show a Van der Waals loop.*

It is noted that the density of the liquid at ambient conditions, corresponds to a site fraction of water molecules, ϕ_w, that is only slightly higher than a half. In section 6 it will be shown that the water-water coordination number is somewhat above 4, and that in the water-water contacts hydrogen bonds prevail.

5 SOLVATION OF SMALL APOLAR MOLECULES AND VACANCIES IS SIMILAR

Pure water has an open structure, containing numerous cavities which are spontaneously present. The interaction energy between water and an apolar molecule has a purely dispersive nature and is low as compared to the energy of a hydrogen bond. Consequently, no qualitative change of structure (such as 'iceberg' formation) upon addition of a small apolar molecule is expected. Rather, the change of water structure upon addition of a small apolar molecule is expected
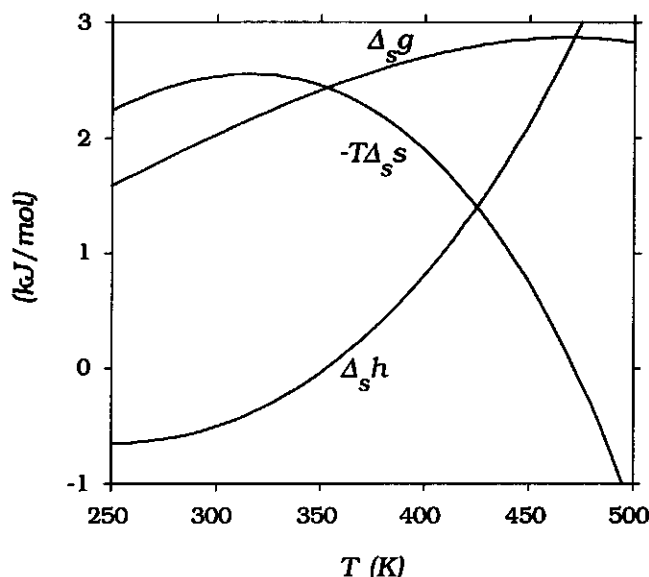
Figure 3. *Temperature dependence of the Gibbs energy of solvation of vacancies or model apolar molecules and its enthalpic and entropic contributions at $\frac{1}{4}p^{*}$.*

to be similar to changes due to expansion of pure water at which additional cavities are created [24]. Obviously this only holds for apolar molecules that are of approximately the same size as the cavities that spontaneously exist in pure liquid water.

Since we are, for the moment, not interested in quantitative results on specific apolar compounds but in the qualitative aspects that all apolar solutes have in common, we introduce a (in our lattice model simplest possible) model-apolar molecule. Such a molecule occupies one lattice site and it does not interact at all with water or with molecules of its own species. Such a molecule is similar to vacancies. Hence, its weighting factor G_a equals that of vacancies G_v.

According to eqs. (9), (12) and (15), the Gibbs energy of transfer of such a molecule a from a fixed position in an a-phase, consisting of a-molecules and vacancies, to a fixed position in water of the same pressure, is related directly to the isobaric density of pure water as plotted in fig. 2:

$$\Delta_s g = -kT \ln G_a = -kT \ln \phi_v - pv \qquad (16)$$

where p is the pressure and v the volume per lattice site.

This $\Delta_s g$ is equal to the change of Gibbs energy upon a similar transfer of a vacancy. The maximum in the isobaric density can be regarded as a minimum of the 'solubility of vacancy', and has the same physical origin as the minimum in the solubility of small apolar molecules. It is clear that this similarity will not hold quantitatively for real apolar molecules. Small differences of molecular sizes and interactions between apolar molecules will have some quantitative effects but the behaviour will be qualitatively the same. For instance, a small Van der Waals interaction between an apolar molecule with water will lead to an additional, approximately constant negative term in $\Delta_s h$ and hence in $\Delta_s g$. This will lead to a positive shift of the temperature where $\Delta_s h$ changes sign from negative to positive, which is the temperature where the solubility is minimal (see also APPENDIX II). This also explains the observation that the temperature of minimum solubility depends somewhat on the nature of the apolar molecule.

The isobar with the lowest pressure presented in fig. 2 was for $\frac{1}{4} p^*$ which corresponds to about forty atm. The liquid branch of the isobars at lower pressures fall between the liquid branch of the binodal and the $\frac{1}{4} p^*$-isobar. Hence qualitatively these isobars and according to eq. (16) $\Delta_s g$ as a function of temperature will be similar. At a pressure that is higher than the atmospheric pressure, the liquid phase is stable over a larger temperature range. This is an advantage since it enables us to examine $\Delta_s g$ and its enthalpic and entropic contributions over a large temperature range.

For a pressure $\frac{1}{4} p^*$, $\Delta_s g$ and its enthalpic and entropic contributions are plotted in fig. 3. At least qualitatively, all aspects of the anomalous temperature dependence of the Gibbs energy of solvation are reproduced. The temperature dependence of $\Delta_s g$, $\Delta_s h$ and $\Delta_s s$ as calculated here for "vacancy-like" molecules is very similar to what is found experimentally for the solvation of apolar compounds by water. The temperature dependence of both $\Delta_s h$ as $T\Delta_s s$ is rather strong, but they compensate each other so that the temperature dependence of $\Delta_s g$ is relatively weak. The value of the solvation
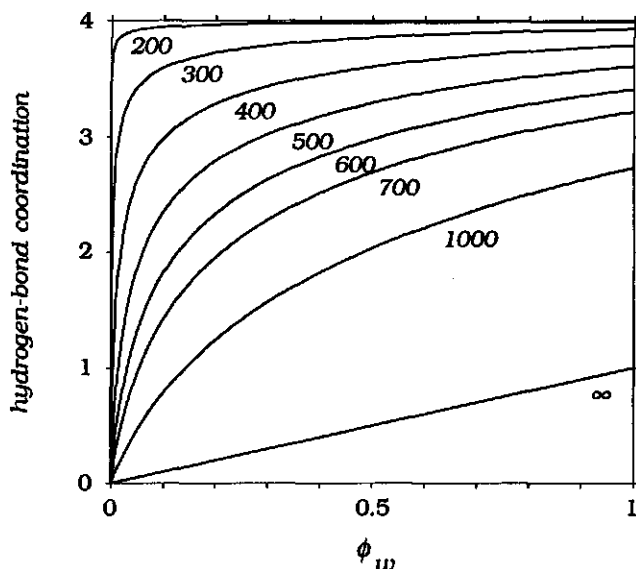
Figure 4. *Coordination of water molecules by hydrogen bonds to other water molecules as a function of water density at various temperatures. Temperatures are indicated along the curves. The random-mixing case is indicated by the symbol ∞. At ambient conditions, ϕ_w is about one half.*

enthalpy, $\Delta_s h$, is low. At low temperatures, the solvation of vacancies is even exothermic, $\Delta_s h < 0$, hence the enthalpy of solvation promotes the solubility of vacancies in liquid water. The entropic contribution to $\Delta_s g$, $-T\Delta_s s$ is positive and larger than $|\Delta_s h|$ and suppresses the solubility of vacancies. As $\Delta_s h$ increases with temperature, the partial heat capacity of vacancies in water, given by $\Delta_s C = (\partial \Delta_s h / \partial T)_p$, is positive at any T. This is also found experimentally for the heat-capacity change due to dissolving apolar compounds in water. Usually, for non-aqueous mixtures, this effect is much smaller [25, 26].

For a molecule that does interact with water molecules, the weighting factors and Gibbs energy of transfer can be calculated quite easily, especially in the limit of low concentration. From eqs. (11) and (10) the weighting factors for any molecule a in a medium can be calculated. From eq. (15) the Gibbs energy of transfer from one medium to another can be calculated. In the limit $\lim_{\phi_a \to 0}$, terms in the
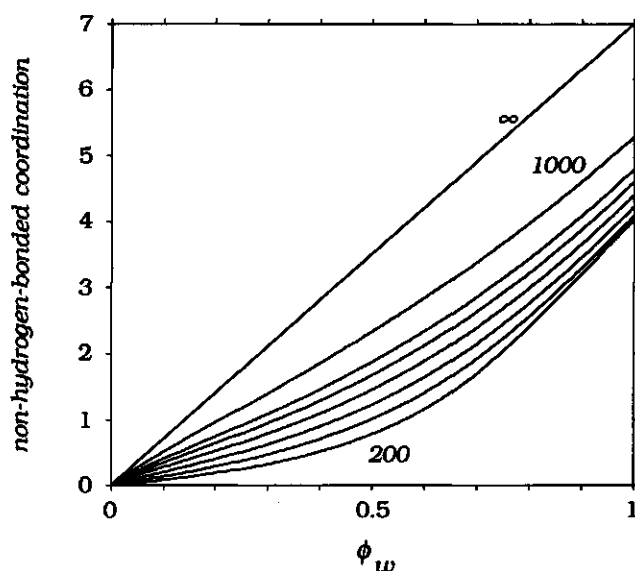
Figure 5. *Non-hydrogen bonded coordination of water molecules by water molecules as a function of water density at various temperatures. Temperatures are 1000 K, 700 K and with steps of 100 K down to 200 K. The random-mixing case is indicated by the* symbol ∞.

sum over β, for faces of a vanish with respect to other terms. So, the sum extends over the faces of the pure medium only. Hence, if the face weighting factors of the pure fluid are known, in the limit of low concentration of the solute, the face weighting factors of the solute are obtained by an explicit closed formula.

For higher solute concentrations the equations (11) have to be solved for the complete ensemble of faces, those of the solute included.

In the present chapter we will not be dealing with more realistic model molecules since at present we are focusing on the characteristic trends associated with the hydrophobic effect. These appear all to be present with the simple vacancy-like solute.
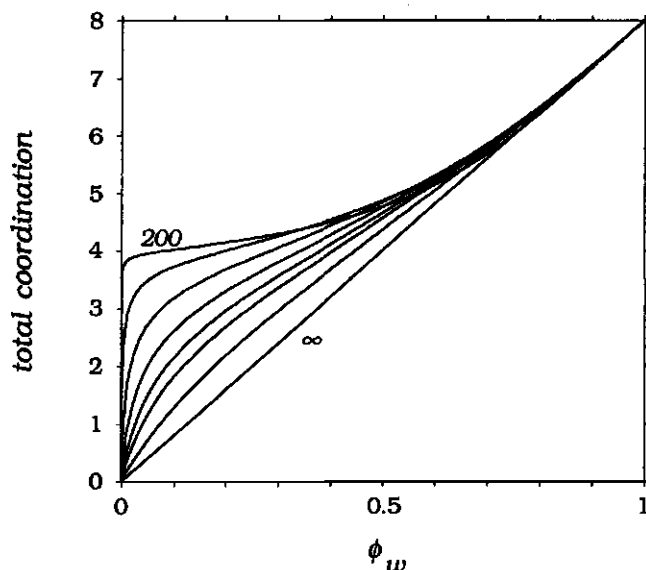
Figure 6. *Total coordination of water molecules by water molecules as a function of water density at various temperatures: 200 K 300 K . . 700 K, 1000 K and infinitely high T indicated by the symbol ∞.*

6 MOLECULAR INTERPRETATION

We have seen in previous sections that the present theory reproduces the experimental trends on hydrophobic solvation. To interpret these phenomena from a molecular point of view, we have to look at the distribution of contacts. Due to the strong directional interactions between water molecules, a pronounced local ordering occurs. The number of hydrogen bonds exceeds by large its random value (see fig. 4). Simultaneously, the frequency of non-hydrogen bonded water-water contacts and, at not too high density, the number of water-vacancy contacts are smaller than their random values (fig. 5). This ordering is most pronounced at low water density where the fluid preserves a large number of hydrogen bonds. Hence, the configurational freedom of the molecules is more severely restricted at low density. According to eq. (7) this leads to a lowering of the entropy as compared to its ideal value. The calculated
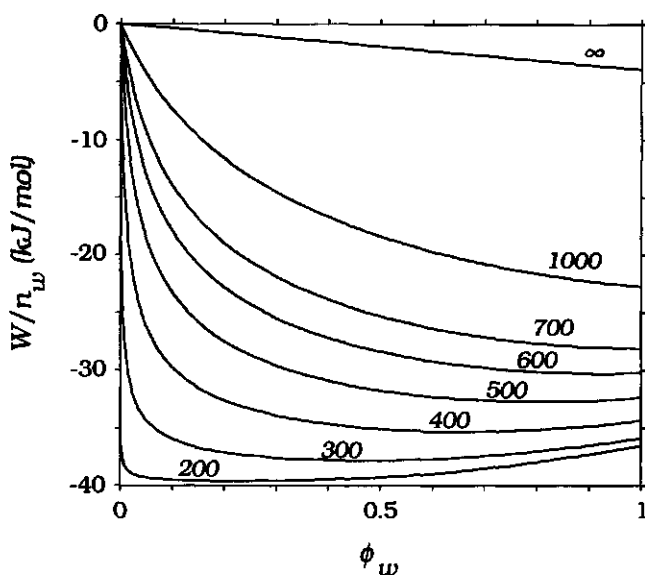
Figure 7.   *Cohesive energy per mole of water as a function of water density at various temperatures. Temperatures are indicated along the curves.*

excess entropy per water molecule as a function of water density is plotted in fig. 8 for several temperatures.

Especially at low temperatures, the excess entropy per water molecule as a function of density has a minimum at a density that is lower than the density of the liquid at ambient pressure $(\phi_w \approx \frac{1}{2}$, see fig. 2). At ambient liquid density, the molecular excess entropy decreases upon decreasing water density. This behaviour is quite unusual and does not occur in simple fluids. It is the origin of the negative solvation entropy of small apolar molecules and vacancies. Addition of an apolar molecule reduces ϕ_w. At ambient conditions this leads to a decrease of S^{exc}/n_w. In APPENDIX I the tangents of fig. 8 are related to other thermodynamic quantities in a more exact manner.

The mean molecular cohesive energy is negative, and for most fluids it decreases with increasing density. However, due to short range intermolecular repulsion, at very high pressures it increases
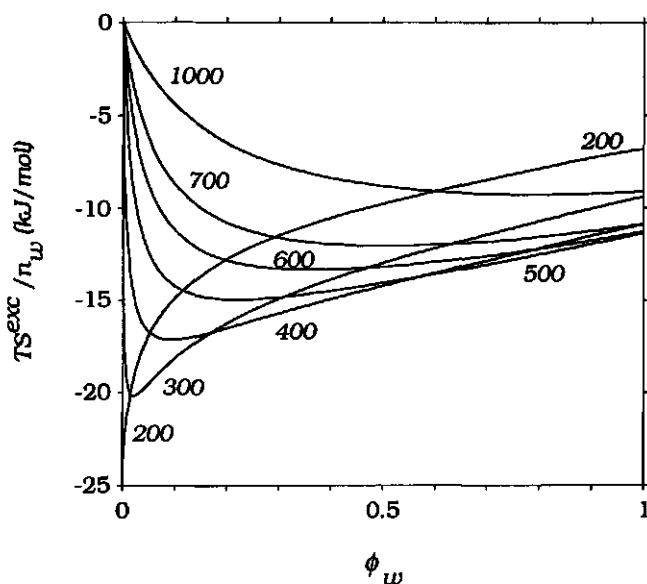
Figure 8. *Excess entropy per water molecule as a function of water density at various temperatures. Temperatures are indicated along the curves.*

with increasing density. According to the present theory, the molecular cohesive energy of water increases with increasing density *at ambient conditions* (see fig. 7). Obviously, this phenomenon is closely related to the orientation-dependent nature of the intermolecular interactions.

Hydrogen bonds have a negative contribution to the cohesive energy but the non-hydrogen bonding water-water contacts contribute positively. As can be seen in fig. 7 the molecular cohesive energy of water decreases steeply upon increasing the density of water from $\phi = 0$. This is due to hydrogen-bond formation (see fig. 4). We have seen that if the temperature is not too high, the increase of the number of hydrogen bonds per molecule levels off at intermediate density. Then the cohesive energy per molecule corresponds to about two hydrogen bonds. Upon further increase of the density, mainly the number of repulsive contacts increases (see fig. 5) and hence the molecular energy (see fig. 7), even though the
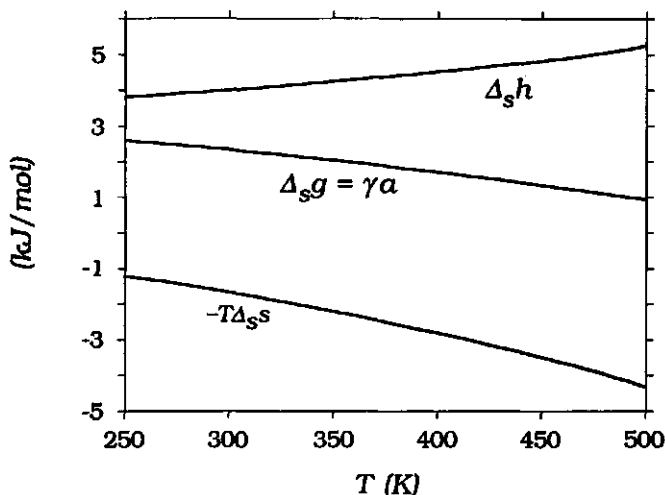
Figure 9. *Temperature dependence of the Gibbs energy of solvation per site, of an inert surface and liquid water at $\frac{1}{4}p^{\bullet}$, and its entropic, $\Delta_s s = -\left(\partial\gamma/\partial T\right)_p$, and enthalpic contribution. Note that $\Delta_s g = \gamma a$, with a the cross-sectional surface area per mole of sites.*

number of hydrogen bonds per water molecule still increases slightly.

Consequently, isothermal expansion of liquid water is predicted to be exothermic (if not the pressure is reduced to the extent that boiling occurs). More importantly, the exothermic effect upon dissolving apolar molecules in water can also be explained by a decrease of repulsive non-hydrogen bonding water-water contacts. Upon addition of an apolar molecule, the water density decreases and hence the cohesive energy. In APPENDIX I, it is indicated how the tangents of fig. 7 relate to other thermodynamic quantities.

7 SOLVATION OF AN EXTENDED HYDROPHOBIC SURFACE

Above, we discussed the solvation of small apolar molecules. These are accommodated in fluid water in such a way that the number of hydrogen bonds is reduced only slightly. As a consequence, the enthalpy of solvation is small but, due to the loss of configurational freedom of the water molecules, the associated entropy loss is considerable. Obviously, bulky particles can not be accommodated in
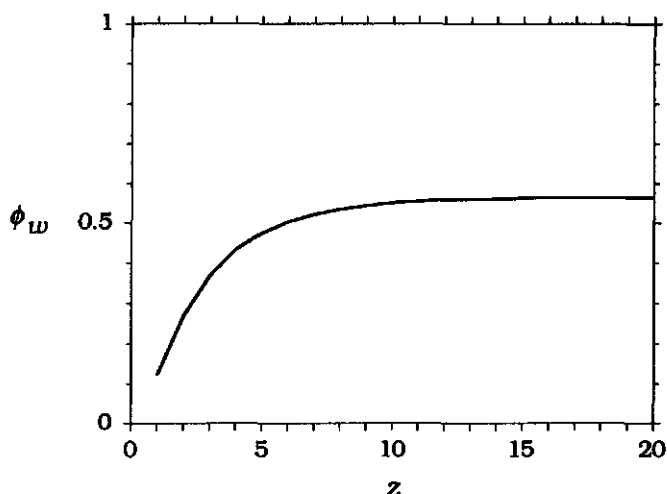
Figure 10. *Density profile of water at the non-interacting surface. The surface is located at z = 0. To guide the eye, calculated values, at the centres of the lattice layers, are connected by straight lines.*

this way. To indicate what consequences this has for the solvation of bulky particles and macroscopic apolar surfaces, we present some theoretical results on liquid water adjoining an extended planar hydrophobic surface.

These calculations require a generalisation of the theory as summarised in section 3. Now we have to account for spatial heterogeneity. Hence coordinates for position and direction have to be introduced. This has been worked out in refs. [19] and [20].

To be able to compare the results with the previous calculations on "vacancy-like" molecules, we will examine a surface that does not interact with water molecules. This surface can be considered as a "surface of vacuum". This allows comparison with the previous discussion of the solvation of single vacancies. The solvation of single vacancies, having a size of one lattice site, and of a flat non-interacting surface can be considered as limiting cases for the size of a solute particle, the smallest and the largest that are possible in the present model.

In fig. 9, which should be compared with fig. 3, the Gibbs energy of solvation of the 'vacuum surface' is plotted together with its
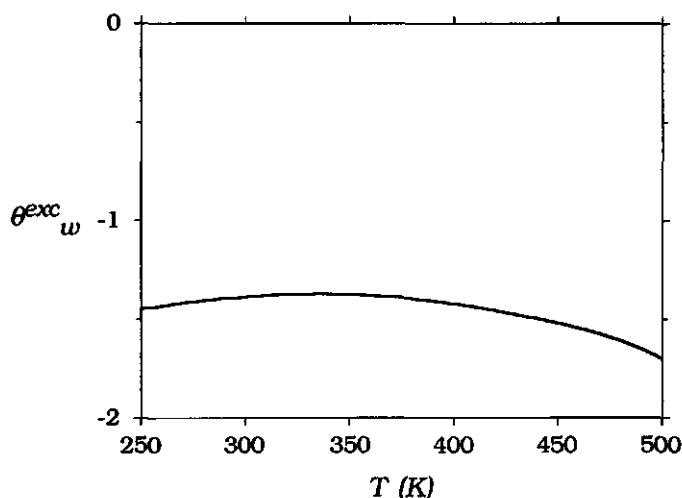
Figure 11. *Temperature dependence of the surface excess of water at the 'solid vacuum surface', given in equivalent lattice layers. Note that the excess of water equals minus the excess free volume.*

entropic and enthalpic contributions. The Gibbs energy of solvation of a mole of sites of the surface equals the surface tension of the solid-liquid surface times the surface area of a mole of surface sites: $\Delta_s g = \gamma a$, with a the cross-sectional surface area per mole of sites. This interfacial tension is somewhat higher than that of the aqueous liquid-vapour interface, as can be calculated within the same theory [20]. This difference is mainly due to the small difference between the density of the liquid coexisting with vapour and the liquid at $\frac{1}{4} p^{*}$. Each site of the inert surface exposes two faces to the liquid. At 300 K the solvation Gibbs energy per unit of surface is about four times higher for the extended flat surface. This agrees qualitatively with the results from molecular-dynamics simulations (on a different model for water) by Postma et all. who studied the solvation of cavities of different sizes [27, 28]. Unfortunately, they did not obtain separately the entropic and enthalpic contributions.

It is remarkable that the entropic and enthalpic contributions are very different as compared to solvation of a small molecule. Over the temperature range examined, the entropic and enthalpic contribution to γa are both positive. These results demonstrate that

the anomalous temperature dependence of solvating small apolar molecules does not exist for bulky particles.

This is mainly due to the reduced density and reduced hydrogen bonding in the fluid layer adjoining the surface as compared to bulk liquid water. At the "vacuum surface" the density of water decreases towards the surface as it does at the liquid-vapour interface see fig. 10 and ref. [20]). Alternatively stated, at the flat surface, a depletion layer exists. The excess surface amount in equivalent lattice layers of some component A is given by $\theta_A^{exc} = \sum_z (\phi_A(z) - \phi_A(\infty))$, where $\phi_A(\infty)$ is the site fraction of A in the bulk, far from the surface. For pure water adjoining a surface, $\theta_v^{exc} = -\theta_w^{exc}$. The surface excess of water is negative; the excess free volume of solvation is positive. In fig. 11 θ_w^{exc} is plotted as a function of temperature.

8 CONCLUDING REMARKS

According to the commonly accepted view, a region of specially structured water is present around a dissolved apolar molecule. However, in the present chapter, we arrive at a different interpretation the notion of these so-called 'iceberg' structures does not have to be invoked to explain the anomalous thermodynamics of solvation of apolar molecules in water. The anomalous temperature dependence of the isobaric density of water can be related to the temperature dependence of the solubility of small apolar molecules. Our model calculations reproduce the experimental trends and make it possible give a molecular interpretation.

The balance between attraction (hydrogen bonds) and repulsion (non-hydrogen bonding contacts) between water molecules leads to the open, approximately four-coordinated structure of liquid water at ambient conditions, to the anomalous temperature dependence of the solubility of apolar molecules.

The energy and entropy changes upon dissolution of small apolar molecules are related to the distribution of intermolecular contacts. In this chapter we concentrated on the interpretation of the thermodynamics of dissolution of small apolar molecules in water. We indicated that this has much in common with the anomalous temperature dependence of the isobaric density of pure water. So

the present discussion also offers a clue to understand the behaviour of pure water.

As an additional argument, we note that there is a certain analogy between the swelling of polymer networks and expansion of water [24]. Upon swelling, by uptake of solvent, the entropy of a polymer network decreases. This is easily explained: since the bonds in a polymer network do not break, the configurational freedom of the polymer segments decreases and hence the entropy. Upon expansion of pure liquid water, or by uptake of small apolar molecules, the number of hydrogen bonds between water molecules does not decrease much and consequently the configurational freedom of the water molecules decreases. This is does not hold for the solvation of bulky molecules and extended surfaces. This will inevitably lead to *qualitative* changes of the structure of water, and to more substantial reduction of the number op hydrogen bonds.

APPENDIX I

The tangents of the curves in several figures where some property X/n_w is plotted as a function of ϕ_w can be related to other interesting quantities:

$$\left(\frac{\partial(X/n_w)}{\partial\phi_w}\right)_{n_w,T} = -\left(\frac{\partial(X/n_w)}{\partial\phi_v}\right)_{n_w,T} = -\frac{1}{\phi_w^2}\left(\frac{\partial X}{\partial n_v}\right)_{n_w,T} = -\frac{v}{\phi_w^2}\left(\frac{\partial X}{\partial V}\right)_{n_w,T}$$

$$(A.1)$$

for pure water (water molecules and vacancies only). Here $\phi_w = n_w/N$ and $\phi_v = n_v/N$. The first identity holds since $\phi_w + \phi_v = 1$, the second follows from $(\partial X/\partial n_v)_{n_w,T} = (\partial X/\partial\phi_v)_{n_w,T}(\partial\phi_v/\partial n_v)_{n_w,T}$, where $(\partial\phi_v/\partial n_v)_{n_w,T} = \phi_w/N$, the third follows from $Nv = V$. Each of the quantities on the ordinate of the figures 4 to 8 can be substituted for X/n_w.

Generally we are more interested in changes at which the pressure is fixed instead of the number of vacancies. We can write

$$\left(\frac{\partial X}{\partial n_a}\right)_{p,n_w,T} = \left(\frac{\partial X}{\partial n_a}\right)_{n_v,n_w,T} + \left(\frac{\partial X}{\partial n_v}\right)_{n_a,n_w,T}\left(\frac{\partial n_v}{\partial n_a}\right)_{p,n_w,T}$$

$$(A.2)$$

If X is a quantity that has the same functional dependence on n_a as on n_v (such as the cohesive energy W, the 'ordering entropy', S^{exc}, the number of hydrogen bonds etc.), then $(\partial X/\partial n_v)_{n_a,n_w,T} = (\partial X/\partial n_a)_{n_v,n_w,T}$.

Now the problem is to determine $(\partial n_v/\partial n_a)_{p,n_w,T}$, the change of the number of vacancies upon isobaric addition of an a-molecule. Note that this quantity is closely related to the partial molecular volume of a: $(\partial V/\partial n_a)_{p,n_w,T} = v\left(1+(\partial n_v/\partial n_a)_{p,n_w,T}\right)$. We will refer to $v(\partial n_v/\partial n_a)_{p,n_w,T}$ as the excess partial free volume of a.

We know

$$dF\big|_{n_w,T} = f_a dn_a + f_v dn_v \tag{A.3}$$

where $f_v = (\partial F/\partial n_v)_{n_a,n_w,T} = -vp$, with v the volume per lattice site.

$$d\left(F - f_v n_v\right)\big|_{n_w,T} = f_a dn_a - n_v df_v$$

From this, we obtain the Maxwell relation

$$\left(\frac{\partial n_v}{\partial n_a}\right)_{f_v,n_w,T} = -\left(\frac{\partial f_a}{\partial f_v}\right)_{n_a,n_w,T} = -\left(\frac{\partial f_a}{\partial n_v}\right)_{n_a,n_w,T}\left(\frac{\partial n_v}{\partial f_v}\right)_{n_a,n_w,T} \tag{A.4}$$

Note that $-(\partial n_v/\partial f_v)_{n_a,n_w,T} = (\partial V/\partial p)_{n_a,n_w,T}$ is the isothermal compressibility. Since $f_a/kT = \ln\phi_a - \ln G_a$ and $f_v/kT = \ln\phi_v - \ln G_v$ where the weighting factor G_a equals G_v since a-molecules and vacancies are supposed to be the same, it is true that $(\partial f_a/\partial n_v)_{n_a,n_w,T} = (\partial f_v/\partial n_v)_{n_a,n_w,T} - kT/n_v$. So

$$\left(\frac{\partial n_v}{\partial n_a}\right)_{f_v,n_w,T} = -\frac{(\partial f_v/\partial n_v)_{n_a,n_w,T} - kT/n_v}{(\partial f_v/\partial n_v)_{n_a,n_w,T}} = \frac{1}{n_v(\partial f_v/\partial n_v)_{n_a,n_w,T}} - 1 \tag{A.5}$$

Further we can write $(\partial f_v/\partial n_v)_{n_a,n_w,T} = (\partial f_v/\partial N)_{n_a,n_w,T} = (\partial f_v/\partial 1/\phi_w)_{n_a,n_w,T}/n_w = -\phi_w(\partial f_v/\partial 1/\phi_w)_{n_a,n_w,T}/N$, so that

$$\left(\frac{\partial n_v}{\partial n_a}\right)_{f_v,n_w,T} = -1 - \frac{1}{\phi_w\phi_v(\partial f_v/kT/\partial\phi_w)_{n_a,n_w,T}} \tag{A.6}$$

Since f_v as a function of ϕ_w can be computed, all elements are now available to obtain the desired derivative of X.

REFERENCES

1   Tanford, C. *The Hydrophobic Effect: Formation of Micelles and Biological Membranes*; Wiley: New York, 1980.
2   Evans, D. F.; Ninham, B. W. *J. Phys. Chem.*, *90*, 226-234 (1986) "Molecular forces in the self-organization of amphiphiles".
3   Murphy, K. P.; Privalov, P. L.; Gill, S. J. *Science*, *247*, 559-561 (1990) "Common features of protein unfolding and dissolution of hydrophobic compounds".
4   Israelachvili, J. *Intermolecular & Surface Forces*; Academic Press: London, 1992.
5   Privalov, P. L.; Gill, S. J. *Adv. Protein Chem.*, *39*, 191-234 (1988) "Stability of protein structure and hydrophobic interaction".
6   Franks, F. in *Water. A Comprehensive Treatise 1*, edited by Franks, F. (Plenum, New York-London, 1972) pp. 115-149. "The properties of ice".
7   Widom, B. *J. Chem. Phys.*, *39*, 2808-2812 (1963) "Some topics in the theory of fluids".
8   Widom, B. *J. Stat. Phys.*, *19*, 563-574 (1978) "Structure of interfaces from uniformity of the chemical potential".
9   Jackson, J. L.; Klein, L. S. *Phys. Fluids*, *7*, 228-231 (1963) "Potential distribution method in equilibrium statistical mechanics".
10   Ben-Naim, A. *Water and Aqueous Solutions: Introduction to a Molecular Theory*; Plenum: New York, London, 1974.
11   Ben-Naim, A. *Hydrophobic Interactions*; Plenum Press: New York, 1980.
12   Lyklema, J. *Fundamentals of Interface and Colloid Science*; Academic press: London, 1991.
13   Prausnitz, J. M.; Lichtenthaler, R. N.; Azevedo, E. G. *Molecular Thermodynamics of Fluid-Phase Equilibria*; Prentice-Hall: Englewood Cliffs, 1986.
14   Frank, H. S.; Evans, M. W. *J. Chem. Phys.*, *13*, 507-532 (1945) "Free volume and entropy in condensed systems III. Entropy in binary liquid mixtures; partial molal entropy in dilute solutions; structure and thermodynamics in aqueous electrolytes".
15   Némethy, G.; Scheraga, H. A. *J. Chem. Phys.*, *36*, 3401-3417 (1962) "Structure of water and hydrophobic bonding in proteins. II. Model for the thermodynamic properties of aqueous solutions of hydrocarbons".
16   Shinoda, K. *J. Phys. Chem.*, *81*, 13001302 (1977) ""Iceberg" formation and solubility".
17   Muller, N. *J. Solution Chem.*, *17*, 661-672 (1988) "Is there a region of highly structured water around a nonpolar solute molecule".
18   Privalov, P. L.; Gill, S. J. *Pure & Appl. Chem.*, *61*, 1097-1104 (1989) "The hydrophobic effect: a reappraisal".
19   Besseling, N. A. M. "Statistical thermodynamics of molecules with orientation-dependent interactions in homogeneous and heterogeneous systems". Chapter II, Ibid.

20   Besseling, N. A. M. "Equilibrium properties of water and its liquid-vapour interface". Chapter III, Ibid.

21   Curtis, L. A.; Frurip, D. J.; Blander, M. *J. Chem. Phys.*, *71*, 2703-2711 (1979) "Studies of molecular association in H2O and D2O vapors by measurement of thermal conductivity".

22   Guggenheim, E. A. *Mixtures*; Clarendon: Oxford, 1952.

23   Hill, T. L. *Introduction to Statistical Thermodynamics*; Addison-Wesley: 1962.

24   Gibbs, J. H. *Ann. New York Acad. Sci.*, *303*, 10-19 (1977) "On the Nature of Liquid Water".

25   Mirejovsky, D.; Arnett, E. M. *J. Am. Chem. Soc.*, *105*, 1112-1117 (1983) "Heat capacities of solution for alcohols in polar solvents and the new view of hydrophobic effects".

26   Gill, S. J.; Dec, S. F.; Olofsson, G.; Wadsö, I. *J. Phys. Chem.*, *89*, 3758-3761 (1985) "Anomalous heat capacity of hydrophobic solvation".

27   Postma, J. P. M. *MD of H2O. A Molecular Dynamics Study of Water*; Thesis. Groningen State University, The Netherlands: 1985.

28   Postma, J. P. M.; Berendsen, J. C.; Haak, J. R. *Faraday Symp. Chem. Soc.*, *17*, (1982) "Thermodynamics of cavity formation in water".

CHAPTER V

HYDRATION FORCES BETWEEN PLANAR SURFACES

A surface immersed in water influences the adjoining liquid. If the ordered regions of two surfaces interfere, this leads to a distance-dependent, solvent-structure mediated interaction between those surfaces. In case of mutual enhancement of the structure of solvation layers, the interaction is attractive, whereas in case of disruptive overlap, the surface force is repulsive. This is inferred from generalising the density-functional theory of Marcelja and Radic: if the profile between the surfaces of the relevant order parameter is symmetric, the associated surface force is attractive and conversely. Both the attractive and the repulsive interaction decay exponentially with the distance between the surfaces. This rather phenomenological approach is complemented by lattice-model calculations. A lattice theory that has been demonstrated to reproduce various properties of water and aqueous solutions is applied to systems containing inert surfaces. This theory also predicts attractive and repulsive surface forces, depending on the properties of the surfaces. These interactions are associated with two different ordering mechanisms, each with its own decay length. According to our calculations, repulsion between similar surfaces ensues if these surfaces influence the orientational distribution of nearby water molecules. However, if the main function of the surface is to affect the density of adjacent water, then the surface force is attractive, even if the surfaces are very hydrophilic. This is at variance with the common idea that the sign of the surface force depends on the hydrophilicity/hydrophobicity of the surfaces.

1 INTRODUCTION

Surfaces will generally induce certain changes in adjoining layers of fluid. Such a zone where the fluid differs from the bulk is called a solvation layer, or, in case of aqueous systems, hydration layer. Overlap of the solvation layers of two surfaces leads to a distance-dependent contribution of the interaction between those surfaces. Such a solvent mediated interaction supplements the well-understood DLVO forces, i.e. the screened electrostatic interaction and the long range Van de Waals interaction.

Very smooth surfaces induce molecular layering and the interaction between such surfaces has an oscillatory contribution with a periodicity of about the molecular diameter. This has also been measured in aqueous systems [1]. In practice, these microstructural effects are often absent due to surface roughness. However, for water this seems not to be the whole story. For various systems including adsorbed layers [2-4], glass and quartz rods [4], mica surfaces in various electrolyte solutions [1, 5-9], lipid bilayers [10-13] (for a review see ref. [14]), DNA double helices [15], and non-ionic surfactant-bilayers [16] there is evidence for the existence of an additional repulsive surface force. This appears to be exponentially decaying with surface separation [4, 10, 15, 16]. Similar forces have been reported for non-aqueous hydrogen-bonding solvents [13, 17, 18]. It should be noted that surface-force measurements are very sensitive to impurities. For instance, recently results for mica in $CaCl_2$ solution have been reported [19] that are at variance with previous results [1, 8].

Hydration forces are important in biological systems such as biological membranes. The interactions between biomembranes are important in regulating processes such as membrane fusion as occurs for instance in exocytosis. Moreover, hydration forces play a role in the interaction of proteins with surfaces [20, 21], the association of proteins and their colloidal stability and in bacterial adhesion [20]. Various possible implications of hydration forces in biological systems where discussed by Parsegian [22]. In various non-biological disperse systems, solvation forces are important for colloidal stability [3, 4, 23].

It is now well established that water-structure mediated forces can be repulsive as well as attractive [9, 12, 14, 23, 24]. For attractive and repulsive water-structure mediated interactions often the terms "hydrophobic attraction" and "hydrophilic repulsion", respectively, are used. However, the results presented in the present chapter indicate that it does not primarily depend on the hydrophilicity/hydrophobicity of the surface whether attraction or repulsion occurs. Therefore we will avoid terms as hydrophobic attraction and hydrophilic repulsion. We will use the term hydration force both for attractive- and for repulsive water-structure mediated interactions.

There is still some debate whether experimentally observed forces should be attributed to water structuring. Israelachvili and Wennerström recently proposed that certain observed non-DLVO forces might not be due to structuring of water but to steric hindrance of chain molecules such as lipids and surfactants that are linked to the surfaces and that are protruding somewhat into the aqueous phase [25]. This explanation is restricted to surfaces that contain such molecules. We shall exclusively consider surfaces where such steric forces are absent.

Theoretical work on these phenomena was initiated by Marcelja and Radic [26]. Immediately after the first report on exponentially decaying hydration forces between lipid bilayers [10], they formulated an elegant mesoscopic theory in which the free energy of the liquid between the surfaces was expressed as a functional of the profile of some order parameter. Their approach confirmed the exponentially decaying repulsive force. In section 3 of the present chapter, we will demonstrate that the same approach, with modified boundary conditions for the order parameter, predicts an attractive force.

A precise molecular interpretation of the order parameter was not given by Marcelja and Radic. Various molecular mechanisms where proposed. For instance, the coupling between spatially varying electric polarisation of water and the electric double layer was considered [27-29]. Molecular-dynamics simulations of water between solid surfaces [30] and between lipid membranes [31, 32] indicate that disrupted hydrogen bonding, rather than electric polarisation is the basis of the hydration force.

The lattice theory of Attard and Batchelor was especially designed to examine this mechanism [33]. They modelled water between two surfaces on a two-dimensional square lattice with each site occupied by a so-called vertex. A vertex represents a water molecule having one of the six orientations that are possible in the model. Each water molecule has two proton donors and two acceptors. To a defect, a donor-donor- or an acceptor-acceptor contact, a positive energy is attributed. By means of the transfer-matrix method, an exponentially decaying repulsion between the surfaces was calculated. In the model of Attard and Batchelor no variation of density is allowed and hence the water-water coordination number is fixed at a value of four.

The lattice model of the present chapter can, in some respects, be considered as an extension of the model of Attard and Batchelor. It is more elaborate however, since we make use of a three-dimensional body-centred cubic lattice and allow sites to be vacant. Therefore our model has a much wider applicability. It has been demonstrated that it is capable of reproducing various trends of the behaviour of water and of the aqueous liquid-vapour interface [34, 35]. In section 4.4 we will see that, according to the present model, the behaviour of water-structure-related forces between surfaces is more complex than in the model of Attard and Batchelor. It will be shown that a variable density can give rise to an attractive surface-force contribution.

In a preceding chapter [36] we introduced a first-order self-consistent field lattice theory for homogeneous as well as heterogeneous systems containing molecules with orientation-dependent interactions. By "first-order" it is indicated that the "Bethe-Guggenheim"- alias "quasi-chemical" approximation [37] is applied. In subsequent chapters, this general method was applied to a lattice-gas model for water. In section 4 of the present chapter this theory for water is applied to phenomena related to the modification of the structure of fluid water adjoining solid surfaces.

The outline of the rest of the present chapter follows a trend from phenomenological towards a more and more microscopic molecular approach. First we will briefly resume the basic thermodynamics of surface forces, then the theory of Marcelja and Radic is generalised
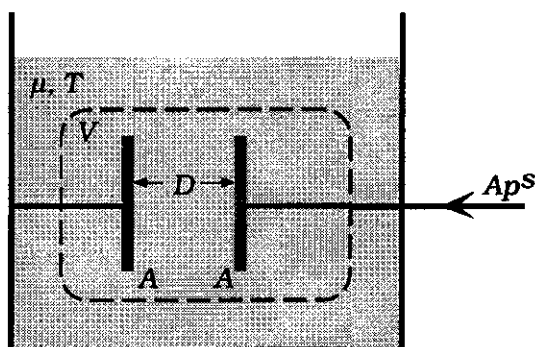
Figure 1. *Schematic picture of a surface-force apparatus: two surfaces immersed in water at a distance D. The area of each surface is A.*

for different boundary conditions and finally, a detailed lattice-gas model for water is applied.

2 THERMODYNAMICS OF SURFACE INTERACTIONS

The change of the Gibbs energy upon an infinitesimal reversible change of the conditions for two parallel identical surfaces immersed in a fluid (see fig. 1) is given by

$$dG = -SdT + \mu dn + Vdp - Ap^s dD + 2\gamma dA \qquad (1)$$

where A is the area of one surface, D the separation between the surfaces and p^s the surface force per unit area, which is chosen to be positive if the surfaces repel each other. The quantity p^s is often called "disjoining pressure" [2]. The interfacial tension of each surface is as γ.

From eq. (1):

$$Ap^s = -\left(\frac{\partial G}{\partial D}\right)_{T,n,p,A} \qquad (2)$$

By cross differentiation between the last two terms of eq. (1) we obtain

$$p^s = -2\left(\frac{\partial\gamma}{\partial D}\right)_{T,n,p,A} \tag{3}$$

This does not generally hold in case of a mixed solvent. Then n has to be replaced by a set of variables: $\{n\}$, specifying the amount of each component of the mixture. Then cross differentiation between the last two terms of eq. (1) leads to

$$\left(\frac{\partial\left(Ap^s\right)}{\partial A}\right)_{T,\{n\},p,D} = p^s + A\left(\frac{\partial p^s}{\partial A}\right)_{T,\{n\},p,D} = -2\left(\frac{\partial\gamma}{\partial D}\right)_{T,\{n\},p,A}$$

where $\left(\partial p^s/\partial A\right)_{T,\{n\},p,D}$ does not generally vanish, due to adsorption and desorption processes. It vanishes if the system contains an infinitely large bulk fluid so that the chemical potential of each component is virtually constant.

The work of bringing the surfaces from infinity to a separation D at constant T, n, p and A, often called free energy of interaction, is given by integrating eq. (3):

$$A\int_{\infty}^{D} p^s(D')dD' = G(D) - G(\infty) = 2A(\gamma(D) - \gamma(\infty)) \tag{4}$$

The change of surface tension upon the above-mentioned process, $\gamma(D) - \gamma(\infty)$ will be denoted as $\Delta\gamma(D)$, $G(D) - G(\infty)$ as $\Delta G^s(D)$.

Often, in a surface-force apparatus, the external force Ap^s is exerted by a spring. In alternative experimental setups, there can be a variable hydrostatic pressure, or osmotic pressure difference between the inside and outside of the slit between the surfaces. In these cases one measures in principle a different quantity since the chemical potential of water is different for different surface separations.

3 MARCELJA-RADIC THEORY REVISITED

Marcelja and Radic formulated an elegant mesoscopic theory for the interaction between two plan-parallel identical surfaces located at $z = -D/2$ and at $z = D/2$. In this theory, the free energy of the fluid between the surfaces was assumed to be a functional of some order

parameter $\eta(z)$ which measures ordering with respect to the bulk of the fluid. A precise physical interpretation for this order parameter was not given. It might be any structural difference as compared to the bulk fluid. It should be something of the form $(\vartheta(z) - \vartheta(\infty))/\vartheta(\infty)$, where ϑ quantifies some aspect of the local structure of the fluid. The Landau expansion of the local Gibbs energy density is [26, 38]:

$$g(z) = g_0 + a\eta^2(z) + ... + c\left(\frac{d\eta(z)}{dz}\right)^2 + ... \tag{5}$$

where g_0 is the free-energy density in the bulk fluid. If $\eta(z)$ is not too large, coefficients of terms of odd degree vanish since $g(z)$ is invariant with respect to reversal of the sign of $\eta(z)$; moreover, terms beyond the quadratic ones are omitted. The coefficients a and c are both positive. The Gibbs energy of the fluid between the surfaces $G[\eta(z)] = A\int_{-D/2}^{D/2} g(z)dz$ has to be minimised with respect to $\eta(z)$. This leads to the differential equation [26]

$$\frac{d^2\eta(z)}{dz^2} - \frac{a}{c}\eta(z) = 0 \tag{6}$$

which has the general solution

$$\eta(z) = C_1 \exp\left(\frac{z}{\xi}\right) + C_2 \exp\left(-\frac{z}{\xi}\right) \tag{7}$$

Here $\sqrt{c/a}$ has been replaced by ξ which can be identified as the correlation length for the order parameter η. It is a measure of the thickness of the ordered layer.

Marcelja and Radic assumed that their order parameter is related to the orientation of the water molecules. Hence, it has opposite values at the two identical face-to-face oriented surfaces: $\eta(-D/2) = -\eta(D/2) = \eta_0$. With these boundary conditions the coefficients in eq. (7) become $C_1 = -C_2 = \eta_0/(\exp(D/2\xi) - \exp(-D/2\xi))$ and hence

$$\eta(z) = \frac{\eta_0 \sinh(z/\xi)}{\sinh(D/2\xi)} \tag{8}$$

which is antisymmetric with respect to $z = 0$. The excess Gibbs energy per unit surface area is given by

$$\frac{G^s(D)}{A} = \int\limits_{-D/2}^{D/2} (g - g_0)dz = 2\varepsilon\xi\coth\left(\frac{D}{2\xi}\right) \approx 2\varepsilon\xi\left(1 + 2\exp\left(-\frac{D}{\xi}\right)\right) \quad (9)$$

where $\varepsilon = a\eta_0^2$ is the change of g due to ordering the fluid to state $\eta = \eta_0$. For one isolated surface, the excess free energy per unit area (i.e. the contribution to γ) due to ordering of the fluid equals $\varepsilon\xi$. Hence, the interaction Gibbs energy per unit area, $2\Delta\gamma(D)$, equals $G^s(D)/A - 2\varepsilon\xi$. The last expression on the right-hand side of the previous and the following equation hold for separations $D > \xi$. The interaction force per unit area is given by

$$p^s = -\frac{1}{A}\left(\frac{\partial G^s}{\partial D}\right)_{T,n,p,A} = \varepsilon\sinh^{-2}\left(\frac{D}{2\xi}\right) \approx 4\varepsilon\exp\left(-\frac{D}{\xi}\right) \quad (10)$$

This is the result obtained by Marcelja and Radic who chose, unlike we do, a negative force to be repulsive. The interaction appears to be repulsive and for not too small separations exponentially decaying. This is in accordance with the first experiments on the hydration force [10] that Marcelja and Radic aimed to interpret. In the period after this pioneering work evidence appeared for attractive hydration forces as well [9, 14]. We will demonstrate that these can also be reproduced by the Marcelja-Radic formalism and that the sign of the force is related to the symmetry of the order-parameter profile between the surfaces.

In the case discussed above, the repulsive character of the surface force is due to the antisymmetric shape of the profile of the order parameter as imposed by the antisymmetric boundary conditions. We will now consider a situation where the order-parameter profile is symmetric. This will occur if the order parameter satisfies symmetric boundary conditions, for instance $\eta(-D/2) = \eta(D/2) = \eta_0$. For an order parameter related to the orientation distribution of the water molecules, this will occur if the two surfaces have an opposite effect on the orientation distribution. For similar surfaces, if the

density is the relevant order parameter, the profile is symmetric as well.

With symmetric boundary conditions the coefficients in eq. (7) become $C_1 = C_2 = \eta_0/\big(\exp(D/2\xi) + \exp(-D/2\xi)\big)$ and hence

$$\eta(z) = \frac{\eta_0 \cosh(z/\xi)}{\cosh(D/2\xi)} \tag{11}$$

which is symmetric with respect to $z = 0$. The surface excess free energy is given by

$$\frac{G^s}{A} = \int_{-D/2}^{D/2} (g - g_0)dz = 2\varepsilon\xi \tanh\left(\frac{D}{2\xi}\right) \approx 2\varepsilon\xi\left(1 - 2\exp\left(-\frac{D}{\xi}\right)\right) \tag{12}$$

The last expression on the right-hand side of the previous and the following equation holds for separations $D > \xi$. The interaction force per unit area is given by

$$p^s = -\frac{1}{A}\left(\frac{\partial G^s}{\partial D}\right)_{T,n,p,A} = -\varepsilon\cosh^{-2}\left(\frac{D}{2\xi}\right) \approx -4\varepsilon\exp\left(-\frac{D}{\xi}\right) \tag{13}$$

The interaction is now attractive and for not too small separations again exponentially decaying.

In this case the order parameter can for instance be the excess density (then the excess adsorbed amount in the slit between the surfaces is given by $\int_{-D/2}^{D/2} \eta(z)dz$ with $\eta(z)$ given by eq. (11)).

In subsequent sections of the present chapter a detailed model for liquid water between interfaces will be evaluated. Depending on the properties of the surface both attractive and repulsive forces are possible. This corresponds to the fact that in these cases the dominant ordering mechanism is different.

It should be noted that in the cases discussed above, it was assumed that η_0 is constant upon variation of D. Hence, at the boundaries the gradient $d\eta/dz$ changes upon changing D. Alternatively, the gradient $d\eta/dz$ can be assumed to have fixed values at the surfaces. Then the values $\eta(-D/2)$ and $\eta(D/2)$ will be changing upon changing D. It is straightforward to work out these cases as well. The conclusion that an antisymmetric order-parameter profile
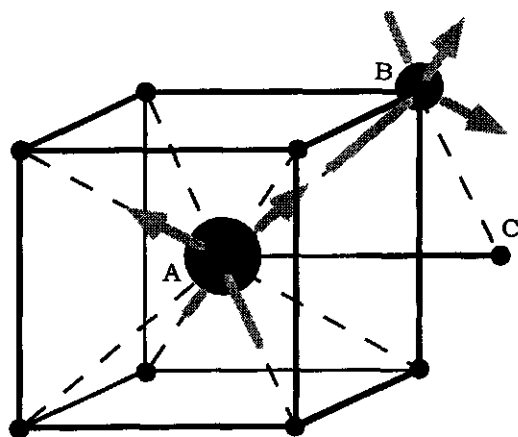
Figure 2. *Section of the body-centred cubic lattice. Site A is occupied by a water molecule. It is surrounded by eight nearest-neighbours of which one is also occupied by a water molecule (site B). Moreover, one next-nearest neighbour is drawn (site C). The proton donors are indicated by arrows, the acceptors by headless sticks. The two molecules are interacting through a hydrogen bond.*

is associated with a repulsive surface force, and a symmetric order-parameter profile with an attractive surface force remains valid. Otherwise stated: if overlap of solvation layers leads to enhancement of ordering, the ensuing surface force is attractive, if it disrupts the order, the associated surface force is repulsive.

The Marcelja-Radic approach can be generalised for cases where two (say $\eta(z)$ and $\varphi(z)$) or more different ordering mechanisms operate at the same time. Generally, the surface-force contributions associated with different types of ordering will not be additive. In eq. (5) cross terms like $\eta(z)\varphi(z)$ and $(\partial\eta(z)/\partial z)(\partial\varphi(z)/\partial z)$ have to be included.

4 A LATTICE-GAS THEORY FOR WATER AT SURFACES

4.1 General

The model was introduced in a previous chapter where we studied the properties of water in absence of rigid surfaces [34]. This model is now applied to water between surfaces. This enables us to get a
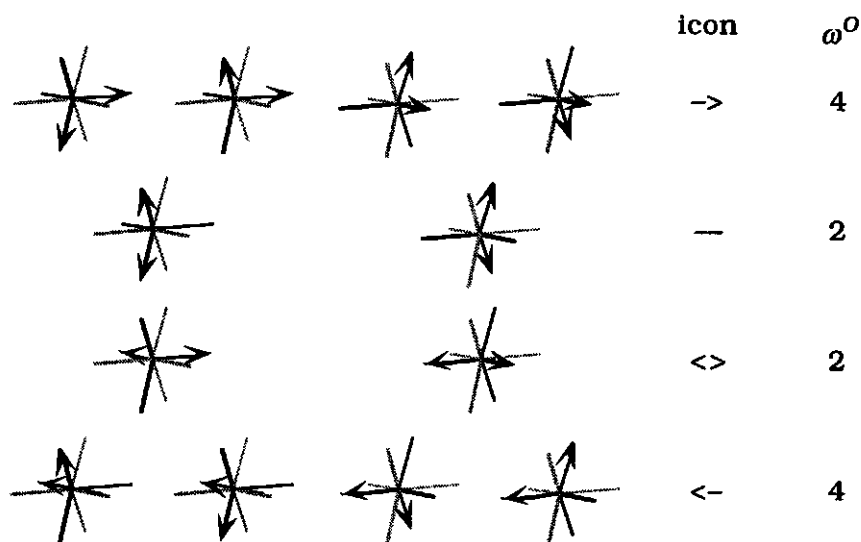
Figure 3. The twelve orientations of the water molecule in the present model grouped in sets with the same projection in the z-direction (the positive z-direction is to the right). Black arrows indicate proton donors, black headless sticks indicate proton acceptors; The directions of the four additional faces are indicated by grey sticks. The orientations of the first set (indicated by ->) present one proton acceptor to the negative z-direction and one proton donor to the positive z-direction. Orientations — present a proton acceptor to the negative- and to the positive z-direction. Orientations <> present a donor to the negative- and to the positive z-direction. Orientations <- present a donor to the negative- and an acceptor to the positive z-direction.

physical picture of the molecular mechanisms of the hydration forces.

The volume V that contains the fluid is divided into a regular lattice of N identical sites. This lattice does not change with temperature or composition. To model water the body-centred cubic (bcc) lattice is a good choice because it has tetrahedral angles (see fig. 2). The bcc lattice has a coordination number of eight; each lattice site is surrounded by eight nearest neighbours.

To be able to model systems that are heterogeneous in the direction normal to the surfaces, the lattice is divided into M parallel layers of L sites each in such a way that each site has four nearest neighbours within the same layer and two in each of the two adjacent

layers. Beyond these layers, at $z = 0$ and at $z = M + 1$, the solid surfaces are located. The number of layers M between the surfaces is a measure for the distance between the surfaces; $D = lM$ where l is the layer spacing. We will be dealing with systems with an infinitely large surface area and hence an infinitely large L. Each layer is denoted by a ranking number z, which runs from 1 until M. Each layer can be filled differently.

As in previous chapters [34, 35], the lattice dimensions are obtained from the density of natural ice (ice Ih at 273.16 K; 916.8 kg/m³). Assuming this density to corresponds to that of a half-filled bcc lattice ($\phi_w = \frac{1}{2}$), a value of, $v = 0.01632$ nm³, is obtained for the lattice site volume. This corresponds to a distance of 0.2767 nm between the centres of nearest neighbours. The cross-sectional surface area per lattice site is given by $a = A/L = 0.7221$ nm². The spacing between the layers is $l = 0.2260$ nm.

The water molecule is modelled as a monomer, i.e. a molecule that occupies one lattice site. Of this monomer, two faces represent the protons. These will be referred to as *proton-donor faces* or *D*. Two other faces represent the *lone pairs of electrons*. These will be referred to as *proton-acceptor faces* or *A*. These four faces have a tetrahedral geometry. The four remaining faces, indicated by *I*, also have a tetrahedral geometry. These faces are directed towards nearest-neighbour sites. Consequently, in this model the water molecule has 12 orientations (see fig. 3). A hydrogen bond is said to exist when a proton-donor face of a water molecule makes contact with a proton-acceptor of a neighbour. This is illustrated by fig. 2. When two neighbouring lattice sites are occupied by water, only in 18 out of 144 distinguishable configurations the two molecules interact trough a hydrogen bond.

Lattice sites are allowed to be vacant. Hence, density variations are accounted for in the model. Empty lattice sites are referred to as *holes* or *vacancies*. In the statistical analysis vacancies can be treated as just another type of isotropic monomer.

Assuming that mainly the difference between the hydrogen bond and other modes of contact is responsible for the anomalous properties of water, the same interaction energy was attributed to all intermolecular contacts, except for the hydrogen bonds. It should be

Table I

interaction energies for surfaces A and B

	u/k	vac	water			surface		
			D	A	I	D	A	I
vac		0	0	0	0	0	0	0
wa-	D	0	210.2	-2414.23	210.2	0	-2414.23	0
ter	A	0	-2414.23	210.2	210.2	-2414.23	0	0
	I	0	210.2	210.2	210.2	0	0	0
sur-	D	0	0	-2414.23	0			
face	A	0	-2414.23	0	0			
	I	0	0	0	0			

noted that with this choice for the interaction parameters the proton-donor- and proton acceptor faces are modelled as being identical, except for the fact that they are complementary with respect to formation of hydrogen bonds. The values for the interaction energies are the same as used in ref. [36] (see table I). They were obtained by fitting the experimental pressure and liquid density at coexistence with vapour at 273.16 K. The value for the hydrogen bond is quite reasonable; it corresponds to a value of –20.1 kJ/mole of hydrogen bonds. Other intermolecular contacts have a positive energy.

4.2 Models for Surfaces

We will always be considering a finite number of layers between two surfaces. To model inert surfaces, surface that do not change upon changing conditions, adjacent to the boundary water layer a surface with a fixed distribution of faces is specified. To clarify the effects of surface characteristics, we will examine a number of relatively simple model surfaces. We will examine two distinct types of surfaces.

1) Surfaces carrying an equal amount of "donors" and "acceptors", $\phi_A^s = \phi_D^s$. The remaining fraction of a surface, $\phi_I^s = 1 - \phi_A^s - \phi_D^s$, does not interact at all with water molecules (see table I). The donors and

acceptors of the surfaces are capable of forming hydrogen bonds with the acceptors and donors of water molecules. For simplicity, to the hydrogen bonds between the surface and water molecules we attribute the same energy as to the water-water hydrogen bonds. To non-hydrogen bonding contacts between molecules and surface a zero energy is attributed (see table I). These surfaces are referred to as "A=D" surfaces. These influence the local density of water near the surface but leave the orientational distribution unaltered as compared to bulk water.

2) Surfaces that do not possess acceptors. They only have donors and non-interacting faces. These can only form hydrogen bonds with the acceptor faces of water molecules. All other contacts between surface and water molecules have zero energy. These surfaces will influence the orientational distribution as well as the density of water layers adjacent to the surface.

4.3 First-Order Self-Consistent Field Equations

The distribution of molecules over orientations and layers can be related to a molecular field. This field is quantified by *face weighting factors*. Simultaneously, these can be expressed in terms of the monomeric distribution. The configuration for which the molecular field and the monomeric distribution are self consistent is identified as the equilibrium state of the system. The self-consistent field equations are derived on the basis of the first-order approximation [37] that was generalised for molecules with orientation-dependent interactions and for heterogeneous systems [36]. Hence, correlations of positions and orientations of the molecules are accounted for in an approximate way. This is especially important for molecules with orientation-dependent interactions such as water. Here we will recapitulate some features that are important for the present system.

For vacancies and for water molecules we can write

$$\phi_A^o(z) = \Lambda_A G_A^o(z) \tag{14}$$

where $\phi_A^o(z) \equiv n_A^o(z)/L$ is the fraction of sites in layer z, occupied by monomers of type A having orientation o, $n_A^o(z)$ is the number of monomers of type A having orientation o, located in layer z. In the present paper A might indicate water ($A = w$) or vacancy ($A = v$). We

will often omit the index if dealing with water and we will simply write ϕ for the fraction of sites occupied by water molecules.

The density distribution of component A is normalised by the factor Λ_A, which has the same value for the heterogeneous system with the surface(s) and for the homogeneous bulk fluid with which the heterogeneous system is in equilibrium. Summation over any selection of orientations o and layers z, of the left- and right-hand side of eq. (14) leads to the expression

$$\Lambda_A = \frac{\sum\limits_{o,z} \phi_A^o(z)}{\sum\limits_{o,z} G_A^o(z)} \tag{15}$$

As $G_A^o(z)$ measures the probability to find a monomer of type A, having orientation o, in layer z, it is referred to as a *monomer weighting factor*. It can be factorised as follows:

$$G_A^o(z) = C \prod_{\alpha,d} G_\alpha^d(z)^{q_{A\alpha}^{od}} \tag{16}$$

As $G_\alpha^d(z)$ represents the contribution of a face of type α (i.e. either a proton donor, acceptor etc.) with direction d to the monomer weighting factor, it is referred to as *face weighting factor*, $q_{A\alpha}^{od}$ equals 1 if the face at direction d of a monomer of type A having orientation o, is of type α, otherwise it equals 0.

For heterogeneous systems, all monomer weighting factors contain a factor C. The interfacial tension of the two surfaces separated by M lattice layers is given by

$$\frac{2\gamma a}{kT} = M \ln C \tag{17}$$

Combining this with eq. (4) the interaction free energy $\Delta G^s(M) = \Delta\gamma(M)$ is obtained. In the calculated interaction curves, the situation for $M = 0$, where the surfaces are in direct contact, is not considered. Within the present theoretical approach this is a trivial situation: the value of the interaction free energy at zero separation depends purely on input parameters for the surface-surface interactions (the values that are omitted in table I).

One manner to obtain the value for C is by considering the equilibrium of the interfacial system with a homogeneous bulk for which $C = 1$. Alternatively, if Λ_w and Λ_v are known C is given by the condition that the total number of molecules and vacancies equals the total number of sites: $\sum_{A,o,z} \phi_A^o(z) = M$.

In addition to density profiles of macroscopic interfaces, the present theory accounts for short-range correlations. In fact the weighting factors of eq. [16] are closely related to the local correlations. The distribution of contacts can be written in terms of the distribution of monomers over orientations and locations and the face weighting factors:

$$\phi_\alpha^d(z)_\beta = \frac{\phi_\alpha^d(z)\phi_\beta^{-d}(z')}{G_\alpha^d(z)G_\beta^{-d}(z')}\exp-\frac{u_{\alpha\beta}}{kT} \tag{18}$$

The direction indicated by $-d$ is the opposite of d. By z' we indicate the layer at which d is directing from layer z (z' and z may be the same layer). The normalised quantities $\phi_\alpha^d(z) \equiv n_\alpha^d(z)/L$ are related to the distribution of monomers: $n_\alpha^d(z) = \sum_{A,o} n_A^o(z)q_{A\alpha}^{od}$. By $\phi_{\alpha\beta}^d(z) = n_{\alpha\beta}^d(z)/L$, we denote the fraction of contacts between a monomer at layer z and a nearest neighbour at direction d, where a face of type α of the first monomer makes contact with a face of type β of the second one. Equation [18] is consistent with a mass-action law for contacts: $\phi_\alpha^d(z)_\beta\phi_\beta^d(z)_\alpha/\phi_\alpha^d(z)_\alpha\phi_\beta^d(z)_\beta = \exp\left((u_{\alpha\alpha} + u_{\beta\beta} - 2u_{\alpha\beta})/kT\right)$.

The $\phi_\alpha^d(z)_\beta$ are related to the nearest-neighbour distribution function:

$$\psi_\alpha^d(z)_\beta \equiv \frac{\phi_\alpha^d(z)_\beta}{\phi_\beta^{-d}(z')} \tag{19}$$

This is the conditional probability of a face of type α, provided that it is located at layer z, has direction d and makes contact with a face of type β. Note that $\phi_\alpha^d(z)_\beta = \phi_\beta^{-d}(z')_\alpha$ but $\psi_\alpha^d(z)_\beta \neq \psi_\beta^{-d}(z')_\alpha$. Within our model for water, the hydrogen-bond ratio of proton-donor faces having direction $-d$ that are located in layer z' is defined as $\psi_A^d(z)_D$, for acceptors as $\psi_D^d(z)_A$.

In eq. (18) the $G_\alpha^d(z)$ account for saturation of faces: the constraints $\sum_\beta n_\alpha^d(z)_\beta = n_\alpha^d(z)$ have to be satisfied, so

$$\frac{1}{G_\alpha^d(z)} \sum_\beta \left(\frac{\phi_\beta^{-d}(z')}{G_\beta^{-d}(z')} \exp- \frac{u_{\alpha\beta}}{kT} \right) = 1 \tag{20}$$

If for the components the normalisation conditions are given, then eq. (20) together with eq. (14) and (16) make up a complete set of self-consistent field equations. These can be solved numerically by the methods of ref. [36].

In the calculation of the present section we have introduced one further approximation: It is assumed that orientations of water molecules that have the same projection in the z-direction, normal to the surfaces (see fig. 3), are equally probable. The monomer weighting factors for such orientations are equal and the face weighting factors for directions that have the same projection in the z-direction are equal.

It has been shown [36] that Λ_A as given by eq. (15) equals $\exp(f_A/kT)$ with $f_A \equiv (\partial F/\partial n_A)_{A,T,\{n_{B\neq A}\}}$. The pressure in a lattice gas can be related to f_v where the subscript v indicates vacancy. Note that he symbol v denotes the volume per lattice site.

$$p \equiv -\left(\frac{\partial F}{\partial V}\right)_{A,T,n_w} = -\frac{1}{v}\left(\frac{\partial F}{\partial n_v}\right)_{A,T,n_w} = -\frac{f_v}{v} \tag{21}$$

For the chemical potential of water we can write

$$\mu_w \equiv \left(\frac{\partial F}{\partial n_A}\right)_{V,A,T} = f_w - f_v \tag{22}$$

4.4 Hydration Attraction

Unless specified differently, results are calculated for a temperature of 300 K and a pressure of 1 atm. This corresponds to $pv/k = 0.11817$ K. This is 33 times the theoretical saturation pressure at this temperature. The corresponding theoretical density is given by $\phi = 0.55476$. The density of the liquid at coexistence with vapour at this temperature is given by $\phi = 0.55456$.
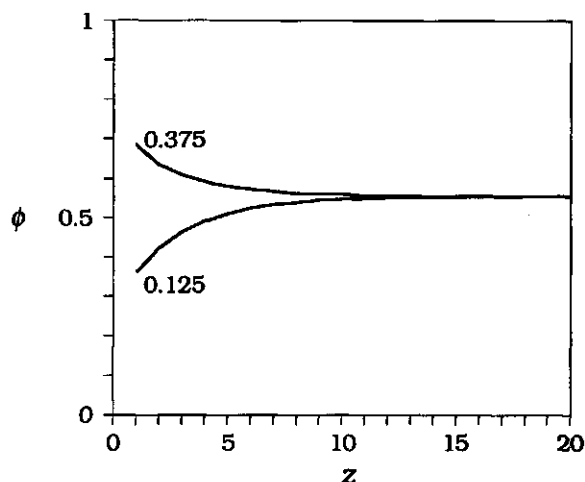
Figure 4.   *Density profiles of water near different isolated "A=D" surface. The surface densities of active faces, $\phi_A^s + \phi_D^s$, are indicated along the curves. The surface is located at z = 0. To guide the eye, calculated points at integer values of z are connected by straight lines.*

To understand the effects upon adjoining water of the surfaces introduced above, the surface density of A- and D faces should be compared with corresponding densities of a slab of undisturbed water. In the present model for water, in the bulk $\phi_A = \phi_D = \phi_w/4$.

The A=D surfaces are expected to influence the density of the boundary water layers. Close to a surface with a large amount of donors and acceptors, the density of water will exceed that of the bulk liquid (fig. 4). There is a positive surface excess of water. However, if the density of donor and acceptor faces on the surface is low, the density of water in the boundary layers is lower than in the bulk liquid (fig. 4), corresponding with a negative surface excess. In all these cases the density gradually decays towards its bulk value. For not too large values of $|\phi(z) - \phi(\infty)|$ this variation is exponential. The density-decay length equals $2.74l$ (the lattice-layer separation, l is 0.226 nm). This is the same as was calculated before for the liquid side of the liquid-vapour interface [34]. Close to the surface, where the deviation from bulk density is largest the profile is not exactly exponential.
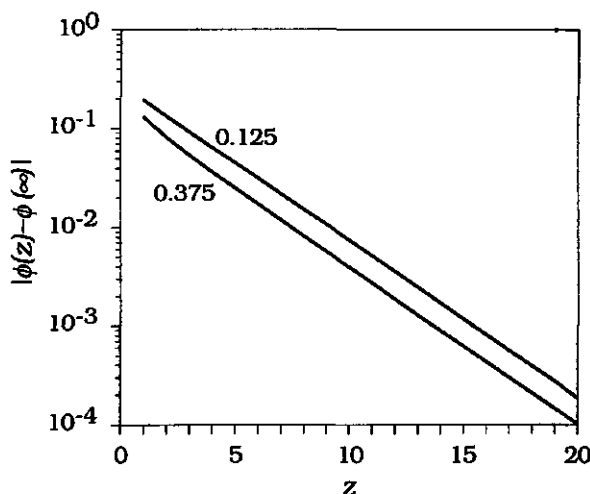
Figure 5. *Logarithmic plot of the profile of the excess density* $|\phi(z) - \phi(\infty)|$ *of water near isolated "A=D" surfaces. The values for the surface density of active faces,* $\phi_A^s + \phi_D^s$, *are indicated. The surface is located at z = 0.*

The "A=D" surfaces will not influence the orientational distribution of the water molecules. As in bulk liquid, near the surface all twelve orientations are equally probable.

The interaction between "A=D" surfaces appears to be attractive (see fig. 6). This holds for surfaces near which the local density exceeds that of bulk water as well as for surfaces with a negative surface excess of water. The strength of the attraction appears to be more or less proportional to the absolute value of the surface excess. Contrary to what is usually thought, the interaction between very hydrophilic surfaces may be attractive. The sign of the interaction (whether it is attractive or repulsive) is not directly related to the affinity between surface and solvent but depends on different properties, as we will see soon. For the surface with $\phi_A^s + \phi_D^s = 0.25$, which nearly matches bulk water, the interaction nearly vanishes. For not-too-small separations, the interaction decays exponentially with distance. The decay length of this surface force is equal to the density-decay length of fluid water: $2.74l$. So the excess density can be pointed out as the relevant order parameter for this attractive

surface force. The present calculations did not reproduce the
extreme long range for the attractive interactions observed by
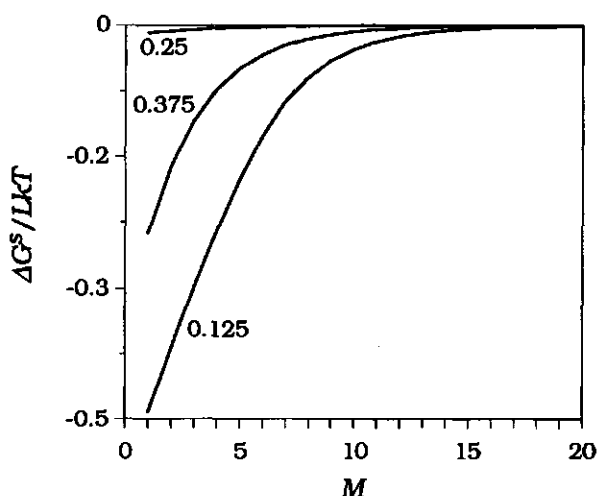Claeson and Christenson [39].

Figure 6. *Gibbs energy of interaction between "A=D" surfaces. The
values for the surface density of active faces,* $\phi_A + \phi_D$, *are indicated
along the curves. The separation between the surfaces is expressed in
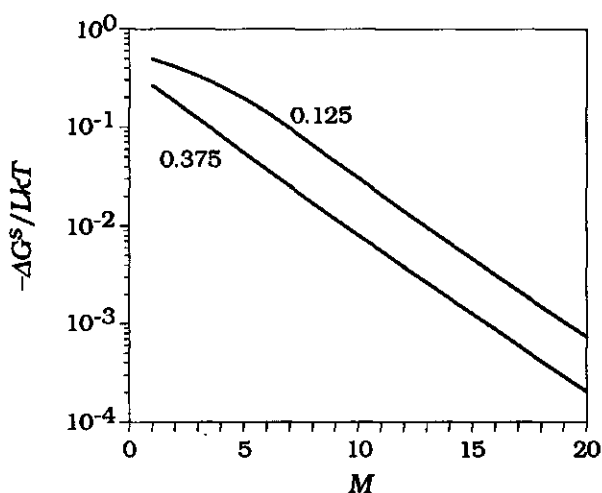the number of lattice layers, M.*

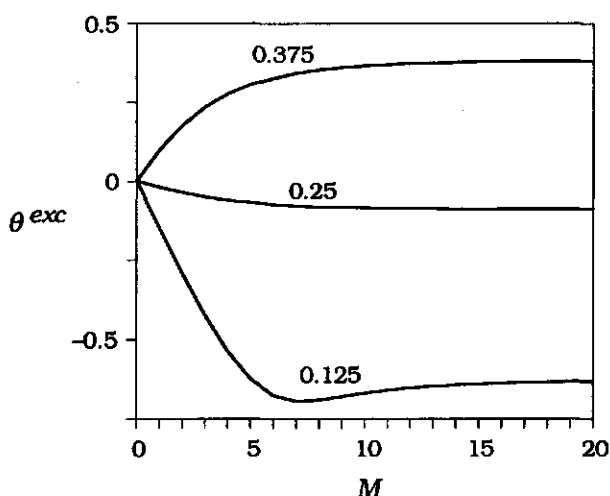Figure 7. *Gibbs energy of interaction between "A=D" surfaces.*

Figure 8. *Excess amount of water between "A=D" surfaces. The values for the surface density of active faces, $\phi_A^s + \phi_D^s$, are indicated.*

In fig. 8 the excess amount of water, given in lattice layers, θ^{exc} is plotted as a function of surface separation. For not too small separations it decays exponentially towards its value for infinite separation. Again the decay length equals $2.74l$. It is remarkable that the curve for the surfaces with $\phi_A^s + \phi_D^s = 0.125$ has a minimum at a separation of 7 lattice layers. This is a foreshadowing of capillary vaporisation, a phenomenon that occurs between more hydrophobic surfaces, in the present model these are for instance surfaces that have a low surface density of active sites. Upon decreasing the separation between hydrophobic surfaces at fixed pressure, the fluid between the surfaces exhibits a transition from a dense, liquid-like state to a dilute vapour-like state (See for instance ref. [40]. This phenomenon is the converse of capillary condensation between hydrophilic surfaces in equilibrium with vapour, see for instance ref. [41]. These phenomena will also be discussed in the following chapter).

4.4 Hydration Repulsion

Surfaces with only donors and no acceptors influence the orientation distribution of the boundary water layers. In general, they will influence the density of the boundary water layers as well. The behaviour of water at surfaces with only acceptors and no donors is similar as at surfaces with only donors and no acceptors. These will not be discussed separately.

The density profiles for some different surface-donor densities are plotted in fig. 9. These look rather similar as the ones of fig. 4. In fig. 10 the corresponding density profile for the different (sets of) orientations of the water molecules is plotted for the surface with $\phi_A^s = 0.25$. At this surface, the total-density profile is nearly uniform (see fig. 9). A set of orientations consists of orientations that have the same projection in the z-direction (see fig. 3). Note that the sets of orientations do have different degeneracies by which the curves of fig. 10 have to be multiplied to obtain the contribution of orientations of one set to the total density.

If the surface density of active sites is not too low, the hydration interaction between those surfaces is repulsive (see fig. 11). Again the interactions are exponentially decaying with surface separation, if the separation is not too small. The decay length of the repulsive interaction is significantly larger (3.83 lattice layers ~ 0.866 (nm)) than that of the attractive force that was discussed before. The calculated decay length is close to the values that are measured for inorganic surfaces such as glass (0.85 nm [4]), quartz (1.0 nm [4]) and mica (0.86 nm [5]). It is true however that for different electrolyte solutions other values are found [8].

If the surface density of donors is low then a relatively weak attraction occurs for larger separations. At a separation of 3 lattice layers the interaction free energy has a minimum.
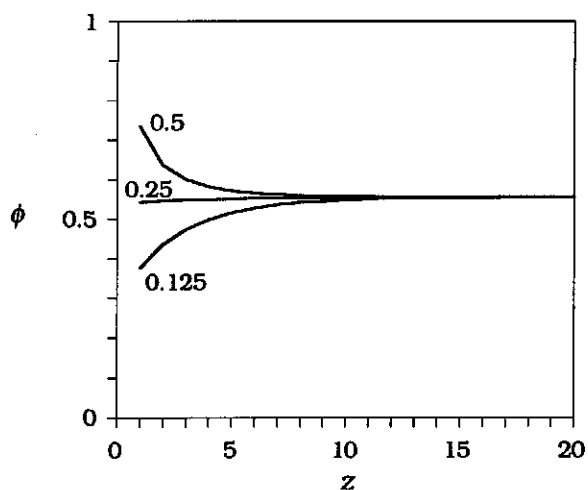
Figure 9. *Density profile at an isolated "D" surface; $\phi_A^s = 0$, the values for the surface density of active faces, ϕ_D^s, are indicated.*
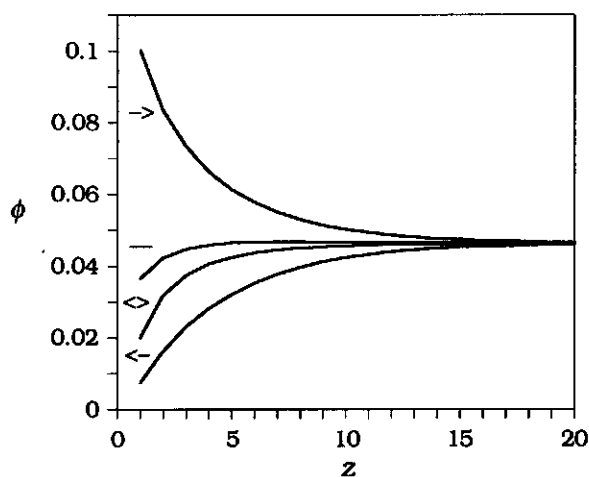
Figure 10. *Profile for the orientations at a surface with $\phi_D^s = 0.25$, $\phi_A^s = 0$. The orientations are indicated along the curves by symbols explained in fig. 3).*
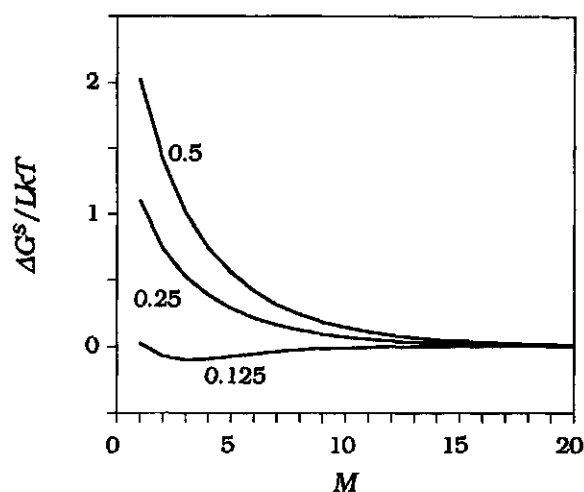
Figure 11. Gibbs energy of interaction between "D" surfaces. The values for the surface density of active faces, ϕ_D^s, are indicated.
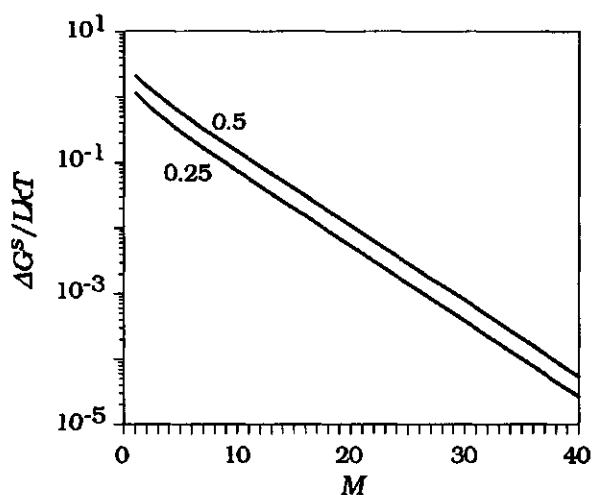
Figure 12. Gibbs energy of interaction between "D" surfaces. The values for the surface density of active faces, ϕ_D^s, are indicated.
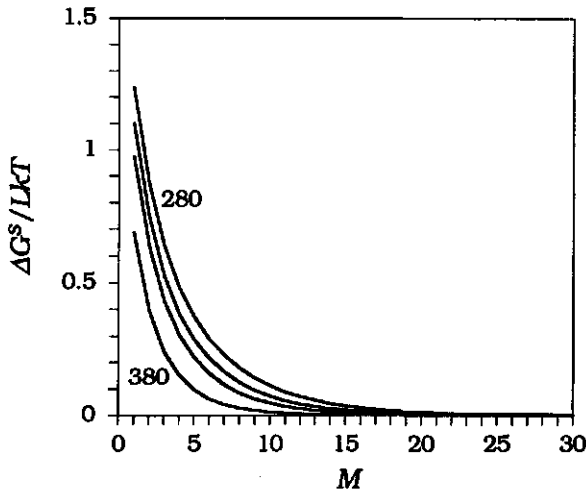
Figure 13. *Interaction free energy between surfaces with $\phi_A^s = 0$ and $\phi_D^s = 0.25$ at different temperatures: from top to bottom $T = 280$, 300, 320, 380 (K). The distance between the surfaces is given in lattice layers.*
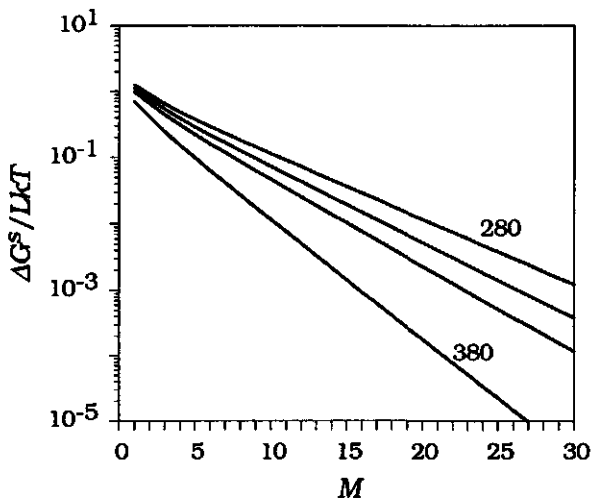
Figure 14. *Interaction free energy between surfaces with $\phi_A^s = 0$ and $\phi_D^s = 0.25$ at different temperatures: from top to bottom $T = 280$, 300, 320, 380 (K). The decay lengths are $4.4l$, $3.8l$, $3.3l$ and $2.4l$. The distance between the surfaces is given in lattice layers.*

4.5 Temperature Dependence of Hydration Repulsion

The temperature dependence of the repulsive surface interaction is illustrated in figs. 13 and 14. the interaction weakens upon increasing the temperature, and its range diminishes as well. This is explained by weakening association of the water molecules by hydrogen bonds.

For certain colloids (for instance quartz), stability is higher than is expected from standard DLVO theory. This has been explained by hydration repulsion [4]. In such cases, it is found that colloidal stability decreases upon increasing the temperature [3]. This is consistent with our present calculations on the repulsive hydration force.

5 CONCLUDING REMARKS

All six model surfaces that are examined in this section are more or less hydrophilic as judged from the excess surface tensions for the isolated surfaces (see table II). Excess here means: excess with respect to the surface in vacuo. The contact angles will for all surfaces be smaller than 90°. The excess surface tension equals the free energy of solvation per unit surface area; the free energy change of immersing a completely dry surface in water.

The surface excess amount correlates with the excess surface tension but a negative excess surface tension does not imply a positive surface excess of water.

The distance dependent surface forces do not correlate simply with the excess surface tension nor with the excess adsorbed amount. This is ad variance with the common conviction that the surface force between hydrophilic surfaces is repulsive and between hydrophobic surfaces attractive. The latter is probably correct but the interaction between hydrophilic surfaces might be attractive as well as repulsive. This depends on the dominant ordering mechanism that occurs at a surface. If a surface influences the orientational distribution of adjacent water, then overlap of the solvation layers of two such surfaces that approach each other disrupts the orientational order. This leads to a repulsive surface force. If the ordering near a surface is such that it is enhanced by overlap of the solvation layers of two surfaces then the surface force is attractive.

Table II

ϕ_A^s	ϕ_D^s	$\dfrac{\gamma^{exc}(\infty)a}{kT}$	θ^{exc}	surface force
0.0625	0.0625	–0.2830	–0.6300	– –
0.125	0.125	–1.346	–0.08900	(–)
0.1875	0.1875	–2.0984	0.3811	–
0	0.125	–0.2106	–0.569	– / +
0	0.25	–1.053	–0.04823	+++
0	0.5	–1.964	0.3843	++++

In this chapter it is shown that the relation between the sign of the distance-dependent surface force and the properties of the surfaces are more delicate than is often suggested [23]. The surface force can not be simply related to the hydrophilicity/hydrophobicity of the surfaces; that is, to the affinity of water for the surface as reflected in the excess (with respect to the surface in vacuo) surface tension (~ solvation free energy per unit area) of an isolated surface. It also depends on the nature of the solvation layers and especially, on the way solvation layers overlap: Generally, if overlap of solvation layers leads to enhancement of the ordering, then the ensuing force will be attractive. If overlap disrupts the order, then the associated surface force is repulsive. In theory, these mechanisms can be separately studied. In practical situations usually more than one ordering mechanisms together with well known DLVO forces operate at the same time. These different mechanisms are generally not independent and can not be simply summated.

Calculations indicate that energetically homogeneous surfaces behave similarly as the surfaces carrying donors and acceptors discussed above.

One should be very careful in relating for instance the disjoining pressure in adsorbed films to that between to immersed solid surfaces. [2]. In the case of an adsorbed film, the two surfaces are different (i.e. a "vapour-liquid"- and a "liquid-solid" surface).

The present results suggest that in so called "secondary-minimum" adhesion of proteins might be more specific, than is believed at present [20]. By means of hydration forces, molecular recognition in biological systems might operate between surfaces that are not in direct contact.

In the previous section, only the interaction between identical surfaces was considered. The interaction between different surfaces might be very different than the interaction between similar surfaces. For instance, the interaction between a surface with only donors and a surface with only acceptors will be attractive since the orientational ordering is enhanced by overlap.

It should be noted that in lattice models like that of Attard and Batchelor [33] and the present model oscillating interaction curves due to molecular layering [1] cannot be reproduced. The spatial resolution for such details of density profiles and interaction curves is restricted by the lattice spacing. In these models, the distances always correspond to integer numbers of lattice layers. On the other hand, in a lattice model where molecules occupy more than one site, oscillations can be reproduced [42, 43].

The results of the present chapter cannot be expected to be quantitatively correct for practical systems. Real surfaces should be represented by some intermediate of the above model surfaces. Further, long range Van der Waals- and electrical double layer interactions should be taken into account. In the lattice model, we did not account for electrostatic interactions: for the coupling between the charge distribution of water molecules with the electrical field normal to the surface. This can in principle be done by combining the present theory with ideas of the so called "multi Stern-layer model" for the charge distribution [44].

REFERENCES

1   Pashley, R. M.; Israelachvili, J. N. *J. Colloid Interface Sci.*, *101*, 510-523 (1984) "Molecular Layering of Water in Thin Films between Mica Surfaces and its Relation to Hydration Forces".

2   Derjaguin, B. V.; Churaev, N. V. *J. Colloid Interface Sci.*, *49*, 249-255 (1974) "Structural component of disjoining pressure".

3   Deryaguin, B. V.; Chureav, N. V. *Croat. Chem. Acta*, *50*, 187-195 (1977) "Structural components of the disjoining pressure of thin layers of liquids".

4   Churaev, N. V.; Derjaguin, B. V. *J. Colloid Interface Sci.*, *103*, 542-553 (1985) "Inclusion of structural forces in the theory of stability of colloids and films".

5   Pashley, R. M. *J. Colloid Interface Sci.*, *80*, 153-162 (1981) "Hydration Forces between Mica Surfaces in Aqueous Electrolyte Solutions".

6   Pashley, R. M. *J. Colloid Interface Sci.*, *83*, 531-546 (1981) "DLVO and Hydration Forces between Mica Surfaces in Li+, Na+, K+, and Cs+ Electrolyte Solutions: A Correlation of Double-Layer and Hydration Forces with Surface Cation Exchange Properties".

7   Pashley, R. M. *Adv. Colloid Int. Sci.*, *16*, 57-62 (1982) "Hydration Forces Between Mica Surfaces in Electrolyte Solutions".

8   Pashley, R. M.; Israelachvili, J. N. *J. Colloid Int. Sci.*, *97*, 446-455 (1984) "DLVO and Hydration Forces between Mica Surfaces in Mg2+, Ca2+, Sr2+ and Ba2+ Chloride Solutions".

9   Claeson, P. M. *Progr. Colloid & Polymer Sci*, *74*, 48-54 (1987) "Experimental evidence for repulsive and atractive forces not accounted for by conventional DLVO theory".

10 Le Neveu, D. M.; Rand, R. P.; Parsegian, V. A. *Nature*, *259*, 601-603 (1976) "Measurement of forces between bilayers".

11 McIntosh, T. J.; Magid, A. D.; Simon, S. A. *Biochemistry*, *26*, 7325-7332 (1987) "Steric repulsion between phosphatidylcholine bilayers".

12 Rand, R. P.; Fuller, N.; Parsegian, V. A.; Rau, D. C. *Biochemistry*, *27*, 7711-7722 (1988) "Variation in hydration forces between neutral phospholipid bilayers: evidence for hydration attraction".

13 McIntosh, T. J.; Magid, A. D.; Simon, S. A. *Biochemistry*, *28*, 7904-7912 (1989) "Range of solvation pressure between lipid membranes: dependence on the packing density of solvent molecules".

14 Rand, R. P.; Parsegian, V. A. *Biochim. Biophys. Acta*, *778*, 224-228 (1989) "Hydration forces between phospholipid bilayers".

15 Rau, D.; Parsegian, V. A. *Proc. Natl. Acad. Sci. USA*, *81*, 2621-2625 (1984) "Measurement of the repulsive force between polyelectrolyte molecules in ionic solution: Hydration forces between parralel DNA double helices".

16 Lyle, I. G.; Tiddy, G. J. T. *Chem. Phys. Letters*, *124*, 432-436 (1986) "Hydration forces between surfactant bilayers:An equilibrium binding description".

17 Persson, P. K. T.; Bergenståhl, B. A. *Biophys. J.*, *47*, 743-746 (1985) "Repulsive forces in lecithin glycol lamellar phases".

18 Bergenståhl, B. A.; Stenius, P. *J. Phys. Chem.*, *91*, 5944-5948 (1987) "Phase diagrams of dioleoylphosphatidylcholine with formamide, methylformamide, and dimethylformamide".

19 Dunstan, D. A. *Langmuir*, *8*, 740-743 (1992) "Forces between Mica Surfaces in Ca.Cl2 Solutions".

20 Norde, W.; Lyklema, J. *Colloids Surf.*, *38*, 1-13 (1989) "Protein adsorption and bacterial adhesion to solid surfaces: A colloid-chemical approach".

21 Lu, D. R.; Lee, S. J.; Park, K. *J. Biomater. Sci. Polymer Edn*, *3*, 127-147 (1991) "Calculation of solvation interaction energies for protein adsorption on polymer surfaces".

22 Parsegian, V. A. *Adv. Colloid Interface Sci, 16*, 49-56 (1982) "Physical Forces due to the State of Water Bounding Biological Materials: Some Lessons for the Disign of Colloidal Systems".

23 Derjaguin, B. V.; Churaev, N. V. *Colloids Surf., 41*, 223-237 (1989) "The current state of the theory of long-range surface-forces".

24 Israelachvili, J. N.; Pashley, R. M. *J. Colloid Interface Sci., 98*, 500-514 (1984) "Measurement of hydrophobic interaction between two hydrophobic surfaces in aqueous electrolyte solutions".

25 Israelachvili, J. N.; Wennerström, H. *Langmuir, 6*, 873-876 (1990) "Hydration or steric forces between amphiphilic surfaces?".

26 Marcelja, S.; Radic, N. *Chem. Phys. Lett., 42*, 129-130 (1976) "Repulsion of interfaces due to boudary water".

27 Gruen, D. W. R.; Marcelja, S. *J. Chem. Soc. Faraday Trans. 2, 79*, 225-242 (1983) "Spatially varying polarization in water".

28 Belaya, M. L.; Feigel'Man, M. V.; Levadny, V. G. *Chem. Phys. Lett., 126*, 361-364 (1986) "Hydration Forces as a Result of Non-Local Water Polarisation".

29 Leikin, S.; Kornyshev, A. A. *J. Chem. Phys., 92*, 6890-6898 (1990) "Theory of hydration forces. Nonlocal electrostatic interaction of neutral surfaces".

30 Kjellander, R.; Marcelja, S. *Chem. Phys. Lett., 120*, 393-396 (1985) "Perturbation of Hydrogen bonding in water near polar surfaces".

31 Berkowitz, M. L.; Raghavan, K. *Langmuir, 7*, 1042-1044 (1991) "Computer Simulation of a Water/Membrane Interface".

32 Raghavan, K.; Rami Reddy, M.; Berkowitz, M. L. *Langmuir, 8*, 233-240 (1992) "A molecular dynamics study of the structure and dynamics of water between dilauroylphosphatidylethanolamine bilayers".

33 Attard, P.; Batchelor, M. T. *Chem. Phys. Lett., 149*, 206-211 (1988) "A mechanism for the hydration force demonstrated in a model system".

34 Besseling, N. A. M. "Equilibrium properties of water and its liquid-vapour interface". Chapter III, Ibid.

35 Besseling, N. A. M. "On the molecular interpretation of the hydrophobic effect". Chapter IV, Ibid.

36 Besseling, N. A. M. "Statistical thermodynamics of molecules with orientation-dependent interactions in homogeneous and heterogeneous systems". Chapter II, Ibid.

37 Guggenheim, E. A. *Mixtures*; Clarendon: Oxford, 1952.

38 Landau, L. D.; Lifshitz, E. M.; Pitaevskii, L. P. *Statistical physics. part 1*; Pergamon press: Oxford, 1980.

39 Claeson, P. M.; Christenson, H. K. *J. Phys. Chem., 92*, 1650-1655 (1988) "Very Long Range Attractive Forces between Uncharged Hydrocarbon and Fluorocarbon Surfaces in Water".

40 Yushenko, V. S.; Yaminsky, V. V.; Shchukin, E. D. *J. Colloid Interface Sci., 96*, 307-314 (1983) "Interaction between particles in a nonwetting liquid".

41 Evans, R.; Marconi, M. B. *J. Chem. Phys., 86*, 7138-7148 (1987) "Phase equilibria and solvation forces for fluids confined between parallel walls".

42 Björling, M. in *Polymers at Interfaces*, edited by (Thesis, University of Lund, Sweden, Lund, 1992) pp. V:2-V:32. "Self consistent field theory for hard sphere chains close to hard walls".

43 Israëls, R.; Meijer, L. A. (1992). Personal communication: The theory of Scheutjens and Fleer applied to small branched molecules at a smooth surface reproduces an oscilatory density profile.

44 Böhmer, M. R.; Evers, O. A.; Scheutjens, J. M. H. M. *Macromolecules*, *23*, 2288 (1990)

CHAPTER VI

WATER-VAPOUR ADSORPTION, WETTING, CAPILLARY CONDENSATION IN SLITS

Some results on water-vapour adsorption and on the behaviour of liquid water adjoining some different surfaces are presented and discussed. It is indicated how these results relate to wetting phenomena. Both complete wetting and partial wetting occurs. This depends on the properties of the surface and on the temperature. The excess surface tension of a surface immersed in liquid water as well as in the vapour is calculated. Since also the tension of the liquid-vapour interface can be calculated, such quantities as the contact angle and the reversible work of adhesion of the liquid at the solid surface can be calculated. Capillary condensation in slits between two surfaces is examined. For narrow slits deviations from Kelvin's law occur. These phenomena are studied for various temperatures and for a number of model surfaces.

1 INTRODUCTION

In the following sections it will be demonstrated that it is possible to calculate the excess surface tension of a surface immersed in liquid water at coexistence with vapour and of the surface in saturated vapour. By 'excess' we mean the difference with respect to the value for the surface in vacuum. In chapter III the interfacial tension of the interface between coexisting liquid and vapour was already calculated. So all ingredients to characterise the equilibrium wetting behaviour are available. Some general reviews on wetting phenomena are refs. [1-4]. Here some relevant aspects are reviewed.

Often, the hydrophobicity or hydrophilicity of a surface is characterised by the contact angle, the angle between the liquid-vapour- and the solid-liquid interface. This angle can be calculated from the above-mentioned interfacial tensions by means of Young's law:

$$\cos\Theta = \frac{\gamma_{sv} - \gamma_{sl}}{\gamma_{lv}} \tag{1}$$

Here, Θ is the contact angle, γ_{sv}, γ_{sl}, and γ_{lv} denote the interfacial tension of the solid-vapour-, the solid-liquid- and the liquid-vapour interface, respectively.

A contact angle between 0° and 180° occurs if $\gamma_{sv} \leq \gamma_{sl} + \gamma_{lv}$ and if $\gamma_{sl} \leq \gamma_{sv} + \gamma_{lv}$. If γ_{sv} would be larger than $\gamma_{sl} + \gamma_{lv}$ then the solid-vapour interface could not exist at the saturation pressure: the liquid then completely wets the solid and a macroscopically thick liquid layer is found at the surface. Alternatively, if γ_{sl} would be larger than $\gamma_{sv} + \gamma_{lv}$ (which never occurs in practice, the Hamaker constant [5] between solid and liquid across vapour will always be positive; the interaction between solid and liquid will be attractive and a macroscopically thick intercalating vapour layer will not be stable), then the solid-liquid interface could not exist at the saturation pressure. Eq. (1) holds for intermediate cases: where partial wetting can occur; at the saturation pressure a part of the surface that is covered by macroscopically thick liquid film can coexist with a part of the surface at which a microscopic adsorbed layer is present.

Another quantity that is related to the three mentioned interfacial tensions is the reversible work of adhesion: the work to create a liquid-vapour and a solid-vapour interface at the cost of a liquid-solid interface:

$$W^{adh} = \gamma_{sv} + \gamma_{lv} - \gamma_{sl} \qquad (2)$$

Note that equations (1) and (2) in principle only hold if liquid and vapour are in equilibrium. Moreover, also the interfaces, for instance, the adsorption layer at the solid-vapour interface has to be in equilibrium. This condition is often does not met in actual contact angle measurements.

Equilibrium wetting transitions at an isolated surface occur in principle at bulk saturation conditions; pressure and chemical potentials have the values at which liquid and solid phases coexist. However, in a slit between two parallel surfaces (or in a capillary of a different geometry), the conditions for phase transitions can be shifted with respect to the bulk. Condensation phenomena in slits between surfaces will be examined in section 4.

In the present chapter some aspects of the equilibrium behaviour of water at solid surfaces will be considered that were not examined in the previous chapters. One purpose of the present chapter is to give an impression of the range of phenomena that can be handled by the theoretical methods introduced in previous chapters. Due to lack of time, this chapter has a provisional character.

The model for water is the same as that of the chapters III to V. Phase behaviour of fluids at surfaces cannot be adequately understood without thorough consideration of the phase behaviour of the fluid in situations where no additional surface is present. Fortunately, in chapter III, the liquid-vapour equilibrium and the liquid-vapour interface of water have already been studied by means of the same lattice-fluid theory that will also be used in the present chapter.

In the present chapter, some of the same types of model surfaces will be examined as in chapter V. These surfaces are partly occupied with proton donors and acceptors that are capable of forming hydrogen bonds with the acceptors and donors of water. The remainder of such a model surface does not interact with water (see
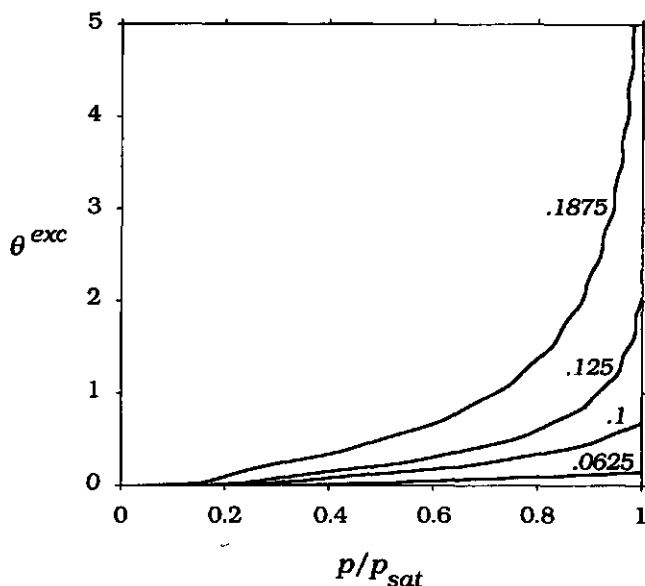
Figure 1. *Water-vapour adsorption isotherms at 300 K. The theoretical saturation pressure at this temperature is given by $p_{sat}v/kT = 1.1940 \cdot 10^5$. On the surface, the amount of proton donor faces equals the fraction of proton acceptor faces. The values of $\phi_A^{surf} = \phi_D^{surf}$ for the surfaces are indicated.*

table I of chapter V). In addition, "capillary vaporisation" in slits between perfectly hydrophobic surfaces will be studied.

2 VAPOUR ADSORPTION

At low surface coverage, the adsorption isotherm is linear and simply given by $\phi(1) = K_{ads}\phi$. The affinity between an inert surface and the molecules of a fluid can be characterised by the Henry coefficient of adsorption K_{ads}. For a lattice model this is given rigorously by

$$K_{ads} = \lim_{\phi \to 0} \frac{\phi(1)}{\phi} = \left\langle \exp - \frac{u}{kT} \right\rangle =$$

$$= \frac{1}{\omega} \sum_{\alpha} \phi_\alpha^{surf} \sum_o \exp - \frac{u_\alpha^o}{kT} = \frac{1}{q} \sum_{\alpha} \phi_\alpha^{surf} \sum_{\beta} q_\beta \exp - \frac{u_{\alpha\beta}}{kT} \tag{3}$$

Figure 2. *Excess interfacial tension due to vapour adsorption as a function of vapour pressure for the same systems as fig. 1.*

Here, ϕ is the site fraction of molecules in the bulk, and $\phi(1)$ in the lattice layer adjoining the surface, u is the int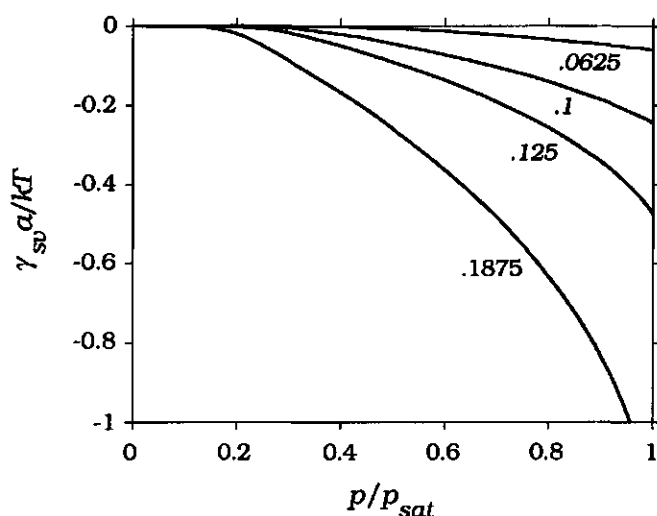eraction between molecule and surface for some specific site on the surface and some specific orientation of the molecule, $\langle \exp(-u/kT) \rangle$ is the average over all molecular orientations and surface sites of $\exp(-u/kT)$. The sum over α extends over the faces belonging the solid surface, ϕ_α^{surf} is the surface fraction of faces of type α. The number of orientations of the monomer is denoted as ω, in the case of water it equals 12. The sum over o extends over all these orientations. u_α^o is the interaction energy between a monomer having orientation o and a face of the solid surface of type α. The coordination number of the lattice is denoted by q, q_β is the number of β-faces on the surface of a molecule, $u_{\alpha\beta}$ is the interaction energy between an α- and a β-face. The first-order theory, developed in the previous chapters, leads for low densities to eq. (3).

According to eq. (3), the temperature dependence of the adsorption coefficient is more pronounced if the interaction between a molecule and the surface depends on the molecular orientation and on the position on the surface. This means that information on surface heterogeneity and on the orientation dependence of the
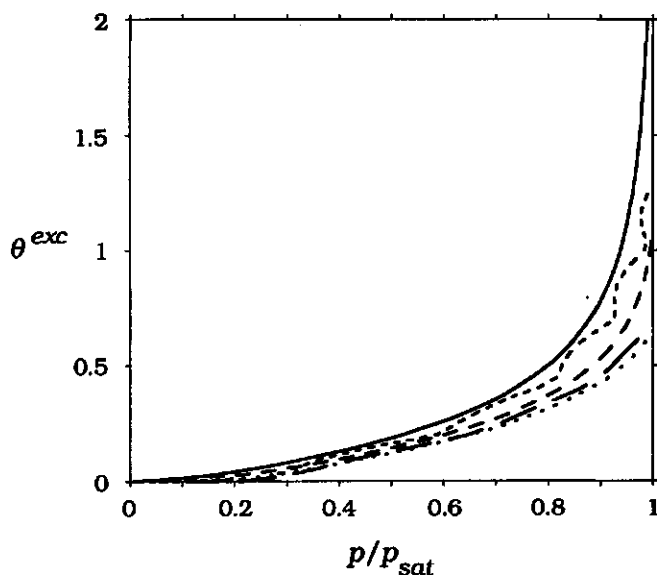
Figure 3. *Water vapour adsorption isotherms at a surface with* $\phi_A^{surf} = \phi_D^{surf} = 0.1$ *at various temperatures:* $T = 200$ *K (------),* $T = 300$ *K (— —),* $T = 400$ *K (······),* $T = 500$ *K (---),* $T = 600$ *K (———). At these temperatures the saturation pressure is given by* $p_{sat}v/kT$ *=* $5.0048 \ 10^{-9}$, $1.1940 \ 10^{-5}$, $5.1695 \ 10^{-4}$, $4.7282 \ 10^{-3}$ *and* $2.0537 \ 10^{-2}$ *respectively. A wetting transition occurs between 500 K and 600 K.*

interaction with the surface can in principle be extracted from the temperature dependence of K_{ads}.

For model surfaces with hydrogen bonding sites, as types A and B of chapter V, eq. (3) reduces to

$$K_{ads} = 1 + \tfrac{1}{4}\left(\phi_A^{surf} + \phi_D^{surf}\right)\left(\exp{-\frac{u_{Hb}}{kT}} - 1\right) \tag{4}$$

where ϕ_A^{surf} and ϕ_D^{surf} are the surface fractions of proton acceptors and proton donors respectively.

At low densities, the bulk vapour satisfies the ideal gas law. This can be written in terms of the lattice-site volume v and the fraction of occupied sites as $p = kT\phi/v$.

Upon increasing $\phi(1)$, lateral interactions between adsorbed molecules and the formation of second and higher adsorption layers
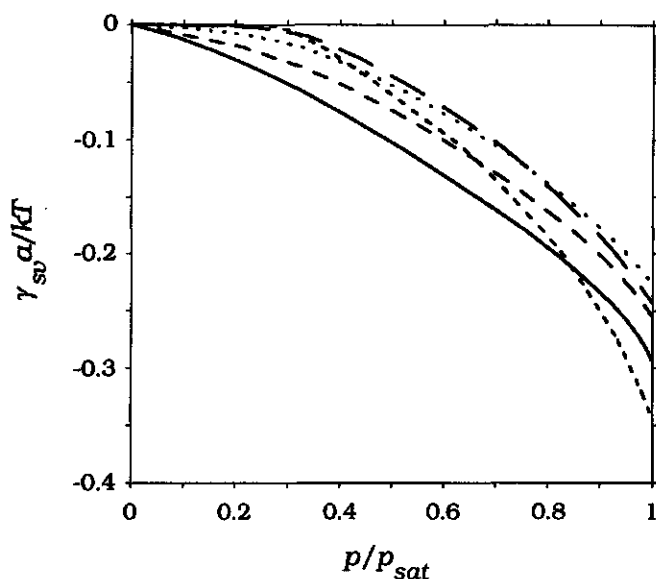
Figure 4. *Interfacial tensions for the same conditions as fig. 3.*

become more and more important. Consequently, the linear adsorption isotherm $\phi(1) = K_{ads}\phi$ does not hold anymore. Using the methods described in previous chapters, the complete adsorption isotherms can be calculated. Unless stated otherwise, results are calculated for a temperature of 300 K.

The pseudo plateaux of the adsorption isotherms, especially of the first layers, are determined by the density of hydrogen bonding sites on the surface. Although especially for lower temperatures some layering can be observed in the isotherms of figs. 1 and 3, pronounced adsorption plateaux do not occur. This is due to strong association of water molecules. Second and higher adsorption layers start building up as soon as first layer starts to contain some water. The density profiles of the adsorbed layers are rather shallow; the density decreases rather gradually towards that of the bulk. This has also been found for other situations: the liquid-vapour interface (chapter III) and liquid water adjoining a surface (chapter IV and V).

In fig. 1 it is shown how the shape of the vapour adsorption isotherms depends on properties of the surface. The isotherms for

the surfaces with $\phi_A^{surf} = \phi_D^{surf}$ = 0.0625, 0.1 and 0.125 show a finite adsorbed amount at the saturation pressure p_{sat}. This indicates that such a surface can be partially wet at p_{sat}; a thin adsorbed layer can coexist with a macroscopically thick liquid layer at the surface. Adsorbed layers having an intermediate thickness cannot exist at saturation. At a three-phase (solid, liquid and vapour) contact line, a contact angle with a value between 0° and 180° will be present.

Because of oscillations of the adsorption isotherms, that are associated with layering, the adsorption isotherm might cross the vertical $p = p_{sat}$ at several values for the adsorbed amount. The higher ones apply for metastable or instable states.

For the surface with $\phi_A^{surf} = \phi_D^{surf}$ = 0.1875, the adsorption diverges upon approaching p_{sat}. In this case the surface is completely wet at p_{sat}, only a macroscopic liquid layer can exist at the surface. Upon increasing pressure, the profile of the adsorbed layer shows a gradual change from a thin adsorption layer to a macroscopically thick liquid layer. At a temperature of 300 K, the change from non wetting to wetting will occur somewhere between $\phi_A^{surf} = \phi_D^{surf}$ = 0.125 and 0.1875.

In fig. 2, we see that for the cases of fig. 1, the surface tension decreases with p. Further, at fixed p, the surface tension decreases with increasing $\phi_A^{surf} = \phi_D^{surf}$. All curves end at some finite value at $p = p_{sat}$. For the case of complete wetting the adsorbed layer gradually increases with p until at $p = p_{sat}$ a macroscopic liquid layer is present and $\gamma = \gamma_{sl} + \gamma_{lv}$.

In fig. 3, the influence of temperature on the shape of the vapour adsorption at the surface with $\phi_A^{surf} = \phi_D^{surf}$ = 0.1 is shown and in fig. 4 the corresponding surface tension. If for a case of partial wetting the temperature is increased, a wetting transition is expected at a temperature below the bulk critical temperature. Cahn has given a mesoscopic analysis for cases where this wetting transition occurs at temperatures not to far below the bulk critical temperature [6]. From the vapour adsorption isotherms of fig. 3 it can be seen that for the surface with $\phi_A^{surf} = \phi_D^{surf}$ = 0.1 a wetting transition occurs between 500 K and 600 K. At 500 K the adsorbed amount at saturation pressure still has a finite value whereas at 600 K, it diverges upon approaching the saturation pressure.

Figure 5. *Excess surface tension for the surface in vapour at the saturation pressure as a function of temperature for two model surfaces. The values for $\phi_A^{surf} = \phi_D^{surf}$ are indicated. The kink in the curve for $\phi_A^{surf} = \phi_D^{surf} = 0.1$ is due to the occurrence of layering transitions.*
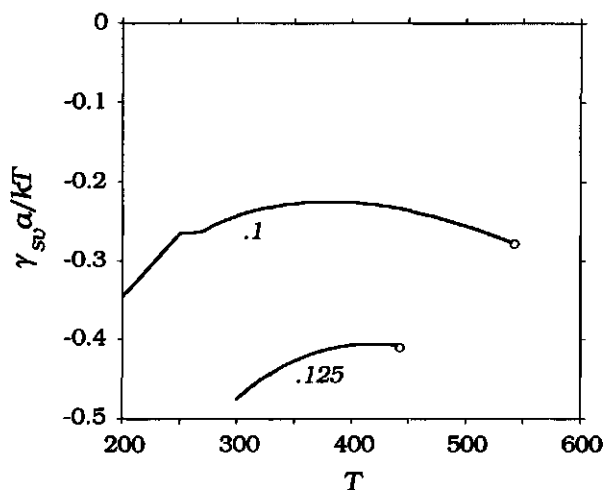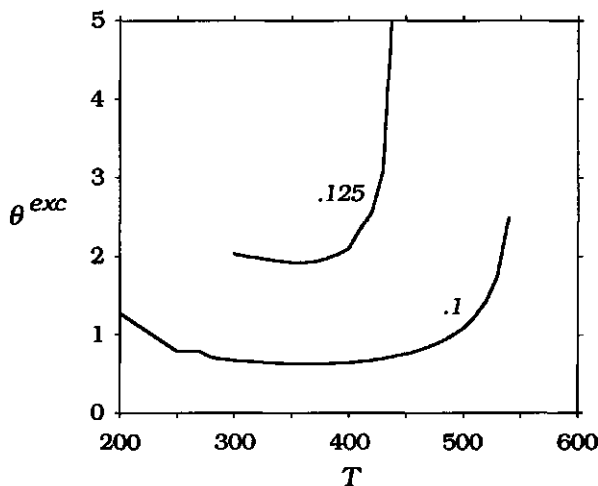

Figure 6. *Excess adsorbed amount for the surface in vapour at the saturation pressure as a function of temperature for two model surfaces. The values for $\phi_A^{surf} = \phi_D^{surf}$ are indicated. The kink in the curve for $\phi_A^{surf} = \phi_D^{surf} = 0.1$ is due to the occurrence of layering transitions.*
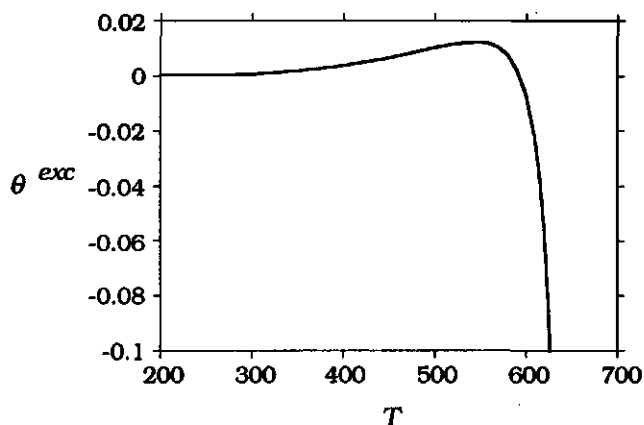
Figure 7. *Excess adsorbed amount from saturated vapour at a surface with $\phi_A^{surf} = \phi_D^{surf} = 0.01$.*

In fig. 6, the adsorbed amount at saturation is plotted as a function of temperature for two surfaces: $\phi_A^{surf} = \phi_D^{surf} = 0.1$ and 0.125. The adsorbed amount at the saturation pressure has a minimum at about 350 K. It becomes infinitely large at the wetting transition. The surface tension γ_{sv} as plotted in fig. 5 ends where it equals $\gamma_{sl} + \gamma_{lv}$ if the wetting transition is reached. The temperature range where partial wetting occurs is smaller for the surface with the higher value of $\phi_A^{surf} = \phi_D^{surf}$, then the wetting transition occurs at a lower temperature. For the presented cases, the temperatures for which total wetting occurs are considerably lower than the bulk critical temperature which is calculated as 639 K for this model [7]. For total wetting to occur, $\phi_A = \phi_D$ on a 'slice' of liquid should be not too far higher than $\phi_A^{surf} = \phi_D^{surf}$.

If $\phi_A^{surf} = \phi_D^{surf}$ is too far below $\phi_A = \phi_D$ of the fluid at the bulk critical point, then no wetting transition occurs (see for instance fig. 7). Moreover, the sign of the excess adsorbed amount changes sign from positive to negative. At the bulk critical temperature, the adsorbed amount diverges since the density decay length diverges there.

Figure 8. *Excess surface tension of the surface with $\phi_A^{surf} = \phi_D^{surf} = 0.1$ immersed in liquid water at coexistence with vapour.*

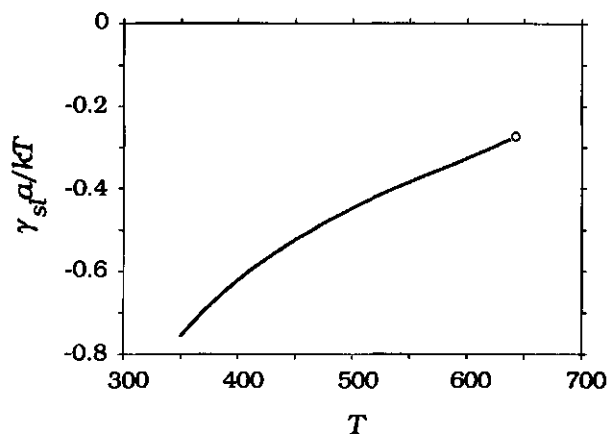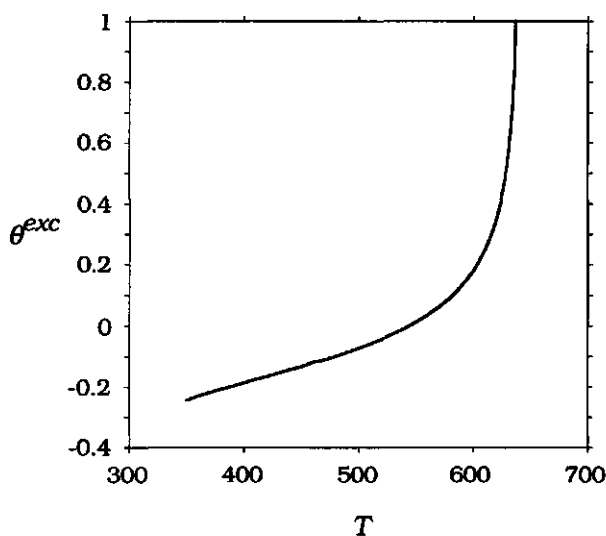Figure 9. *Excess amount of water at the surface with $\phi_A^{surf} = \phi_D^{surf} = 0.1$ immersed in liquid water at coexistence with vapour.*

3 LIQUID WATER AT SOLID SURFACES

At a surface immersed in liquid water, the local density of the fluid adjoining the surface will generally deviate from its bulk value. With

the model surface examined here, the local density at the surface will be lower than in the bulk if the density of hydrogen-bonding sites on the surface is lower than in bulk water. At a surface with $\phi_A^{surf} = \phi_D^{surf}$ = 0.1, this is the case if the temperatures is not too high (see fig. 9). Upon increasing temperature, the density of liquid water decreases and hence the surface excess changes sign from negative to positive at the temperature where $\phi_A = \phi_D \approx \phi_A^{surf} = \phi_D^{surf}$. Since at the bulk critical point, the density coherence length diverges, the thickness of the adsorption layer will also diverge there. The surface tension assumes a finite value.

At a surface for which $\phi_A^{surf} = \phi_D^{surf}$ on the surface is too much lower than $\phi_A = \phi_D$ in water at the bulk critical point, total dewetting occurs at some temperature below the critical temperature. This will not occur in practical systems because of the long range Van der Waals interactions: as noted before, the Hamaker constant between liquid and solid across vapour is always positive.

4 CONDENSATION PHENOMENA IN SLITS BETWEEN SURFACES

At a single surface, a reversible wetting transition occurs at bulk saturation conditions ($p = p_{sat}$). Some examples were discussed in the previous sections. Within a slit between two parallel planar surfaces (or in a capillary of a different geometry), the phase transition from a situation where the contents of the slit are vapour-like to one where the contents are liquid like, occurs at conditions that are shifted with respect to the bulk phase transition. This results in a very long-range force between the surfaces.

If the width of the slit is not too small, these phenomena are adequately described by the phenomenological relations of the Appendix. The shift of the phase transition and the surface force can be calculated from the behaviour of coexisting and of liquid and vapour at a single flat surface: (eqs. (A.3), (A.4) or (A.6)).

Things become slightly more complicated however if the separation between the slits is in the same range as the thickness of the hydration (adsorption, depletion) layers at the surfaces. Then we have to account for overlap of these layers. In the model calculations of the present section such effects are accounted for.

Results are presented for three different surfaces: $\phi_A^{surf} = \phi_D^{surf} =$ 0.0625, 0.125 and 0, respectively. For all these surfaces different separations are examined. For the first two cases, the behaviour of the contents of slit in a vapour environment ($p \leq p_{sat}$) and in a liquid environment ($p \geq p_{sat}$) is examined. For the surface with $\phi_A^{surf} = \phi_D^{surf}$ = 0, not much interesting happens and no plots are shown; the average density is always lower than in the bulk and gradually increases with pressure.

In the graphs of the average density between surfaces with $\phi_A^{surf} = \phi_D^{surf}$ = 0.0625, 0.125 against pressure up to p_{sat} (figs. 10 and 14), sigmoidal condensation loops are observed. The cusped figures in the corresponding graphs of the surface tension are also due to capillary condensation (figs. 11 and 15). At low pressures the surface tension is nearly constant and the corresponding average density in the slit is low (vapour-like). At high pressures, the average density inside the slit is high, liquid-like, and the corresponding surface tension decreases steeply with increasing pressure. Where the vapour branch of the surface tension crosses the liquid branch the two states of the slit can coexist. Experimentally, the average density would make a jump at such a point. Since metastable states exist, hysteresis effects might occur. The pressure at which the phase transition inside the slit occurs, increases with the width of the slit and approaches more and more the bulk saturation pressure.

The average density of the liquid inside the slit is for narrow slits lower than the density of the bulk liquid, especially if $\phi_A^{surf} = \phi_D^{surf}$ is low. The average density as a function of p for various widths appear to have a common intersection point. For wide slits, the surface tension for the slit filled with liquid decreases linearly with $\ln p$, as predicted by eq. (A.7). For narrow slits deviations from this linearity occur.
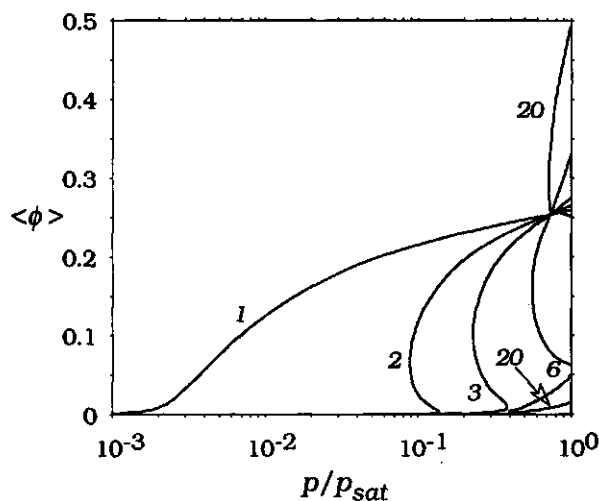
Figure 10. Average density within the slits between surfaces with $\phi_A^{surf} = \phi_D^{surf} = 0.0625$ as a function of vapour pressure for different surface separations. The density is given as the fraction of sites occupied with water. The separation between the surfaces is indicated in lattice layers.

Figure 11. Excess surface tension of surfaces with $\phi_A^{surf} = \phi_D^{surf} = 0.0625$ as a function of vapour pressure for different surface separations. The separation between the surfaces is indicated in lattice layers.

Figure 12. *Average density within the slit between surfaces with* $\phi_A^{surf} = \phi_D^{surf} = 0.0625$ *as a function of pressure for different surface separations. The density is given as the fraction of sites occupied with water. The separation between the surfaces is indicated in lattice layers. The density of the bulk liquid is given by the dashed curve.*

Figure 13. *Excess surface tension of surfaces with* $\phi_A^{surf} = \phi_D^{surf} = 0.0625$ *as a function of vapour pressure for different surface separations. The separation between the surfaces is indicated in lattice layers.*

Figure 14. *Average density within the slit between surfaces with $\phi_A^{surf} = \phi_D^{surf} = 0.125$ as a function of vapour pressure for different surface separations. The density is given as the fraction of sites occupied with water. The separation between the surfaces is indicated in lattice layers.*

Figure 15. *Excess surface tension of surfaces with $\phi_A^{surf} = \phi_D^{surf} = 0.125$ as a function of vapour pressure for different surface separations. The separation between the surfaces is indicated in lattice layers.*
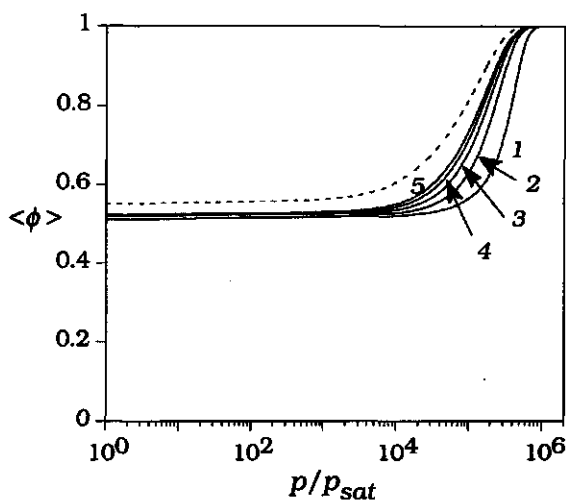
Figure 16.   Average density within the slit between surfaces with $\phi_A^{surf} = \phi_D^{surf} = 0.125$ as a function of pressure for different surface separations. The density is given as the fraction of sites occupied with water. The separation between the surfaces is indicated in lattice layers. The density of the bulk liquid is given by the dashed curve.
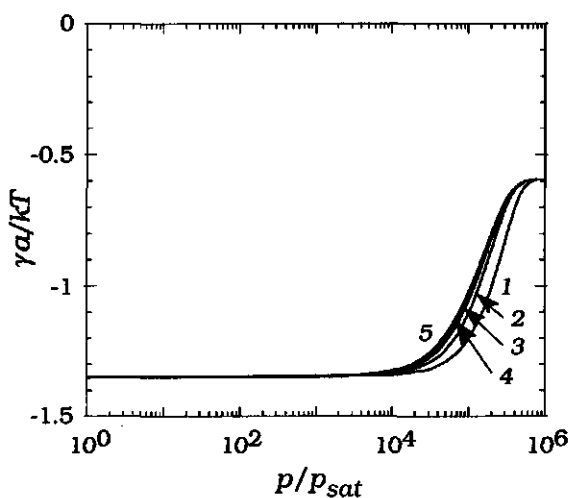
Figure 17.   Excess surface tension of surfaces with $\phi_A^{surf} = \phi_D^{surf} = 0.125$ as a function of vapour pressure for different surface separations. The separation between the surfaces is indicated in lattice layers.

At 300 K, capillary condensation does not occur for a very narrow slit of one lattice layer. The increase of the density upon increasing pressure is gradual and does not exhibit a condensation loop. In a slit, the critical temperature is lowered. This is a manifestation of the general phenomenon that the critical temperature decreases with the dimensionality of the system. For a one-dimensional system, the critical temperature vanishes. A slit between two parallel surfaces can be considered as intermediate between a two- and a three dimensional system. If the slit is so narrow that only one layer of molecules can be accommodated then it can be considered as a genuine two dimensional system.

If $p \geq p_{sat}$, the bulk as well as the contents of the slit are liquid and no condensation phenomena occur between these relatively hydrophilic surfaces (see figs. 12, 13, 16 and 17). Especially for narrow slits, the average density is lower than in the bulk. This is due to the value of $\phi_A^{surf} = \phi_D^{surf}$ which is lower than $\phi_A = \phi_D$ in liquid water. The dependencies of the surface excess of water and of the surface tension upon the separation between the surfaces (that are closely related to hydration forces between the surfaces) have been examined in chapter V.

Finally, in figs. 18 and 19 it is shown that between hydrophobic surfaces ($\phi_A^{surf} = \phi_D^{surf} = 0$, and no other interactions with water), condensation occurs at $p \geq p_{sat}$. At $p = p_{sat}$, the surface tension vanishes. Increasing p from there, the surface tension increases linearly with p. This is in agreement with eq. (A.4), since the depletion layers are negligible in this case. The reversible condensation occurs at the pressure where this branch crosses the liquid branch.
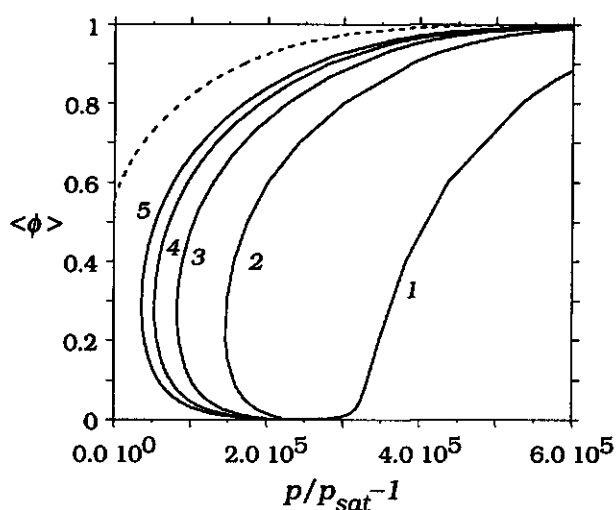
Figure 18. *Average density within the slit between hydrophobic surfaces as a function of pressure for different surface separations. The density is given as the fraction of sites occupied with water. The separation between the surfaces is indicated in lattice layers. The density of the bulk liquid is given by the dashed curve.*
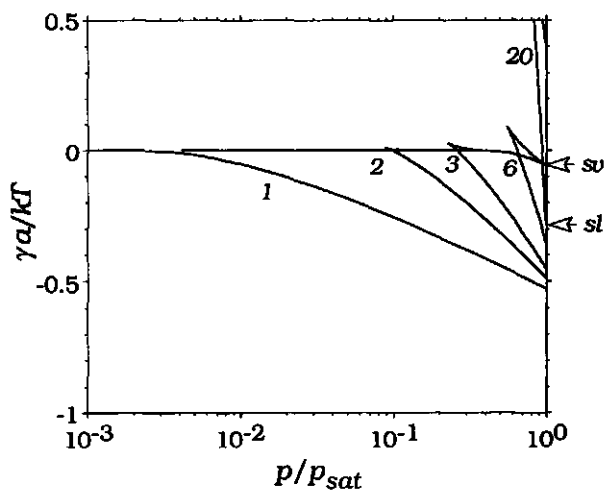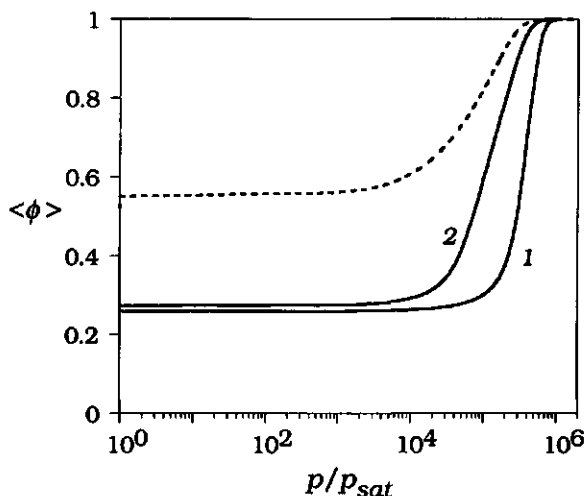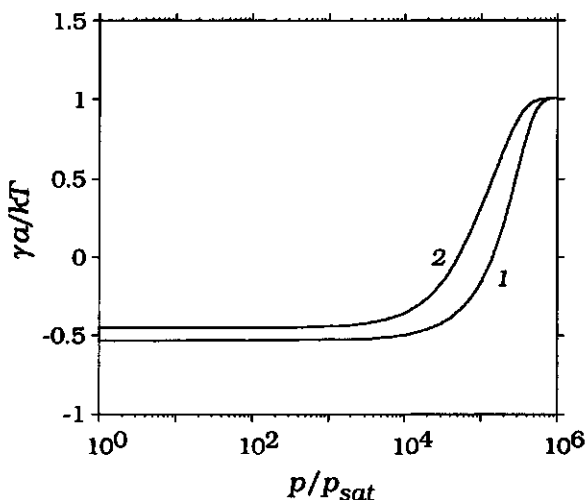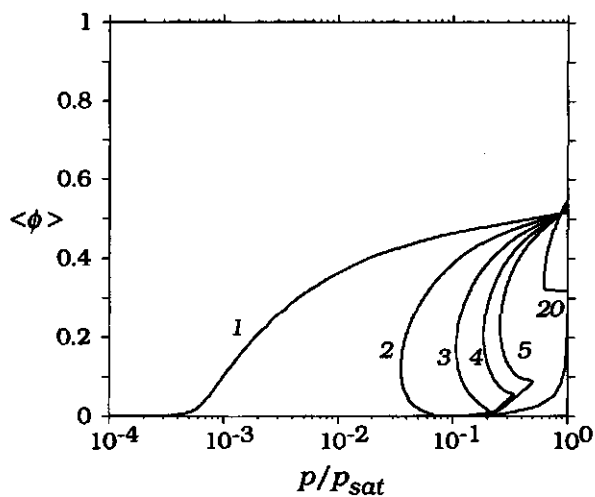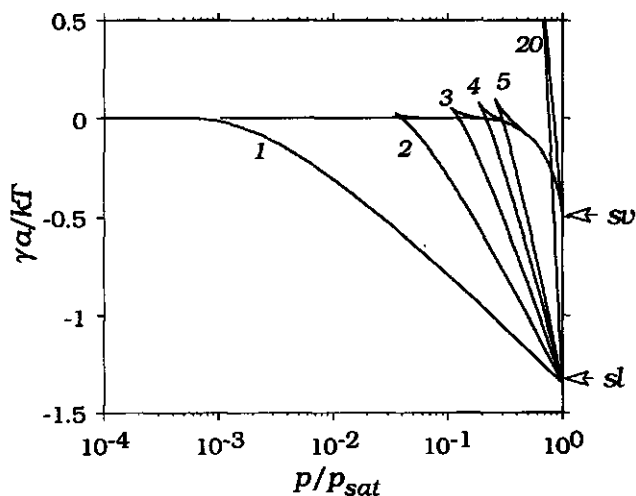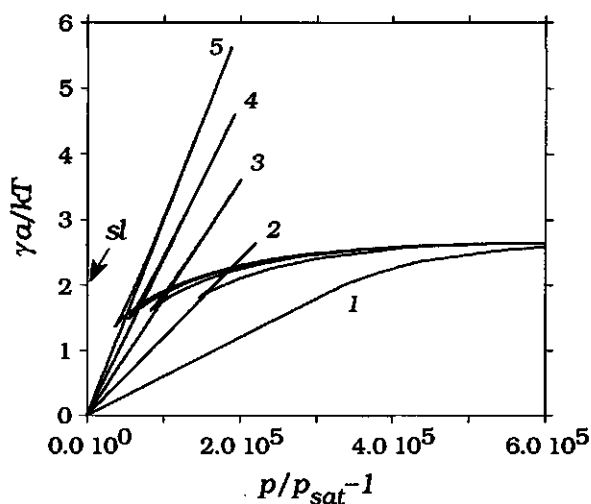

Figure 19. *Excess surface tension of hydrophobic surfaces as a function of vapour pressure for different surface separations. The separation between the surfaces is indicated in lattice layers. The value for the isolated solid-liquid interface is indicated by the arrow.*

APPENDIX *CONDENSATION PHENOMENA IN SLITS*

In the present appendix, some thermodynamic relations for condensation phenomena in slits are reviewed. Most results presented here have been obtained before in a slightly different manner by Evans and Marconi [8]. Consider a slit between two inert surfaces, each of area A at a distance H. The fluid film inside the slit is in equilibrium with bulk fluid characterised by a temperature T, and a pressure p. For the slit between two identical surfaces, the Gibbs adsorption equation can be written as

$$2\left(\frac{\partial \gamma}{\partial p}\right)_{T,H} = -\frac{2\Gamma^{exc}}{\rho} = \frac{H(\rho - \bar{\rho})}{\rho} \qquad (A.1)$$

Here γ is the interfacial tension of one surface, Γ^{exc} is the excess amount per unit of surface area of one surface, ρ is the bulk density and $\bar{\rho}$ is the average density inside the slit. We consider two different thermodynamic states of the slit: liquid- and vapour-like.

If the solvation (adsorption, depletion etc.) layers of the two surfaces do not overlap then γ is independent of H. In this case we can expand γ around p_{sat} making use of eq. (A.1). For the vapour-like state of the slit:

$$\gamma_{sx}(p) = \gamma_{sx}(p_{sat}) + (p - p_{sat})\frac{H(\rho(p_{sat}) - \bar{\rho}_x(p_{sat}))}{2\rho(p_{sat})} \qquad (A.2)$$

where x may indicate the liquid or the vapour state of the slit.

We find the conditions for coexistence of the liquid state with the vapour state inside the slit by equating $\gamma_{sv}(p)$ and $\gamma_{sl}(p)$ as given by eq. (A.2) and obtain

$$\frac{2\rho(\gamma_{sv} - \gamma_{sl})}{H(\bar{\rho}_v - \bar{\rho}_l)} = p - p_{sat} \qquad (A.3)$$

where the arguments (p_{sat}) are omitted and we write γ_{sx} for $\gamma_{sx}(p_{sat})$ etc.. So the pressure at which liquid and vapour coexist inside a slit is shifted with respect to the bulk value. Eq. (A.3)

applies for large H (such that overlap between adsorption or depletion layers is negligible) and for $p \approx p_{sat}$.

For large H, $\bar{\rho}_l$ can be replaced by ρ_l and $\bar{\rho}_v$ by ρ_v (often ρ_v can be disregarded with respect to ρ_l). If the bulk is a liquid then $\rho = \rho_l$ and $\rho/(\bar{\rho}_v - \bar{\rho}_l)$ equals -1. Using Young's law (eq. (1)) we obtain

$$\frac{2\gamma_{lv}\cos\theta}{H} = p_{sat} - p \qquad (A.4)$$

To be a little more accurate, $\bar{\rho}_v$ can be approximated by $(H\rho_v + 2\Gamma_v^{exc})/H$ where Γ_v^{exc} is the excess adsorbed amount at a unit area of an isolated surface in equilibrium with saturated vapour. Similarly, $\bar{\rho}_l$ can be approximated by $(H\rho_l + 2\Gamma_l^{exc})/H$.

If eq. (A.4) holds, then at values $H < 2\gamma_{lv}\cos\theta/(p_{sat} - p)$ the vapour state is stable and in some range beyond those values it will be metastable.

At $p = p_{sat}$, the bulk is a liquid and for not to small H, $(\rho - \bar{\rho}_v)/\rho$ approximately equals unity and the force between the surfaces is obtained by differentiating eq. (A.2):

$$-2\frac{\partial \gamma_{sv}(p)}{\partial H} = p_{sat} - p \qquad (A.5)$$

where the sign of the force is chosen to be positive if the surfaces repel each other. If $H > 2\gamma_{lv}\cos\theta/(p_{sat} - p)$ then the slit is in the liquid state. In as much as $(\rho - \bar{\rho}_l)/\rho$ vanishes, the force will be vanishing. The liquid state will be metastable for values not too far beyond $H > 2\gamma_{lv}\cos\theta/(p_{sat} - p)$.

As an example, we might consider water, $\gamma_{lv} = 73.10^{-3}$ N/m and $p_{sat} = 3.56.10^3$ (Pa.). For typical hydrophobic surfaces (the contact angle is 100^0) in water at 1.10^5 Pa. the liquid and the vapour state of the fluid film will coexist at a distance between the surfaces $H = 263$ nm. At smaller H, the contents of the slit become vapour like in a process that might be called capillary vaporisation. The attraction force between the surfaces will then be $1.10^5 - 3.56.10^3$ (Pa.). This type of attraction between the surfaces of a slit (or a capillary of a different geometry) might be relevant for the stability of porous hydrophobic materials. Such a material that is stable if immersed in

liquid water under some high pressure might collapse if the pressure is reduced.

If some gas is dissolved in the liquid, a 'bubble' between the surfaces occurs sooner than the above analyses predicts.

If the bulk is a low density vapour, the ideal gas law $\rho = p/RT$ applies. Substituting $\ln(p/p_{sat})$ for $p/p_{sat} - 1$, eq. (A.3) leads to

$$\frac{2\gamma_{lv}\cos\theta}{H(\rho_l - \rho_v)} = RT\ln\left(\frac{p}{p_{sat}}\right) \qquad (A.6)$$

and equation (A.2) to

$$\gamma_{sv}(p) = \gamma_{sv}(p_{sat}) + \tfrac{1}{2}H(\rho_l - \rho_v)RT\ln\left(\frac{p}{p_{sat}}\right) \qquad (A.7)$$

Equation (A.6) is known as the Kelvin law for the shift of the saturation pressure associated with a cylindrical surface with a radius of curvature $H/2\cos\theta$. The ratio p/p_{sat} can here be replaced by ρ/ρ_{sat}.

The arguments of the present appendix also apply to a binary mixture; then p should be read as the osmotic pressure $(\partial F/\partial V)_{T,n_1}$, where n_1 is one of the components.

The present discussion applies to a slit between planar surfaces. A similar analysis might be applied to curved surfaces. For example, a concave cylindrical surface could be chosen as a model for a pore. A slit between two convex surfaces as a model for approaching colloidal particles. For convex surfaces the condensation will occur at smaller distances than with planar ones and the force will increase with decreasing distance.

REFERENCES

1 Sullivan, D. E.; Telo de Gama, M. in *Fluid Interfacial Phenomena*, edited by Croxton, C. A. (Wiley, Chichester, 1986) pp. 45-134. "Wetting Transitions and Multilayer Adsorption at Fluid Interfaces".

2 Schick, M. in *Les Houches, Session XLVII, 1988-Liquids at Interfaces*, edited by Charvolin, J., et al. (Elsevier, Amsterdam, 1990) pp. 415- 498. "Introduction to Wetting Phenomena".

3 Dietrich, S. in *Phase Transitions and Critical Phenomena*, edited by Domb, C., et al. (Academic Press, London, 1988) pp. 2-218. "Wetting Phenomena".

4   Schrader, M. E. *Modern Approach to Wettability. Theory and Applications.*; Loeb, G. I.; Plenum: 1992.

5   Lyklema, J. *Fundamentals of Interface and Colloid Science. I: Fundamentals*; Academic Press: London, 1991.

6   Cahn, J. W. *J. Chem. Phys.*, *66*, 3667-3672 (1977) "Critical point wetting".

7   Besseling, N. A. M. "Water and its liquid-vapour interface". Chapter II, ibid.

8   Evans, R.; Marino Bettolo Marconi, U. *J. Chem. Phys.*, *86*, 7138-7148 (1987) "Phase equilibria and solvation forces for fluids confined between parallel walls".

A Lattice Theory for Chain Molecules in Homogeneous and Heterogeneous Systems Accounting for Correlation Effects

A lattice theory for chain molecules is presented, in which correlations for the occupations of nearest-neighbour sites is accounted for. In this respect, the present treatment is a generalisation of the quasi-chemical or Bethe-Guggenheim approximation. Parallel lattice layers may be differently occupied, so that heterogeneous systems can also be modelled. The present formulation is fairly general, It applies to any collection of chain molecules and monomers; the segments can possess different internal states; the intersegmental interactions may be orientation dependent; the systems may be isotropic or anisotropic, homogeneous or spatially heterogeneous. The packing statistics for given distributions of chain configurations and intersegmental contacts on a lattice are evaluated. Subsequently, a partition function is formulated as a sum over these distributions. From this, the self-consistent field equations for the equilibrium distributions are obtained. The segment-density distribution is efficiently evaluated by means of a propagator formalism, a recurrence relation for the statistical weight of chain fragments of increasing lengths. Methods to obtain numerical results are given.

1 INTRODUCTION

In a previous chapter [1] we presented a first-order self-consistent field lattice theory for interacting molecules. By *first-order* it is indicated that the theory goes beyond the random-mixing (Bragg-Williams) approximation, which is often denoted as *zeroth-order* [2]. This zeroth-order approximation ignores all correlations, even if non-zero interactions are present. To reproduce the temperature dependence of the thermodynamic properties especially of compounds with orientation-dependent intermolecular interactions, it is essential to account for local correlations [1]. This is illustrated particularly well in the application of the first-order approximation to a lattice-gas model for water [3-5]. Accounting for correlations due to the orientation-dependent interactions between water molecules, various properties of water, such as the maximum of the isobaric density as a function of temperature [3, 4] and the solvation of apolar molecules, could be reproduced. Moreover, interesting interfacial phenomena such as hydration forces could be considered [5].

In ref. [1], a theory was developed for lattice models of heterogeneous systems containing small anisotropic molecules, molecules with orientation-dependent interactions. Although formulated in a rather general manner, this treatment was restricted to monomeric components. It seems well worth while to extend the approach of ref. [1] towards chain molecules. The first-order approximation can also be applied to account for correlations due to connectivity of segments of chain molecules. For homogeneous isotropic mixtures this has been done by Huggins [6] and by Guggenheim [2, 7, 8]. DiMarzio has generalised this approach to homogeneous systems with oriented rigid rods [9] and to rigid rods near a surface [10]. Leermakers and Scheutjens [11] and, independently, Cantor and McIlroy [12] presented a statistical analysis for chain molecules in heterogeneous systems in which they accounted in first-order approximation for correlations due to bonds between segments. Somewhat inconsistently, Leermakers and Scheutjens as well as Cantor and McIlroy combined that with the Bragg-Williams approximation of random mixing and did not account for correlations

due to non-zero interactions. In the present chapter, we will treat correlations due to chemical bonds and those due to short range interactions on the same first-order footing.

In many statistical mechanical theories for chain molecules, evaluation of the segment distribution is facilitated by invoking a recurrence relation for the statistical weight (single-chain partition function) of chain fragments of different lengths [13, 14]. Such a propagator formalism has found many applications in the statistical thermodynamics of chain molecules. For instance, for a chain with excluded volume interactions [15], for polymers at surfaces [13, 16-21] and in colloidal systems [22], or for nematic ordering of semi-flexible polymers [16]. Some of these theories are based on a lattice model [17-21].

By combining a propagator formalism proposed by DiMarzio and Rubin for chains on a lattice [17] with the mean field approximations of Flory and Bragg and Williams [2, 23, 24], Scheutjens and Fleer derived a self-consistent field theory for the adsorption of interacting homopolymers [20, 21]. In the decade following these publications, various workers extended this approach in different directions and for a variety of applications [11, 18, 19, 25]. These include, the adsorption of polyelectrolytes [26, 27], block-copolymers [19], polymers with segments with different internal states [18, 25]. Apparently very different phenomena such as surfactant micelles [28], surfactant monolayers [12], emulsion droplets and bilayer vesicles [29], the bending elasticities of surfactant films [29], as well as biological membranes [11, 30, 31] and lipid vesicles [32] were also successfully modeled by this strategy.

The present chapter provides a generalisation of the first-order approximation towards all kinds of chain molecules. In principle this approach has the same versatility as the one initiated by Scheutjens and Fleer. In addition the effects of orientation dependent interactions can be accounted for. In the following section, the model will be defined in a rather general way. Any combination of molecular species, monomeric, linear and branched chains can be accommodated. The chains may consist of any combination of segment types. Moreover, the present treatment accounts for different (conformational) states of segments. By attributing to a

segment different states in which the connected bonds make different angles, semi-flexible chains can be modelled. The segments may or may not possess orientation-dependent interactions. It is straightforward to allow for vacant lattice sites and hence for free-volume effects. The thermodynamic consequences of this are considered. Moreover, most variables that will be used to describe the micro states of a system will be introduced.

In section 3 the combinatory analyses, that forms the basis of the theory, is presented. In section 4 appropriate partition functions are formulated and self-consistent field equations for the equilibrium distributions of chain configurations and contacts are derived. In section 5 expression for thermodynamic quantities are given. In section 6 a propagator formalism is derived, permitting an efficient evaluation of the segment distribution. As much as possible, the notation and routes of derivation of ref. [1] will be retained.

2 THE MODEL

General

The volume V that contains the system is imagined to be divided into a regular lattice of N sites, each of volume v. Each site is surrounded by an equal number of nearest neighbours. This lattice coordination number is denoted by q.

We distinguish parallel layers of sites. The layers are numbered by the variable z. To model heterogeneous systems, layers at different z are allowed to be different occupied. The number of sites of one layer, denoted by L, will be taken to be infinitely large. The number of layers, denoted by M, is finite. Boundary conditions have to be defined for the contents beyond the boundary layers, $z = 1$ and $z = M$. By means of reflecting boundary conditions a virtually infinitely large system can be considered. Alternatively, inert surfaces can be defined [1].

The present treatment applies to collections of molecules that can be of different sizes. The molecules consist of segments, each segment occupying one lattice site. A molecule that consists of r segments is called an r-mer. Model molecules occupying one lattice site are referred to as *monomers*. Sites can be allowed to be vacant.

This makes it possible to account for free-volume effects. In the statistical treatment, vacancies can be handled as just another monomeric species.

Segments of a chain molecule are connected by bonds. The number of segments of a chain of type a is denoted by r_a. For any linear or branched chain a that does not have closed rings, the number of bonds is given by $l_a = r_a - 1$. A monomer has q faces with which it makes contact with neighbours. For a chain segment this number is lowered by the number of bonds in which it is involved. The number of faces of a chain of type a is given by $q_a = qr_a - 2l_a$. These faces may be different or identical.

Segmental States

In previous chapters [1, 3-5], anisotropic monomers could assume distinguishable orientations. The monomers where considered rigid; the arrangement of faces on the surface of a monomer and other monomeric properties where fixed. However, in many cases, molecules or molecular segments possess some flexibility and internal degrees of freedom. Hence, we introduce the concept "state". The monomers and chain segments can assume different states. These states include the orientations as introduced previously [1] but, in addition, the arrangement of faces or bonds or other segmental properties may be different for different states. By definition, with the state of a segment the directions of its different faces and bonds are given.

To a segmental state, an intrinsic potential energy, denoted by w_A^σ, and an intrinsic degeneracy, denoted by ω_A^σ, can be attributed. We define an intrinsic weighting factor

$$g_A^\sigma = \omega_A^\sigma \exp- \frac{w_A^\sigma}{kT} \tag{1}$$

The a priori probability p_A^σ, for segment A to be in a state σ, is given by

$$p_A^\sigma = \frac{g_A^\sigma}{\sum\limits_{\sigma} g_A^\sigma} \tag{2}$$

Due to interactions of the segment with its environment, the probability of state σ will generally be different from p_A^σ. Such effects will be accounted for in the following statistical analysis.

The formal concept of segmental states enlarges the versatility of the present method. For instance, it makes it possible to model semi-flexible chains by attributing different a priori weights to states with different angles between successive bonds. This determines the flexibility of chain molecules that consist of these segments. The degree of stiffness of a chain molecule is commonly quantified by its *persistence length*, l_p, or by the length of its *statistical segments* or *Kuhn segments*, $2l_p$. The persistence length is defined as the average projection of the end to end vector of a chain onto the directional vector of its first bond if the chain were infinitely long. For a lattice model of a chain consisting of segments of type A only, l_p is given by

$$l_p = \frac{l}{1 + \sum_\sigma p_A^\sigma \cos\theta^\sigma} \tag{3}$$

Here l is the distance between the centres of nearest-neighbour lattice sites. The sum extends over all angles between consecutive bonds that are possible in the lattice.

Interactions between segments

Each segment exposes a number of faces that is equal to the lattice coordination number minus the number of chemical bonds in which the segment is involved. We distinguish different types of faces. The state of a segment is partly characterised by the directions of its various faces. This is quantified by numbers $q_{A\alpha}^{\sigma d}$, the number of faces of type α with direction d, on a segment of type A in state σ, it can assume values 0 and 1.

The total numbers of faces of type α in layer z with direction d, and the distribution of segments are related as

$$n_\alpha^d(z) = \sum_{A,\sigma} n_A^\sigma(z) q_{A\alpha}^{\sigma d} \tag{4}$$

for each α, z and d.

The numbers $n_A^\sigma(z)$ of segments of type A in layer z and state σ, and the number of chains of type a with conformation c are related as

$$n_A^\sigma(z) = \sum_{a,c} n_a^c r_{aA}^{c\sigma}(z) \tag{5}$$

Here n_a^c is the number of chains of type a, with configuration c. The *configuration* of a chain is completely defined by the state and layer number of each of its segments. Consequently the state of each segment of a chain is also known if the chain configuration is known. By $r_{aA}^{c\sigma}(z)$ we denote the number of segments of type A, in state σ and layer z that belong to such a chain. We denote the total number of chains of type a by n_a. Obviously, $n_a = \sum_c n_a^c$. A complete distribution of configurations is indicated as $\{n_a^c\}$.

The total number of faces of type α with direction d, originating from layer z, is denoted by $n_\alpha^d(z)$. Indices α, β, . . . are used for unbonded faces only. The total number of not chemically bonded faces for a certain layer and direction is given by $n^d(z) = \sum_\alpha n_\alpha^d(z)$

The number of contacts between faces of type α having a direction d and originating from a site of layer z, and a face of type β, is denoted by $n_\alpha^d(z)_\beta$. The complete frequency distribution of contacts is denoted by $\{n_\alpha^d(z)_\beta\}$. In the present model, the interaction energy between two segments on nearest-neighbour sites depends on the face types involved in the contact. Interaction parameters for $\alpha\beta$ contacts are symmetrical with respect to exchange of α and β. Further, for each face type a reference has to be chosen. Let the number of face types be x, then there are in principle $(x^2 - x)/2$ independent interaction parameters. It is convenient to work with *exchange energies*. The exchange energy of an $\alpha\beta$-contact equals half the amount of energy necessary to break contacts $\alpha\alpha$ and $\beta\beta$ between identical faces, and to make two $\alpha\beta$ contacts. It can be calculated according to

$$v_{\alpha\beta} = u_{\alpha\beta} - \tfrac{1}{2}\left(u_{\alpha\alpha} + u_{\beta\beta}\right) \tag{9}$$

Accordingly, the exchange energy for contacts between identical faces vanishes; $v_{\alpha\alpha} = 0$ for each α. Alternative possibilities for quantifying the interactions are discussed in ref. [1].

It is convenient to define the fractions $\phi_A^\sigma(z) \equiv n_A^\sigma(z)/L$, $\phi_\alpha^d(z) \equiv n_\alpha^d(z)/L$ and $\phi_\alpha^d(z)_\beta \equiv n_\alpha^d(z)_\beta/L$. The number of segments per lattice-site surface area belonging to chains of species a is given by

$\theta_a = n_a r_a / L$. The joint probability distribution for the occupations of two nearest-neighbour sites, $\phi_\alpha^d(z)_\beta$, is related to the nearest-neighbour distribution function

$$\psi_\alpha^d(z)_\beta \equiv \frac{\phi_\alpha^d(z)_\beta}{\phi_\beta^{-d}(z')} \tag{6}$$

This is the conditional probability of a face of type α in layer z at direction d, provided it makes contact with a face of type β. Sometimes, the term surface fraction is used for such quantity: $\psi_\alpha^d(z)_\beta$ is the fraction of α-faces at the surface of β-faces with direction $-d$ at layer z'.

Moreover, we introduce the nearest-neighbour correlation function

$$g_\alpha^d(z)_\beta \equiv \frac{\phi_\alpha^d(z)_\beta}{\phi_\alpha^d(z)\phi_\beta^{-d}(z')} = \frac{\psi_\alpha^d(z)_\beta}{\phi_\alpha^d(z)} \tag{7}$$

If the contacts are formed at random, then the nearest-neighbour distribution, $\psi_\alpha^d(z)_\beta$, is independent of β, and simply given by

$$\psi_\alpha^{*d}(z)_\beta = \frac{\phi_\alpha^d(z)}{\phi^d(z)} \tag{8}$$

Then, the distribution of contacts is given by $\phi_\alpha^{*d}(z)_\beta = \phi_\alpha^d(z)\phi_\beta^{-d}(z')/\phi^d(z)$, and for each α, β, z and d, the nearest-neighbour correlation function, $g_\alpha^{*d}(z)_\beta$, equals $1/\phi^d(z)$. In a systems with monomeric compounds only, it equals 1 for all z, d, α, β.

Configurational Energy

The energy of the system is assumed to be a sum of the energies of all intersegmental contacts and of segmental states. Only interactions between segments on nearest-neighbour sites are accounted for.

The overall potential energy of a system having a certain configuration is given by

$$U\left(\left\{n_a^c\right\}, \left\{n_\alpha^d(z)_\beta\right\}\right) = \sum_{A,\sigma} n_A^\sigma w_A^\sigma + \tfrac{1}{2} \sum_{z,d,\alpha,\beta} n_\alpha^d(z)_\beta v_{\alpha\beta} \tag{10}$$

Here, the first sum on the right-hand side of eq. (10) contains the contributions of the internal segmental energy, the second one accounts for contact interactions. The factor $\frac{1}{2}$ is needed because the summation over α, β and d counts each contact twice.

3 COMBINATORICS

In a previous chapter [1], a first-order combinatory formula was derived for a collection of monomers with a given distribution over orientations and layers and, simultaneously, a given distribution of contacts. Hence, correlations within a sequence of lattice sites are accounted for in a first-order Markov approximation. In the present chapter we will, in addition, account for chemical connectivity within chain molecules, on the same level of approximation.

It is assumed that all contacts are independent, apart from the conditions

$$\sum_{\beta} n_{\alpha}^d(z)_{\beta} = n_{\alpha}^d(z) \tag{11}$$

for each α, d and z. The $n_{\alpha}^d(z)$'s are related to the distribution of chain configurations via eqs. (4) and (5). Equation (11) implies that each layer contains the same number of segments. If, in addition, the constraint

$$\sum_{a} n_a r_a = ML \tag{12}$$

is satisfied, then each layer of L sites contains L segments.

At first, we will derive an approximate expression for $\Omega\left(\left\{n_a^c\right\}\right)$, the number of ways to arrange on the lattice a collection of chains (monomers and vacancies included) with a specified distribution of configurations without specifying the distribution of contacts. We apply a counting scheme which is a modification of that of Flory and Huggins [6, 23]. The chains are imagined to be inserted one by one. For the first segment of a chain of certain type and conformation, a site is selected at random in the layer where it is placed. The sites on which the following segments are placed are then known since we work with a fixed conformation. We write $P_s(\tau)$ for the probability

that segment s of the τth chain arrives at an unoccupied site, provided all preceding segments of that chain have found an unoccupied site. Accordingly, the probability that an attempt to insert the τth chain is successful (does not encounter any site that is already occupied), is given by $\prod_{s(\tau)} P_s(\tau)$, where the multiple product extends over all segments of this chain. The total number of ways to insert the chain equals $L\prod_{s(\tau)} P_s(\tau)$ (where the degeneracy of segmental states is not counted yet). The segmental states contribute a factor $\prod_{A,\sigma} \omega_A^{\sigma\ n_A^\sigma}$ to $\Omega(\{n_a^c\})$. For the total number of ways to arrange the ensemble of chains on the lattice we can hence write rigorously

$$\Omega(\{n_a^c\}) = \prod_{A,\sigma} \omega_A^{\sigma\ n_A^\sigma}\ \frac{L^n}{\prod_{a,c} n_a^c!} \prod_{\tau=1}^{n}\prod_{s(\tau)} P_s(\tau) \tag{13}$$

Here n denotes the total number of chains $\sum_{a,c} n_a^c$. If volume exclusion is not accounted for, the number of ways to place n distinguishable chains with specified configurations is L^n. Factorials $n_a^c!$ correct for indistinguishability of chains of the same type having the same configuration. The factor $L^n/\prod_{a,c} n_a^c!$ is essentially the configurational partition function for an ideal gas. This is corrected for site exclusion by the multiple product of $P_s(\tau)$. Strict exclusion of configurations with multiple occupancy of one or more sites, by rigorously evaluating all $P_s(\tau)$'s, is impracticable for macroscopic systems containing chain molecules. Scheutjens and coworkers applied Flory's mean field approximation [2, 23] to an equation like (13) and accordingly assumed that for each segment, the probability that it arrives at an unoccupied site equals the fraction of sites that are still unoccupied in the layer where that site is placed [19-21]. If the number of chains of type a having configuration c that are already placed in the lattice at stage τ is denoted as $n_a^c(\tau)$, and the number of segments in layer z, of a chain with configuration c as $r_a^c(z)$, then the number of sites in layer z that are not yet occupied is given by $n_\emptyset(z,\tau) = L - \sum_{a,c} n_a^c(\tau) r_a^c(z)$, and the fraction of such sites by

$$\phi_\emptyset(z,\tau) = \frac{n_\emptyset(z,\tau)}{L} \tag{14}$$

Only for the first segment of each chain, it is exact to substitute $\phi_\varnothing(z,\tau)$ for $P_s(\tau)$. For a lattice filled with monomers this leads to the exact expression (see eq. (10) of ref. [1]). For chains, it does not, since all correlations due to the connected nature of segments are neglected. It can be said that the Flory approximation ignores the connected nature of chain segments in the way site exclusion is accounted for. We will apply a more accurate approximation which is a generalisation of that of Huggins [6] and of Guggenheim [2, 7].

The probability that a segment arrives at an unoccupied site, provided previous segments have found empty sites, will generally be larger than the unconditional probability to arrive at an empty site, $\phi_\varnothing(z,\tau)$. The conditional probability that a segment finds a site empty in layer z at stage τ, given that the previous segment of the same chain has found room at the adjacent site in direction d, is denoted as $\psi_\varnothing^d(z,\tau)_\varnothing$. Remember that in the imaginary insertion process, contacts are formed at random. Hence, for similar reasons as invoked in eq. (8), by substituting $\varnothing$ for α and β, we obtain

$$\psi_\varnothing^d(z,\tau)_\varnothing = \frac{n_\varnothing(z,\tau)}{n^d(z,\tau)} \tag{15}$$

where $n^d(z,\tau) = L - \sum_{a,c} n_a^c(\tau) \lambda_a^{cd}(z)$ is the number of pairs of sites, consisting of one located in layer z and its nearest neighbour in direction d, that are not occupied by bonded segments.

For the probability of a successful insertion of a complete chain, $\prod_{s(\tau)} P_s(\tau)$, a Markov approximation will be used: the transition probability for each subsequent segment to arrive at an unoccupied site is assumed to be independent of the preceding steps. Hence, in eq. (13) $\phi_\varnothing(z,\tau)$ is substituted for the first segments of each chain, and $\psi_\varnothing^d(z,\tau)_\varnothing$ for all other segments. We obtain (see APPENDIX I)

$$\Omega\big(\{n_a^c\}\big) = \prod_{A,\sigma} \omega_A^{\sigma\,n_A^\sigma} \frac{L!^M}{\prod\limits_{a,c} n_a^c!} \prod_{z,d} \left(\frac{n^d(z)!}{L!}\right)^{1/2} \tag{16}$$

The exponent $\tfrac{1}{2}$ is needed since in the product over all z and d, each factor occurs twice. For one-dimensional systems this formula is

exact. For two- and three-dimensional systems it is exact for
situations where all bonds are parallel.

Making the additional assumption, that all configurations of a
chain occur with the same frequency (hence the system is
homogeneous and isotropic, the parameter z can be omitted, for M a
value of 1 can be substituted and for L: N) eq. (16) reduces to
Guggenheim's eq. 10.10.2 (apart from the factor $\prod_{A,\sigma} \omega_A^{\sigma}{}^{n_A^\sigma}$ and
different symbols) [2]. DiMarzio has derived a combinatory formula for
oriented rigid rods on a cubic lattice, for homogeneous systems [9] and
for rigid rods adjoining a surface [10] which are also special cases of
our equation. Moreover, eq. (16) is equivalent to eq. (7) of
Leermakers and Scheutjens [11].

As in ref. [1], the effects of a specified distribution of contacts,
$\left\{n_\alpha^d(z)_\beta\right\}$, are also evaluated on the level of a first-order Markov
approximation for correlations within sequences of sites. The
configurational degeneracy of the system for given distributions of
chain configurations and of contacts, $\Omega\!\left(\left\{n_a^c\right\},\left\{n_\alpha^d(z)_\beta\right\}\right)$, is assumed to
have the functional form

$$\Omega\!\left(\left\{n_a^c\right\},\left\{n_\alpha^d(z)_\beta\right\}\right) = \frac{f\!\left(\left\{n_a^c\right\}\right)}{\left(\displaystyle\prod_{\alpha,\beta,d,z} n_\alpha^d(z)_\beta!\right)^{1/2}} \tag{17}$$

where factorials $n_\alpha^d(z)_\beta!$ in the denominator account for
indistinguishability of identical contacts; the exponent $\frac{1}{2}$ is needed
since in the product over all α, β, d and z, the number of contacts of
each type occurs twice. The numerator $f\!\left(\left\{n_a^c\right\}\right)$ is some function of
the distribution of chain configurations only. It follows from the
condition $\Omega\!\left(\left\{n_a^c\right\},\left\{n_\alpha^{*d}(z)_\beta\right\}\right) = \Omega\!\left(\left\{n_a^c\right\}\right)$ that

$$\Omega\!\left(\left\{n_a^c\right\},\left\{n_\alpha^d(z)_\beta\right\}\right) = \Omega\!\left(\left\{n_a^c\right\}\right)\!\left(\prod_{\alpha,\beta,d,z} \frac{n_\alpha^{*d}(z)_\beta!}{n_\alpha^d(z)_\beta!}\right)^{1/2} \tag{18}$$

The second factor on the r.h.s. vanishes if the distribution of
contacts is completely random. Applying Sterling's theorem,
$\ln n! = n\ln n - n$ for large n, to eq. (18) we obtain

$$\ln \Omega\left(\left\{n_a^c\right\}, \left\{n_\alpha^d(z)_\beta\right\}\right) = \ln \Omega\left(\left\{n_a^c\right\}\right)$$

$$-\tfrac{1}{2} \sum_{z,d,\alpha,\beta}\left(n_\alpha^d(z)_\beta \ln \phi_\alpha^d(z)_\beta - n_\alpha^{*d}(z)_\beta \ln \phi_\alpha^{*d}(z)_\beta\right) \qquad (19)$$

where the last terms on the r.h.s account for non-randomness of the distribution of contacts. According to eq. (16)

$$\ln \Omega\left(\left\{n_a^c\right\}\right) = -\sum_{a,c} n_a^c \ln \frac{n_a^c}{L} + \sum_{A,\sigma} n_A^\sigma \ln \omega_A^\sigma + \tfrac{1}{2}\sum_{z,d} n^d(z) \ln \phi^d(z) \qquad (20)$$

where the last term on the r.h.s accounts for correlation effect due to chain connectivity. To obtain eq. (20), we have used $\tfrac{1}{2}\sum_{d,z} n^d(z) = \tfrac{1}{2}qML - \sum_a n_a l_a$ with $\sum_a n_a l_a = ML - \sum_a n_a$. This last equality only holds if none of the chains contains closed rings of segments.

Since $\tfrac{1}{2}\sum_{z,d,\alpha,\beta} n_\alpha^{*d}(z)_\beta \ln \phi_\alpha^{*d}(z)_\beta$ equals $\sum_{z,d,\alpha} n_\alpha^d(z) \ln \phi_\alpha^d(z) - \tfrac{1}{2}\sum_{z,d} n^d(z) \ln \phi^d(z)$, eqs. (19) with (20) can be rewritten as

$$\ln \Omega\left(\left\{n_a^c\right\}, \left\{n_\alpha^d(z)_\beta\right\}\right) = -\sum_{a,c} n_a^c \ln \frac{n_a^c}{L} + \sum_{A,\sigma} n_A^\sigma \ln \omega_A^\sigma$$

$$-\tfrac{1}{2}\sum_{z,d,\alpha,\beta} n_\alpha^d(z)_\beta \ln \phi_\alpha^d(z)_\beta + \sum_{z,d,\alpha} n_\alpha^d(z) \ln \phi_\alpha^d(z) \qquad (21)$$

or as

$$\ln \Omega\left(\left\{n_a^c\right\}, \left\{n_\alpha^d(z)_\beta\right\}\right) = -\sum_{a,c} n_a^c \ln \frac{n_a^c}{L} + \sum_{A,\sigma} n_A^\sigma \ln \omega_A^\sigma - \tfrac{1}{2}\sum_{z,d,\alpha,\beta} n_\alpha^d(z)_\beta \ln g_\alpha^d(z)_\beta \qquad (22)$$

Here, the last term on the right-hand side accounts for correlation effects due to bonds (between segments of the same chain) and to contacts. It vanishes for systems containing monomers only, in which the contacts are formed at random.

4 PARTITION FUNCTIONS AND EQUILIBRIUM CONFIGURATION

With the expressions for the configurational energy, $U\left(\left\{n_a^c\right\},\left\{n_\alpha^d(z)_\beta\right\}\right)$, and the degeneracy, $\Omega\left(\left\{n_a^c\right\},\left\{n_\alpha^d(z)_\beta\right\}\right)$, the configurational canonical partition function can be formulated

$$Q\left(\left\{n_a\right\},L,T\right) = \sum_{\left\{n_a^c\right\},\left\{n_\alpha^d(z)_\beta\right\}} \Omega\left(\left\{n_a^c\right\},\left\{n_\alpha^d(z)_\beta\right\}\right) \exp- \frac{U\left(\left\{n_a^c\right\},\left\{n_\alpha^d(z)_\beta\right\}\right)}{kT}$$

(23)

where the sum extends over all distributions of configurations that satisfy $\sum_c n_a^c = n_a$ for each component a, and over all distributions of contacts that satisfy the constraints (11) with eqs. (4) and (5); the symbol k denotes Boltzmann's constant.

The characteristic thermodynamic function for the independent variables $\left\{n_a\right\}$, L and T is the Helmholtz energy, $F = -kT \ln Q\left(\left\{n_a\right\},L,T\right)$. We define the partial Helmholtz energy of a component as

$$f_a \equiv \left(\frac{\partial F}{\partial n_a}\right)_{L,T,\left\{n_{b\neq a}\right\}}$$

(24)

The f_a's can be related to pressure and chemical potentials, as will be explained in section 5. The partition function for an ensemble of systems where for each system, instead of $\left\{n_a\right\}$, all f_a's and M are fixed, is obtained as a Laplace transform of $Q\left(\left\{n_a\right\},L,T\right)$

$$\Xi\left(\left\{f_a\right\},M,L,T\right) = \sum_{\left\{n_a\right\}} Q\left(\left\{n_a\right\},L,T\right) \exp \sum_a \frac{n_a f_a}{kT}$$

(25)

where the sum extends over all distributions of chains $\left\{n_a\right\}$ that satisfy the constraint (12).

It should be noted that the sum $\sum_a n_a f_a$ includes the term $-pV$ (see section 5). Accordingly, the characteristic function for the variables $\left\{f_a\right\}$, M, L and T is $F - \sum_a n_a f_a = \gamma A$, where γ is the interfacial tension and A the surface area.

For macroscopic systems, the most probable distributions of contacts and of chain configurations dominate the equilibrium properties of a system. These distributions, at which the summands of eqs. (25) and (23) are at their constrained maximum with respect to variations of $\left\{n_a^c\right\}$ and $\left\{n_\alpha^d(z)_\beta\right\}$, can be obtained by means of the Lagrange method (see for instance ref. [24]). We will locate the maximum of the unconstrained function

$$\mathcal{L}\left(\left\{n_a^c\right\},\left\{n_\alpha^d(z)_\beta\right\}\right) = \ln \Omega\left(\left\{n_a^c\right\},\left\{n_\alpha^d(z)_\beta\right\}\right) - \frac{U\left(\left\{n_a^c\right\},\left\{n_\alpha^d(z)_\beta\right\}\right)}{kT} + \sum_a \frac{n_a f_a}{kT} +$$

$$\sum_{\alpha,d,z} \lambda_\alpha^d(z)\left(\sum_\beta n_\alpha^d(z)_\beta - n_\alpha^d(z)\right) + \lambda\left(\sum_a n_a r_a - LM\right) \qquad (26)$$

where $\ln \Omega\left(\left\{n_a^c\right\},\left\{n_\alpha^d(z)_\beta\right\}\right)$ is given by eq. (21) and $U\left(\left\{n_a^c\right\},\left\{n_\alpha^d(z)_\beta\right\}\right)$ by eq. (10); $\lambda_\alpha^d(z)$ and λ are undetermined multipliers.

The most probable distribution of contacts is obtained from the equations

$$\frac{\partial \mathcal{L}}{\partial n_\alpha^d(z)_\beta} = -\ln \phi_\alpha^d(z)_\beta - 1 + \lambda_\alpha^d(z) + \lambda_\beta^{-d}(z') - \frac{v_{\alpha\beta}}{kT} = 0 \qquad (27)$$

for each α, β, d and z. Direction $-d$ is the opposite of d and z' is the layer number of the site at which d is directing from a site of layer z. Introducing $G_\alpha^d(z) = \phi_\alpha^d(z)\exp\left(\frac{1}{2} - \lambda_\alpha^d(z)\right)$, eq. (27) can be rewritten as

$$\phi_\alpha^d(z)_\beta = \frac{\phi_\alpha^d(z)\phi_\beta^{-d}(z')}{G_\alpha^d(z)G_\beta^{-d}(z')}\exp-\frac{v_{\alpha\beta}}{kT} \qquad (28)$$

The $G_\alpha^d(z)$, that are referred to as *face weighting factors*, account for saturation of faces in eq. (28). Substituting these expressions into the saturation constraints (11) we obtain the set of equations

$$\frac{1}{G_\alpha^d(z)}\sum_\beta \frac{\phi_\beta^{-d}(z')}{G_\beta^{-d}(z')}\exp-\frac{v_{\alpha\beta}}{kT} = 1 \qquad (29)$$

for each α, z and d.

Although the equations (28) and (29) are similar to eq. (19) and (20) of the previous chapter [1], in the present case effects of the presence of bonds are included. For homogeneous athermal systems, all products $G_\alpha^d(z)G_\beta^{-d}(z')$ are equal to $\phi^d(z)$ and the distribution of contacts is given by eq. (8).

The number of segments of type A in layer z and state σ, that belong to a chain of type a with configuration c, is $\partial n_A^\sigma(z)/\partial n_a^c = r_{aA}^{c\sigma}(z)$. Similarly, the number of faces of type α with direction d belonging to a segment of type A in layer z in state σ, is $\partial n_\alpha^d(z)/\partial n_A^\sigma(z) = q_{A\alpha}^{\sigma d}$. So the number of faces of type α in layer z, having direction d, belonging to a chain of type a having configuration c is $\partial n_\alpha^d(z)/\partial n_a^c = \sum_{A,\sigma} r_{aA}^{c\sigma}(z)q_{A\alpha}^{\sigma d}$. For each chain a with $l_a = r_a - 1$ (the chain does not have closed rings) and each conformation c we obtain

$$\frac{\partial \mathcal{L}}{\partial n_a^c} = -\ln\frac{n_a^c}{L} - 1 + \sum_{A,\sigma,z} r_{aA}^{c\sigma}(z)\left(\sum_{\alpha,d} q_{A\alpha}^{\sigma d}\left(\ln\phi_\alpha^d(z) - \lambda_\alpha^d(z)\right)\right)$$

$$+ \sum_{A,\sigma} r_{aA}^{c\sigma} \ln g_A^\sigma + r_a q - 2r_a + 2 + r_a\lambda + \frac{f_a}{kT} = 0 \qquad (30)$$

This expression for the distribution of chain configurations can be rewritten in a more convenient way. To this end, we define the *chain weighting factor* G_a^c in such a way that

$$\frac{n_a^c}{L} = \Lambda_a G_a^c \qquad (31)$$

where $\Lambda_a = \exp(f_a/kT)$.

Moreover, we define the *free-segment weighting factor* $G_A^\sigma(z)$ for a segment of type A in layer z and state σ, in such a way that the chain weighting factor can be written as a product of free-segment weighting factors of all its segments

$$G_a^c = \prod_{A,\sigma} G_A^\sigma(z)^{r_{aA}^{c\sigma}(z)} = \prod_s G_s\big|_a^c \qquad (32)$$

where s indicates a segment by its position in the chain, $G_s\big|_a^c$ is the free-segment weighting factor of segment s of a chain of type a with

configuration c. According to the definition for *chain configuration* used in this chapter, the state and layer number of all segments of a chain are fixed if the configuration of the chain to which they belong is fixed.

Free-segment weighting factors can also be factorised. If in eq. (30) the combination of terms $\ln \phi_\alpha^d(z) - \lambda_\alpha^d(z) + \frac{1}{2}$ are recognised to be equal to $\ln G_\alpha^d(z)$, and if we introduce C such that $\ln C = \frac{1}{2}q - 1 + \lambda$, then we can write

$$G_A^\sigma(z) = Cg_A^\sigma \prod_{d,\alpha} G_\alpha^d(z)^{q_{A\alpha}^{\sigma d}} = Cg_A^\sigma \prod_d G^d \big|_A^\sigma(z) \tag{33}$$

Here $G^d\big|_A^\sigma(z)$ is the face weighting factor of the face with direction d of a segment of type A in state σ located at layer z. Formally it equals 1 if there is a chemical bond at direction d. The product over α extends over all faces that are not occupied in a chemical bond.

Equation (33) reflects that the distribution of segments over states is generally influenced by the interactions with the other segments in the system. the probability that a segment A in layer z is in state σ is given by $G_A^\sigma(z) / \sum_\sigma G_A^\sigma(z)$ which will generally differ from the a priori probability given by eq. (2).

The factor Λ_a normalises the total amount of component a. Taking the sum over all configurations c of both sides of eq. (31) we obtain

$$\Lambda_a = \frac{n_a}{LG_a} = \frac{\theta_a}{r_a G_a} \tag{34}$$

where $LG_a = L\sum_c G_a^c$ can be considered as the configurational partition function of a single chain of type a in an external (molecular) field; it normalises the probability distribution of chain configurations: eq. (31) with (34) can be rewritten as $n_a^c/n_a = G_a^c/G_a$. If the chains do not experience any interactions, LG_a simply equals $LM\omega_a$ where ω_a is the number of configurations of an a-chain if one of its segments is fixed at a site.

If in a system with fixed M and L, for component a either Λ_a or n_a/L is fixed, the system is either open or closed with respect to that component. For systems to be in equilibrium it is required that for each component a, Λ_a has a common value in each system. It will

be clear that at given M and T the normalisation conditions of all components are not independent because a system is subject to condition (12).

5 THERMODYNAMIC FUNCTIONS

From the equilibrium distribution of the system, all thermodynamic quantities can be obtained. The configurational entropy follows from the equilibrium distribution with $S = k \ln \Omega\left(\left\{n_a^c\right\}, \left\{n_\alpha^d(z)_\beta\right\}\right)$. Substituting for n_a^c/L the expressions for the most probable distribution given by eqs. (31) to (33) and for $n_\alpha^d(z)_\beta$ and $n_\alpha^{*d}(z)_\beta$ expressions given by eq. (28) and eq. (8), respectively, we obtain

$$\frac{S}{Lk} = -\sum_a \frac{\theta_a f_a}{r_a kT} - M \ln C + \sum_{z,A,\sigma} \frac{\phi_A^\sigma(z) w_A^\sigma}{kT} + \tfrac{1}{2} \sum_{z,d,\alpha,\beta} \frac{\phi_\alpha^d(z)_\beta v_{\alpha\beta}}{kT} \quad (35)$$

Expression (35) is useful because it does not explicitly contain the (possibly very large number of) configurational frequencies.

Substituting the most probable distributions into eq. (10), the equilibrium value for the configurational energy is obtained. Comparing eqs. (35) and (10) it is noted that the last two terms on the right-hand side of eq. (35) equal U/LkT. Accordingly, the Helmholtz energy, $F = U - TS$, is given by

$$\frac{F}{LkT} = \sum_a \frac{\theta_a f_a}{r_a kT} + M \ln C \quad (36)$$

Moreover, since $F = \sum_a n_a f_a + A\gamma$ we obtain

$$\frac{\gamma a}{kT} = M \ln C \quad (37)$$

Where $\gamma = (\partial F/\partial A)_{T,V,\{n_a\}}$ is the surface tension and $a = A/L$ is the cross-sectional area per lattice site. For homogeneous systems $F = \sum_a n_a f_a$, and hence $C = 1$. This condition also determines the value of C for inhomogeneous systems that are at equilibrium with some homogeneous system.

The quantity f_0, where the subscript 0 indicates vacancy, can be related to the pressure

$$p = -\left(\frac{\partial F}{\partial V}\right)_{T,n_{a\neq0}} = -\frac{1}{v}\left(\frac{\partial F}{\partial n_0}\right)_{T,n_{a\neq0}} = -\frac{f_0}{v} \qquad (38)$$

where $v = V/N$ is the volume of a lattice site. For each molecular component (not vacancies), f_a can be related to the chemical potential of component a

$$\mu_a = \left(\frac{\partial F}{\partial n_a}\right)_{T,\{n_{b\neq a,0}\}} = f_a - r_a f_0 \qquad (39)$$

From the relations between the f_A's and the chemical potentials and the pressure, and from the condition $dV = \sum_a r_a v dn_a$, the familiar expressions for the Helmholtz energy are recovered: $dF = -SdT + \gamma dA - pdV + \sum_{a\neq0}\mu_a dn_a$ and $F = A\gamma - pV + \sum_{a\neq0}\mu_a n_a$.

6 PROPAGATOR FORMALISM FOR THE SEGMENT DISTRIBUTION

In principle, using eqs. (31) with (32), from the free-segment weighting factors and specified normalisation conditions, the frequency of each configuration of each chain can be calculated. From these, the density distribution of all segment types can be obtained. We will define the *chain-segment weighting factor* as the statistical weight of a chain of which the state and layer number of one of its segments, s, is specified.

$$G_a\big|_s^\sigma(z) = \sum_{c\big|_s^\sigma(z)} G_a^c \qquad (40)$$

The sum on the right-hand side extends over those chain configurations for which segment s is located in layer z and has state σ. Obviously, $\sum_{\sigma,z} G_a\big|_s^\sigma(z) = \sum_c G_a^c = G_a$ for each segment s of chain a, and hence $\sum_{\sigma,z,s} G_a\big|_s^\sigma(z) = G_a r_a$. Note that the chain-segment weighting factor, $G_a\big|_s^\sigma(z)$, differs from the free-segment weighting factor, $G_s^\sigma(z)$, that appeared in eq. (32). In the first, the statistical weights of the chain fragments that are bonded to the segment are included.

The number of chains of species a, with its segment s in state σ at layer number z, which equals the number of segments s in state σ and at layer number z, that belong to chains of species a, is given by $n_s^\sigma(z)$ = $\sum_{c|_s^\sigma(z)} n_a^c$. Obviously, the total number of a chains equals $\sum_{z,\sigma} n_s^\sigma(z)$ = n_a for each segment s of a. Summation of the left- and right-hand side of eq. (31) over configurations for which segment s is located in layer z and assumes state σ, leads to the following expression for the segment density distribution:

$$\phi_s^\sigma(z) = \Lambda_a G_a \big|_s^\sigma(z) \tag{41}$$

where $\phi_s^\sigma(z) = n_s^\sigma(z)/L$ is fraction of sites of layer z occupied by s segments (that belong to a chains), in state σ. So, for each separate segment of each chain type the distribution over layers and states can be obtained. The density distribution is normalised by Λ_a. Taking the sum over σ and z of the left-, and right-hand side of eq. (41), eq. (34) can be rewritten as, $\Lambda_a = \sum_{z,\sigma} \phi_s^\sigma(z) \big/ \sum_{z,\sigma} G_a \big|_s^\sigma(z) = \theta_a \big/ \sum_{z,\sigma,s} G_a \big|_s^\sigma(z)$.

The number of configurations of a flexible chain can be exceedingly large. This makes it very time consuming to calculate the weighting factor for each separate chain configuration and to perform the summation of eq. (40) in order to obtain the distribution of segments and subsequently, using the equations of section 5, the thermodynamic functions. Fortunately, as anticipated in section 1, a more efficient method can be devised. Within the framework of the Markov approximation introduced in section 3, it is possible to derive a recurrence relation that allows an efficient evaluation of the distribution of chain conformations.

First we note that the chain weighting factors, G_a^c, of all configurations included in the sum of eq. (40) have the free-segment weighting factor, $G_s^\sigma(z)$, in common. Hence, this factor can be taken outside the sum. The remaining sum can be written as a product of weighting factors of the chain fragments that are connected to segment s:

$$G_a \big|_s^\sigma(z) = G_s^\sigma(z) \prod_{d,a'} G_{a'} \big|^d(z) \tag{42}$$

where $G_{a'}\big|^d(z)$ is the statistical weight of a chain fragment a' that is connected to segment s at layer z, with a bond (s to a') that has direction d. The product on the right-hand side of eq. (42) extends over all directions. A value 1 should be substituted for $G_{a'}\big|^d(z)$ for directions where no chain fragment is bonded to segment s in state σ. The quantity, $G_{a'}\big|^d(z)$, will be referred to by the term *end weighting factor*. Comparison of eq. (42) with (33) reveals that the end weighting factors of chemically bonded chain fragments play similar roles in the statistical weight of a chain segment as the face weighting factors. The latter account for the interactions that are not chemical bonds.

The end weighting factor can be expressed as

$$G_{a'}\big|^d(z) = \sum_{\sigma'\big|^d_{s \to s'}} G_{a'}\big|^{\sigma'}_{s'}(z') \tag{43}$$

Here, we write $G_{a'}\big|^{\sigma'}_{s'}(z')$ for the statistical weight of chain fragment a' with its end segment s' in state σ'. The sum extends over the states of segment s' for which the bond from segment s to s' has direction d. For similar reasons as in eq. (42), the statistical weight of a chain fragment, $G_{a'}\big|^{\sigma'}_{s'}(z')$ can be written as a product of a free-segment weighting factor and of end weighting factors

$$G_{a'}\big|^{\sigma'}_{s'}(z') = G^{\sigma'}_{s'}(z') \prod_{d \neq s' \to s} G_{a''}\big|^d(z') \tag{44}$$

where the product extends over all directions except that at which segment s is bonded to s'. Obviously, for linear chains, the product over directions reduces to one factor. Factor $G_{a''}\big|^d(z')$ denotes the statistical weight of a chain fragment a'' that is bonded to segment s' at layer z', with a bond (s' to a'') that has direction d. If at direction d no chain fragment is bonded to s', then for $G_{a''}\big|^d(z')$ a value 1 should be substituted.

Combining eqs. (44) and (43), from the end weighting factors of chain fragments a'' that are bonded to segment s', the end weighting factor of the larger chain fragment a', that includes segment s', can be calculated. These two equations constitute a recurrence relation for chain-end weighting factors.

Equations (31) and (32) and the treatment of this present section are rather general and will also be valid in treatments that start from a differently approximated partition function. For example, it incorporates the matrix method of DiMarzio and Rubin [17] and Scheutjens and Fleer [20, 21] as special cases. These authors do not distinguish segment states and they write the recurrence relation in terms of a sum over possible locations of the segment preceding the end segment. In the present treatment, if the location and state of a segment is known, then the location of the preceding one is also known as well as the direction of the bond between the two. Hence, we write a sum over possible states of the preceding segment for which the bond has the right direction (eq. (43)).

In the treatment of DR and SF, the segments are completely flexible. In the present terminology these segments would have $q^2/2!$ distinguishable states. If backfolding of the bonds is forbidden the number of states is $q!/(2!(q-2)!)$.

7 CONCLUDING REMARKS

The first-order self consistent field lattice theory for monomers with orientation-dependent interaction of chapter II has been generalised for chain molecules. This results in a versatile method for modelling all kinds of complicated fluid systems.

The statistical handling of segmental states has quite general applicability. For instance it applies to dissociation / association of weakly acidic or basic segments. The statistics of this phenomenon has previously been incorrectly evaluated in theoretical treatments of the adsorption of polyelectrolytes [26, 27]. Further the concept of segmental states can be applied to vary the flexibility of chain molecules. By attributing a high a priori probability to states for which successive bonds are more or less parallel, de stiffness of chains of such segments is increased.

The present treatment can be applied to nematic ordering of semi-flexible chain molecules. One advantage over the approach by Khokhlov and Semenov [16] would be that the "dominant Eigenfunction approximation" can be avoided since the recurrence relation is evaluated throughout. This approximation implicates that the

orientational distribution of the segments is assumed independent of their position within the chain; end effects are neglected. This is formally analogous to the effects of the "dominant Eigen-function approximation" in polymer-adsorption theory. Further the present approach is capable of handling heterogeneous systems. So nematic ordering in interfacial systems might be studied.

Since the effects of orientation-dependent interactions can easily be accounted for within the present theory, the phase diagrams of aqueous solutions of such polymers as poly(propylene oxide) and poly(ethylene oxide) [33] can be modelled.

APPENDIX I. COMBINATORY FORMULA

Using eqs. (14) and (15), eq. (13) can be rewritten as:

$$L^n \prod_{\tau=1}^{n} \prod_{s(\tau)} P_s(\tau) = \prod_{\tau=1}^{n} \frac{n_\emptyset(z,\tau)^{r(z,\tau)}}{\prod_d n^d(z,\tau)^{l^d(z,\tau)/2}}$$

This equation can be simplified considerably. With $(n-kr)^r = (n-kr)!/(n-(k+1)r)!$ for $n \gg r$, we obtain

$$\prod_{\tau=1}^{n} n_\emptyset(z,\tau)^{r(z,\tau)} = L!^M$$

and

$$\prod_{\tau=1}^{n} n^d(z,\tau)^{\frac{1}{2}l^d(z,\tau)} = \prod_z \left(\frac{L!}{n^d(z,\tau)!} \right)^{1/2}$$

substitution into eq. (13) leads to eq. (16).

APPENDIX II. REDUCTION OF THE NUMBER OF VARIABLES

In the preceding derivations, parallel layers are allowed to be differently occupied. Moreover, all directions were allowed to be differently occupied. The number of variables (for example face weighting factors) can be reduced by restricting the configurational freedom of the system, by assuming a higher symmetry for the system.

For example, to study homogeneous systems it is unnecessary to consider more than half a lattice layer between reflecting boundaries. To study nematic ordering in a homogeneous system, only directions having different angles with respect to a director need to be discriminated. If a homogeneous system is isotropic, all directions are equally populated with bonds and contacts.

An important reduction of variables can be achieved when for the sites of a layer, subsets of directions are equally occupied by bonds and contacts. For example, all directions with a common angle with respect to the z-axis. For the number of directions belonging to a subset D we write q^D. Faces of the same type, belonging to the same subset of directions, have equal weights: $G_\alpha^d(z) = G_\alpha^D(z)$ for all directions d, belonging to the subset of directions D.

Segmental states belong to the same subset Σ if for the different states the directions of faces differ but belong to the same subset. These states have equal weights: $G_A^\Sigma(z) = \sum_{\sigma \in \Sigma} G_A^\sigma(z) = \omega_A^\Sigma G_A^\sigma(z)$ for each $\sigma \in \Sigma$.

$$G_A^\Sigma(z) = \omega_A^\Sigma \prod_{\alpha,D} G_\alpha^D(z)^{q_{A\alpha}^{\Sigma d}} \tag{II.1}$$

where ω_A^Σ is the number of segmental states belonging to the subset of states Σ, $q_{A\alpha}^{\Sigma D}$ is the number of faces of type α, having a direction belonging to the subset D, on a segment of type A, with an orientation belonging to the subset Σ.

Chain configurations can also be grouped in subsets. If the segments of different configurations are in states that belong to the same subsets then these configurations belong to the same subset of configurations. Such configurations have equal weights, $G_a^C = \sum_{c \in C} G_a^c = \omega_a^C G_a^c$ for each $c \in C$. This is illustrated in fig. {}. Taking the sum over all $c \in C$ of the left and right hand side of eq. (31) we obtain

$$\frac{n_a^C}{L} = \Lambda_a G_a^C \tag{II.2}$$

The weighting factor for chains with configurations belonging to subset C can be written as $G_a^C = \omega_a^C \prod_{A,\Sigma,\alpha,D} G_\alpha^D(z)^{q_{A\alpha}^{\Sigma D} r_{\alpha A}^{C\Sigma}(z)}$. The

number of configurations of subset C is given by $\omega_a^C = \prod_{A,\Sigma} \omega_A^{\Sigma^{r_{aA}^{C\Sigma}}} \prod_{A,\Sigma,D} q_{Ab}^{\Sigma D}! / \prod_D q^{D^{\frac{1}{2}l_a^{CD}}}$. Division by the multiple product of q^D is necessary because a factor q^D for the number of directions of the bond between two segments is included in the degeneracy factor ω_A^Σ of each of the two segments, the bond reduces the orientational freedom of the segments. Factorials $q_{Ab}^{\Sigma D}!$ account for the number of ways to arrange $q_{Ab}^{\Sigma D}$ bonds at q^D directions. The number of segments of type A, in a state that belongs to subset Σ, that belong to a chain of type a with a configuration belonging to subset C that are located in layer z is written as $r_{aA}^{C\Sigma}(z)$. The number of chemical bonds having direction D of such a chain is denoted as l_a^{CD}. Combining these we obtain the following analogue of eq. (32):

$$G_a^C = \frac{\prod_{A,\Sigma}\left(\prod_D q_{Ab}^{\Sigma D}!^{r_{aA}^{C\Sigma}} \prod_z G_A^\Sigma(z)^{r_{aA}^{C\Sigma}(z)}\right)}{\prod_{z,D} q^{D^{\frac{1}{2}l_a^{CD}}}} = \frac{\prod_{s=1}^{r_a}\left(q_a^C(s)_b! G_a^C(s)\right)}{\prod_{s=1}^{r_a-1} q_a^C(s)_{s'}} \tag{II.3}$$

Here $q_a^C(s)_{s'}$ is the number of directions the bond s to s' can have provided it belongs to a chain of type a that has a configuration belonging to set C. The weighting factor $G_a^C(s)$ is identical to $G_A^\Sigma(z)$ if segment s of a chain of type a is of type A and if this segment has an state belonging to Σ provided the chain has a configuration belonging to C.

Taking the sum over all $\sigma \in \Sigma$ in eq. (41), we obtain for the segment distribution the expression

$$\phi_a(z,\Sigma,s) = \Lambda_a G_a\left(z,\Sigma,s|\{s'\}\right) \tag{II.4}$$

Here

$$G_a\left(z,\Sigma,s|\{s'\}\right) = \sum_{C(z,\Sigma,s)} G_a^C = G_a(z,\Sigma,s) \prod_D G_a(z,s)_{s'}^{D^{q(\Sigma,s)_{s'}^D}} \tag{II.5}$$

The appropriate recurrence relation is

$$G_a(z,s)_{s'}^D = \frac{1}{q^D} \sum_{\Sigma'(D:s)}\left(G_a(z',\Sigma',s') \prod_{D'\neq D(s's)} G_a(z',s')_{s''}^{D'^{q(\Sigma',s')_{s''}^{D'}}}\right) \tag{II.6}$$

APPENDIX III. *NUMERICAL METHODS*

In the previous sections it has been shown that distributions of contacts and monomers are determined by the face weighting factors $G_\alpha^d(z)$, and vice versa. The set of equations can be solved using a Newton iteration method. We define a number of variables x_i, from which all properties of the system can be derived, and need an equal number of equations $f_i = 0$, that are satisfied uniquely if eqs. (29) and (41) with (42) and (43) are satisfied.

The method described previously has to be modified to cope with chemically bonded chains efficiently.

In the subsequent sections the following averages will be used:

$$\overline{x_\alpha}^\alpha = \frac{\sum\limits_\alpha x^\alpha}{\sum\limits_\alpha 1} \qquad\qquad \overline{x^d}^d = \frac{\sum\limits_d x^d}{q} = \frac{\sum\limits_D q^D x^D}{q}$$

$$\overline{x(z)}^z = \frac{\sum\limits_z x(z)}{M} \qquad\qquad \overline{x^d(z)}^* = \tfrac{1}{2}\Big(x^D(z) + x^{-D}(z')\Big)$$

Scheme I, general method.

The variables are defined as:

$$x_\alpha^D(z) = \ln G_\alpha^D(z) - \overline{\ln G_\alpha^D(z)}^\alpha + \overline{\ln G_\alpha^D(z)}^{\alpha,d} + \ln C$$

$$x_{link}^D(z) = -\overline{\ln G_\alpha^D(z)}^{\alpha,*} + \overline{\ln G_\alpha^D(z)}^{\alpha,d,*} + \ln C \qquad\qquad (\text{III.1})$$

Accordingly:

$$\overline{x_\alpha^D(z)}^\alpha = \overline{x_\alpha^D(z)}^{\alpha,d} = \overline{\ln G_\alpha^D(z)}^{\alpha,d} + \ln C \qquad\qquad (\text{III.2})$$

and

$$x_\alpha'^D(z) = x_\alpha^D(z) - \overline{x_\alpha^D(z)}^\alpha = \ln G_\alpha^D(z) - \overline{\ln G_\alpha^D(z)}^\alpha \qquad\qquad (\text{III.3})$$

We introduce:

$$G_A'^{\Sigma}(z) = \omega_A^{\Sigma} \exp \sum_D \left(\sum_\alpha q_{A\alpha}^{\Sigma D} x_\alpha^D(z) + q_{Alink}^{\Sigma D} x_{link}^D(z) \right) \quad \text{(III.4)}$$

It can be verified that $G_A'^{\Sigma}(z)$ is related to $G_A^{\Sigma}(z)$ as $G_A'^{\Sigma}(z) = G_A^{\Sigma}(z) \prod_D x^D(z)^{q_{Alink}^{\Sigma D}}$ where $x^D(z) = x^{-D}(z')$. Hence $G_A'^{\Sigma}(z)$ can be substituted for $G_A^{\Sigma}(z)$ since all $x^D(z)$ will cancel in calculating chain weighting factors.

Applying eqs. (III.4), the recurrence relation and the composition relation, all $\phi_A^{\Sigma}(z)$ are computed and since $\phi_\alpha^D(z) = \sum_{A,\Sigma} \phi_A^{\Sigma}(z) q_{A\alpha}^{\Sigma D}/q^D$ also all $\phi_\alpha^D(z)$ are known. Appropriate functions are:

$$f_\alpha^D(z) = 1 - \frac{1}{\sum\limits_{A,\Sigma} \phi_A^{\Sigma}(z)} + \overline{x_\alpha^D(z)}^\alpha - \overline{x_\alpha^D(z)}^{\alpha,d} - g_\alpha^D(z) + \overline{g_\alpha^D(z)}^{\alpha,d,*}$$

$$f_{link}^D(z) = 1 - \frac{1}{\sum\limits_{A,\Sigma} \phi_A^{\Sigma}(z)} + x_{link}^D(z) - \overline{x_\alpha^D(z)}^{\alpha,d,*} + \overline{g_\alpha^D(z)}^{\alpha,d,*} \quad \text{(III.5)}$$

here

$$g_\alpha^D(z) = -x_\alpha'^D(z) + \ln \sum_\beta \phi_\beta^{-D}(z') \exp- \left(x_\beta'^{-D}(z') + \frac{v_{\alpha\beta}}{kT} \right) \quad \text{(III.6)}$$

If the self-consistent field equations (29) and (41) with (42) and (45) are satisfied, all $f_\alpha^D(z)$ vanish: It is obvious that the first two terms of eq. (III.5) have to cancel. According to eqs. (29) and (III.3) $g_\alpha^D(z)$ equals $\overline{\ln G_\alpha^D(z)}^\alpha + \overline{\ln G_\alpha^{-D}(z')}^\alpha$, for each α, D and z, and hence cancels the last term.

Taking the average over all layers of the left and right hand side of eq. (III.2) and substituting $\frac{1}{2}\overline{g_\alpha^D(z)}^{\alpha,d,z}$ for $\overline{\ln G_\alpha^D(z)}^{\alpha,d,z}$ an expression for C can be obtained:

$$\ln C = \overline{x_\alpha^D(z)}^{\alpha,d,z} - \frac{1}{2}\overline{g_\alpha^D(z)}^{\alpha,d,z} \quad \text{(III.7)}$$

The distribution of contacts can be obtained using eq. (28) with

$$G_\alpha^D(z) G_\alpha^{-D}(z') = \exp\left(x_\alpha'^D(z) + x_\alpha'^{-D}(z') + \overline{g_\alpha^D(z)}^\alpha \right) \quad \text{(III.8)}$$

Usually calculations are made on two systems that are in equilibrium, an inhomogeneous interfacial system and a homogeneous bulk system. The latter is adequately represented by half a layer between two reflecting boundaries.

Using eq. (41) with (III.4) and (45) all volume fractions can be computed if the Λ_A are known. For a component Λ_A can be given directly. It also can be computed from a given total amount, θ_A, in one of the systems that are in equilibrium.

In accordance with the phase rule, normalisation conditions for components are not all independent. As a consequence, using this iteration scheme for a system consisting of more than one layer, not all components can be normalised by a fixed θ_A. Then the equations (III.5) would not be independent. For one component $\phi_A(b)$ is computed as $1 - \sum_{A \neq B} \phi_A(b)$. If for all components but one, bulk concentrations or Λ_A are given, all unknown Λ_A can be computed first by a separate iteration for the bulk. However if for one or more components θ_A, is given this iteration has to be carried out each time the functions (III.5) are to be computed.

Scheme II, System with fixed overall composition.

If for one of the systems, that are to be in equilibrium, the overall composition is fixed, then a good strategy is to compute the internal equilibrium of that system first, using a modified iteration method:
Each component is normalised by a given amount, θ_A. In order to avoid the functions to be dependent, they have to be supplemented by an additional term (the right hand side of eq. (III.7)). This implies that C will attain a value of one. Using scheme I, the resulting values of Λ_A can be used for normalisation in a computation for an other system, that is in equilibrium with the first. The values for C can be renormalised afterward using the condition that C equals 1 for homogeneous systems. Also the Λ_A will have to be renormalised.

APPENDIX IV SYMBOLS

subscripts:
A, B monomer types, all uppercase roman subscripts refer to monomer types. A value 0 refers to vacancies.

α, β face types. All lower case Greek subscripts refer to face types. A value 0 refers to the face of vacancies.

superscripts

d face direction.

D set of directions.

σ segment state.

Σ set of segment states.

If in an equation the parameters d, $-d$, z and z' appear they are related as follows: $-d$ indicates the opposite of direction d. z indicates the layer from which the face with direction d originates, z' the layer at which it is pointing.

In the following list, each parameter o or d can be replaced by O or D.

A surface area.

a $= A/L$, cross-sectional surface area per lattice site.

C normalisation constant for the whole system.

f_a $= (\partial F/\partial n_a)_{\{n_{b \neq a}\}}$, partial Helmholtz energy of component a

F Helmholtz energy.

g_A^σ a priori weighting factor for state σ of segment A

$g_\alpha^d(z)_\beta$ $= \phi_\alpha^d(z)_\beta / \phi_\alpha^d(z)\phi_\beta^{-d}(z')$, nearest-neighbour correlation function.

G Gibbs energy.

G_a weighting factor for chains of type a, $G_a = \sum_c G_a^c$.

G_a^c chain weighting factor for a chains in configuration c.

$G_A^\sigma(z)$ free-segment weighting factor of a segment of type A in state σ at layer z.

$G_{s|a}^{|c}$ free-segment weighting factor of segment s belonging to a chain of type a with configuration c.

$n_\alpha^d(z)$ number of faces of type α, at layer z, with direction d.

k Boltzmann's constant.

L number of lattice sites in a layer.

$\mathcal{L}$ Lagrangian function.

M number of layers.

N $= LM$, number of lattice sites of a system.

n_a number of chains of type a.

n_a^c number of a chains in configuration c.

$n_A(z)$ number of monomers of type A in layer z .

$n_A^\sigma(z)$ number of A-monomers in state σ located at z.

$n_\alpha^d(z)$ number of faces of type α, at layer z, with direction d.

$n_\alpha^d(z)_\beta$ number of contacts between faces of type α, at layer z, with direction d, and faces of type β. an asterisk indicates the random value.

p pressure.

Q canonical partition function.

q coordination number of the lattice, number of nearest neighbours of each site.

q^D number of directions belonging to set D.

$q_{A\alpha}^{\sigma d}$ number of faces of type α, having direction d, on a monomer of type A, in state σ. It can have values 0 and 1.

$q_{A\alpha}^{\Sigma D}$ number of faces of type α, having direction belonging to subset D, on a monomer of type A, having in one of the states of subset Σ

S   entropy.

T absolute temperature.

U energy of the system.

V volume of the system.

v $= V/N$ volume of one lattice site.

$v_{\alpha\beta}$ exchange energy for an $\alpha\beta$-contact.

w_A^σ internal energy of a segment of type A in state σ.

z layer number.

γ surface tension.

θ_a $= n_a r_a / L$.

Λ_a $= \exp(f_a/kT)$ if there are no vacancies in the model, it is the absolute activity.

λ, $\lambda_\alpha^d(z)$ Lagrange undetermined multiplier.

μ_a $= (\partial F/\partial n_a)_{N,\{n_{b \neq a,0}\}}$, chemical potential

Ξ partition function.

$\phi_A^\sigma(z)$ $= n_A^\sigma(z)/L$, volume fraction of monomers of type A, in state σ and z.

$\phi_\alpha^d(z)$ $= n_\alpha^d(z)/L$, fraction of faces in layer z having direction d that are of type α.

$\phi_\alpha^d(z)_\beta$ $= n_\alpha^d(z)_\beta/L$, fraction of contacts with direction d, originating from a site in layer z between an α face and a β face.

$\psi_\alpha^d(z)_\beta$ $= \phi_\alpha^d(z)_\beta/\phi_\beta^{-d}(z')$, nearest-neighbour distribution function.

Ω combinatory factor.

ω_A^Σ number of states of a monomer of type A, belonging to the subset of states Σ,

REFERENCES

1   Besseling, N. A. M. "Statistical thermodynamics of molecules with orientation-dependent interactions in homogeneous and heterogeneous systems". Ibid. Chapter II.

2   Guggenheim, E. A. *Mixtures*; Clarendon: Oxford, 1952.

3   Besseling, N. A. M. "Equilibrium properties of water and its liquid-vapour interface". Ibid. Chapter III.

4   Besseling, N. A. M. "On the molecular interpretation of the hydrophobic effect". Ibid. Chapter IV.

5   Besseling, N. A. M. "Hydration forces betwee planar surfaces". Ibid. Chapter V.

6   Huggins, M., L. *Ann. N. Y. Acad. Sci.*, 43, 1-32 (1942) "Thermodynamic properties of solutions of long-chain compounds".

7   Guggenheim, E. A. *Proc. R. Soc. (London)*, A183, 203-212 (1944) "Statistical thermodynamics of mixtures with zero energies of mixing".

8   Guggenheim, E. A. *Proc. R. Soc. (London)*, A183, 213-227 (1944) "Statistical thermodynamics of mixtures with non-zero energies of mixing".

9   DiMarzio, E. A. *J. Chem. Phys.*, 35, 658-669 (1961) "Statistics of orientation effects in linear polymer molecules".

10   DiMarzio, E. A. *J. Chem. Phys.*, 66, (1977) "Configurational packing statistics of polymers near a surface. I. The generalization of the rigid rod case to include both orientation dependence and spatial variation".

11   Leermakers, F. A. M.; Scheutjens, J. M. H. M. *J. Chem. Phys.*, 89, 6912-6924 (1988) "Statistical thermodynamics of association colloids. III. The gel to liquid phase transition of lipid bilayer membranes".

12   Cantor, R. S.; McIlroy, P. M. *J. Chem. Phys.*, 91, 416 (1989) "Statistical thermodynamics of monolayers of flexible-chain amphiphiles: adding nearest-neighbour correlations to a Scheutjens_Fleer approach".

13   de Gennes, P. G. *Rep. Prog. Phys.*, 32, 187-205 (1969) "Some conformation problems for long macromolecules".

14   Lifshitz, I. M.; Grosberg, A. Y.; Khokhlov, A. R. *Rev. Mod. Phys.*, 50, 683-713 (1978) "Some problems of the statistical physics of polymer chains with volume interaction".

15 Edwards, S. F. *Proc. Phys. Soc.*, *85*, 613-624 (1965) "The statistical mechanics of polymers with excluded volume".

16 Khokhlov, A. R.; Semenov, A. N. *Physica*, *112A*, 605-614 (1982) "Liquid-crystaline ordering in the solution of partially flexible macromolecules".

17 DiMarzio, E. A.; Rubin, R. J. *J. Chem. Phys.*, *55*, 4318-4336 (1971) "Adsorption of a chain polymer between two plates".

18 Björling, M.; Linse, P.; Karlström, G. *J. Phys. Chem.*, *94*, 471-481 (1990) "Distribution of segments for terminally attached poly (ethylene oxide) chains".

19 Evers, O. A.; Scheutjens, J. M. H. M.; Fleer, G. J. *Macromolecules*, *23*, 5221-5233 (1990) "Statistical thermodynamics of block copolymer adsorption. 1. Formulation of the model and results for the adsorbed layer structure".

20 Scheutjens, J. M. H. M.; Fleer, G. J. *J. Phys. Chem.*, *83*, 1619-1635 (1979) "Statistical theory of the adsorption of interacting chain molecules. 1. Partition function, segment density distribution, and adsorption isotherms".

21 Scheutjens, J. M. H. M.; Fleer, G. J. (1980) "Statistical theory of the adsorption of interacting chain molecules. 2. Train, loop, and tail size distribution".

22 Meijer, E. J. *Computer simulation of molecular solids and colloidal dispersions*; Rijksuniversiteit Utrecht: 1993.

23 Flory, P. J. *Principles of Polymer Chemistry*; Cornell: Ithaca/London, 1971.

24 Hill, T. L. *Introduction to Statistical Thermodynamics*; Addison-Wesley: 1962.

25 Linse, P.; Björling, M. *Macromolecules*, *24*, 6700-6713 (1991) "Lattice theory for multicomponent mixtures of copolymers with internal degrees of freedom in heterogeneous systems".

26 Böhmer, M. R.; Evers, O. A.; Scheutjens, J. M. H. M. *Macromolecules*, *23*, 2288 (1990)

27 Evers, O. A.; Fleer, G. J.; Scheutjens, J. M. H. M.; Lyklema, J. *J. Colloid Interface Sci.*, *111*, 446-454 (1986) "Adsorption of weak polyelectrolytes from aqueous solution".

28 Leermakers, F. A. M.; Scheutjens, J. M. H. M. *J. Colloid Interface Sci.*, *136*, 231-241 (1990) "Statistical thermodynamics of association colloids: V. Critical micelle concentration, micellar size and shape".

29 Barneveld, P. A.; Scheutjens, J. M. H.; Lyklema, J. *Langmuir*, *8*, 3122-3130 (1992) "Bending moduli and spontaneous curvature. 1. Bilayers and monolayers of pure and mixed nonionic surfactants".

30 Leermakers, F. A. M.; Scheutjens, J. M. H. M. *J. Chem. Phys.*, *89*, 3264-3274 (1989) "Statistical thermodynamics of association colloids. 1. Lipid bilayer membranes".

31 Leermakers, F. A. M.; Scheutjens, J. M. H. M. *Biochim. Biophys. Acta*, *1024*, 139-151 (1990) "Statistical thermodynamics of association colloids. IV. Inhomogeneous membrane systems".

32 Leermakers, F. A. M.; Scheutjens, J. M. H. M. *J. Phys. Chem.*, *93*, 7417-7426 (1989) "Statistical thermodynamics of association colloids. 2. Lipid vesicles".

33 Saeki, S.; Kuwahara, N.; Nakata, M.; Kaneko, M. *Polymer*, *17*, 685-689 (1976) "Upper and lower critical solution temperatures in poly (ethylene glycol) solutions".

SUMMARY

The aim of the present study was to develop a lattice theory for systems, homogeneous as well as heterogeneous, containing molecules with orientation-dependent interactions such as water. It was soon recognised that the so-called Bragg-Williams mean-field approximation is not capable of reproducing the typical temperature dependence of the thermodynamic properties of such systems. This is due to the neglect of correlations between positions and orientations of the molecules. To improve this, we based ourselves on the so called quasi-chemical approximation.

In **chapter I**, some background information is given on the systems with which the present study is concerned and the theoretical methods that are employed.

In **chapter II** the theory is derived in a general fashion, for an arbitrary collection of monomeric species. To model heterogeneous systems, the lattice is divided into parallel layers. The density of each monomeric species and the orientational distribution are allowed to be different for each layer. A partition function is derived as a sum over distributions of molecules over orientations and positions and over distributions of intermolecular contacts. From this, self-consistent field equations are obtained for the equilibrium distributions. Further, it is indicated how free-volume effects can be accounted for by allowing sites to be vacant. Expressions are obtained for energy, entropy, chemical potentials, pressure and surface tension etc..

The self-consistent field equations are solved numerically by means of a modified Newton iteration. A major complication in the numerical problem associated with this theory is the necessity to simultaneously iterate the density distribution of the various molecular orientations as well as the distribution of contacts between molecules. With self-consistent field theories that are based on the Bragg-Williams approximation such as that of Scheutjens and Fleer, the distribution of contacts is simply assumed to be random, even if there are non-zero interactions.

At the end of chapter II, the capabilities of the method are illustrated by applying it to a number of specific systems containing molecules

with orientation-dependent interactions. The coexistence curves that are calculated show that orientation-dependent interactions can give rise to an increasing solubility with decreasing temperature. Also for the interfacial properties the orientation-dependent nature of the intermolecular interactions is shown to be of great importance. For special model systems it is found that the tension of the interface between coexisting phases increases with increasing temperature. Of a system that exhibits a closed-loop coexistence curve, the interfacial tension of the interface between the coexisting phases vanishes at the lower critical solution temperature. Upon increasing temperature it increases, passes a maximum and decreases until it vanishes again at the upper critical solution temperature. The structural differences at the interface between temperatures at which the interfacial entropy is negative and where it is positive are discussed.

Chapters III to VI are concerned with various properties of water.

In **chapter III**, a lattice-gas model for water is introduced that is elaborated by the formalism of chapter II. This theory appeared to be capable of reproducing various anomalous thermodynamic properties of water. The calculated equation of state and liquid-vapour phase diagram agree at least qualitatively with the experimental behaviour of water. For instance, the maximum of the isobaric density as a function of temperature is reproduced. Within this model it is possible to analyse the relation between macroscopic behaviour and the microscopic structure of liquid water. The amount of intact hydrogen bonds can be calculated as well as that of the other intermolecular contacts. Over a large range of temperatures and densities, the fraction of intact hydrogen-bonds is close to unity. This confirms that liquid water can be considered as a percolating hydrogen-bonded network.

The liquid-vapour interface is also investigated. A salient result is the increase of the interfacial thickness and the density-coherence length of liquid water upon decreasing temperature. This result still awaits experimental verification. Further, the minimum of the temperature coefficient of the interfacial tension as a function of temperature is reproduced by the theory.

In **chapter IV** the so-called hydrophobic effect is addressed. It is made plausible that the physics underlying the anomalous thermodynamics of solvation by water of small apolar molecules is

similar to that of the isobaric density maximum of pure water. An explanation is given for the exothermic solvation of apolar compounds below room temperature. This is attributed to a decrease of repulsive non-hydrogen bonding interactions between water molecules. The large entropy effect of solvating apolar compounds is also reproduced by the theory. For the explanation of these phenomena it appears to be unnecessary to invoke so-called iceberg formation around apolar molecules. Another interesting result is that the solvation thermodynamics of small molecules and of extended surfaces appears to be very different.

In **chapter V**, hydration forces, water-structure mediated forces between surfaces, are the main subject. There is experimental evidence for the occurrence of such forces in systems as different as biological membranes and inorganic colloids. Both within a phenomenological approach based on a Landau expansion of the free-energy density as in results from the lattice-theory, it is found that these forces can be attractive or repulsive, depending on the properties of the surfaces. More specifically, the sign of the interaction depends on the type of ordering induced by the surfaces in adjoining water. If the solvation layers of two surfaces overlap in such a way that the ordering is enhanced, the ensuing interaction between the surfaces is attractive. This indicates that the accepted view, that the water-structure mediated interaction between hydrophilic surfaces is always repulsive, needs reconsideration. If the structuring is distorted by overlap, then a repulsive force is the result.

Chapter VI contains some preliminary results on vapour adsorption and on wetting phenomena. For various model surfaces and temperatures vapour-adsorption isotherms are calculated. In this way, the understanding of the relation between the properties of surfaces and the adsorption of water vapour is improved. For a number of surfaces a transition from partial wetting to complete wetting is found with variation of the properties of the surface or of temperature. The interfacial tension of the solid-vapour and the solid-liquid interface at the saturation pressure has been calculated, as well as that of the liquid-vapour interface. Consequently, using Young's law, the contact angle can be obtained together with related quantities such as the reversible work of adhesion and the spreading coefficient.

In **chapter VII**, the formalism of chapter II is extended towards systems containing chain molecules. Such molecules consist of segments, each occupying one lattice site. Generally, they can have a large number of conformations. It is indicated how the (semi)flexibility of chain molecules can be accounted for within the theory. Correlations due to the connected nature of segments are accounted for in first-order approximation. This is consistent with the way correlations due to energetic interactions are accounted for. It has been possible to derive a recurrence relation for the statistical weight of chains of different lengths which allows an efficient evaluation of the statistical weight of each possible chain conformation.

STATISTISCHE THERMODYNAMICA VAN VLOEISTOFFEN
MET ORIËNTATIE-AFHANKELIJKE INTERACTIES
TOEPASSINGEN OP WATER IN HOMOGENE EN HETEROGENE SYSTEMEN

SAMENVATTING

Op het eerste gezicht is water niet erg interessant. Het is een kleurloze, smaakloze en geurloze vloeistof. Het is niet explosief, het kan niet eens branden. Het is totaal niet zeldzaam en ontzettend goedkoop. We wassen ons met water, en drinken het alleen als niets beters voorhanden is. Ieder kind weet wat water is. Waarom zou dan een riant OIO-salaris moeten worden besteed aan een onderzoek aan water?

Bij nader inzien blijkt water een bijzonder interessante stof. Het is een van de meest voorkomende stoffen op aarde. Alle levende wezens bestaan voor het grootste deel uit water. In ons lichaam komen daarnaast ook stoffen voor als zouten, eiwitten, vetten, suikers en alcoholen.

Vergeleken met stoffen met een vergelijkbaar molekuulgewicht gedraagt water zich tamelijk uitzonderlijk. Bij een druk van één atmosfeer en bij kamertemperatuur zijn bijvoorbeeld ammoniak en methaan gasvormig terwijl water vloeibaar is. Het kookpunt van water ligt bij een veel hogere temperatuur dan dat van ammoniak of methaan. Dit geldt ook voor de smeltpunten. Verder zijn ook de warmtecapaciteit en de verdampingswarmte van water relatief hoog. Dit is onder andere belangrijk voor de stabiliteit van het klimaat op aarde en voor de regulering van de temperatuur van ons lichaam. In water lossen veel stoffen zoals bijvoorbeeld zout, suiker en alcohol goed op. Olie- en vetachtige stoffen lossen zoals bekend slecht op in water. Dit is belangrijk voor de chemische processen die zich in levende wezens afspelen.

Voor een goed begrip van allerlei belangrijke verschijnselen is dus een goed begrip van water belangrijk. In dit proefschrift wordt een theorie beschreven waarmee de eigenschappen van een stof als water verklaard kunnen worden uit de eigenschappen van de molekulen waaruit het is opgebouwd. In de volgende alinea's wordt de inhoud van ieder hoofdstuk beschreven.

Hoofdstuk I, de algemene inleiding, geeft wat informatie over het soort systemen en het type eigenschappen waar het in dit proefschrift over gaat. Daarnaast worden enkele achtergronden van de gebruikte theorie besproken.

Hoofdstuk II is hoofdzakelijk gewijd aan de afleiding van de theorie. Deze wordt zo algemeen mogelijk geformuleerd zodat ze kan worden toegepast op allerlei verschillende systemen. Als eerste benadering wordt een roostermodel geïntroduceerd. Hierin bevinden alle molekulen zich op een regelmatig rooster van plaatsen en hebben anisotrope molekulen een discreet aantal oriëntaties. De interactie tussen naast elkaar gelegen molekulen kan afhangen van hun onderlinge oriëntatie. Voor dit model wordt een toestandssom opgesteld. Hierbij wordt de zogenaamde quasi-chemische benadering veralgemeniseerd. Omdat parallelle lagen van het rooster een verschillend bezetting kunnen hebben kunnen heterogene systemen gemodelleerd worden. Uit de toestandssom worden uitdrukkingen afgeleid voor de evenwichtstoestand van een systeem. Belangrijke karakteristieken van de toestand van een systeem zijn in dit verband: het dichtheidsprofiel, de verdeling van molekulaire oriëntaties en van intermolekulaire contacten. Verder worden uitdrukking afgeleid voor alle relevante thermodynamische grootheden zoals inwendige energie, vrije energie, grensvlakspanning, druk en chemische potentialen.

Aan het eind van hoofdstuk II wordt de theorie toegepast op een aantal mengsels waarbij oriëntatie-afhankelijke intermolekulaire interacties een rol spelen. Eén van deze systemen vertoont een gesloten binodaal. Bij een ander is de binodaal asymmetrisch t.o.v. een molfractie gelijk aan $\frac{1}{2}$, doordat één van de componenten anisotroop is en de ander niet. Voor deze gevallen wordt tevens de structuur van het grensvlak tussen de coëxisterende fasen berekend en de bijbehorende grensvlakspanning. In bepaalde gevallen is de grensvlak-entropie negatief en blijkt het grensvlak sterk gestructureerd te zijn.

In **hoofdstuk III** wordt de bovengenoemde theorie toegepast op water. Als basis wordt het lichaams-gecentreerde kubische rooster gebruikt. De oriëntatie-afhankelijke interacties van watermolekulen worden in dit model in rekening gebracht. Voor bepaalde onderling oriëntaties is de interactie tussen naburige watermolekulen sterk attractief, voor andere zwak repulsief. Dit model reproduceert een

aantal karakteristieke eigenschappen die uniek zijn voor water. Een voorbeeld is het maximum van de dichtheid als functie van de temperatuur. Het vloeistof-damp evenwicht van water is onderzocht. Ook het grensvlak tussen coëxisterende vloeistof en damp is bestudeerd. De berekende grensvlakspanning als functie van de temperatuur vertoont een buigpunt, zoals ook experimenteel wordt gevonden. Opvallend is verder dat voor niet te hoge temperatuur, de dikte van het grensvlak en de correlatielengte van de vloeistof toeneemt bij dalende temperatuur.

In **hoofdstuk IV** wordt op basis van de theorie van hoofdstuk III het hydrofobe effect geanalyseerd. Met 'hydrofobe effect' doelt men in het algemeen op een aantal opvallende verschijnselen die zich voordoen bij het oplossen van apolaire stoffen in water. Deze oplosbaarheid is laag en vertoont vaak een minimum als functie van de temperatuur. Hieruit blijkt dat de oplos-entropie hoog is en de voornaamste factor bij de slechte oplosbaarheid. De oplos-enthalpie is laag en soms zelfs negatief. Dit laatste bevordert de oplosbaarheid. Deze verschijnselen worden gewoonlijk verklaard door aan te nemen dat rond een apolair molekuul een laagje sterk gestructureerd water ontstaat waarin de waterstofbruggen zelfs sterker en/of talrijker zijn dan in zuiver water. In hoofdstuk IV wordt een alternatief voorgesteld: de strukturering rond een apolair molekuul is niet kwalitatief anders dan in zuiver water. De negatieve enthalpie is het gevolg van een afname van repulsieve interacties tussen watermolekulen door toevoeging van apolaire molekulen. Deze effecten treden ook op bij het uitzetten van zuiver water. De molekulaire verklaring voor het dichtheids-maximum van zuiver water en voor het minimum in de oplosbaarheid van apolaire stoffen als functie van temperatuur is gelijk.

Hoofdstuk V: Een laagje water aan een oppervlak dat verschilt van de bulkvloeistof wordt een hydratatielaag genoemd. De lokale dichtheid en/of de verdeling over oriëntaties in de nabijheid van een grensvlak kan van die in de bulk afwijken. Als de hydratatielagen van twee parallelle oppervlakken elkaar overlappen zal een kracht tussen die oppervlakken het gevolg zijn, de hydratatie-kracht. Volgens berekeningen met bovengenoemde methode kunnen zowel attractieve als repulsieve krachten optreden. Als twee gelijke oppervlak voornamelijk de lokale dichtheid van water beïnvloedt dan zal de

resulterende kracht altijd attractief zijn. Dit geldt voor hydrofobe en hydrofiele oppervlakken en is onafhankelijk van het feit of die lokale dichtheid hoger of lager is dan in de bulkvloeistof. Als voornamelijk de oriëntatie-verdeling van de watermolekulen wordt beïnvloed dan zal een repulsieve kracht optreden tussen twee gelijke oppervlakken.

Hoofdstuk VI bevat een aantal resultaten met betrekking tot andere verschijnselen die optreden bij water aan grensvlakken. Aan de orde komen: dampadsorptie, bevochtiging en capillair-condensatie in een spleet tussen twee oppervlakken. Het blijk dat ook deze verschijnselen onderzocht kunnen worden met de bovengenoemde methodiek. De dampadsorptie-isothermen van water vertonen geen duidelijk plateau. Voor een aantal oppervlakken wordt een bevochtigings-overgang gevonden. Het blijkt dat de temperatuur waarbij de bevochtigings-overgang optreedt afhangt van de eigenschappen van het oppervlak. Naarmate de affiniteit van het oppervlak voor water groter is, is de temperatuur waarboven volledige bevochtiging optreedt lager.

In **hoofdstuk VII** wordt de theorie van hoofdstuk II nog wat verder veralgemeniseerd zodat ook ketenmolekulen kunnen worden gemodelleerd. Deze bestaan uit segmenten; elk segment bezet een roosterplaats. Pakkingseffecten als gevolg van bindingen tussen de segmenten worden in rekening gebracht op een wijze die consistent is met de manier waarop correlaties als gevolg van energetische wisselwerkingen worden behandeld.

LEVENSLOOP

De schrijver van dit proefschrift werd geboren op 15 januari 1960 te Zwaag. In 1978 behaalde hij het diploma Atheneum B aan de Scholengemeenschap Werenfridus te Hoorn. Daarna begon hij de studie aan de landbouwuniversiteit. Na aanvankelijk begonnen te zijn aan de studie Tuinbouwplantenteelt zwaaide hij in 1980 om naar Moleculaire Wetenschappen. In 1986 studeerde hij af met afstudeervakken Fysische Chemie, Natuurkunde en Moleculaire fysica en een bijvak Wijsbegeerte. Bovendien behaalde hij de eerste-graads onderwijsbevoegdheid Scheikunde. Van 1987 tot 1988 vervulde hij de vervangende dienstplicht en was 'tewerkgesteld' bij de vakgroep Fysische en Macromoleculaire Chemie van de Rijksuniversiteit te Leiden. In juli 1988 werd begonnen aan het promotieonderzoek bij de vakgroep Fysische en Kolloïdchemie van de Landbouwuniversiteit, in dienst van NWO. Dit heeft geleid tot dit proefschrift. Vanaf mei 1993 werkt hij bij de afdeling Toegepaste Wiskunde van Akzo Research Laboratories te Arnhem.

NAWOORD

Het is voor iemand met een beperkt literair talent onmogelijk recht te doen aan alle ervaringen die tijdens de afgelopen periode van bijna vijf jaar zijn opgedaan. Zo'n promotieonderzoek is zeker geen 'negen-tot-vijf' baan. Je moet het uit interesse doen en het houdt je ook in je vrije tijd nog vaak bezig. Mijn belangstelling voor de Statistische Thermodynamica is lang geleden gewekt door het college van Hans Lyklema, o.a. door zijn prikkelende opmerking dat dit het moeilijkste vak zou worden dat we in onze studie zouden tegenkomen. De combinatie van een elegant formalisme en de mogelijkheid/noodzaak om een fysische voorstelling te maken van de microscopische wereld die schuilgaat achter alledaagse macroscopische verschijnselen boeit me nog steeds. Toch zijn het bij een onderzoek vaak triviale, op zich oninteressante problemen, die het meeste tijd kosten. Zo ben ik bijvoorbeeld zo'n drie jaar bezig geweest om een numerieke methode te bedenken, zoals nu beschreven staat in Appendix II van het tweede hoofdstuk van dit boekje. Zonder zo'n methode had dit proefschrift er niet kunnen komen. Al die tijd ben ik er maar van uit gaan dat het op tijd zou lukken, zonder enige zekerheid daarover te hebben. In zo'n situatie is het onvermijdelijk dat je je zo nu en dan enige zorgen maakt.

Een belangrijk tegenwicht voor dit soort beslommeringen werd gevormd door de plezierige sfeer op de vakgroep en de activiteiten buiten werktijd zoals de jaarlijkse Veluweloop, het wekelijks volleybal, allerlei etentjes en feestjes en het inmiddels internationaal vermaarde 'vergaderen' op Loburg. Mijn begeleider, Jan Scheutjens, was bijna altijd te porren voor dit soort gezellige dingen. Het was een enorme schok om te horen dat hij niet meer terug zou komen van vacantie omdat hij was verongelukt. De eerste zin van dit nawoord geldt des te sterker als ik wat wil zeggen over Jan. Een paar trefwoorden die iedereen die hem gekend heeft wel zal kunnen plaatsen zijn: zachtaardigheid, originaliteit en creativiteit die zich uitte in een bijzondere humor en veel verassende ideeën, die ook nog vaak juist bleken te zijn. Dit proefschrift was ongetwijfeld beter geweest als hij bij de afronding betrokken was geweest.

Frans Leermakers en Hans Lyklema hebben het verlies van Jan zoveel mogelijk opgevangen, onder meer door het manuscript kritisch te lezen en van kanttekeningen te voorzien. Daarvoor wil ik ze hier bedanken. De collega's van de theoriegroep wil ik bedanken voor hun plezierige gezelschap en voor het op orde houden van de computervoorzieningen. Zonder anderen hierbij tekort te willen doen verdient Peter Barneveld in dit verband wel een eervolle vermelding. Met mijn kamergenoten, de meeste jaren Johan Kijlstra, later Chris Wijmans, was het altijd plezierig om van gedachten te wisselen over allerlei onderwerpen. Dit geldt ook voor "m'n" doctoraalstudenten Philip Lijnzaad en Henk Visser. Met Joost van Opheusden, heb ik plezierig samengewerkt bij de begeleiding van Henk. Het is niet mogelijk om iedereen aan wie ik goede herinneringen heb apart te noemen, daarom stop ik nu maar met schrijven.

U, de lezer, wil ik nog even feliciteren: U heeft dit proefschrift nu helemaal uit!

Tot ziens,

Klaas